Developing a process control strategy for the consistent and scalable manufacture of human mesenchymal stem cells

by

Thomas Richard James Heathman

A Doctoral Thesis
Submitted in partial fulfillment of the requirements
for the award of

DOCTOR OF PHILOSOPHY

Loughborough University
October 2015

ABSTRACT

Human mesenchymal stem cells (hMSCs) have been identified as a promising cell-based therapy candidate to treat a number of unmet clinical indications, however, *in vitro* expansion will be required to increase the available number of cells and meet this demand. Scalable manufacturing processes, amenable to closed, single-use and automated technology, must therefore be developed in order to produce safe, effective and affordable hMSC therapies. To address this challenge, a controlled serum-free end-to-end microcarrier process has been developed for hMSCs, which is amenable to large-scale manufacture and therefore increasing economies of scale. Preliminary studies in monolayer culture assessed the level of variability in growth between five hMSC donors, which was found to have a variance of 25.3 % after 30 days in culture. This variance was subsequently reduced to 4.5% by the development of a serum-free monolayer culture process with the maintenance of critical hMSC characteristics and an increased number of population doublings. In order to transfer this into a scalable system, the serum and serum-free expansion processes were transferred into suspension by the addition of plastic microcarriers in 100 mL spinner flasks without control of pH or dissolved oxygen (DO). This achieved a maximum cell density of $0.08 \pm 0.01 \cdot 10^6$ cells.mL^{-1} in FBS-based medium, $0.12 \pm 0.01 \cdot 10^6$ cells.mL^{-1} in HPL-based medium and $0.27 \pm 0.03 \cdot 10^6$ cells.mL^{-1} in serum-free medium after six days. In order to drive consistency and yield into the manufacturing process, a process control system was developed for the FBS-based microcarrier expansion process in a 100 mL DASbox bioreactor platform to control DO, pH, impeller rate and temperature. Reduced impeller rates and DO concentrations were found to be beneficial, with a final cell density of $0.11 \pm 0.02 \cdot 10^6$ cells.mL^{-1} and improved post-harvest outgrowth and colony-forming unit (CFU) potential compared to uncontrolled microcarrier and monolayer culture. This controlled bioreactor expansion process was then applied to the previously developed serum-free microcarrier process, eventually achieving a final cell density of $1.04 \pm 0.07 \cdot 10^6$ cells.mL^{-1}, whilst retaining key post-harvest hMSC characteristics. Following the controlled serum-free expansion and harvest of hMSCs, a downstream and cryopreservation process was developed to assess the impact of prolonged holding times and subsequent unit-operations on hMSC quality characteristics. This showed that hMSCs are able to maintain key characteristics throughout the entire end-to-end process, demonstrating their potential for commercial scale manufacture.

Key words: cell-based therapy, consistency, cryopreservation, downstream process development, human mesenchymal stem cell, manufacture, microcarrier, process control, regenerative medicine, serum-free.

Acknowledgements

List of Publications and Presentations

Journal Publications

Heathman TRJ, Glyn VAM, Picken A, Rafiq QA, Coopman K, Nienow AW, Kara B, Hewitt CJ. Expansion, harvest and cryopreservation of human mesenchymal stem cells in a serum-free microcarrier process. Biotechnology & Bioengineering, (2015) 112 (8): 1696-1707

Heathman TRJ, Nienow AW, McCall MJ, Coopman K, Kara B, Hewitt CJ. The translation of cell-based therapies: clinical landscape and manufacturing challenges. Regenerative Medicine, (2015) 10 (1): 49-64.

Heathman TRJ, Rafiq QA, Chan AK, Coopman K, Nienow AW, Kara B, Hewitt CJ. Characterisation of human mesenchymal stem cells from multiple donors and the implications for large scale bioprocess development. Biochemical Engineering Journal, (2016) 108: 14-23.

Heathman TRJ, Stolzing A, Fabian C, Rafiq QA, Coopman K, Nienow AW, Kara B, Hewitt CJ. Serum-free process development: Improving the yield and consistency of human mesenchymal stem cell production. Cytotherapy, (2015) 17 (11): 1524-1535.

Heathman TRJ, Stolzing A, Fabian C, Rafiq QA, Coopman K, Nienow AW, Kara B, Hewitt CJ. Scalability and process transfer of mesenchymal stem cell production from monolayer to microcarrier culture using human platelet lysate. Cytotherapy, (2016) 18 (4): 523-535.

Heathman TRJ, Rafiq QA, Coopman K, Nienow AW, Kara B, Hewitt CJ. Developing a process control strategy for the serum-free production of human mesenchymal stem cells on microcarriers. Biotechnology & Bioengineering, (2015) (*in preparation*)

Heathman TRJ, Picken A, Glyn VAM, Cheeseman E, Rafiq QA, Nienow AW, Kara B, Hewitt CJ, Coopman K. Controlled microcarrier expansion, harvest, downstream processing and cryopreservation of mesenchymal stromal cells from multiple donors under serum-free conditions. Journal of Biotechnology, (2016) (*in preparation*)

Heathman TRJ, Rafiq QA, Coopman K, Nienow AW, Kara B, Hewitt CJ. Developing a microcarrier coating protocol to allow for the serum-free production of human mesenchymal stem cells on microcarriers. <u>Biotechnology letters</u>, (2016) (*in preparation*)

Rafiq QA, **Heathman TRJ**, Fonte G, Coopman K, Nienow AW, Hewitt CJ. Monolayer expansion of hMSCs in multiple brands of serum-free medium. <u>Cytotherapy</u>, (2016) (*in preparation*)

Nienow AW, Hewitt CJ, **Heathman TRJ**, Glyn VAM, Fonte G, Hanga MP, Coopman K, Rafiq QA. Agitation Conditions for the Culture and Detachment of hMSCs from Microcarriers in Multiple Bioreactor Platforms. <u>Biochemical Engineering Journal</u>, (2016) 108: 24-29.

Chan AK, **Heathman TRJ**, Coopman K, Hewitt CJ. Multiparameter flow cytometry for the characterisation of extracellular markers on human mesenchymal stem cells. <u>Biotechnology letters</u>, (2014) 36 (4): 731-41.

Book Chapters

Heathman TRJ, Rafiq QA**,** Coopman K, Nienow AW, Hewitt CJ. The scale-up of human mesenchymal stem cell expansion and recovery. Bioprocessing for Cell-Based Therapies. <u>John Wiley & Sons</u>, (2015).

Rafiq QA, **Heathman TRJ,** Coopman K, Nienow AW, Hewitt CJ. Scale-up of stem cell manufacture for cell therapy needs. Bioreactors: Design, Operation and Novel Applications. <u>Wiley-VCH</u>, (2015).

Nienow AW, **Heathman TRJ,** Coopman K, Rafiq QA, Hewitt CJ. Bioreactor Engineering Fundamentals for Stem Cell Manufacturing. Stem Cell Manufacturing. <u>Elsevier</u>, (2015).

Rafiq QA, **Heathman TRJ,** Coopman K, Nienow AW, Hewitt CJ. Culture of human mesenchymal stem cells on microcarriers in multiple stirred-tank bioreactor platforms. Bioreactors for Stem Cells Biology: Methods and Protocols. <u>Springer's Methods in Molecular Biology</u>, (2015).

Invited Oral Presentations

Heathman TRJ, Medcalf N. Regulation and development in cell-based therapeutics: The need for comparability and Implications for new business models. <u>Cell & Gene Therapy</u>, Las Vegas, USA.

Heathman TRJ, Kara B, Nienow A, Coopman K, Hewitt C. Serum-free expansion, harvest and preservation of mesenchymal stem cells from a scalable microcarrier process. <u>Cell & Gene Therapy</u>, Las Vegas, USA.

Oral Presentations

Heathman TRJ, Kara B, Nienow A, Coopman K, Hewitt C. Process development to drive the consistency of mesenchymal stem cell production from multiple donors. <u>ECI Manufacture of Cell-Based Therapies IV</u>, San Diego, USA.

Heathman TRJ, Kara B, Nienow A, Coopman K, Hewitt C. Developing a process control strategy for the manufacture of human mesenchymal stem cells. <u>FIRM Symposium</u>, Girona, Spain.

Heathman TRJ, Kara B, Nienow A, Coopman K, Hewitt C. Developing a process control strategy for the manufacture of human mesenchymal stem cells. <u>IChemE Young Researchers Meeting</u>, University of Birmingham, UK.

Heathman TRJ, Kara B, Nienow A, Coopman K, Hewitt C. Application of quality-by-design principals to the upstream manufacture of human mesenchymal stem cells. <u>Health & Life Sciences Conference</u>, Loughborough University, UK.

Selected Poster Presentations

Heathman TRJ, Kara B, Nienow A, Coopman K, Hewitt C. Development of a controlled bioreactor process to drive the consistent manufacture of human mesenchymal stem cells from multiple donors. <u>ISCT Annual Conference</u>, Las Vegas, USA.

Heathman TRJ, Glyn VAM, Picken A, Coopman K, Nienow AW, Kara B, Hewitt CJ. Expansion, harvest and cryopreservation of human mesenchymal stem cells in a serum-free microcarrier process. <u>ECI Manufacture of Cell-Based Therapies IV</u>, San Diego, USA

Heathman TRJ, Kara B, Nienow A, Coopman K, Hewitt C. Manufacture of Cell-Based Therapies: Evaluating Mesenchymal Stem Cell Input Variability. <u>ECI Manufacture of Cell-Based Therapies III</u>, San Diego, USA.

Heathman TRJ, Kara B, Nienow A, Coopman K, Hewitt C. Application of quality-by-design principals to the upstream manufacture of human mesenchymal stem cells. <u>Advanced Course in Stem Cell Manufacturing</u>, Algarve, Portugal.

Table of Contents

List of Figures

List of Tables

List of Equations

List of Abbreviations

BM-hMSC – Bone marrow-derived human mesenchymal stem cell

DAPI - 4',6-diamidino-2-phenylindole

DMEM - Dulbecco's Modified Eagle Medium

DMSO - Dimethyl sulfoxide

DNA - Deoxyribonucleic acid

DO – Dissolved oxygen

FBS – Fetal bovine serum

FDA – Food and Drug Administration

FN – Fibronectin

GAG - Glycosaminoglycan

hESC – Human embryonic stem cell

HIF - Hypoxia-inducible factor

hMSC – Human mesenchymal stem cells

HPL – Human platelet lysate

iPSC – Induced pluripotent stem cells

ISCT – International Society for Cellular Therapy

MNC – Mononuclear cell

MOA – Mechanism of action

PBS – Phosphate buffered saline

PCR – Polymerase chain reaction

PFA - Paraformaldehyde

PI - Propidium iodide

RNA - Ribonucleic acid

SCNT - Somatic cell nuclear transfer

SFM – PRIME-XV® MSC expansion serum-free medium

STR – Short tandem repeat

VVM - Gas volume flow per unit of liquid volume per minute

1 Introduction

Regenerative medicine is a growing field that aims to develop treatments to restore or maintain tissue function (Mason and Dunnill 2008; Mather *et al.* 2009) and draws upon therapies from all four pillars of healthcare: pharmaceuticals, biologics, devices and cell therapies (Mason and Manzotti 2009). Cell therapy is the therapeutic application of cells regardless of cell type or clinical indication – a platform technology (Mason *et al.* 2011) with global sales of well over £1 billion and growth predicted to follow (Mason 2013). Human mesenchymal stem cells (hMSCs) have been identified as a promising cell-based therapy to target a number of unmet clinical indications such as heart disease and stroke, due to their ease of isolation, relative immune privilege and their ability to respond to local environmental cues, to release a cascade of trophic factors to initiate repair (Caplan 2009; Caplan and Correa 2011; Pittenger *et al.* 2015).

For the majority of clinical indications, the transplantation of primary donor hMSCs may not be sufficient to achieve a therapeutic benefit and the expansion of cells *in vitro* will be required to address the shortage of functional cells available in the patient. The aim of these manufacturing processes is to significantly increase cell numbers without negatively affecting the therapeutic potential of the cell, which is known to deteriorate with time in culture (Hourd *et al.* 2008). It is possible that the commercial manufacturing lot size required to meet this need will be in the order of trillions of cells (Rowley *et al.* 2012a), though this is dependent on the dose requirements per patient and market size of each indication to be treated (Wappler *et al.* 2013). Many of the manufacturing processes for these cell-based therapies, for example Prochymal® (Osiris Therapeutics), are based on manual planar culture technology which has proven difficult to cost-effectively operate at the commercial scale. It is clear therefore, that this current manual planar culture technology will not be sufficient to meet this need and scalable manufacturing processes, amenable to closed, single-use and potentially automated technology, must be developed in order to produce safe, effective and affordable cell-based therapies.

Humans MSCs are complex biological entities that are sensitive to their environment and display intrinsic variability within a tightly regulated industry. The two major sources of variation in the product are introduced by the process input material and process conditions (Williams *et al.* 2012), which must be controlled in order to reduce product costs. A key aspect of reducing variation in the process input material will be reducing and eventually eliminating the use of fetal bovine serum (FBS) from the cell culture medium (Wappler *et al.* 2013). In addition to lot-

to-lot variability, there are further process constraints on the use of FBS such as limited supply, increasing costs, potential for pathogen transmission (Brindley *et al.* 2012) and reduced scope for process optimisation. All of these considerations mean that moving towards a serum-free process would be beneficial in the development of a scalable and consistent manufacturing process.

A lack of online process control is a key barrier for the consistent manufacture of hMSC therapies, as it has the potential to reduce the variation associated with the process conditions during manufacture. Without effective process control metrics, expansion technology will suffer when attempting to maintain product consistency and will therefore incur a higher cost of production. Effective monitoring and control systems will provide assurance of continued suitability and process capability, under the guidance of quality risk management (International Conference on Harmonisation of Technical Requirements for Registration of Pharmaceuticals for Human Use 2008). Process control systems for conventional bioreactor technology are well-understood and have the potential to be adapted for the manufacture of hMSC therapies (Butler 2005; Trummer *et al.* 2006) and subsequently reduce variation in the hMSC product.

One of the key differences between traditional cell bioprocesses to manufacture therapeutic proteins and the development of cell-based therapy manufacturing processes is that the cellular identity and functional characteristics must be maintained throughout the entire process. This means that the development of scalable and cost-effective off-the-shelf hMSC manufacturing processes must consider the harvest, downstream processing and long-term preservation of the hMSC product and its functional characteristics. The successful development of these end-to-end manufacturing processes should be systematically evaluated as a set of sequential unit-operations, rather than developing each step of the process in isolation, as changes in the upstream process will have a fundamental impact on the product quality throughout the following process steps. Accordingly, the scalable end-to-end manufacture of hMSC therapies, to consistently obtain clinically relevant cell numbers of the desired quality for commercial production, remains a key challenge for the successful development of off-the-shelf hMSC manufacturing processes.

2 Literature Review

Regenerative medicine and tissue engineering are expanding research areas in which living human cells and tissues are being developed as potential therapeutic products. Clinical applications of cell based therapies are wide ranging, but are predominantly aimed at degenerative conditions, organ failure, and tissue damage (Thomas *et al.* 2007). Of increasing interest in the field is the use of stem cells, which have demonstrated the potential to treat or even cure chronic diseases such as diabetes, cancer, cardiac disease and neurological disorders, effecting billions of people throughout the world (Mimeault and Batra 2006; Mimeault *et al.* 2007). Stem cells are defined as cells that have the ability to perpetuate themselves through self-renewal with the ability to generate mature cells of a particular tissue (Reya *et al.* 2001). It is this ability to self-perpetuate and produce large quantities of therapeutically active cells that have generated significant interest around the use of stem cells to not only treat, but potentially cure many diseases.

2.1 Historical perspective of stem cells

The transplantation of bone marrow from healthy donors to treat patients for bone degeneration dates back to the 19th century (Goujon 1869) with abysmal results and no survivors. The research slowly continued and it was not until the pioneering work of Dr Edward "Don" Thomas in the 1950s that patients began to go into remission from leukemia, for which he won the Nobel Prize for Medicine in 1990. Despite the number of bone marrow transplantations, the discovery of mammalian bone marrow stem cells was not made until 1961 at the University of Toronto by James Till and Ernest McCulloch who demonstrated that the number of marrow cells injected into a mouse produced a linear correlation with the number of colonies formed in the spleen (Till 1961; Till and McCulloch 1961). This work developed the hypothesis that each of these colonies was produced by a single cell or clone, which was verified by further experiments (Becker *et al.* 1963; Siminovitch *et al.* 1963). The impact of this research cannot be underestimated, as it was the first set of experiments to conclusively prove that bone marrow contained cells with clonogenic potential and sparked a new research area, which aimed to harness this potential and further the development of bone marrow transplantation (Tavassol.M and Crosby 1968).

Despite the realisation that bone marrow contained cells with the potential to proliferate *in vivo*, the presence of non-hematopoietic stem cells could not be confirmed until they were isolated. This critical step was taken in the late 1960s by a Russian scientist Alexander Friedenstein with colleagues at the University of Moscow. The group showed that "fibroblast-like" clonogenic cells from rat bone marrow could be isolated from hematopoietic progenitor cells by adherence to tissue culture plastic as well as *in vivo* differentiation down the osteogenic lineage *via* heterotopic transplantation (Friedens.Aj *et al.* 1966). This proved vital in their development, as it provided not only the proof that these "stromal stem cells" are a distinct population in the bone marrow but also provided a method for isolation, allowing for more detailed studies to characterise these cells. Studies soon followed to show that discrete colonies could be formed from single cells, bringing about the concept of a bone marrow colony-forming unit fibroblast (CFU-f) (Friedens.Aj *et al.* 1970; Friedens.Aj *et al.* 1974; Friedenstein *et al.* 1976), as well as the ability to form multiple skeletal tissues (bone, cartilage, adipose and fibrous tissues) *in vivo* by the progeny of a single cell which Friedenstein and Owens termed "osteogenic stem cells" (Friedenstein *et al.* 1987; Owen and Friedenstein 1988).

It was not until the work of Arnold Caplan in the early 1990s that the potential for "mesenchymal stem cells" to regenerate skeletal tissues was considered for clinic indications (Caplan 1991). This idea of a cell therapy, whereby hMSCs could be taken from a patient, expanded *ex vivo* and returned to the same patient for therapeutic benefit (autologous therapy) initiated the need for *in vitro* expansion technologies to obtain these clinically relevant cell numbers, due to the rarity of these cells *in vivo*. This shift to *in vitro* isolation and culture meant that many more research groups could investigate hMSCs using conventional cell culture techniques combined with the highlighted potential for multiple target therapeutic indications. This led to the formation of the first cell therapy company Osiris Therapeutics (NASDAQ:OSIR) in 1992 who quickly began pre-clinical development of an hMSC therapy for the treatment of Graft vs. Host disease (GvHD) along with continuing research in the field (Bruder *et al.* 1994; Wakitani *et al.* 1995; Jaiswal *et al.* 1997; Johnstone *et al.* 1998; Caplan and Dennis 2006a; Caplan 2007). It was not until 1999 that the true potential of hMSC therapies received worldwide attention after Osiris Therapeutics published a research paper in Science suggesting a broad therapeutic utility for hMSCs (Pittenger *et al.* 1999). This breakthrough coincided with the isolation of human embryonic stem cells (hESCs) by James Thomson in 1998 (Thomson *et al.* 1998) which produced significant interest around the broad therapeutic potential of stem cells. On the crest of a wave, the stem cell world changed dramatically with hMSCs being proposed for the treatment of many

indications (mirroring hESCs), far outside of the original limits proposed by Friedenstein *et al* in the 1970s.

This broad therapeutic utility is still being considered today, with cell therapy companies such as Mesoblast Ltd (Australia), Athersys Inc. (USA), Pluristem Therapeutics Inc. (Israel) and Celgene (USA) currently in clinical development with hMSCs products for the treatment of acute myocardial infarction, ischemic stroke, multiple sclerosis, limb ischemia, pulmonary disease and diabetes. Clearly there is a push to commercialise cell therapy products targeting these major indications, however, rigorous product characterisation must be considered to ensure hMSC have the functional ability to treat this broad range of clinical indications.

2.1.1 The sobering years

Reality soon hit at the turn of the millennium. The hype surrounding the potential of hMSCs to treat a vast number of clinical indications sparked by the work of Osiris Therapeutics (Pittenger *et al.* 1999) and the groundbreaking developments within embryonic stem cell research led many academic institutions to invest heavily in hMSC research. Conversely, the green shoots of industry that began to emerge in the 1990s soon disappeared as the failure rate of clinical trials, the huge cash-burn and increased bankruptcy of cell therapy companies caused investors to lose confidence in the industry and as a result, the capital value of publically traded companies plummeted from $2.5 billion in 2000 to $300 million by 2003 (Lysaght and Hazlehurst 2004).

2.1.2 Induced pluripotent stem cells

Fueled in part by the lack of government funding for embryonic stem cell research, academia was in search of an alternative cell line which would provide the benefits of a pluripotent cell line without the associated ethical constraints. Based on work by Sir John B. Gurdon at Oxford University in 1962 (Gurdon 1962), Shinya Yamanaka *et al* of Kyoto University successfully reprogrammed murine (Takahashi and Yamanaka 2006) followed by human (Takahashi *et al.* 2007) mature cells to become pluripotent using a technique known as somatic-cell nuclear transfer (SCNT) in 2006 and 2007, respectively. SCNT allows for the creation of primitive embryonic-like stem cells by combining the nuclei from a somatic cell with an enucleated egg potentially allowing for the development of patient-specific pluripotent stem cells (Byrne *et al.* 2007), termed induced pluripotent stem cells (iPS cells).

The derivation of human iPS cells in 2007 had a significant impact on the stem cell world, with the US research funding for non-embryonic cell lines more than doubling by 2009. At the same time, embryonic stem cell research experienced no significant increase in research funding even following the US government's decision to pass the Stem Cell Research Enhancement Act and reinstate federal funding for embryo-derived cells lines in 2009. It seems that as the field develops, iPS cells are increasingly taking the place of ESCs as the pluripotent cell of choice with reduced ethical constraints associated with the destruction and manipulation of human embryos.

2.1.3 Industry and early adopters

The development of iPS cells in 2006 coincided with a large number of biotechnology companies becoming involved in the commercialisation of hMSC therapies. This has led to a large jump in the number of clinical trials for hMSC therapies from 2008 with peak interest for cardiac repair, skeletal disorders and disease of the immune system (Li *et al.* 2014). The development of systems such as the Celution by Cytori Therapeutics, began to drive the commercial interest in developing autologous cell-based therapy clinical trials. These point-of-care devices allow for the isolation of a patient's own adipose derived hMSCs in the clinic, for re-implantation in the same procedure under the regulatory policy of minimal manipulation (Trainor *et al.* 2014). This has the benefit of a shorter regulatory pathway compared to manufactured products which is considered to be desirable due to shorter perceived reimbursement timelines, therefore reducing the risk to investors (O'Cearbhaill *et al.* 2014).

The minimum guidelines for defining hMSCs published in 2006 by the International Society for Cellular Therapies (ISCT) came at a time when many big companies where getting involved in hMSC therapies, a fantastic demonstration of the give and take between academia and industry that will be imperative to achieve successful commercialisation. Industry creates the need that academia is charged with fulfilling and although the argument is still active about the issue of *in vitro* characterisation of hMSCs, the ISCT went some way to addressing the issue and gave industry and academia direction on the minimum definition of what constitutes an hMSC, which will be discussed further in Section 2.2.4.

2.2 Mesenchymal stem cells

Ever since the term mesenchymal stem cell was first introduced by Arnold Caplan in 1991 (Caplan 1991), much excitement has been generated around the potential for hMSCs to treat and in some cases cure human disease. This has been mainly due to their ease of isolation as well as their ability to proliferate *ex vivo* under the appropriate culture conditions. Human MSCs have now been reportedly isolated from many tissue types such as bone marrow (Friedens.Aj *et al.* 1966; Friedens.Aj *et al.* 1970; Pittenger *et al.* 1999), adipose tissue (Zuk *et al.* 2001; Zuk *et al.* 2002), umbilical cord (Wang *et al.* 2004) and cord blood (Erices *et al.* 2000; Kogler *et al.* 2004) with the therapeutic benefit thought to be achieved *via* a combination of:

1. Modulation of the patients' immune system.
2. Release of trophic factors to stimulate native tissue regeneration.
3. Reducing the inflammatory response.

Part of the defining criteria for an hMSC is the ability to differentiate into different cell types (Figure 2.1) including osteoblasts, chondrocytes, adipocytes, neural cells and connective tissues (Pittenger *et al.* 1999; Pittenger and Martin 2004). Along with the desirable characteristics described above, hMSCs have also received a lot of attention due to their ability for donor mismatched transplantation without ectopic formation and their non-engraftment following treatment, achieving their mode of action *via* a "hit and run" mechanism (von Bahr *et al.* 2012). This introduced the possibility of off-the-shelf (allogeneic) hMSC therapies, whereby many doses can be manufactured from a single batch to treat multiple patients. This allows for increasing economies of scale and the development of a business model that is far more akin to current biopharmaceuticals, a highly attractive proposition for pharmaceutical companies.
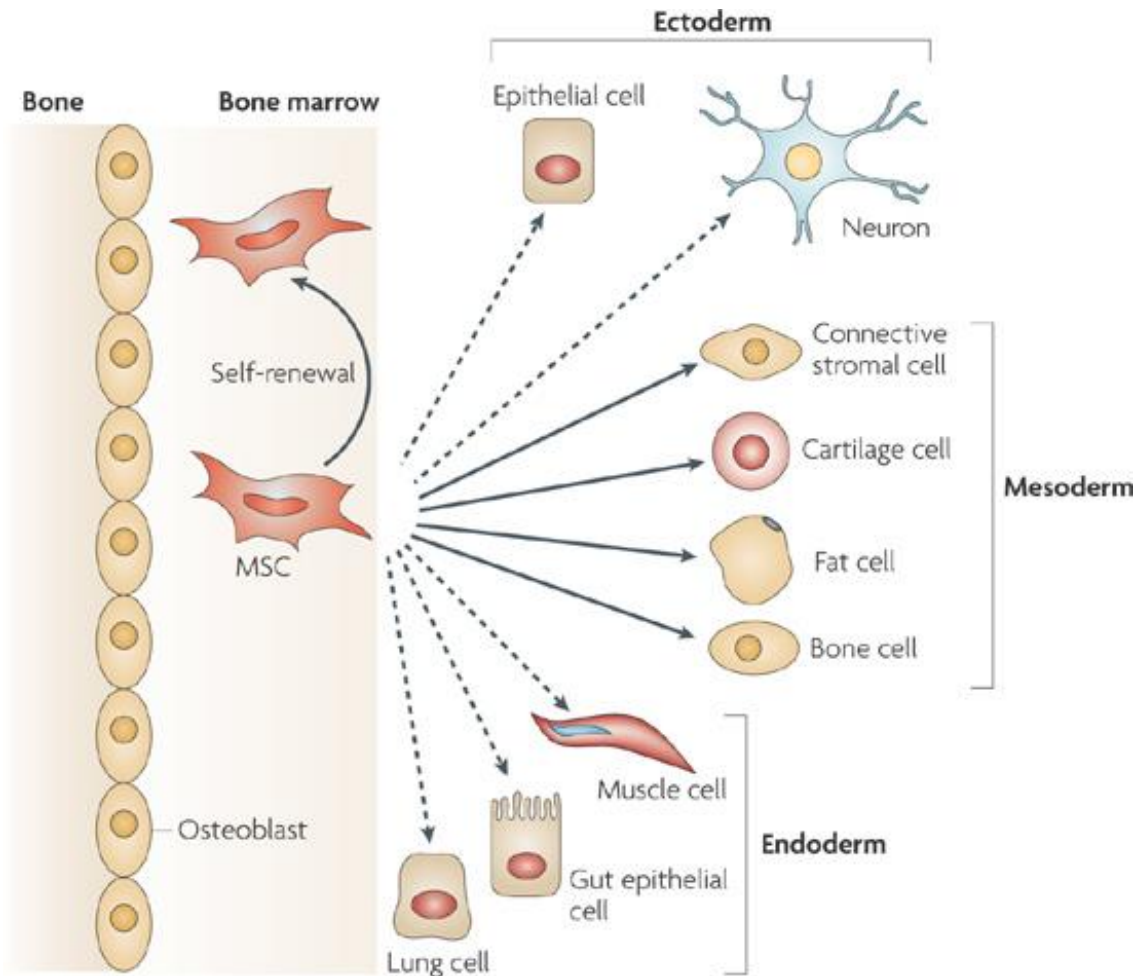
Figure 2.1. Ability of mesenchymal stem cells in the bone-marrow cavity to self-renew (curved arrow) and to differentiate (straight, solid arrows) towards the mesodermal lineage. The reported ability to trans-differentiate into cells of other lineages (ectoderm and endoderm) is shown by dashed arrows, as trans-differentiation has not been fully demonstrated *in vivo*. Taken from (Uccelli *et al.* 2008)

2.2.1 hMSC nomenclature

The term "mesenchymal stem cell" proposes a ubiquitous *in vivo* potential that has yet to be fully demonstrated (Bianco *et al.* 2008; Bianco *et al.* 2013a; Bianco *et al.* 2013b). The term mesenchymal stem cell suggests that they can be derived from skeletal and non-skeletal tissues as well as having the ability to act as a "drugstore" (Caplan and Correa 2011) delivering trophic factors (Caplan and Dennis 2006b) when infused *in vivo* to successfully treat a multitude of diseases, including those effecting non-skeletal tissues (Pittenger and Martin 2004; Caplan 2005). This multilineage potential of hMSCs has yet to be proven *in vivo*, with a limited amount

of positive human clinical data to support this broad therapeutic utility. By applying the appropriate chemical cues to cells *in vitro* one could form almost any human tissue type. A good example of this is bone morphogenetic protein (BMP) which can cause adult myocytes to form osteoblast-like cells (Yamaguchi *et al.* 1991; Katagiri *et al.* 1994), but does not demonstrate that these cells are functional. It is important, therefore, that the *in vivo* mechanism of action of hMSCs is well understood so that manufacturing processes can be developed in order to maximise these desired cell attributes.

Human MSCs represent an entirely heterogeneous population of cells, making it very difficult to standardise and compare research since there is no universal method for positively selecting a homogenous population. Although efforts are being made to do so based on $CD271^+$ cells from human bone marrow (Jones *et al.* 2006; Jones *et al.* 2010), it is unlikely that a single cell surface marker will define the entire functional hMSC population. It is important, however, that efforts are made to positively select the input material for hMSC manufacturing processes, as this will reduce variation in the product and facilitate the development of consistently efficacious therapies. That said, it is also possible that the infusion of a heterogeneous population of hMSCs is part of the therapeutic benefit, with different subpopulations of hMSCs contributing to the variety of clinical effects.

Despite the many names given to hMSCs (Table 2.1) it is clear that much more work is required to fully understand and characterise these cells, to ensure that researchers in the field do not lose sight of the fact that these cells must demonstrate their therapeutic potential *in vivo* if the full potential of hMSC therapies is to be realised.

Table 2.1. **Summary of the various names given to "hMSCs" demonstrating the uncertainty and conflict in the field as to the identity and function of these cells.**

Nomenclature	Year	Reference
Stromal Stem Cell	*1966*	(Friedens.Aj *et al.* 1966; Friedens.Aj *et al.* 1970; Friedens.Aj *et al.* 1974; Friedenstein *et al.* 1976; Owen and Friedenstein 1988)
Marrow Stromal Cell	*1975*	(Kharlamova 1975; Prockop 1997; Woodbury *et al.* 2000)
Osteogenic Stem Cell	*1987*	(Friedenstein *et al.* 1987)
Mesenchymal Progenitor Cell	*1988*	(Pensler *et al.* 1988; Johnstone *et al.* 1998)
Mesenchymal Stem Cell	*1991*	(Caplan 1991; Bruder *et al.* 1994; Pittenger *et al.* 1999; Caplan and Dennis 2006a; Caplan 2007)
Skeletal Stem Cell	*2001*	(Kuznetsov *et al.* 2001; Bianco and Robey 2004; Bianco *et al.* 2006; Bianco *et al.* 2010)
Multipotent Adult Progenitor Cell	*2001*	(Reyes and Verfaillie 2001; Jiang *et al.* 2002b; Schwartz *et al.* 2002)
Multipotent Mesenchymal Stromal Cell	*2006*	(Dominici *et al.* 2006; Le Blanc 2006; Horwitz 2008; Horwitz and Dominici 2008)
Medicinal Signaling Cell	*2010*	*(Caplan and Sorrell ; Caplan 2010)*

2.2.2 Isolation and sources

Although much of the research has focused on bone marrow derived hMSCs, they can also be found and isolated from many other organs and tissues (Table 2.2).The work of Meirelles *et al* showed hMSC-like colonies derived from various tissues, all with similar morphology and immunophenotype even after several passages (Kolf *et al.* 2007). This raises the question: is there an hMSC niche that is common to all of these tissues?

Table 2.2. Summary of isolation sources for hMSCs.

Source	Reference
Bone Marrow	(Friedens.Aj *et al.* 1966; Friedens.Aj *et al.* 1970; Pittenger *et al.* 1999; Pittenger and Martin 2004)
Adipose Tissue	(Zuk *et al.* 2001; Zuk *et al.* 2002; Wang *et al.* 2006)
Placenta	(Soncini *et al.* 2007; Brooke *et al.* 2009; Yu *et al.* 2009; Timmins *et al.* 2012)
Umbilical Cord	(Wang *et al.* 2004; Sarugaser *et al.* 2005; Hartmann *et al.* 2010; Hatlapatka *et al.* 2011)
Cord Blood	(Erices *et al.* 2000; Kogler *et al.* 2004; Hong *et al.* 2005; Moon *et al.* 2005)
Muscle	(Bosch *et al.* 2000; Qu-Petersen *et al.* 2002; Wada *et al.* 2002; Peault *et al.* 2007)
Brain	(Kang *et al.* 2010; Rowley *et al.* 2012a)
Pancreas & Liver	(Petersen *et al.* 1999; Faris *et al.* 2001; Oh *et al.* 2002; Seaberg *et al.* 2004)
Dermis	(Toma *et al.* 2001; Shih *et al.* 2005)

Studies have suggested that the hMSC niche could be of perivascular nature, due to the expression of α-smooth muscle actin (α-SMA) by all hMSCs isolated from various tissues (Meirelles *et al.* 2006) as well as $CD45^-/CD31^-/Sca-1^+/Thy-1^+$ cells found to be localised to perivascular sites (Blashki *et al.* 2006). Further supporting this theory, hMSCs have been found lining blood vessels in human bone marrow and dental pulp using markers Stro-1 and CD146 (Shi and Gronthos 2003). Some researchers have taken it so far as to say that hMSCs are pericytes, due to their ability to repair many different tissues, outside of the mesoderm lineage (Doherty and Canfield 1999; Farrington-Rock *et al.* 2004; Caplan 2008). This would explain why hMSCs seemingly have the ability to home in on sites of injury as by this theory they would be localised to the perivascular niche of a particular tissue, in a position to initiate repair. It should be noted, however, that *in vivo* experiments have not shown that hMSCs are solely located in the perivascular niche.

Part of the evidence against the "pericyte" theory is that hMSCs isolated from various tissues of the same patient differ in terms of their differentiation potential, proliferative ability and functionality. It has been found that hMSCs from the umbilical cord have a higher proliferative capacity than those isolated from both adipose tissue and bone marrow although the number of hMSCs in the latter tissues is higher (Kern *et al.* 2006). In terms of differentiation potential, it has been shown that synovium-derived hMSCs display a greater potential for chondrogenic differentiation, whilst bone marrow derived hMSCs show the greatest potential for osteogenic differentiation (Sakaguchi *et al.* 2005). This shows that hMSCs isolated from different tissues have unique properties and therefore it is a reasonable assumption that the hMSC niche is not the same in every tissue. Further to this, hMSCs seem to display a higher differentiation potential for the tissues from which they were isolated, pointing towards a unique *in vivo* niche environment that they are adapted to maintain.

2.2.3 Characterisation of hMSCs

Scalable manufacturing processes for hMSC based therapies would benefit from online measurement and control of quality parameters (James 2011). Broadly speaking, these quality parameters can be broken up into identity, potency, purity and safety which must all be optimised during the manufacturing process (Carmen *et al.* 2012b). This characterisation of hMSCs is critical within a highly regulated healthcare environment, particularly considering that the regulatory framework was designed for the manufacture of chemical products, not biological products (Mason and Dunnill 2007). Process development must be based on a foundation of detailed characterisation data, to ensure the continuity of quality necessary for Good Manufacturing Practice (GMP) compliant cell therapy manufacturing (Mason and Hoare 2006). To this end, robust tools and technologies for cell characterisation are imperative for the successful development of scalable cell therapy manufacturing processes (Bravery 2010).

2.2.3.1 Identity of hMSCs

The purpose of identity assays are to verify that the product in the master cell bank, working cell bank and final product at the manufacturing facility have the correct identity (FDA 2008b). In addition to this it is important to ensure that the manufacturing process has not had any adverse effects on the phenotype of the cell product within or between batches. This is particularly important when scaling up a process, modifying the process during development or

manufacturing at multiple sites as comparability of product identity must be demonstrated throughout. It is possible for these phenotypic changes to occur when process changes are made to reduce serum, increase culturing periods or modify harvesting protocols. There are a number of methods available to assess hMSC identity both quantitative and qualitative; however, many of these methods rely on an operator intervention and efforts should be made to develop online testing methods to facilitate automated and reproducible manufacturing controls.

By far the most common method to assess hMSC identity, used by laboratories all over the world is by morphology. This simply involves looking at the cells down a microscope to verify the typical size and shape expected of hMSCs and has been previously used as a release test, for example Carticel®, an autologous cartilage therapy produced by Genzyme® (FDA 1997). Despite morphology being a good indication of cell identity, it is heavily reliant on operator judgment which is not validated and therefore introduces process variability. Regulatory authorities will require quantitative approaches for reliable product monitoring and release testing which morphology cannot provide alone.

One method which has been widely used for some time in biological research to assess the cell surface phenotype is flow cytometry. Flow cytometry is a high-throughput analytical technique that can be used, amongst other applications, to study protein expression properties of a cell using fluorescently labeled monoclonal antibodies. This provides a qualitative method for characterising the hMSC population based on key positive and negative markers and has become a routine method for identifying stem cell populations from many tissue sources such as the eye and peripheral blood (Adams *et al.* 2009; Tarnok *et al.* 2010). Whilst these single marker methods are useful, they do not often take into account the expression of multiple surface markers simultaneously which provides a far better understanding of the target hMSC population by the co-positive (> 95%) and co-negative (< 5%) expression of surface antigens (Preffer and Dombkowski 2009; Chan *et al.* 2014a). Multiparameter (also known as multicolour) flow cytometry has been applied to clinical diagnostics and immunology, providing the high-resolution information needed to identify subtle phenotypic differences with statistical robustness (Peters and Ansari 2011). Despite the potential of flow cytometry to deliver semi-quantitative product data, there are a number of issues that mean that this information is not a definitive representation of identity. Flow cytometry requires the use of manufactured antibodies and in some cases fixing agents such as paraformaldehyde which mean that the measured cells cannot always be used for clinical applications. These types of destructive

measurement methods can only be applied to batch testing at the end of the process and are unlikely to be used for real-time process monitoring as they require a level of manual operator intervention to set up gating strategies.

Polymerase chain reaction or PCR, is a method to amplify just a few copies of a piece of DNA or RNA over several orders of magnitude by successive heating and cooling cycles (Saiki *et al.* 1985; Saiki *et al.* 1988; Mullis *et al.* 1992). Briefly, short DNA fragments containing sequences complementary to a known region (or primers) are used to target a gene of interest. DNA polymerase is then used to assemble a new DNA strand based on the targeted primer region and the process repeated throughout the thermal cycles to initiate a chain reaction to exponentially amplify the desired gene sequence (Kubista *et al.* 2006). This genetic profiling of the desired hMSC population can be used to characterise the identity of a cell therapy product by obtaining a detailed knowledge of the cell gene expression, indicating the cell's potential for protein production (Stroncek *et al.* 2009). Quantitative PCR (qPCR) can be used to collect data in "real time" by attaching a fluorescent marker to each new strand of DNA, which can be monitored *via* illumination during the thermal cycling (Heid *et al.* 1996; Livak and Schmittgen 2001). The use of PCR is reliant on a well-defined reference cell line to compare the genes of interest against or alternatively can be used to monitor the identity of a cell line throughout a manufacturing process to assess whether the process is causing changes to the cell identity. This can be achieved by developing a cell line and indication specific genetic panel or array, to target a number of key genes that will be important to the manufactured product and to ensure these genes are not affected by the process itself, in an economic and time efficient manner (Carmen *et al.* 2012b).

Attempts have been made by the International Society for Cellular Therapies (ISCT) to standardise the defined minimum identity of hMSCs (Dominici *et al.* 2006; Rasini *et al.* 2013) and have focused on three key identity assays:

1. Human MSCs must adhere to and proliferate on tissue culture plastic.
2. Human MSCs must express CD105, CD73 and CD90, and lack expression of CD45, CD34, CD14 or CD11b, CD79α or CD19 and HLA-DR surface markers.
3. Human MSCs must demonstrate differentiation into osteoblasts, adipocytes and chondroblasts *in vitro*.

In addition to this, hMSCs must retain the desired karyotype throughout culture, to ensure genomic integrity of the cell for both research and therapeutic applications. Although this is a more important consideration for pluripotent cells such as embryonic stem cells (Lefort *et al.* 2009), it is still important to ensure that hMSCs retain genetic stability during manufacture. Despite the number of methods currently available to assess the identity of hMSCs, there is still no consensus on their true *in vitro* identity. It is imperative that reliable cell therapy manufacturing processes are developed using fully characterised hMSC lines to first of all ensure processes are consistent but also to demonstrate that processes are comparable. It is important that hMSC characterisation panels take into account the target clinical indication, particularly for genetic assays, since the desired genetic expression will largely depend on the therapeutic use of the hMSC. Despite the introduction of this minimum identity criteria for hMSCs, it is clear that more rigorous characterisation is required to assess the quality of the product, based on the *in vivo* therapeutic mechanism of action (MOA).

2.2.3.2 Potency of hMSCs

Described by the US FDA as an appropriate measure of biological function, potency provides the basis for the *in vitro* measure of relative efficacy for a cell therapy product (Burger and Bravery 2011; FDA 2011b). Potency assays should evaluate this biological function for a specific clinical indication, which is important for cell therapy products that are likely to use one manufacturing platform for multiple clinical indications, a strategy adopted by almost all companies developing hMSC-based products.

Key to developing these potency assays is the cell therapy putative MOA, which identifies how the cell therapy delivers its therapeutic benefit, either by mesoderm differentiation potential (Caplan and Correa 2011), secretion of trophic factors (Caplan and Dennis 2006b), or immunomodulatory activity (Aggarwal and Pittenger 2005) but more likely a combination of all three as well as additional undefined mechanisms. Defining the indication specific MOA for hMSCs will have far reaching implications in the development of potency assays (FDA 2011b) and must be addressed to avoid "a race to the bottom" where the cheapest cell therapies will prevail, owing to the lack of product quality assessment for competing treatments.

Ever since Arnold Caplan published research outlining the multilineage potential of hMSCs in 1991 (Caplan 1991) it was envisaged that hMSC potency would be defined by differentiation

potential (Pittenger *et al.* 1999). The proposed hMSC MOA was by engraftment and differentiation into the target tissue type, most commonly osteoblasts within damaged bone as demonstrated by Prockop *et al (1995)* and colleagues in mice (Pereira *et al.* 1995; Pereira *et al.* 1998) and subsequently in humans by Horwitz *et al* (Horwitz *et al.* 1999; Horwitz *et al.* 2002). This theory of hMSCs as progenitor cells solely for bone formation has faded, as pre-clinical animal models of hMSC therapies have shown therapeutic potential for disorders outside of the bone *niche*, such as myocardial infarction and neuronal diseases although this is contested by some (Herzog *et al.* 2003). In these clinical models, the documented engraftment of donor cells at the presumed site of activity was low or even completely absent (Horwitz and Dominici 2008). This mounting evidence that the therapeutic effect of hMSCs was not mediated by engraftment and terminal differentiation was further demonstrated by Le Blanc *et al* in 2012. Their group examined autopsy material from 18 patients who had received HLA-mismatched hMSCs and found no ectopic tissue formation as well as only detecting donor DNA in the lungs, lymph nodes and intestine at levels from 1/100 to <1/1000 (von Bahr *et al.* 2012).

Despite this low level of engraftment, a substantial clinical benefit is seen from animal models and clinical trials resulting from the infusion of hMSCs, which begs the question, how are the hMSCs able to deliver clinical benefit without engraftment into native tissue? The idea that hMSCs act as trophic mediators to produce and deliver biologically active molecules to aid regeneration was introduced by Arnold Caplan in the early 2000s (Caplan and Dennis 2006b; Caplan 2009; Caplan and Correa 2011). It should be noted that this ability to secrete trophic mediators does not preclude the notion that hMSCs can act as progenitors in the local bone environment to induce regeneration *via* differentiation, but is part of the multitude of mechanisms in which hMSCs elicit a therapeutic benefit.

Due to their native location in the bone marrow niche, hMSCs are able to secrete biochemical mediators from the lympho-hematopoietic system, such as stromal derived factor-1 (SDF-1 or CXCL12) (Ponomaryov *et al.* 2000), which initiates hematopoietic stem cells to home to the bone marrow niche (Peled *et al.* 1999). In terms of leukocyte mediated response, hMSCs are able to secrete interleukin (IL)-6, IL-7, IL-8, IL-11, IL-12, IL-14, IL-15, macrophage-colony-stimulating factor (M-CSF), Flt-3 ligand and stem cell factor (SCF) (Deans and Moseley 2000). Human MSCs can also be stimulated by these factors to produce alternative chemokines, for example stimulation with IL-1α induces hMSCs to express further IL-1α, leukemia inhibitory factor (LIF), granulocyte-colony-stimulating factor (G-CSF) and granulocyte-macrophage colony-stimulating

factor (GM-CSF) (Majumdar *et al.* 1998; Deans and Moseley 2000). Human MSCs have also been shown to secrete chemokine ligands, CCL2, CCL4, CCL5, CCL20, CX_3CL1 and CXCL8 (Honczarenko *et al.* 2006).

Much of the excitement around the use of hMSCs as a cell therapy has been due to their apparent ability to secrete biochemical mediators unrelated to the bone marrow niche, raising their potential to treat diseases from outside of their native environment. Subsets of hMSCs have been shown to secrete brain-derived neurotropic factor (BDFN), nerve growth factor (β-NGF) (Crigler *et al.* 2006) and Nestin (Tondreau *et al.* 2004), suggesting potential to target neurological disorders. Further to this, hMSCs have been shown to induce angiogenesis *via* the secretion of vascular endothelial growth factor (VEGF) (Wang *et al.* 2006; Zisa *et al.* 2009) and basic fibroblast growth factor (bFGF) (Kinnaird *et al.* 2004), demonstrating the potential for hMSC therapies to treat cardiac and ischemic disorders. Although much of this work has been completed *in vitro* and it can be argued that this does not demonstrate the *in vivo* potential of hMSCs, however, clinical trials are well underway to assess the ability of hMSCs to treat disorders outside of the bone marrow niche with some promising early results. Considering that hMSCs represent a heterogeneous population of cells from the same source (Tremain *et al.* 2001; Wagner *et al.* 2006) and also show heterogeneity between various isolation sources (Wagner *et al.* 2005; Kern *et al.* 2006), one can assume that the local stem cell environment plays a key role in the biochemical activity of hMSCs.

A promising method for quantitatively determining hMSC potency is the colony-forming unit fibroblast (CFU-f). CFU-fs provide a measure of the biological activity of an individual cell, or clone and have been previously used in the quality assessment of hematopoietic cell-based products (Yang *et al.* 2005; Kasten *et al.* 2008). A potential drawback with the use of CFU-fs is that they require operator input in the form of colony counting and assessment, although this can be alleviated *via* bioluminescence which has been employed to quantify the number of colonies without operator intervention (Rich and Hall 2005). Further to this, it takes weeks of culture to assess whether hMSC have retained this potential and is therefore not amenable to online monitoring and feedback. Applying this technique to hMSCs may however provide a relatively inexpensive method for assessing biological activity that would require little material from the final product.

2.2.3.3 Purity of hMSCs

Purity tests ensure that cell therapy products are free from unwanted material, such as endotoxins, unwanted cell types, residual proteins, mycoplasma or any other agents used in the manufacturing process (FDA 1997). For cell therapy applications, where the cell is the product there is potential for unwanted cell types to be present in the final product. This presents an issue when the final product in itself is a heterogeneous population of cells, generating the need for cell screening tools to positively select or negatively exclude desired and undesired cell types respectively. This becomes particularly important during the manufacture of pluripotent cell types which have the potential to differentiate into many undesired cell types given the appropriate chemical and mechanical cues. The particulate content in the final product must also be sufficiently reduced to ensure the purity of the hMSC therapy. Considering that hMSCs require a plastic surface to adhere to and proliferate on, manufacturing processes must minimise the level of plastic particulates in the final product, which will be particularly important for agitated processes, where the formation of such particulates is perceived to be higher than in static culture.

One of the challenges associated with the manufacture of hMSC is in the use of animal products, typically in the form of foetal bovine serum (FBS) and trypsin which are still common within cell therapy manufacture (Brandenberger *et al.* 2011). The FDA Code of Regulations states that the animal serum levels must be reduced to below 1 ppm in the final formulation of a medicinal product (FDA 2002). There are no stated guidelines for the allowable levels of trypsin in product formulations (Carmen *et al.* 2012b), however, there is a push to eliminate the use of all xeno-based products in cell therapy manufacture. As these purity release assays are developed, it is probable that multiplexed ELISA assays will be used to streamline the product release testing process (Ellington *et al.* 2010).

2.2.3.4 Safety of hMSCs

Product safety is of paramount importance in the successful development of a cell-based therapy as negative safety data will impact patient care and has been given the highest priority by regulatory bodies (FDA 1997). It is likely that sterility will need to be tested during the manufacturing process and as part of the product release testing panel for bacterial, viral and mycoplasma agents (Rayment and Williams 2010; Goldring *et al.* 2011). A further key aspect for ensuring product safety is in mitigating the risk of the cell therapy product containing unwanted

cell types, which could be tumorigenic, if the manufacturing process contains a differentiation step (Anisimov *et al.* 2005; Ben-David and Benvenisty 2011). It is likely that characterisation techniques such as qPCR and flow cytometry, in combination, will play a role in ensuring that the product does not contain those cell types that have the potential to form tumors *in vivo* (Lavon *et al.* 2004; Noaksson *et al.* 2005; Adewumi *et al.* 2007).

In order to minimise the risk of safety implications in cell therapy products, closed processes (including supply chain materials and expansion) must be used and in some cases, disposable systems may be beneficial from a cost and risk basis. It is important to note that release tests to confirm product sterility can take up to 14 days to complete (FDA 2010), which is problematic for cell therapy products designed to undergo short term preservation. An accepted way to overcome this can be seen with the former cell product Provenge®, an autologous treatment for prostate cancer from Dendreon® (USA) which administers the cell product prior to the results of the sterility panel (FDA 1998). Finally, it is important that cell therapy products are tested for karyotypic abnormalities to ensure genetic stability of the product (Muntion *et al.* 2012), although it is not known how critical these abnormalities are *in vivo* (Sun *et al.* 2008; Carpenter *et al.* 2009; Hwang *et al.* 2013; Ruan *et al.* 2014).

Traditionally, it was thought that hMSCs would present safety issues with respect to immunogenicity if cells from one patient were infused into another, in the form of an allogeneic therapy (Pittenger and Martin 2004). It has been shown, however, that hMSCs display relative 'immune-privilege', meaning that they do not initiate a full immune reaction in the same way as donated tissues and organs, with little major histocompatibility complex (MHC) class I molecules and no MHC II expression (Uccelli *et al.* 2006). Although there is growing evidence for this relative immune-privilege, hMSCs have not yet demonstrated absolute immune-privilege. Allogeneic hMSCs have shown donor-specific cellular immune responses *in vivo* by measurable anti-donor B cell mediated responses (Beggs *et al.* 2006; Isakova *et al.* 2010). This means that there is potential for minor immune response to allogeneic hMSC infusion and it is likely that it is dependent on hMSC delivery route (Isakova *et al.* 2014), with systemic infusion producing an increased allograft reaction.

In contrast, hMSCs have demonstrated immunosuppressive potential *via* the inhibition of T cell proliferation (Di Nicola *et al.* 2002; Tse *et al.* 2003; Klyushnenkova *et al.* 2005). This ability will also be effective for the treatment of diseases causing an immune overreaction by modulating

the leukocyte population. This ability not only applies to hMSCs in their undifferentiated state, but has also been shown by hMSCs differentiated *in vitro*, which show that these differentiated cells do not elicit an allo-reactive lymphocyte proliferative response, supporting transplant of hMSCs between HLA-incompatible patients (Le Blanc *et al.* 2003). This relative immune-privilege is a large part of the reason that hMSCs have gained so much attention as a candidate for cellular therapies as reduction in patient immune response allows for biotechnology companies to pursue the 'off-the-shelf' business model, which is akin to current bio-pharmaceutical products.

2.2.4 Serum-free expansion of hMSCs

As stated previously, the levels of animal serum must be reduced to below 1 ppm in the final formulation of a medicinal product and therefore eliminating it from the hMSCs manufacturing process will be highly desirable. In addition to this, there is a large amount of lot-to-lot variability between batches of animal serum, as well as a limited supply (Brindley *et al.* 2012), spiraling cost, potential for pathogen transmission, increased risk of recipient immune reaction (Spees *et al.* 2004) and reduced scope for process optimisation. Furthermore, FBS has been shown to contain immunogenic contaminants which have the potential to negatively impact post-transplant clinical results (Heiskanen *et al.* 2007), potentially increasing the regulatory burden placed upon these products. All of these considerations mean that moving towards a serum-free process would be beneficial in achieving scalable, tunable and consistent hMSC manufacturing processes. In addition, hMSCs grown in a serum-free medium have demonstrated increased proliferation rates, up-regulation of genes important to hMSC function and down-regulation of genes involved in the production of proinflammatory cytokines (Crapnell *et al.* 2013). As such, there has been a trend towards reducing or eliminating serum from the process (Jung *et al.* 2012) and even towards developing completely serum and xeno-free processes (Dos Santos *et al.* 2011b).

2.3 Clinical trial landscape for cell-based therapy

A search of the clinical trial database yielded a total of 1342 active clinical trials that were judged to be true cell-based therapies from the BSI definition. The vast majority of these cell-based therapies are using hematopoietic cells (n=444), hMSCs (n=382), lymphocytes (n=253) and dendritic cells (n=91) (Figure 2.2). The use of tissue specific cells was less prevalent, representing 114 of current cell-based therapy activity with a mixture of cell types such as chondrocytes (n=12), endothelial cells (n=15), fibroblasts (n=14), hepatocytes (n=16), islet cells (n=13) and neural cells (n=13).
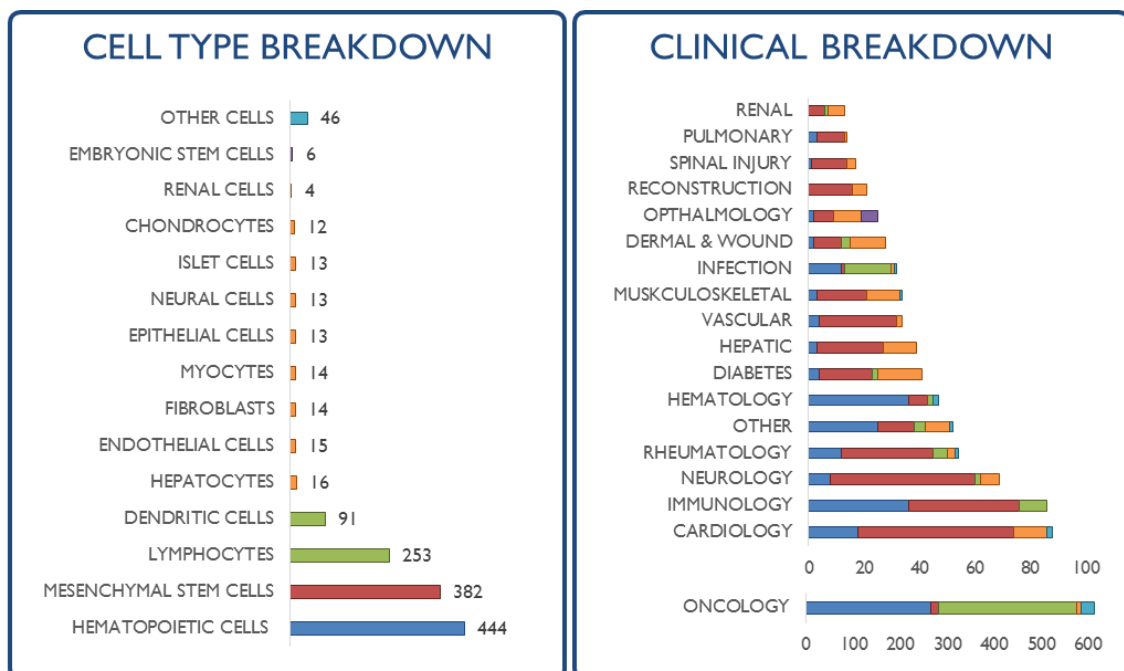
Figure 2.2. Number of currently active clinical trials by cell type and target clinical indication. Displaying broader cell type categories of Hematopoietic (Blue), Mesenchymal Stem Cells (Red), Immune Cells (Green), Tissue specific cells (Orange), Embryonic stem cells (Purple) and Other (Aqua). *From (Heathman et al. 2015b)*

Figure 2.3 shows the diversity of cell isolation sources represented from hematopoietic and hMSC trials. The rapid increase in hMSC activity is clear, with 382 clinical trials in progress from a number of isolation sources most notably 237 of which are from the bone marrow, 61 from

umbilical cord and 59 from adipose tissue. The use of pluripotent stem cell-derived products was rare, though there are six clinical trials involving embryonic stem cells. Interestingly, all six involve differentiation into retinal pigment epithelium cells and were initiated by industry: CHA Bio & Diostech in Korea (n=2), Advanced Cell Technology (n=3) and Pfizer in the UK (in collaboration with University College London).
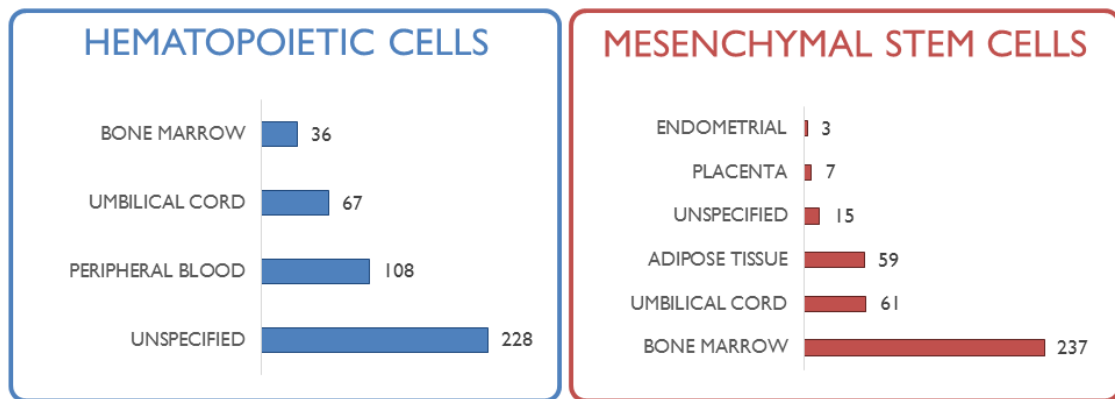
Figure 2.3. Current active cell therapy clinical trials showing the breakdown of the hematopoietic and mesenchymal stem cell groups the by cell isolation source. *From (Heathman et al. 2015b)*

2.3.1 Disease indications targeted by cell-based therapy clinical trials

It is clear that the most common target for cell-based therapy clinical trials is oncology, which represents 46% of all cell-based therapy clinical trials identified (Figure 2.2), due to the use of traditional blood cell and immune cell-based therapies for the treatment of various cancers. Aside from these traditional cell-based therapies, cardiology was the second largest clinical target with 88 clinical trials (Figure 2.2), 51 of which were using hMSCs (Figure 2.4). Immunological disorders remain a key target for cell-based therapies (Figure 2.5) with disorders such as graft vs. host disease (n=33), immune modulation following transplantation (n=17) and Crohn's disease (n=16), as well as rheumatic disorders osteoarthritis (n=15), lupus erythematosus (n=9) and rheumatoid arthritis (n=6) currently in Phase 1 and above. Neurological indications also represented a significant target for novel cell-based therapies for indications such as multiple sclerosis, stroke and motor neuron disease (Figure 2.5). Figure 2.4

shows the broad therapeutic utility adopted for hMSCs, with clinical indications covering all 18 clinical categories with the majority within cardiovascular, neurological and autoimmune indications predominantly in Phase 1. Likewise, tissue specific cells cover the majority of clinical indication categories, due to the diversity of cell populations within this category.
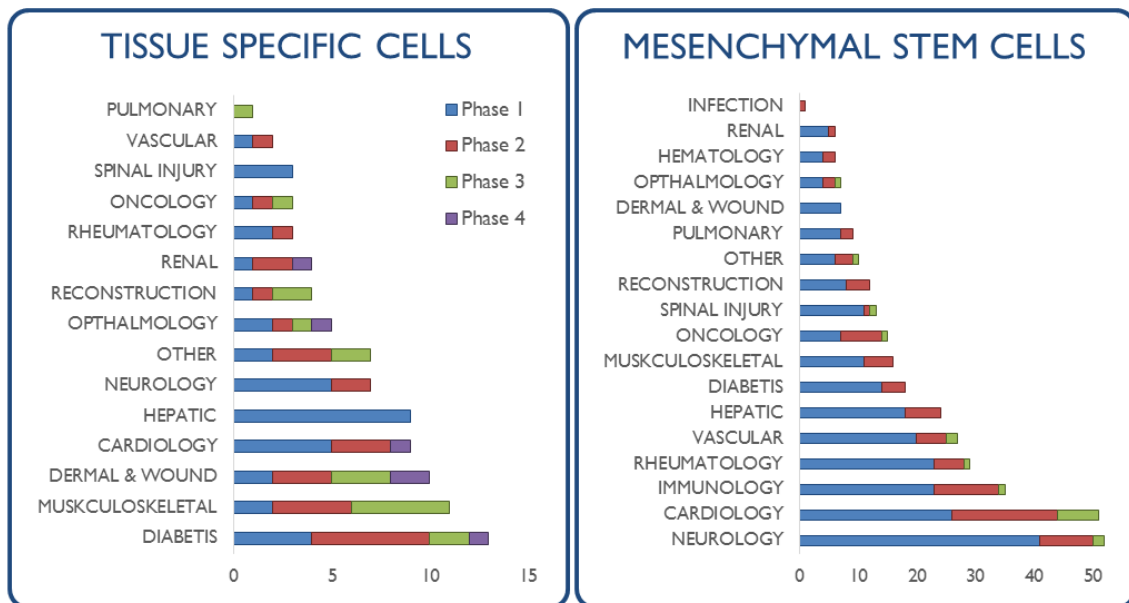
Figure 2.4. Current active cell therapy clinical trials involving tissue specific cells (see Figure 2.2) and mesenchymal stem cells showing target clinical indication and current clinical trial phase. *From (Heathman et al. 2015b)*
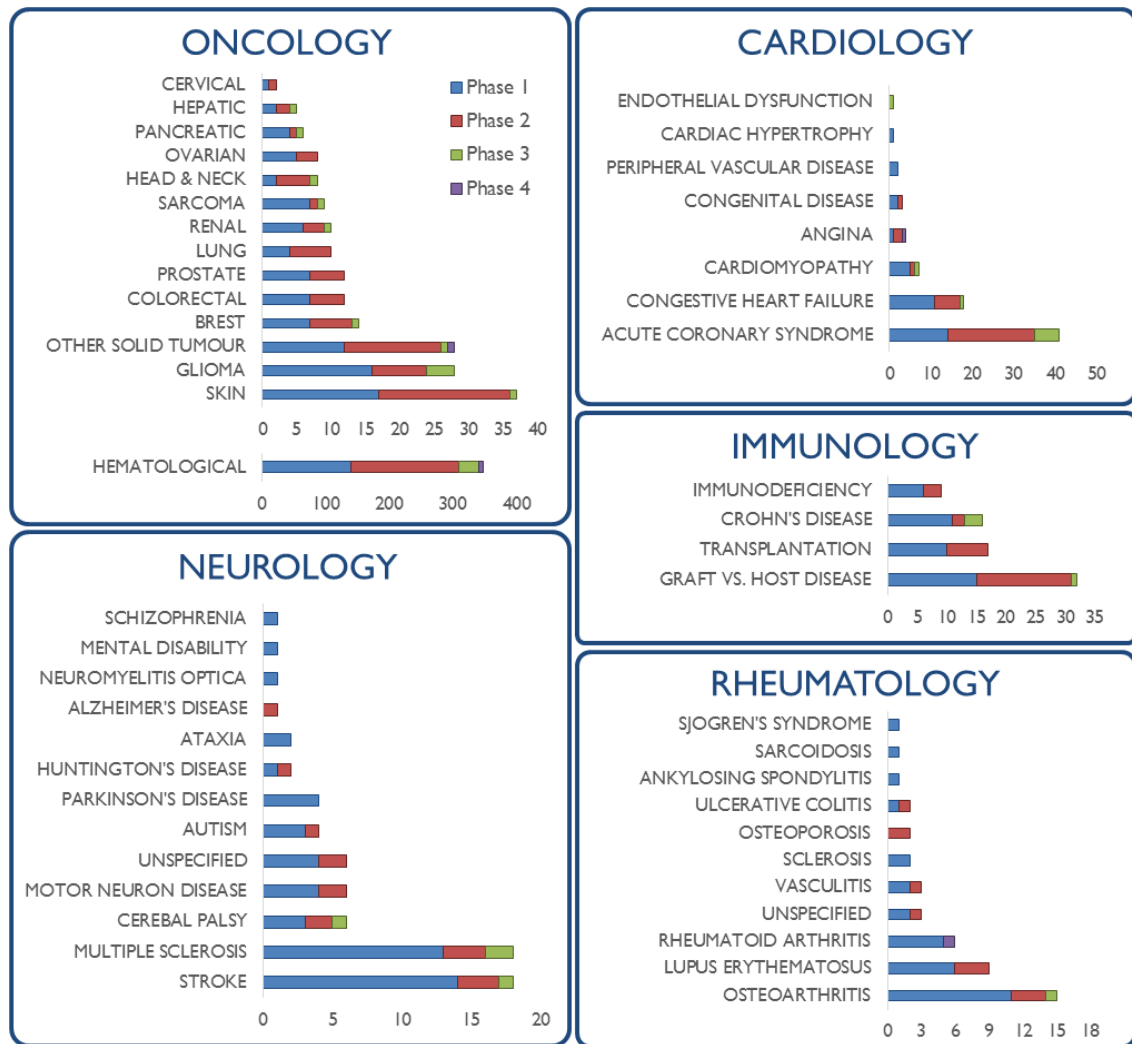
Figure 2.5. Breakdown of the most prevalent clinical targets from cell therapy clinical trials by target disease and clinical trial phase. *From (Heathman et al. 2015b)*

2.3.2 Cell-based therapy clinical trial phase

Considering the relative age of the industry, it is unsurprising that by January 2014 the majority of cell-based therapy clinical trials were in Phase 1, with 232 hMSC, 146 lymphocyte and 118 hematopoietic cell clinical trials (Figure 2.6). There was however, an increase in hematopoietic cell clinical trials moving to Phase 2 with 187 compared to 116 in Phase 1. There were also four tissue specific cell-based clinical trials that reached post-market surveillance, or Phase 4 (Figure 2.6). Most notable of these was the use of dermal fibroblasts for wound repair from Arita Medical (ReCell™) and Organogenesis (Apligraf™) as well as cell-based therapies to treat type 2 diabetes and for cornea replacement. Figure 2.5 shows the major clinical categories by specific disease targets, with the vast majority targeting hematological malignancies within oncology,

with equal weighting in Phase 1 and Phase 2. Cardiovascular indications also had a similar number of clinical trials in Phase 1 and Phase 2, with 10 clinical trials in Phase 3 and above. Human MSC clinical trials were also well represented in Phase 2 (n=88) and were even seeing progression to Phase 3 (Figure 2.6). Neurology and rheumatology based indications that involve hMSCs were mostly in Phase 1 (Figure 2.7), however clinical development using bone marrow-derived hMSCs to treat acute coronary syndrome, Crohn's disease and graft vs. host disease were progressing into Phase 2 and above, with clinical trials taking place all over the world.

	Phase 1	Phase 2	Phase 3	Phase 4
■ HEMATOPOIETIC CELLS	118	187	39	10
■ MESENCHYMAL STEM CELLS	232	88	19	0
■ LYMPHOCYTES	146	72	7	2
■ DENDRITIC CELLS	43	30	3	0
■ HEPATOCYTES	9	3	0	0
■ ENDOTHELIAL CELLS	9	3	0	0
■ FIBROBLASTS	3	3	3	2
■ MYOCYTES	5	4	2	0
■ EPITHELIAL CELLS	2	2	2	1
■ NEURAL CELLS	10	2	0	0
■ ISLET CELLS	3	6	2	0
■ CHONDROCYTES	2	3	4	0
■ RENAL CELLS	1	0	0	1
■ EMBRYONIC STEM CELLS	6	0	0	0
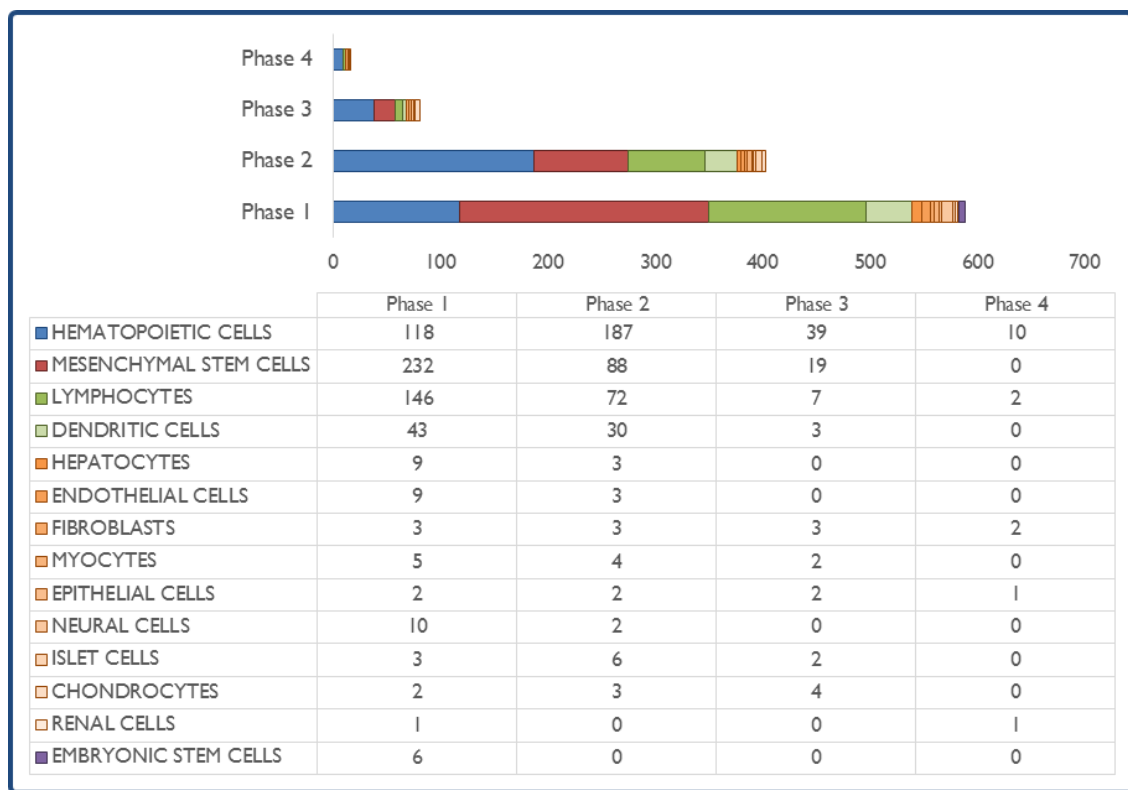
Figure 2.6. Breakdown of current active cell therapy clinical trials by cell group and trial phase. *From (Heathman et al. 2015b)*

2.3.3 Clinical translation of mesenchymal stem cell-based therapies

It is clear that outside of the traditional cell-based therapies using blood and immune cells to treat cancer, the majority of novel clinical trial activity was involving hMSCs. The rebranding of hMSCs has been used to generate intellectual property by defining a specific set of characterization criteria for the cell, for example, Athersys Inc. are developing a product termed

MultiStem[TM], a Multipotent Adult Progenitor Cell (MAPC) therapy which has been patented under this name (Jiang *et al.* 2002a; Breyer *et al.* 2006).
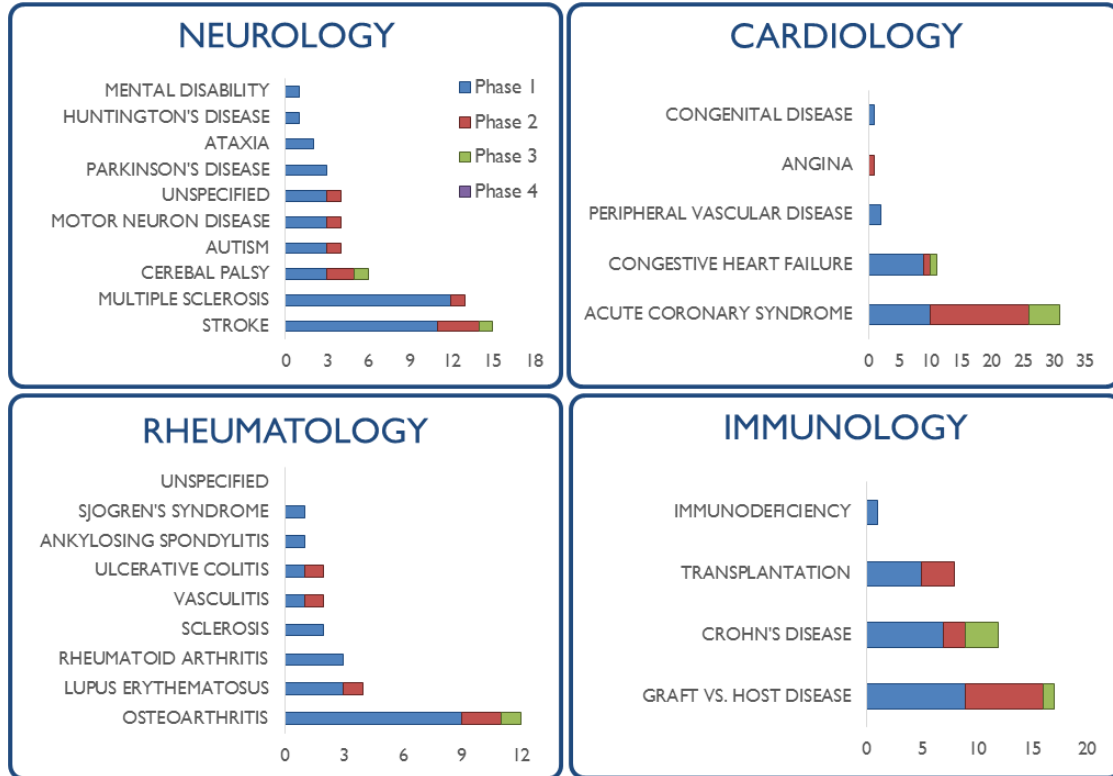
Figure 2.7. Current active cell therapy clinical trials involving mesenchymal stem cells showing target clinical indications by target disease and trial phase. *From (Heathman et al. 2015b)*

2.3.4 Case study: product manufacture during Phase 1 clinical trial

Since the discovery of embryonic stem cells in 1998 (Thomson *et al.* 1998), pluripotent stem cells have been considered a promising source of allogeneic stem cells for regenerative therapies. In 2010 Geron Co. went into Phase 1 clinical trials with an allogeneic hESC derived oligodendrocyte progenitor product for the treatment of spinal cord injury. Despite no adverse safety issues with this hESC derived therapy, Geron Co. halted the clinical trial citing financial and regulatory issues (Atala 2012). Currently, all of the clinical trials involving hESCs are targeting ophthalmology related indications, in Stargardt's macular dystrophy and dry age-related macular degeneration. Advanced Cell Technologies are sponsoring three of these clinical trials in the UK and USA, treating these disorders with hESC-derived retinal pigment epithelium (RPE) cells. One of the key challenges in the manufacture of a pluripotent product is in the

differentiation of the hESC into the therapeutically active cell, which can dramatically impact product yield. The Advanced Cell Technologies RPE product is manufactured from the GMP-grade MA09 hESC line, cultured on mitomycin-inactivated murine embryonic fibroblasts for three passages. Following the formation of embryoid bodies, pigmented RPE patches are isolated and purified (Lu *et al.* 2009), before further expansion and cryopreservation for clinical use. Product characterisation takes place in-process and post-cryopreservation, in the form of pathogen testing, karyotype analysis and purity (Schwartz *et al.* 2012). Much of this manufacturing process is labor-intensive and requires operator intervention, which may not be amenable to automated and scalable manufacture. Therefore, despite the positive safety data from these ESC clinical trials (Atala 2012), it is clear that there are many manufacturing challenges that must be overcome before these therapies can be translated through clinical trial and into commercial production.

2.3.5 Case study: manufacture for commercial production

It is clear from the clinical trial results in Figure 2.2, that the most prevalent clinical category for cell based therapies is oncology, with immune cells contributing to around half of these cell-based therapies. Sipuleucel-T is an autologous active cell-based immunotherapy product designed to stimulate an immune response against prostate cancer from Dendreon Corporation (Seattle, USA) (Small *et al.* 2006). In 2010, Sipuleucel-T (Provenge®) became the first FDA approved autologous cell-based therapy, providing a scale-out service based approach to product manufacture and delivery. Patient cells are collected *via* leukapheresis (Kantoff *et al.* 2010) and cold shipped to a manufacturing site, where the cells are manipulated under GMP conditions to isolate and activate the target immune cells. The activated cell-based immune therapy is then cold shipped back to the patient to be re-infused, which is repeated three times to deliver the full therapeutic dose. Dendreon Corporation (USA) operates patient logistics from a central location, with distributed manufacturing taking place at multiple sites across the USA. This product handling and manipulation is largely manual and has led to high product operating costs, increasing the product cost of goods and therefore creating a high reimbursement price, which is ~$100,000 per patient. Efforts have been made to reduce the cost of goods by implementing automated process steps, with the intention of reducing these high operating costs. This case study highlights the importance of considering functionally closed and automated scale out processes early in clinical development as this will reduce the overall cost of goods during commercial production (Hampson 2014).

A proposed clinical development pathway would be to produce Phase 1 material in a manual, semi-closed process which could then be transferred to a scalable, closed and automated manufacturing process following the success of the initial clinical trials. This model would allow for reduced capital investment to evaluate the product at Phase 1 but then would transfer the process in a timely manner, ensuring a scalable and cost effective product supply for late stage clinical development and commercial supply. Considering the high cost and increased risk of validating sterilization cycles, it is likely that these closed-processes will utilize disposable technology, mimicking current therapeutic protein process development (Kuczewski *et al.* 2011).

2.3.6 Progress from clinical development to product manufacture

Industry progression towards the successful manufacture of cell-based therapies is evident by international cooperation on the formation of global reference 'ruler' standards and protocols to facilitate manufacturing comparability of hMSCs (Viswanathan *et al.* 2014). This will facilitate the development of consistent manufacturing processes across multiple sites and allow for a method to define each cell line. Defining desirable product characteristics is critical and will form the basis of release tests as well as setting the tolerances on the process, allowing for systematic product development and optimisation.

A further sign that the commercial market for hMSC application is increasing in competiveness is the drive by companies such as Athersys Inc. (USA) and Mesoblast Ltd (Australia) to clearly differentiate their product and its production process from "generic" hMSCs. This phenomenon parallels the clinical development of MACI™ (by Genzyme) and CCI™ (by TiGenix) where companies actively sought to distance their products from legacy clinical data on the use of Autologous Chondrocyte Implantation (ACI), which was inconclusive in demonstrating cost effectiveness (Hourd *et al.* 2008). This approach to cell-based product development is largely driven by a fundamental lack of understanding of the product's mechanism of action, as companies must differentiate their product to avoid a race to the bottom, whereby a lower cost therapy has an increased chance of reimbursement. Without the knowledge of the how these cell-based therapies elicit therapeutic benefit, manufacturing processes cannot be optimised to maximize this function and will inevitably be surpassed by lower cost therapies. Given the importance of regulation on the production of cell-based therapies, it is perhaps unsurprising that in the race to successfully commercialize cell products, companies have begun to raise the

regulatory bar as a tactic to disrupt competitor companies. This action has the potential to hinder smaller companies who do not have the financial resource to comply with this increasing regulatory burden.

A further hallmark of the commercial progress of hMSC therapies is the move towards developing automated processes as well as the implementation of functionally closed manufacturing systems and consideration of the associated logistics, supply chain and cost of goods (Hampson *et al.* 2008). Significant UK government investment in the form of the Cell Therapy Catapult has been tasked with 'de-risking' cell-based therapy development for industry by providing a 'centre of excellence' to bridge the current translation gap in the industry (Mason and Manzotti 2010). Outside of the UK, additional institutes have been established to provide resources, in Canada (Centre for Commercialization of Regenerative Medicine) and the USA (California Institute for Regenerative Medicine and the National Institutes of Health) to facilitate this translational process. Despite this progress, there remains a requirement for a better understanding of potential manufacturing platforms and how they can be best utilized for cell-based therapy production.

2.3.7 Expansion technologies to achieve clinical scale manufacture

With cell-based therapies moving towards commercialization and multiple clinical trials in late stage development, it is clear that selecting suitable manufacturing technologies is becoming increasingly important. It is imperative that potential pitfalls in developing scalable manufacturing methods are identified at an early stage and strategies are implemented that can streamline this development pathway. A key consideration for streamlining this pathway is the tradeoff between clean room space and on-going commercial supply as patient numbers increase from clinical development to commercial production. For an autologous therapy if you were treating, for example, 100 patients in a typical two week process for a Phase 3 clinical trial, you would likely require four clean room facilities in order to separate each patient lot. This is assuming that the process is not entirely closed and therefore each lot must be segregated to avoid cross contamination. The issues then arise if the product is successful and commercial production is carried out using the same process for say 1,000 or even 10,000 patients per year, where the clean room and personnel requirements increase 10-fold or 100-fold respectively, making the product cost-prohibitive at this scale. This will drive the development of expansion platforms that are fully closed, so that multiple patient lots can be manufactured in the same

facility, greatly reducing fixed and operating costs as the product moves toward commercial production. Table 2.3 shows the number of doses per lot achievable for multiple expansion technologies currently available based on an allogeneic hMSC treatment for myocardial infarction (Hare *et al.* 2009) requiring 35 – 350 million cells per dose. This demonstrates the challenge of manufacturing an hMSC based product for 10,000 patients per year, given the number of doses per lot achievable using current expansion technology.

Table 2.3. Potential scale per lot and harvest constraints for various cell therapy manufacturing platforms. *From (Heathman et al. 2015b)*

Expansion Technology		Estimated Scale per Lot			Estimated Doses per Lot		Adherent Cell Harvest	
		Surface Area cm^2	Harvest Volume, L	Number of cells (billion)	35 M cells per dose	350 M cells per dose	Detachment Efficiency	Pooling Time
Adherent	Rotating flasks	850,000	100	21.30	609	61	LOW	HIGH
	Packed/Fluidized	440,000	5	11.00	314	31	MEDIUM	MEDIUM
	Hollow Fibre	210,000	5	0.50	14	1	MEDIUM	MEDIUM
	T-Flask (Automated)	225,000	50	0.56	16	2	HIGH	HIGH
	Multi-layer Flask	400,000	30	10.00	286	29	HIGH	HIGH
Adherent & Suspension	Stirred Tank	>4,000,000	>1,000	>100.00	>2857	>286	HIGH	LOW
	Rocking-Motion	2,000,000	500	50.00	1429	143	LOW	LOW
	Pneumatically Driven	2,000,000	500	50.00	1429	143	LOW	LOW

In Situ Detachment Efficiency: Low < 50%, Medium 50-90%, High >90%
Pooling time: Low < 1 hour, Medium 1-5 hours, High > 5 hours

A manufacturing process that reduces biological divergence will inevitably yield a more consistent and higher quality product. This biological divergence is typical of cell expansion processes, whereby small changes to the cell environment at the start of culture will lead to large changes by the time the product is harvested. This has been demonstrated for the culture of embryonic stem cells whereby changes to dissolved oxygen levels in the culture medium can lead to changes in cell growth characteristics (Wu *et al.* 2014) and differentiation potential (Prado-Lopez *et al.* 2010). This potential divergence can be limited by reducing the heterogeneity of the culture conditions *via* mixing, so that the cell microenvironment remains consistent throughout the culture. Technology that does not induce mixing such as T-flasks will potentially suffer from heterogeneity in physical, chemical and hence physiological conditions

(Nienow 2006), although it can also exist in other forms. Packed/fluidized-bed bioreactors, due to their high density will invariably suffer from axial concentration gradients as medium flows though the bed, particularly as the scale and cell density increases. Hollow fibre reactors have the potential to introduce heterogeneity *via* longitudinal concentration gradients as medium or dissociation reagent flowing down the bioreactor changes with distance through the fibre (under plug flow conditions). Although these factors could impact the consistency of the product, there is a lack of evidence to back this up and far more work will be required to fully understand and develop the various manufacturing processes for cell-based therapies.

A lack of online process control is a key barrier for the consistent manufacture of cell-based therapies. Expansion technologies such as rotating flasks and multilayer flasks lack the capability for online cell visualization which could form the basis for a non-invasive control strategy based on cell coverage of a surface (Joeris *et al.* 2002). These technologies as well as T-flask automation currently lack the ability for online medium sampling which prohibits the control of key nutrient and metabolite concentrations, a staple of process control in the bioprocessing industry. Without an effective process control metric, expansion technology will suffer when attempting to maintain product consistency and will incur a higher cost for product validation. Process control strategies are poorly understood for novel cell expansion technologies, however they are routine in stirred tank bioreactors for current bioprocesses (Butler 2005; Trummer *et al.* 2006). In addition to this, the physical characterization of the stirred reactor system is well understood and can also be directly translated from traditional bioprocesses (Vrábel *et al.* 2000; Langheinrich *et al.* 2002; Nienow 2006). This development is analogous to process analytical technology (PAT) (FDA 2004) in the current biopharmaceutical industry (Ganguly and Vogel 2006) and could be used as a model for cell-based therapy process development.

The efficient harvest of cell-based therapies represents one of the few deviations from traditional bioprocessing and must be designed based on cell sensitivity and the pooling time limitations of the product. Scale-out processes such as rotating flasks (Merten *et al.* 1997; Kedong *et al.* 2010), T-flasks (Thomas *et al.* 2007) and multilayer flasks (Abraham *et al.* 2011) will require high cell pooling times which will limit the effective scale to which these therapies can be manufactured as product quality will likely reduce during the pooling process (Table 2.3). For cell-based therapies that are surface-adherent, the dissociation of the cell from the surface is required during the expansion process. This unique constraint of cell-based therapy manufacture is often overlooked but has been considered for packed/fluidized bed (Kasuto *et*

al. 2014), hollow fibre (Antwiler *et al.* 2014) and stirred tank bioreactors (Nienow *et al.* 2014). Rocking-motion (Singh 1999; Mikola *et al.* 2007) and pneumatically driven bioreactors (Zeikus 2009; Kim *et al.* 2013) have been previously employed for suspension cell culture. However, transferring these systems to surface-adherent cell types will likely require an additional process step to transfer the culture to a harvest vessel, allowing for increased agitation to promote efficient detachment and harvest of cells from microcarriers, which may not be sufficient in these systems (Lee *et al.* 2011)**.** A further challenge will emerge if the cells are required to be dissociated during the process (i.e. if bead-to-bead transfer does not occur at a high enough rate to support one step expansion). This will add additional steps to the process and will likely influence the design and optimization of other aspects of the process, such as agitation strategy and culture medium.

Although much work is yet to be done on calculating the optimum volume for expanding cell-based products in stirred tank reactors, current estimates put the maximum value at around 1000 liters (Rowley *et al.* 2012b). It should be noted however, that industrial scale mammalian cell culture, once considered to be limited to a similar scale is now routinely operated at greater than 10,000 liters (Nienow 2006). Similar gains in effective cells per batch can also be made by increasing the microcarrier concentration, which is currently far from optimal for suspension based systems (Rafiq *et al.* 2013b). One feature that is a fundamental aspect of all culture processes is the need to supply oxygen to the cells. Due to its limited solubility, this supply is required to be provided continuously. As the cell density increases, it becomes necessary to provide oxygen by sparging; typically with air, which also strips out the carbon dioxide produced (Sieblist *et al.* 2011). For free suspension animal cells, sparging has required the inclusion in the medium of protective agents, almost always the surfactant, Pluronic™ F68, as the energy released from bursting bubbles damages the cells, resulting in a loss of cell viability (Nienow 2006). The addition of a surfactant such as Pluronic™ F68 reduces the adhesion of cells to these bubbles during sparging, reducing the prevalence of cell damage as the bubbles burst at the gas-liquid interface. Due to the fact that the cell densities reached to date and the specific oxygen uptake rate of hMSCs (Rafiq *et al.* 2013b) and hESCs (Oh *et al.* 2009) for example, are both low, such issues have not yet been addressed but will need to be as the density increases, especially since the presence of these protective agents in final product formulations may be an issue. For pneumatically driven bioreactors (Zeikus 2009; Kim *et al.* 2013), bubbling gas is inherent to the way they function and therefore potential cell damage must be considered during the appraisal of expansion technology.

It is clear that other than stirred bioreactors, there is a distinct lack of comparable and peer reviewed data for the majority of manufacturing platforms discussed in this study. This could potentially be to the detriment of the field, as without reliable information to inform technology appraisal, process development is likely to default to stirred tank bioreactors due to the strong legacy data that exists for large scale mammalian cell culture. On the other hand, there is nothing to be gained by innovating unnecessarily. Many of the potential manufacturing platforms mentioned here were considered in the 1980s for culturing animal cells, when it was considered that because they lacked a cell wall, it would be impossible to do so in the presence of rotating stirrers. Yet today, whether in single use systems (SUBs), at bench scale or the largest commercial scale, stirred bioreactors are commonplace in the biotechnology industry (Kehoe *et al.* 2010). Indeed, they are now being preferred industrially even for clone selection in robotically-controlled microbioreactors (ambr^{TM}) at the 15 mL scale (Nienow *et al.* 2013).

Although, several manufacturing systems are already available for the expansion and manipulation of therapeutically relevant cells, an optimal and universal manufacturing platform does not yet exist and may not be attainable due to the variety of cell types and clinical applications. With the exception of hMSCs, most therapeutically relevant cell types have only been demonstrated on a subset of the broad range of available platforms. Developers considering the range of available manufacturing technologies need to balance the competing pressures discussed. Nevertheless, the fact that both hMSC culture and harvest have now been effectively demonstrated in stirred bioreactors based on sound physical principles is encouraging, especially given the inherent flexibility and controllability of this technology; and its success with free suspension and adherent animal cells from the 15 mL to the 25,000 L scale.

As an industry, cell-based therapies are still in the early stages of clinical development. It is clear that we must better understand the quality of our cell-based products in order to form a stable base for process evaluation and development. Investment in cell-based therapy manufacturing in the UK has created an urgent need to better understand these cell-based therapy products to facilitate successful manufacture based on strong clinical data demonstrating product efficacy. It is likely that there will be bespoke manufacturing processes for each of these cell-based products as well as 'generic' cell-based therapy products driven by this fundamental lack of product understanding, with a move toward functionally closed and single-use technology (Simaria *et al.* 2014).

Publications arising from this Chapter:

Heathman TRJ, Nienow AW, McCall MJ, Coopman K, Kara B, Hewitt CJ. The translation of cell-based therapies: clinical landscape and manufacturing challenges. <u>Regenerative Medicine</u>, (2015) 10 (1): 49-64.

2.4 Aims and objectives

It is clear that there is a significant amount of clinical activity around the use of hMSCs, driven by their potential to treat a variety of diseases that currently only have limited or palliative treatment options. Current manufacturing processes for these BM-hMSC therapies are largely based on manual expansion technology and therefore are not readily scalable to cost-effectively meet the patient need on a large-scale. Considering that the input to this process will need to be from multiple donors, it will be important to consider the impact of the variation in donor material as well as establishing a mechanism to select input material based on desired product attributes and drive consistency into the process at an early stage of development. In conjunction with this, variation in culture materials must also be controlled during development and moving towards a serum-free process provides a mechanism to reduce supply chain risk as well as reducing the batch-to-batch variation associated with FBS. Finally, the development of a process control strategy within an agitated microcarrier process has the potential to consistently produce BM-hMSCs within a process that has the potential to cost-effectively meet the batch sizes required at the commercial scale. Accordingly, the objectives of this work are as follows:

- Characterise BM-hMSCs from multiple donors in monolayer culture to understand the variation in cell growth, metabolism and quality attributes.

- Assess the impact of different culture media on the yield, quality and consistency of BM-hMSC expansion.

- Process transfer from the small-scale monolayer process to a potentially scalable microcarrier process under serum-free conditions.

- Develop a process control strategy for the microcarrier culture of BM-hMSCs to maximise growth, consistency and BM-hMSC quality characteristics.

- Develop a potentially scalable downstream and cryopreservation process to assess the impact of multiple integrated unit operations on BM-hMSC attributes.

3 Materials and Methods

3.1 Materials

All materials used were analytical grade or better. Sterilisation of liquids and equipment was achieved *via* autoclaving with a Systec VX-95 autoclave (Systec, Germany) at 121°C on a 40 minute cycle. Aqueous solutions were prepared using filtered water from a MilliQ ultrafiltration unit (Millipore, UK).

3.2 Culture of human mesenchymal stem cells

3.2.1 Medium formulation

Human mesenchymal stem cells were cultured using three different medium formulations, firstly with Dulbecco's Modified Eagle Medium (DMEM; Lonza, UK) supplemented with 10 % (v/v) foetal bovine serum (FBS) (Lot: RVC35874, Hyclone, Belgium) and 2 mM ultraglutamine (Lonza, UK). Complete growth medium was stored at 2 to 8°C and used within one month of preparation.

For culture using human platelet lysate (HPL), Dulbecco's Modified Eagle Medium (DMEM; Lonza, UK) was supplemented with 2, 5 and 10 % (v/v) HPL (Stemulate™, Cook Regentec, USA) and 2 mM ultraglutamine (Lonza, UK). Complete growth medium was stored at 2 to 8°C and used within one month of preparation.

For serum-free culture, the growth surface of T-flasks was coated with 0.4 µg.cm^{-2} PRIME-XV® human fibronectin (FN) (Irvine Scientific, USA) and cultured in PRIME-XV® SFM (Irvine Scientific, USA) as per manufacturer's instructions. Growth medium was stored at -18°C and thawed immediately before use. The selection of PRIME-XV® SFM was made following a pre-screen of six commercially available serum-free media.

3.2.2 Acquisition and isolation of BM-hMSCs

Bone marrow derived mesenchymal stem cells were purchased or donated as mononuclear cells (MNCs) from Lonza (USA) after the patient had given informed consent (Table 3.1). MNCs from Lonza were initially plated at a cell density of 100,000 MNCs.cm^{-2} with the first medium exchange taking place after 48 hours and every 72 hours thereafter. Cells donated from

Southampton University were received at passage 1 and initially plated at a density of 5000 cells.cm^{-2} with a medium exchange taking place every 72 hours. The five BM-hMSC donors were selected at random in order to obtain a sample from representative BM-hMSC donors so that process development would account for input material from multiple, random donors.

Table 3.1. Summary of the BM-hMSC line donor information as well as the chosen nomenclature to identify the various donor cell lines. Bone marrow derived mesenchymal stem cells were purchased[1] or donated[2] as mononuclear cells.

BM-hMSC line Nomenclature	Donor Age (years)	Donor Gender	Donor Ethnicity	Lot Number
[2]M0	20	MALE	CAUCASIAN	4625A
[1]M1	27	MALE	BLACK	080004A
[1]M2	19	FEMALE	BLACK	071313B
[1]M3	24	MALE	CAUCASIAN	701150B
[1]M4	25	FEMALE	HIPANIC	0000327825

3.2.3 Cryostorage

BM-hMSCs were cryopreserved at passage 0 to passage 3 at a density of either 1×10^6 or 2×10^6 cells.mL^{-1} in a freeze medium containing 90% (v/v) FBS (Lot: RVC35874, Hyclone, Belgium) and 10% (v/v) dimethylsulphoxide (DMSO). Cells suspended in 1 mL freeze medium were placed into 2 mL cryovials, placed in a freezing container (Panasonic, UK) and stored in a -80 °C freezer to cool at a rate of 1 °C.min^{-1}. After 24 hours, cells were placed in the vapour phase of a monitored liquid nitrogen cryostorage bank for long term storage.

3.2.4 Resuscitation

A cryovial of BM-hMSCs was removed from liquid nitrogen storage and rapidly thawed in a water bath at 37 °C until a sliver of ice remained. The contents of the vial were pipetted drop wise into 10 mL of culture medium pre-warmed to 37 °C, centrifuged at 220 g for 5 minutes at room temperature, supernatant aspirated and re-suspended in 5 mL of fresh pre-warmed culture medium. Cells were counted using the method below and seeded into a T-flask at 5000

cells.cm^{-2} with the appropriate volume of pre-warmed culture medium (see Table 3.2), labeled and placed into a humidified incubator at 37 °C in air containing 5% CO_2 for culture.

3.2.5 T-Flask culture of human mesenchymal stem cells

Cells were grown in T-flasks seeded at 5,000 cells.cm^{-2} in a humidified atmosphere at 37°C in air containing 5% CO_2. A complete medium exchange was performed after 72 h culture and cells were passaged at day 6 of culture. On passage, the hMSCs were washed with Ca^{2+} and Mg^{2+} free phosphate buffered saline (PBS) (Lonza, UK). PBS free from Ca^{2+} and Mg^{2+} was used in order to reduce cell adhesion and enzyme denaturation caused by the presence of these components in the PBS. Cells were then incubated for 5 min with trypsin (0.25 %)/EDTA solution (Lonza, UK) or TrypLE Express (Life Technologies, UK) for serum-free culture to aid cell detachment from the surface. The dissociation reagent was then inactivated by the addition of fresh growth medium equivalent to three times the volume of the trypsin solution used for cell detachment. This cell suspension was centrifuged at 220g for 5 min at room temperature, the supernatant discarded and the remaining pellet re-suspended in an appropriate volume of culture medium. Viable cells were counted using a NucleoCounter NC-3000 automated mammalian cell counter (Chemometec, Denmark) and an appropriate number of cells were then re-seeded into a fresh T-flask.

Table 3.2. Volume of culture medium and Trypsin used in monolayer culture of BM-hMSCs

Culture Vessel	Growth Surface Area (cm^2)	Medium Volume (mL)	Trypsin Volume (mL)
24 well plate	1.9	0.5	0.15
12 well plate	3.8	1	0.25
6 well plate	9.5	3	0.50
T-25	25	5	1
T-75	75	15	3
T-175	175	35	7
T-225	225	50	9

3.3 Microcarrier culture of human mesenchymal stem cells

3.3.1 Microcarrier preparation

To sterilise the microcarriers, 1.39 grams of polystyrene P102-L microcarriers (SoloHill, UK) and 15ml of distilled water were added to each flask, giving a microcarrier surface area of 500 cm^2. The flasks were sealed and autoclaved at 121 °C for 40 mins. The supernatant was then aspirated and 20 ml of sterile culture medium was added to each flask and incubated at room temperature for at least 20 mins to coat the microcarrier surface in serum protein. The supernatant was once again aspirated and replaced with 100ml of fresh culture medium and placed into a humidified incubator at 37 °C in air containing 5% CO_2 for culture. The microcarrier type used in these studies was selected following a screening of multiple commercially available microcarriers.

3.3.2 Spinner flask preparation

The glass surfaces of 100 mL Spinner flasks (diam. T = 60 mm) (BellCo, USA) were siliconised with Sigmacote (Sigma-Aldrich, UK) to prevent cell attachment to the glass surface. Spinner flasks were operated with a magnetic, horizontal stirrer bar and a vertical paddle (diam. D = 50 mm).

3.3.3 Spinner flask operation

Each spinner flask was seeded with 3 million BM-hMSCs (6000 cells.cm^{-2}) and left to settle in a humidified incubator at 37 °C and 5% CO_2 in air, for one hour. After this initial period the spinner flasks were placed on a magnetic stirrer plate (Bell-Ennium^{TM} Compact 5, USA), at an impeller speed of 30 rpm, the minimum speed required to achieve microcarrier suspension (Rafiq *et al.* 2013a). The spinner flasks side-arm caps were loosened (to allow for gas exchange) and were incubated at 37 °C in a humidified atmosphere of 5% CO_2 in air. A 50% medium exchange was performed every three days. 1 ml samples of the medium from the spinner flasks were taken daily as well as samples of fresh medium on days when a medium exchange occurred. The medium samples were centrifuged at 220g for 5 minutes and 1 ml of the supernatant is removed to ensure that no microcarriers were present. Daily samples of the cell suspension were also taken for cell counting using the NucleoCounter NC-3000 method below.

3.3.4 Spinner flask harvest

On the sixth day of culture the BM-hMSCs were harvested from the spinner flasks using a previously published method (Nienow *et al.* 2014). The microcarriers were left to settle at the bottom of the spinner flasks, the supernatant was aspirated and the microcarriers were washed in 50 ml of Ca^{2+} and Mg^{2+} free PBS for 3 minutes at an impeller speed of 30 rpm. The microcarriers were left to settle once more and the PBS aspirated before adding 50 mL of Trypsin for 7 minutes at an impeller speed of 150 rpm (ending with 5 seconds at 200 rpm). The Trypsin was then quenched with 50 ml of medium and a 2 mL sample placed in a single well of a 6 well plate for analysis under a light microscope to assess detachment efficiency. The remainder of the solution was filtered through a 60 μm Steriflip Filter Unit (Merck Millipore, Germany) to separate the microcarriers from the cells and medium. The cell suspension was centrifuged, the supernatant aspirated and the cell pellet re-suspended in culture medium. A cell count was then performed using a NucleoCounter NC-3000 to assess the overall BM-hMSC growth and the culture harvest efficiency.

3.3.5 DASGIP DASbox bioreactor culture

DASGIP, DASbox bioreactors (Figure 3.1), were used for all controlled bioreactor experiments, with a working volume of 100 ml and a vessel diameter (T) of 63 mm. The bioreactor was equipped with a 3-blade 30°-pitch down pumping impeller (diameter, D = 30.25 mm, Figure 3.2), a temperature probe, a dissolved oxygen (dO2) probe (Hamilton, UK) a pH probe (Hamilton, UK), an off-gas analyser (Eppendorf, Germany) and two sample ports. The DASbox system was set up, calibrated and controlled using Eppendorf, DASGIP control unit and accompanying software.
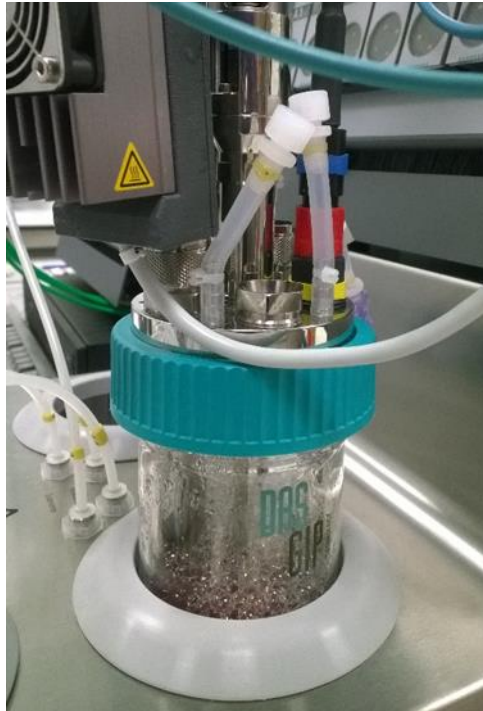
Figure 3.1. DASGIP DASbox Controlled stirred bioreactor system
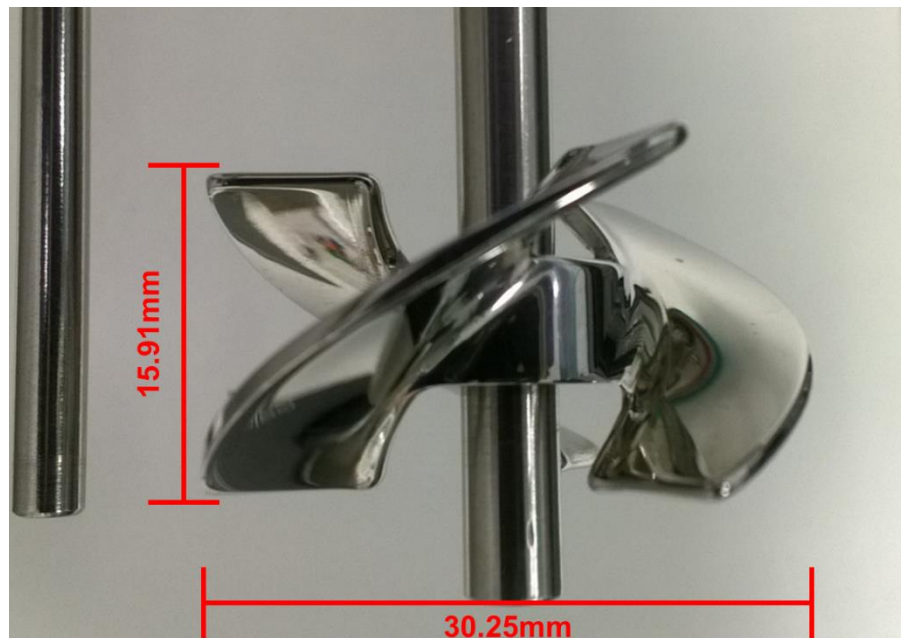
Figure 3.2. DASGIP DASbox impeller and geometry

The DASbox system was operated with headspace aeration to achieve sufficient gas supply, unless otherwise stated. For sparged culture, the gas inlet port was lowered into the culture medium with an aeration rate of 0.1 VVM. For sparged bioreactor cultures, Antifoam C (Sigma, UK) was made up to a concentration of 2% (v/v) in water and sterilised by autoclaving. Antifoam was added to the bioreactors to reduce foaming at a concentration of 0.01% (v/v) per day. If Pluronic^TM F68 (Life Technologies, UK) was used in culture as a shear protectant, it was added directly into the culture medium at a concentration of 0.1% (v/v) as per the manufacturer's instructions.

To allow for sampling and harvest of the culture medium in the DASbox bioreactor without requiring the microcarriers to settle, one of the DASbox sample ports was modified (Figure 3.3). Briefly, a 40 µm nylon mesh was placed over the sample port and held in place using silicone sample tubing which prevented the microcarriers from entering the sample port during culture and harvest. This modification was made prior to autoclave sterilisation of the bioreactor so that the nylon mesh and tubing was sterilised during the autoclave process.
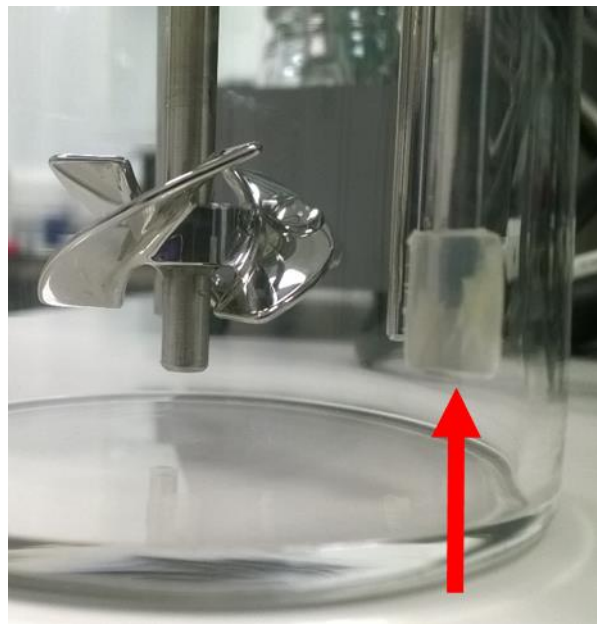
Figure 3.3. DASGIP DASbox impeller and sample port modification (red arrow)

3.3.6 DASGIP DASbox bioreactor harvest

To initiate the microcarrier harvest process, the DASbox control was switched off and the microcarriers allowed to settle. The spent culture medium was extracted through the modified sample port (Figure 3.2) and the microcarriers were washed twice in 50 ml of Ca^{2+} and Mg^{2+} free PBS. The PBS was aspirated before adding 80 mL of dissociation reagent for 10 minutes at an impeller speed of 375 rpm (ending with 5 seconds at 400 rpm). The dissociation reagent was then quenched with 70 ml of medium and a 2 mL sample placed in a single well of a 6 well plate for analysis under a light microscope to assess detachment efficiency. The remainder of the solution was filtered through a 60 µm Steriflip Filter Unit (Merck Millipore, Germany) to separate the microcarriers from the cells and medium. The cell suspension was centrifuged, the supernatant aspirated and the cell pellet re-suspended in culture medium. A cell count was then performed using a NucleoCounter NC-3000 to assess the overall BM-hMSC growth and the culture harvest efficiency.

3.3.7 Downstream processing and cryopreservation from microcarrier culture

Following detachment and separation from the microcarriers, BM-hMSCs were held in culture medium for four hours to simulate an expected process pooling time. Harvested cells were then suspended in Prime-XV™ Cryopreservation medium (Irvine Scientific, USA) at $2x10^6$ viable cells.ml^{-1}. Cells were equilibrated in freezing medium for 30 minutes at room temperature and aliquots (0.5 ml) were loaded into 1.8 ml cryovials during equilibration. Vials were cooled at 4°C for 5 minutes then cooled with a Stirling cryocooler (EF600, Asymptote, UK) set to cool at -1°C.min^{-1} to -80°C. Cooled vials were stored under liquid nitrogen vapour for at least one month. Vials were rapidly thawed in a 37°C water bath and cells recovered by growth medium dilution followed by centrifugation. The resultant cell pellet was suspended in growth medium then the cells were seeded into T-flasks to monitor outgrowth and into fibronectin-coated multiwell plates to assess cell adhesion.

3.4 Analytical Techniques

3.4.1 NC-100 determination of viable cell number

Human MSC viability was determined *via* propidium iodide (PI) exclusion using a NucleoCounter NC-100 automated mammalian cell counter. Briefly, the non-viable cell number was determined by direct measurement of the cell suspension using a NucleoCassette (Chemometec, Denmark) containing PI (with the assumption that viable cells exclude the PI) and run on the NucleoCounter NC-100. The total cell number was obtained by first mixing 50 µL of the cell suspension with 50 µL of NucleoCounter Buffer A (Chemometec, Denmark) to permeabilise the cell membrane, vortexing for 3 seconds and leaving for a minimum of 10 seconds. Next, 50 µL of NucleoCounter Buffer B (Chemometec, Denmark) was added to the solution for stability and the solution aspirated using a NucleoCassette (Chemometec, Denmark) and run on the NucleoCounter NC-100 to obtain the total cell number (taking into account the 3x dilution). To calculate the viable cell number, the non-viable cell number was subtracted from the total cell number and multiplied by the cell re-suspension volume.

3.4.2 NC-3000 determination of viability, mean cell diameter and cell aggregation

The cell suspension was taken up into a Via-1 Cassette and loaded into the NucleoCounter NC-3000 automated mammalian cell counter (Chemometec, Denmark) to determine mean cell diameter, viability (via acridine orange uptake and DAPI exclusion) and percentage cell aggregation.

3.4.3 NC-3000 determination of cell number from microcarrier culture

For microcarrier cultures, cells were counted directly from microcarrier culture, whilst still attached to the microcarrier surface. The total cell number was obtained by first mixing 200 µL of the cell-microcarrier suspension with 100 µL of NucleoCounter Buffer A (Chemometec, Denmark) to permeabilise the cell membrane, vortexing for 30 seconds and leaving for a minimum of 10 seconds. Next, 100 µL of NucleoCounter Buffer B (Chemometec, Denmark) was added to the solution to stabilise, vortexed for 10 seconds and the solution taken into a Via-1 Cassette (Chemometec, Denmark) and run on the NucleoCounter NC-3000 to obtain the total cell number (taking into account the 2x dilution).

3.4.4 Demonstration of multilineage potential

The assessment of BM-hMSC multilineage potential was made according to the International Society for Cellular Therapies (ISCT) guidelines (Dominici *et al.* 2006; Rasini *et al.* 2013) which states that human mesenchymal stem cells should demonstrate the ability to differentiate down the osteogenic, adipogenic and chondrogenic lineages.

A StemPro osteogenesis kit (Life Technologies, UK) was used to verify BM-hMSC osteogenic potential combined with dual staining of calcium and alkaline phosphatase; briefly the 10 mL osteogenic supplement was thawed at room temperature and added to 90 mL of the supplied basal medium and stored at 4-8°C. Cells were seeded in a 12 well plate at 5×10^3 cells cm^{-2} with DMEM and placed into an incubator at 37°C for 72 hours, after which 1 mL osteogenic differentiation medium was added to each well. The cells are then returned to the incubator with a medium exchange taking place every 2 to 3 days. After 28 days under differentiation conditions the medium is removed, cells were rinsed once in PBS and fixed in a 1 mL solution of 4% (v/v) PFA for 5 minutes at room temperature. After fixation, cells were washed with distilled water and 1 mL 2.5% (v/v) silver nitrate (Sigma, UK) is added to each well for 30 minutes. Cells were rinsed three times with distilled water and a fast violet solution (Sigma, UK) containing 4% (v/v) napthol AS-MX phosphate alkaline (Sigma, UK) was added to the cells for 45 minutes at room temperature in the dark. Finally, cells were washed three times in distilled water and visualised under a light microscope.

A StemPro chondrogenesis kit (Life Technologies, UK) was used to verify BM-hMSC chondrogenic potential combined with Alcian blue staining of extracellular matrix containing glycosaminoglycans. Briefly, the 10 mL chondrogenic supplement was thawed at room temperature and added to 90 mL of the supplied basal medium and stored at 4-8°C. Chondrogenic differentiation involves the formation of a micromass of BM-hMSCs, generated by seeding multiple 5 μl cell suspensions at 1.6×10^7 cells.ml^{-1} into a 12 well plate. The 12 well plate is placed into a humidified incubator at 37°C for 20 minutes, after which 2 mL chondrogenic differentiation medium is added to each well. The cells were then returned to the incubator with a medium exchange taking place every 2 to 3 days. After 14 days under differentiation conditions the medium was removed, cells are rinsed once in PBS and fixed in a 2 mL solution of 4% (v/v) paraformaldehyde (PFA) (Sigma, UK) for 20 minutes at room temperature. After fixation, cells were rinsed in PBS and stained with 1% Alcian blue (w/v) (Sigma, UK) in 0.1 N hydrochloric acid (HCl) (Sigma, UK), passed through 0.2 μm filter (Nalgene,

UK) and incubated for 30 minutes at room temperature. After incubation, cells were rinsed three times with 0.1 N HCl, distilled water is added to dilute the acidity and cells were visualised under a light microscope (Nikon Eclipse TS-100, UK).

A StemPro adipoogenesis kit (Life Technologies, UK) was used to verify BM-hMSC adipogenic potential combined with Oil Red O staining of lipid vacuoles; briefly the 10 mL adipogenic supplement was thawed at room temperature and added to 90 mL of the supplied basal medium and stored at 4-8°C. Human MSCs were seeded in a 12 well plate at 1×10^4 cells cm^{-2} with growth medium and placed into an incubator at 37°C for 24 hours, after which 1 mL adipogenic differentiation medium was added to each well. The cells were then returned to the incubator with a medium exchange taking place every 2 to 3 days. After 21 days under differentiation conditions the medium was removed, cells rinsed once in PBS and fixed in a 1 mL solution of 4% (v/v) PFA for 20 minutes at room temperature. A stock solution of 0.3% (w/v) Oil Red O (Sigma, UK) was prepared in 99% isopropanol, stable for one year at room temperature. The working Oil Red O solution was prepared by mixing 3 parts Oil Red O stock solution with 2 parts distilled water, passed through a 0.2 µm filter and incubated for 10 minutes at room temperature (stable for 2 hours). After fixation, cells were rinsed with distilled water and 1mL 60% (v/v) isopropanol was added to each well for 5 minutes, removed and 1 mL of filtered Oil Red O working solution is added for 5 minutes at room temperature. Oil Red O solution is removed, cultures were rinsed with distilled water three times or until water is clear and visualised under a light microscope.

3.4.5 Immunophenotype by multiparameter flow cytometry

Detached BM-hMSCs were suspended at 0.5×10^6 cells.ml^{-1} in culture medium, loaded into a 96 well plate (200µl per well) and centrifuged for 5 minutes at 300 g. The aspirate was removed and the cells re-suspended, washed in flow cytometry stain buffer (R&D Systems, UK) and centrifuged for 5 minutes at 300 g. The cells were stained for 20 minutes in the dark at room temperature with fluorescent monoclonal antibodies against CD34 (PE-CY5), CD45 (APC-Cy7), CD73 (PE-Cy7), CD90 (APC), CD105 (PE), HLA-DR (FITC) (BD Biosciences, UK) along with corresponding isotype controls. After incubation the cells were washed twice with staining buffer as before and 200µl of stain buffer is used to re-suspend the samples before analysis.

All data was obtained using a Guava EasyCyte 8HT flow cytometer (Merck Millipore, UK) equipped with 488nm and 640nm lasers running guava SoftIncyte acquisition software (v2.5). A minimum of 10,000 gated (forward scatter/side scatter) events were recorded for each sample. Compensation values were determined using anti-mouse Ig, κ antibody capture beads (CompBeads, BD Bioscience, UK) according to the manufacturer's instructions. Post-acquisition analysis and compensation was performed with FlowJo v7.6.5 (TreestarInc, USA) software.

3.4.6 Nutrient and metabolite analysis

To assess the metabolic activity of the BM-hMSCs during culture, 1 mL medium samples were taken from each culture vessel (T-flask, spinner flask or bioreactor), stored initially at -18°C and transferred to -80°C for permanent storage. Multiple medium samples were thawed, randomised and analysed for glucose, lactate and ammonium using the BioProfile FLEX (Nova Biomedical, USA). Alternatively, the medium sample were thawed and analysed for glucose, lactate, ammonia, lactate dehydrogenase (LDH) and total protein using the Cedex Bio-HT metabolite analyser (Roche, Germany).

3.4.7 Plastic adherence and morphology by phase contrast microscopy

According to the minimum criteria as defined by the ISCT (Dominici *et al.* 2006; Rasini *et al.* 2013), BM-hMSCs must adhere to tissue culture plastic. During the culture of BM-hMSCs this ability to adhere to tissue culture plastic has been assessed *via* daily imaging of the BM-hMSCs over multiple passages. In conjunction with this, qualitative morphology analysis of the BM-hMSCs is carried out by taking a representative image of each T-75 flask on every day of culture throughout serial passage. This information was then used to assess changes in BM-hMSC morphology throughout the multiple passages as well as morphological differences between the various donor BM-hMSC cell lines.

3.4.8 Quantitative osteogenic potential of BM-hMSCs

Osteogenesis was quantified by BM-hMSC collagen production using the Sircol Assay (Biocolour, UK) following osteogenic differentiation. Collagen standards of acid-soluble collagen Type I at 0, 0.1, 0.2 and 0.4 $g.L^{-1}$ were used to quantify the collagen production. BM-hMSCs were seeded at 10,000 $cells.cm^{-2}$ in a 12 well plate with previously described cell culture medium; after 3 days culture growth medium was exchanged to PRIME-XV® Osteogenesis Serum-Free Medium (Irvine Scientific, USA) and cultured for 9 days with a medium exchange taking place every 3 days. To

quantify the collagen production cells were fixed with a solution of 5% acetic acid (v/v) (Sigma, UK) and 9% formaldehyde (v/v) (Sigma, UK) for 30 minutes at room temperature. The monolayer was washed and Sircol Dye Reagent (Biocolour, UK) was added to each well for 30 minutes, removed and the cell monolayer was washed with Acid-Salt Wash Reagent (Biocolour, UK). Alkali Reagent (Biocolour, UK) was added to each well to release the collagen-bound Sircol Dye Reagent and the resulting solution along with the collagen standard was quantified on a microplate reader (BMG Labtech, UK) at an absorbance of 555 nm.

3.4.9 Colony forming unit-fibroblast (CFU-f) efficiency

To assess the CFU-f efficiency, BM-hMSCs were seeded in a T-flask at 10 cells.cm^{-2} and cultured with a medium exchange every 3-5 days. Following 14 days culture, cells were washed with PBS and fixed in 4% formaldehyde (v/v) (Sigma, UK) for 30 minutes. Colonies were stained with 1% crystal violet (Sigma, UK) in 100% methanol (w/v) for 30 minutes. Stained colonies that were made up of more than 25 cells were recorded as CFU-fs.

3.4.10 RNA isolation

Total RNA was collected using TriFastTM Reagent (Peqlab, Germany) according to the manufacturer's instructions. Potential genomic DNA contamination was removed by digestion with DNase (Life Technologies, Germany) followed by reverse transcription at 50 °C for 60 min using Superscript III (Life technologies, Germany) and 250 ng Oligo(dT)18-primer (Life Technologies, Germany).

3.4.11 Quantitative real-time-polymerase chain reaction (PCR) analysis

Quantitative real-time PCR was done with SYBR GreenER qPCR Supermix Universal (Life Technologies, Germany), additionally added 1x SybrGreenI (Life Technologies, Germany) and 0.2 µM primer each on the DNA engine Opticon2 (Biorad, Germany) using these cycling conditions: Primary denaturation at 95 °C for 3 min, followed by 35 cycles: 95°C for 30s, 60°C for 30s (36B4, p21, CCL2) / 55 °C (Oct4) and 72°C for 30s followed by fluorescence measurement. The following primers for cell markers were used: CCL2 (recruits monocytes, memory T cells, and dendritic cells to the sites of inflammation produced by either tissue injury or infection, NM_002982.3) (Fw) 5¢-CCA AGG GCT CGC TCA GCC AGA TGC-3¢, (Re) 5¢-CGG AGT TTG GGT TTG

CTT GTC CAGG-3¢; p21 (regulates the cell cycle and mediates cellular senescence, NM_000389.4) (Fw) 5¢-CCG CCT GCC TCC TCC CAA CT-3¢, (Re) 5 ¢-GAG GCC CGT GAG CGA TGG AA-3¢, OCT4 (pluripotent marker associated with self-renewal of undifferentiated cells, NM_002701.4) (Fw) 5¢-GAG GAG TCC CAG GAC ATC AA-3¢, (Re) 5¢-CAT CGG CCT GTG TAT ATC CC-3¢ and VEGF (associated with vascularization and growth of blood vessels, NM_001171623.1) (Fw) 5¢- GGAAGGAGCCTCCCTCAGGGTTTCG -3¢, (Re) 5¢-GCCGGAGTCTCGCCCTCCGG -3¢. Serial dilutions of plasmid standards were used as positive controls and for quantification. Expression was normalized to the reference gene 36B4 (ribosomal protein large P0 RPLP0, NM_001002.3).

3.4.12 Short tandem repeat (STR) analysis

Short Tandem Repeat analysis was completed by LGC Standards (UK) under their cell line authentication program.

3.4.13 Post-thaw BM-hMSC adhesion and F-actin staining

For the cell adhesion assay, cultured cells were washed with PBS then fixed and permeabilised with BD Cytofix/Cytoperm™ kit at 4°C for up to 1 week. After repeated washing, cellular F-actin was stained with 100 nM Alexa Fluor® Phalloidin with 100 nM 4',6-diamidino-2-phenylindole counterstain for 30 minutes in the dark. Stained cells were visualized with a Nikon Eclipse TS100 fluorescence microscope (Nikon Instruments Europe B.V. UK). Cells were harvested during outgrowth and diluted 1:1 with viability stain (10 nM calcein-AM + 50 μg/ml propidium iodide in PBS) and incubated at 37°C for 7 minutes in 96 well plates. Stained cells were counted using a Guava EasyCyte 8HT flow cytometer using a standardized analysis protocol with GuavaSoft 2.6 (Merck Millipore, UK).

3.5 Statistical analysis

Results were deemed to be significant if $P < 0.05$ using a 2 tailed Students T-test in SPSS (IBM, USA) statistical software.

3.6 Equations

Equation 1: Specific growth rate

$$Specific\ growth\ rate, \mu = \frac{\ln\left(C_x(t)/C_x(0)\right)}{\Delta t}$$

Where μ is the net specific growth rate (h^{-1}), $C_x(t)$ and $C_x(0)$ are the cell numbers at the end and start of the exponential growth phase, respectively and t is time (h).

Equation 2: Fold increase

$$Fold\ incresae = \frac{C_x(f)}{C_x(0)}$$

Where $C_x(f)$ is the final cell number at the end of passage and $C_x(0)$ is the initial cell number at the start of passage.

Equation 3: Population doublings

$$Population\ Doublings, P_d = \frac{1}{\log(2)} \cdot \log\left(\frac{C_x(t)}{C_x(0)}\right)$$

Where P_d is the number of population doublings, $C_x(t)$ and $C_x(0)$ are the cell numbers at the end and start of the exponential growth phase, respectively.

Equation 4: Doubling time

$$Doubling\ time, t_d = \frac{\ln 2}{\mu}$$

Where t_d is the cell doubling time (h) and μ is the net specific growth rate (h^{-1}).

Equation 5: Specific metabolite consumption and production rate

$$Specific\ metabolite\ flux, q_{met} = \left(\frac{\mu}{C_x(0)}\right) \cdot \left(\frac{C_{met}(t) - C_{met}(0)}{e^{\mu t} - 1}\right)$$

Where q_{met} is the net specific metabolite consumption or production rate, μ is the specific growth rate (h^{-1}), $C_x(0)$ is the cell number at the end of the exponential growth phase, $C_{met}(t)$ and $C_{met}(0)$ are the metabolite concentrations at the end and start of the exponential growth phase, respectively and t is time (h).

Equation 6: Yield of lactate from glucose

$$Yield\ of\ lactate\ from\ glucose, Y_{\frac{Lac}{Gluc}} = \left(\frac{\Delta[Lac]}{\Delta[Gluc]}\right)$$

Where $Y_{Lac/Glc}$ is the yield of lactate from glucose, $\Delta[Lac]$ is the lactate production over specific time period and $\Delta[Glc]$ is the glucose consumption over same time period.

Equation 7: Colony-Forming Unit Fibroblast (CFU-f) Efficiency

$$CFUf\ Efficiency = \left(\frac{N_c(0)}{N_c(t)}\right) \cdot 100$$

Where $N_c(0)$ and $N_c(t)$ are the number of cells seeded and the number of colonies formed, respectively.

Equation 8: Mean specific energy dissipation rate

The mean specific energy dissipation rate during culture at N_{JS} (numerically equal to the specific power, $(P/M)_{JS}$ imparted to the medium) is given by:

$$(\bar{\varepsilon}_T)_{JS} = (P/M)_{JS} = P_O \cdot \rho_L \cdot N_{JS}^3 \cdot D^5 / M_{JS}$$

Where Po is the impeller power number (dependent on the impeller type), D is the impeller diameter, ρ_L is the fluid density, kg.m^{-3} and M_{JS} is the mass of medium and microcarriers in the vessel.

Equation 9: Kolmogorov scale

The Kolmogorov scale, λ_K is given by:

$$(\lambda_K)_{JS} = \left(v^3 / (\varepsilon_T)_{JS\ max}\right)^{1/4}$$

Where $\varepsilon_{T\ max}$ is the maximum local specific energy dissipation rate close to an impeller and v is the kinematic viscosity.

Equation 10: Reynolds number

$$Re = N \cdot D^2 \cdot \rho_L / \mu$$

Where Re is the Reynolds number, N is the impeller speed (s^{-1}), D is the impeller diameter (m), ρ_L is the fluid density (kg.m^{-3}) and μ is the fluid viscosity (kg.ms^{-1}).

3.7 Equipment and suppliers

Becton Dickinson, UK

- BD FACSCanto II

BellCo, USA

- Bell-Ennium^{TM} Compact 5 position magnetic stirrer platform

- 100 mL spinner flasks

BMG Labtech, UK

- Omega plate reader

Chemometec, Denmark

- NucleoCounter NC-100 automated mammalian cell counter

- NucleoCounter NC-3000 automated mammalian cell counter

Eppendorf, UK

- DASGIP DASbox controlled bioreactor system

- Eppendorf 5804 Centrifuge

Hamilton, Germany

- DASbox OxyFerm dissolved oxygen probe

- DASbox EasyFerm pH probe

Merck Millipore, UK

- Guava EasyCyte 8HT flow cytometer

Nikon Instruments, UK

- Nikon TS-100 inverted microscope

- Fluorescent Inverted microscope

Nova Biomedical, USA

- BioProfile FLEX Bioanalyser

Roche, Germany

- Cedex Bio-HT metabolite analyser

Thermo Scientific, UK

- Benchtop centrifuge Megafuge 16

- Herasafe KS Class II Biosafety Cabinet

- Heraeus HERAcell 150 CO2 Incubator

4 Characterisation of BM-hMSCs from Multiple Donors

4.1 Chapter introduction

Autologous cell-based therapies, where the cell donor and recipient is the same individual, are patient specific and their manufacture must be scaled-out to ensure that patient material is segregated and cross-contamination of material is avoided. Scale-out of autologous therapies will likely necessitate multiple manufacturing facilities, creating the need for local automation and the demonstration of comparability between these sites (Hourd *et al.* 2014a; Rafiq *et al.* 2015a). The main advantage of autologous cell-based therapies is the lack of immune rejection associated with donor transplant material, eliminating the need for immunosuppressive medication, which would add significant cost to the treatment. Autologous therapies may also benefit from the development of point-of-care devices, where functional closed devices can be used to manufacture cell-based therapies at the bedside. These typically involve the isolation and enrichment of cells directly from the patient and are returned on-site as "minimally manipulated" therapies. Despite these advantages, many challenges remain in the development and commercialisation of autologous cell-based therapies. It is possible that the route of the target disease might be with the patient's own cells and it would therefore be better to avoid using them, or indeed the patient is unable to undergo the procedure required for cell isolation. Furthermore, issues surrounding the quality test burden and logistics add to the complexity for the production and delivery of a cost effective autologous cell-based therapy and failure of product batches would be likely to lead to an inability to treat patients.

Regenerative cell-based therapies where the donor and the recipient are different individuals are termed "allogeneic". This creates an off-the-shelf business model, which is far more akin to current biopharmaceuticals, representing an attractive commercial opportunity. Assuming cell products can be stored long-term i.e. their manufacture is decoupled from delivery to the patient; the cells can be made available on demand. In contrast to autologous therapies, allogeneic products have the potential to be scaled-up, potentially benefitting from the economies of scale experienced by traditional bioprocesses (Jung *et al.* 2012; Rafiq *et al.* 2013b). As such, manufacturing technologies employed for allogeneic therapies are likely to differ in terms of nature and scale including the use of traditional scale-up technology such as stirred-tank bioreactors. Allogeneic therapies will however create a product that is "more than

minimally manipulated", which means that the regulatory pathway requires far more time and resource to complete.

For the development of both autologous and allogeneic cell-based therapies, the characterisation of the input material from different donors will be necessary to assess any potential variation in the manufacturing and delivery process. The aim of this Chapter, therefore, is to characterise the input material for a BM-hMSC therapy bioprocess and then assess the implications for the development and operation of a large scale "more than minimally manipulated" cell-based therapy bioprocess.

4.2 Growth characteristics of BM-hMSCs from multiple donors

4.2.1 Experimental overview

The development of both patient specific and off-the-shelf BM-hMSC manufacturing processes will have to consider the effect of donor variation and therefore it is important to assess the potential impact of this variation on the process. With this in mind, an experiment was designed to compare the growth and metabolite flux of five BM-hMSC lines over five passages (30 days) in small-scale monolayer culture. Four T-75 flasks were seeded for each donor BM-hMSC line in accordance with the protocol described in Section 3.2.5 and passaged every six days for a total of five passages. At passage the viable cell number was determined (Section 3.4.1) and the growth kinetics calculated (Equation 1). The culture medium supplemented with FBS (Section 3.2.1) was exchanged after three days and daily medium samples were taken and analysed for glucose, lactate and ammonium as in Section 3.4.6 on the Nova BioProfile FLEX. The metabolite concentrations and per cell metabolite flux was then calculated from these measurements (Equation 5 and 6).

4.2.2 Human MSC growth kinetics over multiple passages

It will be important to consider the growth kinetics of multiple BM-hMSC donors for manufacturing processes that require cell expansion, in order to meet the cell numbers required for each product dose. The specific growth rate of each of the donor BM-hMSC lines can be seen in Figure 4.1, with clear differences between them. Cell lines M0, M2 and M4 generally maintained their expansion potential over the five passages with the specific growth rate of M0 decreasing by only 0.066 ± 0.007 day^{-1}, M2 decreasing by 0.056 ± 0.009 day^{-1} and M4 decreasing by 0.069 ± 0.018 day^{-1} from passage four to passage eight. In contrast, BM-hMSC lines M1 and M3 showed a dramatic reduction in growth kinetics over the expansion period with M1 decreasing by 0.138 ± 0.022 day^{-1} and M3 decreasing by 0.123 ± 0.043 day^{-1} over the same time period. The specific growth rates measured here are in the range of other studies of BM-hMSCs and many display the same reduction in growth kinetics throughout expansion (Sethe *et al.* 2006; Higuera-Sierra *et al.* 2009). This reduction in growth kinetics as the number of population doublings increases is largely due to the onset of cellular senescence (Estrada *et al.* 2013; Carlos Sepúlveda *et al.* 2014). This onset of cellular senescence is induced through replicative exhaustion, DNA damage, or other stresses (Tchkonia *et al.* 2013) and is irreversible in primary BM-hMSCs, limiting the expansion potential during manufacture.
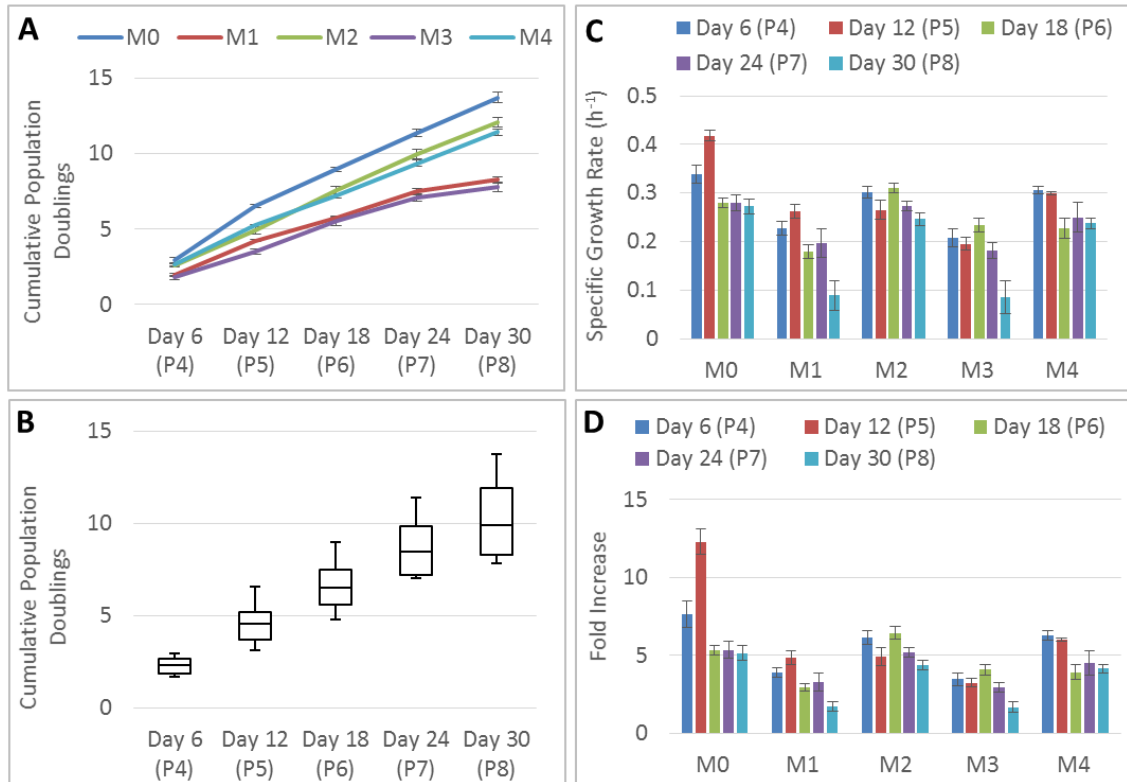
Figure 4.1. Growth potential of the five BM-hMSC lines over five passages. Showing (A) Cumulative population doublings; (B) Variation in cumulative population doublings across all six BM-hMSC lines; (C) Specific growth rate; (D) Fold Increase. (Data shows mean ± SD, n = 4).

As mentioned in Section 4.1, autologous cell-based therapy products must be scaled-out to meet demand and the process must have the capability to deal with innate variation that exists when manufacturing each product batch from a different donor. With this in mind, the variation in input material should be assessed in order to inform product and process development, increase efficiency and reduce costs (Naing *et al.* 2015a). The variation in growth kinetics of the five BM-hMSC lines can be seen in Figure 4.1, with 13.74 ± 0.33 cumulative population doublings achieved by M0 over 30 days in culture, compared to M3 which only achieved 7.81 ± 0.32 over the same period of time. The measured variation in growth kinetics will likely have implications for BM-hMSC products that require culture expansion, as a minimum number of cells will be required to be generated within a set time frame, to meet the specification of the product. With such differences in the growth of BM-hMSCs between donors this makes the manufacture of autologous cell-based products a real challenge and solutions have been proposed to alleviate this, such as reducing the expansion of the product and utilising functionally closed automated manufacturing devices (Hourd *et al.* 2014b). The implications of this difference in growth

kinetics will also impact the logistics and timing, as the process will typically have to operate at the "worst-case-scenario". Table 4.1 shows the variation in process time for each of these donor BM-hMSC lines for a theoretical process with the batch requirement of 350 million BM-hMSCs (Heathman *et al.* 2015b). The range in the process time between these donor BM-hMSC lines for this hypothetical product is over 13 days, creating potential batch timing issues when manufacturing products from multiple patients. This also creates differences in the medium utilisation to achieve each patient dose, for example M1 requires almost double the volume of medium per million cells compared to M0 (Table 4.1). This will likely impact of the overall cost of goods for patient specific processes, as medium and particularly the serum component of medium is likely to be a key cost driver during process scale-out (Brindley *et al.* 2012). Table 4.1 also shows the inter batch range for each of these donor BM-hMSC lines, with cells requiring higher processing times showing increased batch variation (Figure 4.2). Increased inter batch range has the potential to reduce productivity as process timing will need to be flexible enough to accommodate this variation and production rates are likely to be decreased.

The logistics of isolating cells from the patient, processing these cells and returning them to the patient will have to take place in a limited time period, for example, Provenge® (Dendreon Corporation, USA) a non-expanded cell-based therapy has a processing time of up to 18 hours. Process timings must therefore be clearly defined which will be challenging when the difference in growth kinetics is so variable and the process must be run assuming the minimum possible expansion rate of the product to avoid creating a production bottleneck. The implications of this are that low growth rate cells greatly reduce the efficiency of the process, which is likely to increase the cost of developing autologous cell-based products.

Table 4.1. Process time required to manufacture a theoretical batch of 350 million BM-hMSCs demonstrating variation in process time between and within donor material. Assumptions – Starting population of 2M BM-hMSCs, expanded in a T-flask process.

BM-hMSC line	Per dose of 350 million BM-hMSCs			mL culture media per million cells
	Process Time (days)	Number of Passages	Inter Batch Range (days)	
M0	14.2	3	0.5	87
M1	23.3	4	5.0	159
M2	17.6	4	1.6	117
M3	27.4	5	6.8	151
M4	18.7	4	0.9	129

The development of allogeneic cell-based therapies represents an off-the-shelf business model more akin to current biopharmaceutical production. These allogeneic processes can be scaled-up to treat multiple patients from a single batch which is likely to increase the cost-effectiveness of the product due to increasing economies of scale, simpler supply logistics and larger amounts of material for quality control (QC)/quality assurance (QA) testing in comparison to autologous processes. Material from multiple donors must therefore be assessed in order to create a master cell bank with enough material to manufacture cells to meet the commercial demand for the cell-based therapy.
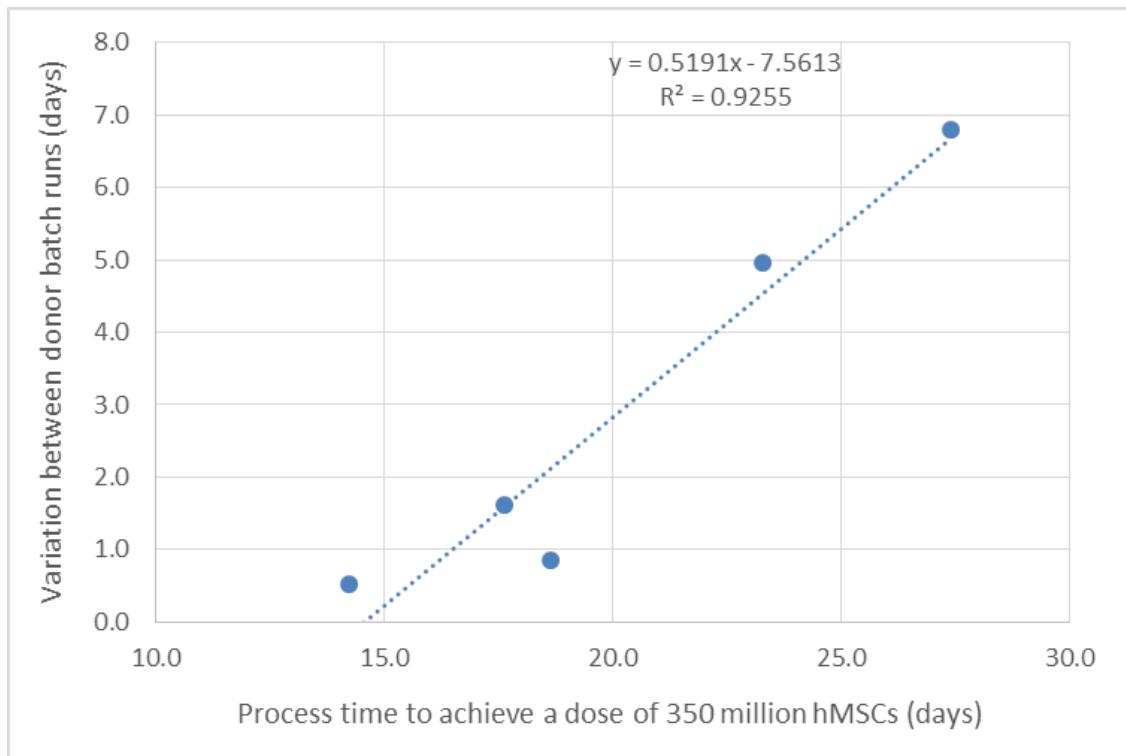
Figure 4.2. Correlation showing that the BM-hMSC donors with increased process times to achieve a therapeutic dose of 350 million cells have increased variation between batch production runs

Figure 4.1b shows the box and whisker plots for the variation across five BM-hMSC lines, which increases with passage number and time in culture. The divergence in cell growth will create an issue for processes with a high expansion ratio, as a consistent process will be harder to obtain the longer the cells are in culture. This highlights the importance of developing a process control strategy that is capable of reducing this divergent culture, minimising the time required for *in vitro* expansion, or ideally producing a convergent process, once it is transferred to a large-scale bioreactor system.

The divergence in growth characteristics of BM-hMSCs from multiple donors has implications for the development of allogeneic cell-based therapy manufacturing processes, as they will require a high cell expansion ratio at large scale in order to produce sufficient cell numbers to meet the product demand. Furthermore, as the cells are cultured for a longer period of time, the number of manipulations increases, which has the potential to introduce increased variability into the process. Automated and closed processes have the potential to reduce the

inherent variability in each of these process manipulations and are likely to play a key role in the development of allogeneic cell-based therapies.

The development of an allogeneic product also necessitates a master cell bank, from which the final product can be manufactured (Wuchter *et al.* 2014). The cost of developing a master cell bank is typically high and cannot be recovered until the product receives market approval, adding to the funding gap in development of allogeneic cell-based therapies. The quality and consistency of the master bank is critical, as once it has been created it cannot be changed and therefore a high level of product and process understanding is required, coupled with rigorous safety and quality testing to ensure that the product in the master cell bank is suitable for the manufacture of the cell-based therapy product. The key advantage of an allogeneic process over an autologous process, however, is that the cellular material in the master cell bank can be selected based on rigorous product screening to control the variation in process input material. This will allow for increased consistency in desired product attributes throughout the manufacturing process, driving down the cost of these therapies as they increase in scale.

4.2.3 Human MSC metabolite flux over multiple passages

The relative metabolite production rate and nutrient consumption rate can be seen in Figure 4.3, with the per cell metabolite flux showing differences across the five BM-hMSC lines over the 30 days in culture. The net glucose consumption rate for the BM-hMSC lines remained relatively stable throughout the 30 days of culture with the exception of M3, which showed an increase at the end of the culture period. The increase in net glucose consumption of M3 is linked with an increase in the net lactate production rate (Figure 4.3b). This is primarily associated with a reduction in the proliferative rate of the M3 cell line towards the end of the culture process. Variation in net metabolite flux across the cell lines has implications for the operation and control of autologous bioprocesses, as this will change the required nutrient feeding strategy employed during the manufacturing process.
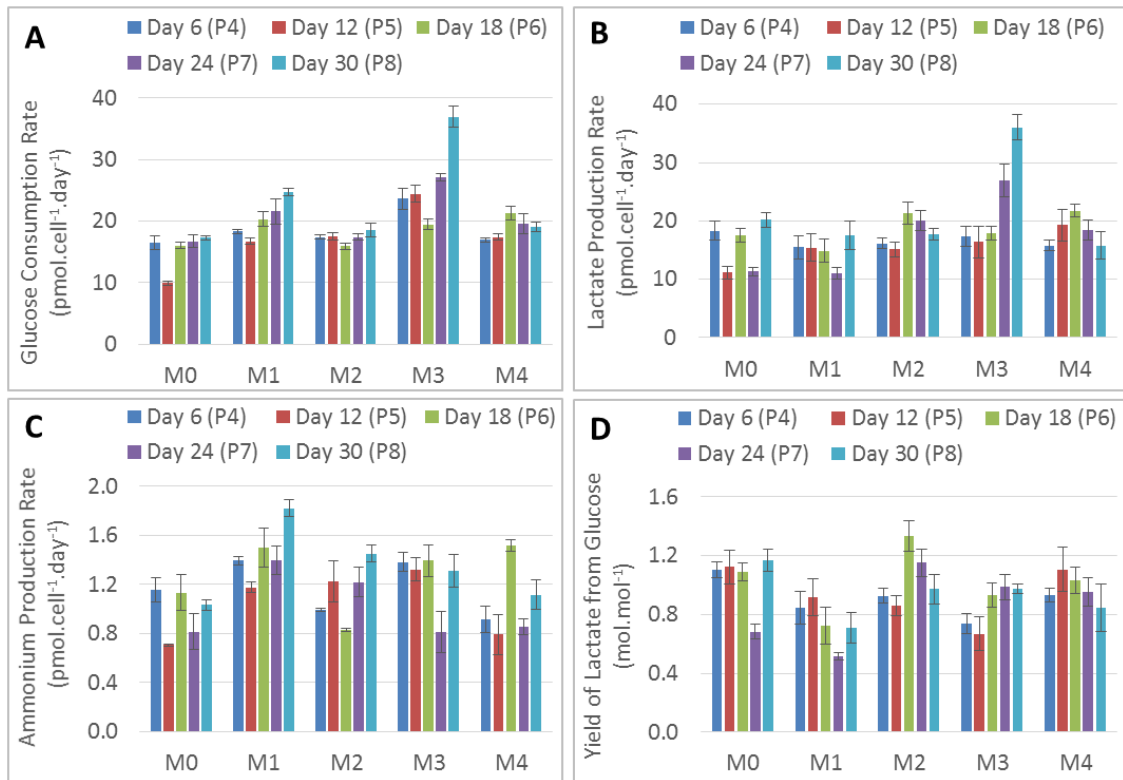
Figure 4.3. Metabolite consumption and production of the five BM-hMSC lines over five passages. Showing (A) Specific glucose consumption rates; (B) Specific lactate production rates; (C) Specific ammonium production rates; (D) Specific yield of lactate from glucose. (Data shows mean ± SD, *n = 4*)

The increase in the lactate production of M3 (Figure 4.4) has the potential to cause the build-up of toxic components that would need to be limited either by dilution (medium exchange) or removal from the process. If the levels of nutrient utilisation and metabolite production vary between donors in this way, control systems must be developed and integrated within the manufacturing process with the ability to neutralise this effect and maintain a consistent process, which will be critical for the successful regulation of an autologous manufacturing process. As well as metabolites, process parameters such as dissolved oxygen concentration and pH should also be controlled as they will have a profound impact on the critical product attributes (Lavrentieva *et al.* 2010c), which could be different for each donor BM-hMSC line. Control of nutrients and metabolites will become particularly important if the bioreactor process is operated at high cell densities, as the consumption of nutrients and production of metabolites will occur at an increasing rate.

Figure 4.4 shows the live metabolite concentrations of glucose, lactate and ammonium over the five experimental passages for each of the donor BM-hMSC lines. During the expansion process for BM-hMSCs, it is important that the concentration of glucose is maintained as it represents the main carbon source for anaerobic glycolysis, the primary metabolic pathway for glucose utilisation of BM-hMSCs (Higuera-Sierra *et al.* 2009). The concentration of glucose generally reaches a minimum at day six of culture, as the number of cells.ml^{-1} reaches a maximum. M0 showed the lowest concentration of glucose which occurred on day six of the first experimental passage at 2.80 ± 0.26 mmol.L^{-1}. In contrast to this, BM-hMSC donor M3 reached a minimum glucose concentration on day six of experimental passage five with 2.88 ± 0.12 mmol.mL^{-1} when the cell growth rate was at its lowest. This is likely due to the increased cellular stress as the BM-hMSCs undergo senescence and consuming increasing amounts of glucose, with reducing the available glucose concentration in culture shown to reduce this onset of senescence (Lo *et al.* 2011).
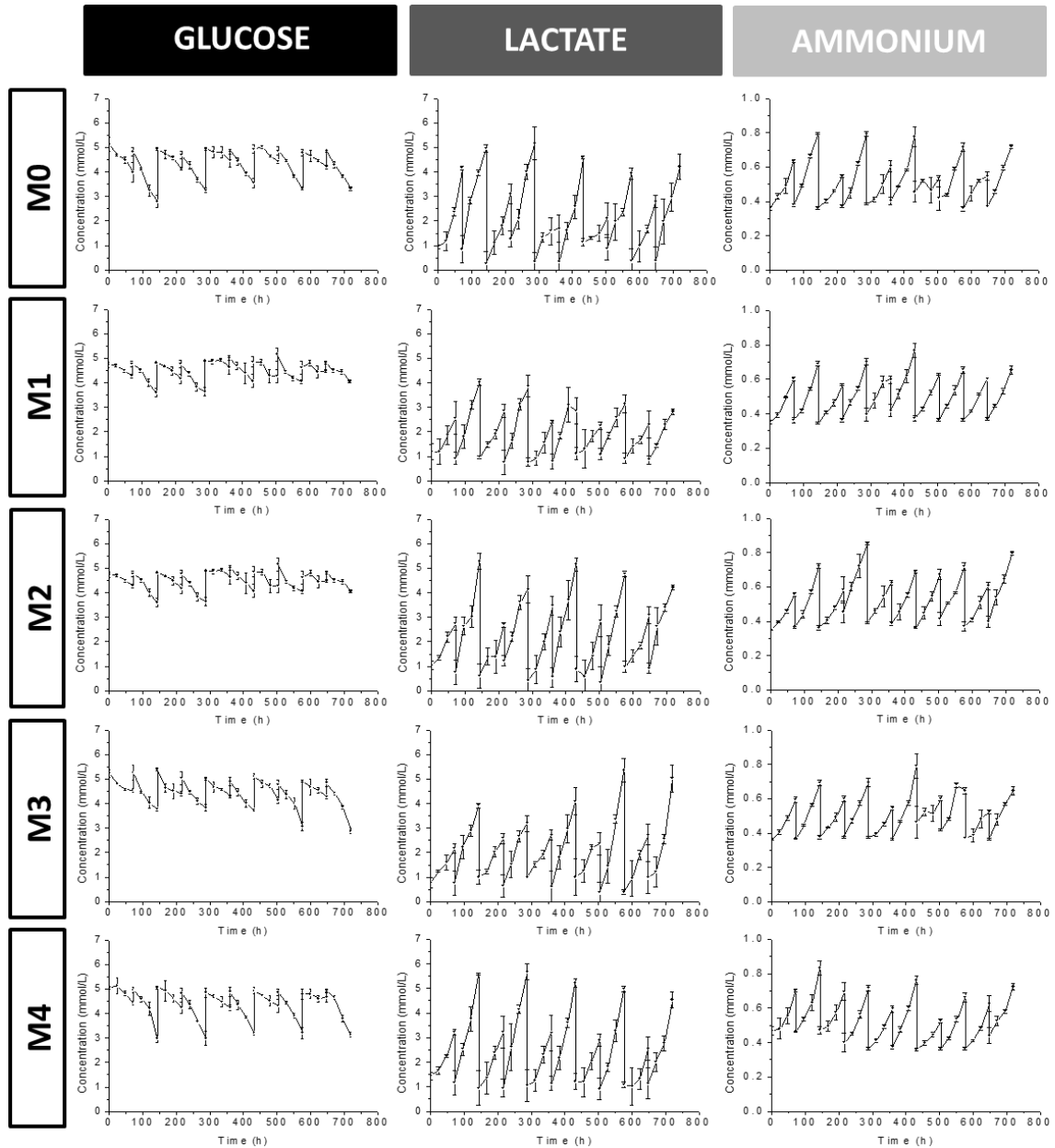
Figure 4.4. Metabolite consumption and production showing the difference between the BM-BM-hMSC lines over five passages. Daily medium samples were taken and analysed for glucose, lactate and ammonium concentration. (Data shows mean ± SD, n = 4)

In addition to the maintenance of glucose concentration during culture, the levels of lactate and ammonium must be minimised as they have the potential to inhibit the growth of the BM-hMSCs. These have previously been determined experimentally to be greater than 20 mmol.L^{-1} for lactate and 2 mmol.L^{-1} for ammonium (Schop *et al.* 2009b). As with the minimum concentration of glucose, the concentration of lactate generally reaches a maximum at day six

of culture, as the number of cells.ml^{-1} reaches its maximum. M0 produced the highest concentration of lactate which occurred on day six of the first experimental passage with 4.96 ± 0.17 mmol.L^{-1}. In contrast to this, BM-hMSC donor M3 reached a maximum lactate concentration on day six of experimental passage four with 5.36 ± 0.48 mmol.mL^{-1} when the cell growth rate was at its lowest. This is again likely due to the increased cellular stress as the BM-hMSCs undergo senescence, consuming increasing amounts of glucose and concurrently producing increasing amounts of lactate. Despite the increase, this concentration of lactate is still below the inhibitory level of 20 mmol.L^{-1} as determined previously for BM-hMSCs.

Similarly, the concentration of ammonium generally reaches a maximum at day six of culture, as the number of cells.ml^{-1} reaches its maximum. M0 produced the highest concentration of ammonium on day six of the first experimental passage with 0.80 ± 0.01 mmol.L^{-1}. Again, in contrast to this, BM-hMSC donor M3 reached a maximum ammonium concentration on day six of experimental passage three with 0.79 ± 0.07 mmol.mL^{-1}. Despite the increase throughout culture, this concentration of ammonium is still well below the inhibitory level of 2 mmol.L^{-1} as determined previously for BM-hMSCs, demonstrating in all instances that the medium exchange regime employed in this monolayer process is sufficient to maintain the required levels of glucose, lactate and ammonium required for sustained BM-hMSC expansion.

4.3 Identity of BM-hMSCs from multiple donors

4.3.1 Experimental overview

Perhaps one of most important aspects of the manufacture of cell-based therapy products is the definition and measurement of cell characteristics (Williams *et al.* 2012). These can be broken down into identity, potency, purity and safety which must all be considered during product development (Carmen *et al.* 2012a). The identity of BM-hMSCs must be maintained throughout the expansion process and establishing a baseline for the monolayer process is important to ensure the donor cells meet the minimum criteria of a BM-hMSC. The BM-hMSC morphology has been assessed during the expansion process outlined in Section 4.3, using a representative phase contrast microscopy image of the BM-hMSCs adhered to the surface of a tissue culture flask. Additionally, the tri-lineage differentiation potential of each BM-hMSC donor has been assessed after five experimental passages (total of seven cell passages) using the protocol outlined in Section 3.4.4 with representative images taken of each donor. Multicolour flow cytometry has been used to assess the co-expression of surface markers on the BM-hMSCs after five passages, using the protocol in Section 3.4.5. Finally, the genotype of three of the BM-hMSC donors has been verified by short tandem repeat (STR) analysis after five experimental passages to ensure the BM-hMSC cultures have remained genetically stable and have not become contaminated during subsequent culture.

4.3.2 Morphology of BM-hMSCs from multiple donors

Morphology has been used for decades as a qualitative assessment of BM-hMSC identity and has also been used as part of the release test for approved cell-based therapies, for example Carticel® (Genzyme, USA) includes morphology as part of their wider product release tests. Figure 4.5 shows the difference between the morphology of the BM-hMSC lines after five days in culture, with clear differences between them. Despite this, the majority of the BM-hMSC donors display the spindle-shaped, elongated morphology outlined by Pittenger *et al* (Pittenger *et al.* 1999), particularly at day six of monolayer culture.

The implications for this difference in cell morphology can be appreciated when considering that an adherent cell manufacturing process will be based upon a fixed surface area for cell expansion. With such differences in cell morphology in terms of size and alignment, the effective number of cells per square centimeter of these two cell lines when confluent varies greatly, creating an issue for these manufacturing processes based upon a fixed surface area. In

these processes, the final cell number at harvest will vary greatly between patients due to these morphological differences. Considering that manufacturing processes for autologous cell-based therapies will likely have a minimum number of cells per dose, this variation will greatly increase the risk of suffering product batch failure as this minimum number of cells per dose may not be met. Increased batch failure rate will likely increase the inherent risk and inevitably the cost of autologous cell-based therapy products. In addition to the challenges relating to the number of cells obtainable per unit area, the cell size will likely play a role in the downstream processing and delivery of the cells to the patient.

The isolation procedure and subsequent positive selection of input material for these patient specific processes will be critical in reducing the failure rate of these manufacturing processes. Robust and reproducible isolation protocols need to be established to minimise variability of source material and selection criteria based on desired product attributes should be identified at an early stage of development. These isolation and selection processes will likely reduce process variation by placing controls on the input to the process, which will be critical to the success of these personalised cell-based therapies.
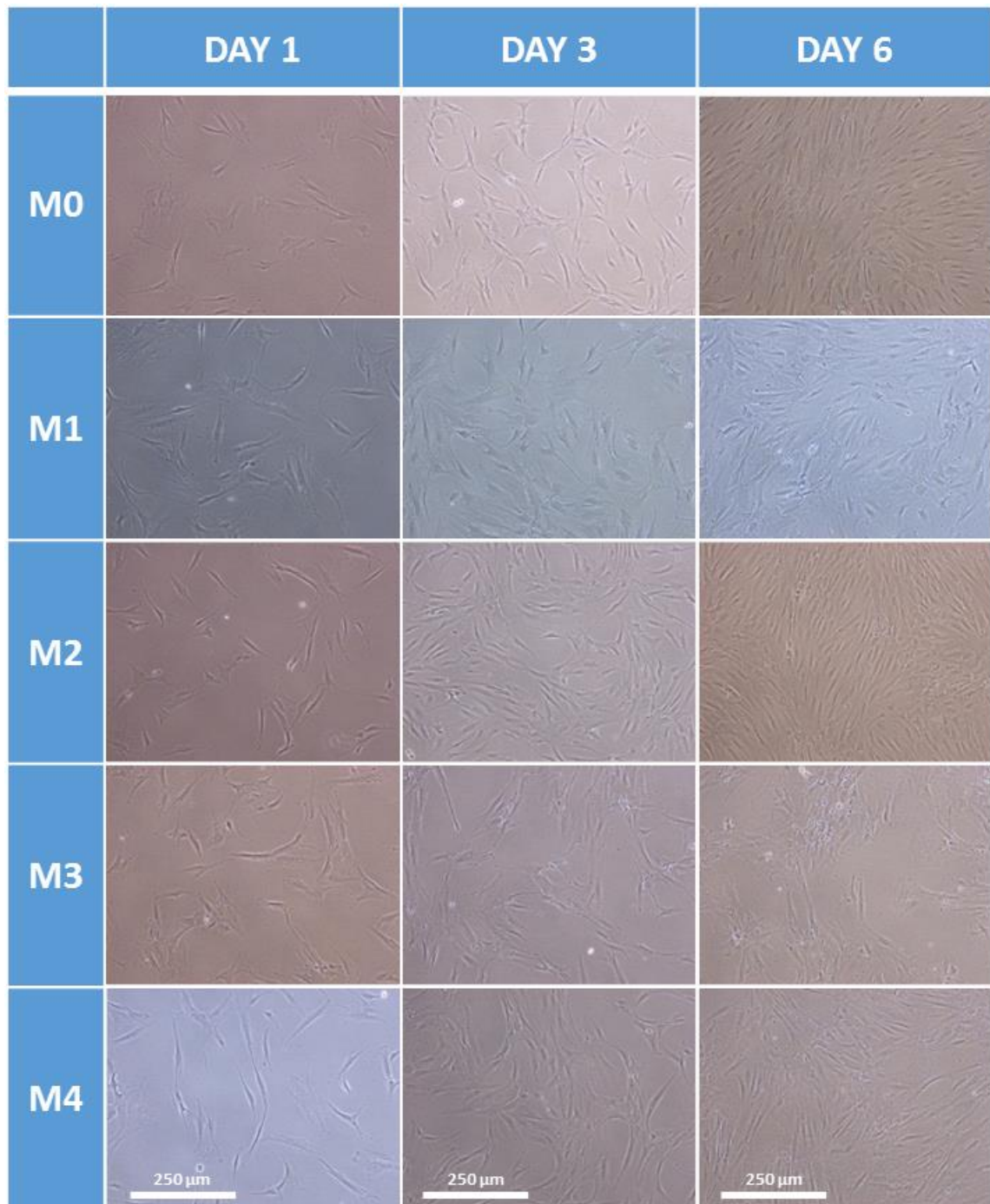
Figure 4.5. Phase contrast images showing the difference in BM-hMSC morphology throughout six days of culture

As well as the cost implications of a product batch failure it is also important to consider the implications of such an occurrence in terms of not being able to treat a patient with an autologous therapy (Hampson *et al.* 2008). This represents a limitation to the use of such therapies and creates a challenge that has not been experienced with traditional medical

treatments. Depending on the severity of the clinical indication, this has the potential to cause complications and repetition of the isolation, expansion and delivery process may not be possible. It is clear that autologous therapies represent an opportunity to deliver cell-based therapies from a scale-out process and require innovation beyond current biopharmaceutical manufacture, however, subtle differences in this approach as highlighted above must be considered during product development and commercialisation.

4.3.3 Tri-lineage differentiation of BM-hMSCs from multiple donors

In addition to the BM-hMSC plastic adherence described in Section 4.3.2, BM-hMSCs from all donors must demonstrate the ability to differentiate down the osteogenic, chondrogenic and adipogenic lineages *in vitro* as defined by the International Society of Cellular Therapy (ISCT) (Dominici *et al.* 2006). This qualitative demonstration of tri-lineage differentiation potential for all donor BM-hMSCs can be seen in Figure 4.6, despite the differences discussed in Section 4.2. The BM-hMSCs cultured in chondrogenic medium as micromasses have stained positive for the presence of glycosaminoglycans (GAGs) with Alcian Blue, indicative of chondrogenic differentiation. In addition, BM-hMSCs cultured in adipogenic medium have formed lipid vacuoles (stained with Oil Red-O) and BM-hMSCs cultured in osteogenic medium have demonstrated the production of alkaline phosphatase and calcium, stained black with silver nitrate.
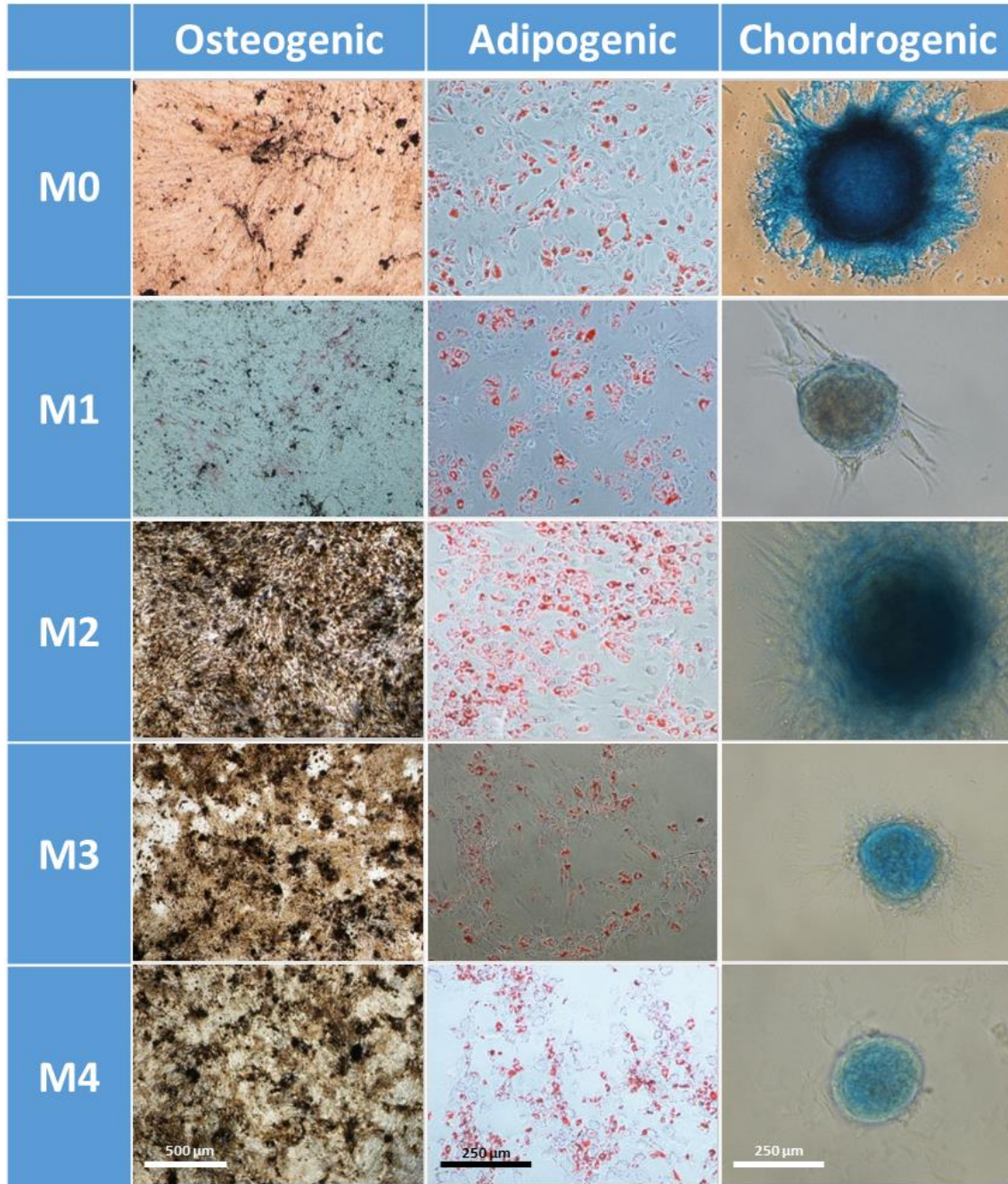
Figure 4.6. Tri-lineage differentiation potential of BM-hMSC lines using phase contrast microscopy. Showing osteogenic differentiation by staining for alkaline phosphatase and calcium deposition, adipogenic differentiation by staining with Oil Red O and chondrogenic differentiation by staining with Alcian Blue.

4.3.4 Immunophenotype of BM-hMSCs from multiple donors

The development of a multiparameter flow cytometry method to assess the co-expression of surface markers on BM-hMSCs represents a step forward in immunophenotype analysis (Chan *et al.* 2014a). The simultaneous expression of positive and negative surface markers identities the cell population that meets all of the immunophenotype requirements, providing enhanced analytical resolution over the conventional method of assessing a single marker at a time. In addition, by taking a multiparameter approach, the phenotype analysis of BM-hMSCs requires fewer cells and reagents as well as a decreased operator time representing a significant cost and time saving during the process.

Despite the differences in cell growth and net metabolite flux described in Section 4.1, all of the BM-hMSC lines displayed the expected immunophenotype by the positive co-expression of CD73, 90 and 105 and negative co-expression of CD34 and HLA-DR at the start and end of the culture process (Table 4.2). This level of expression has been maintained above 90% for all of the BM-hMSC donors across five experimental passages and 30 days in culture, demonstrating that cellular changes in growth kinetics and net metabolite flux do not have an effect on the expression of BM-hMSC surface markers.

Table 4.2. Multiparameter flow cytometry showing percentage co-expression of CD90+, CD73+, CD105+, CD34- & HLA-DR- of each BM-hMSC line at day 0 (passage 1) and after day 30 (passage 5). Mean value ± SD, in all cases 10,000 events were measured.

BM-hMSC line	Day 0 (P3) Culture	Day 30 (P8) Culture
M0	98.97 ± 0.19 %	97.78 ± 2.26 %
M1	96.21 ± 0.22 %	95.97 ± 0.42 %
M2	98.19 ± 0.09 %	95.13 ± 2.53 %
M3	93.60 ± 2.51 %	96.56 ± 0.42 %
M4	98.14 ± 0.94 %	93.17 ± 1.60 %
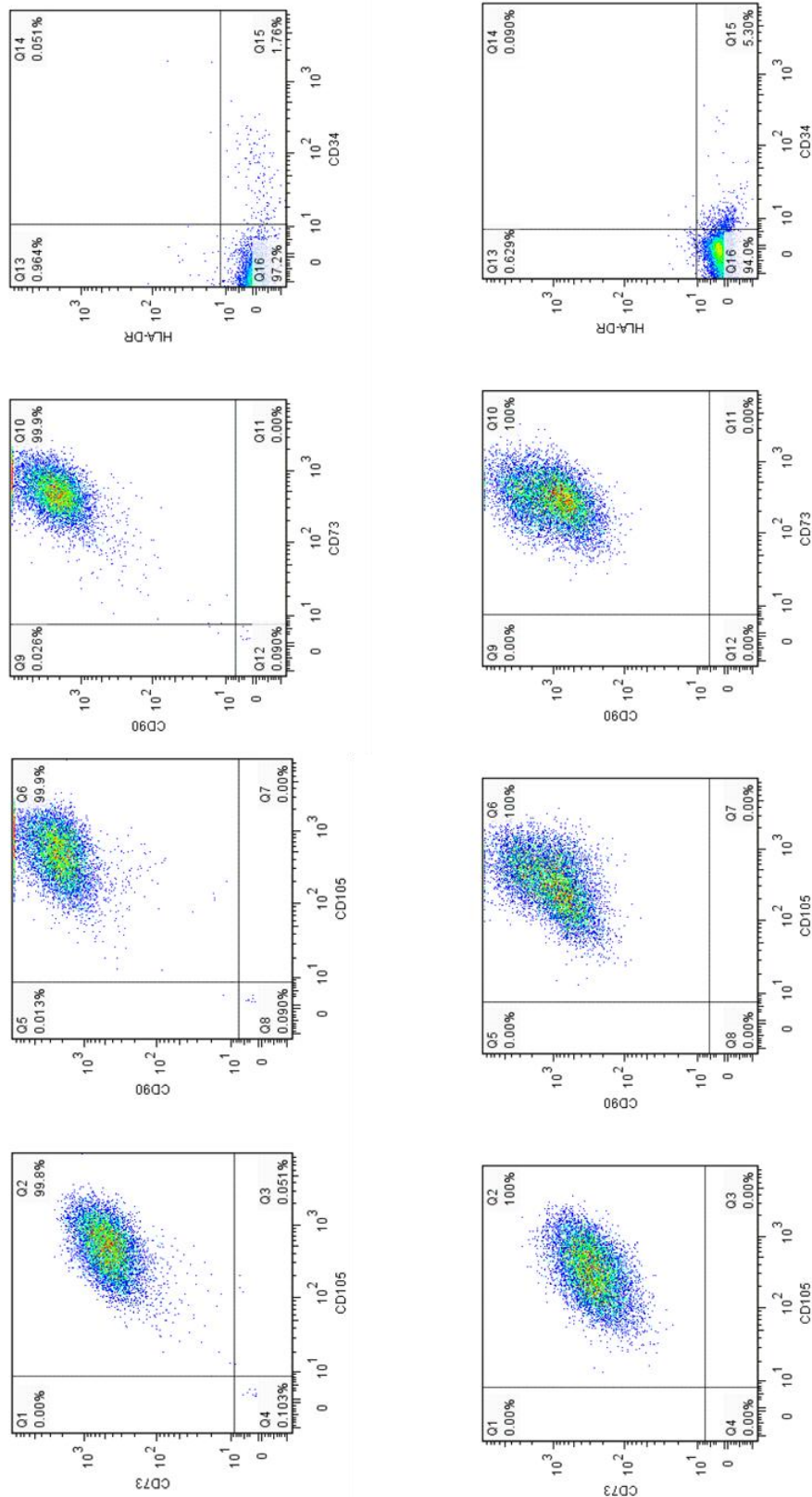
Figure 4.7. Exemplar multiparameter flow cytometry plots showing co-expression of CD90+, CD73+, CD105+, CD34- & HLA-DR- at the start (passage 1, top) and end (passage 5, bottom) of expansion.

4.3.5 Short tandem repeat analysis of BM-hMSCs

Short tandem repeat (STR) analysis of M2, M3 and M4 BM-hMSC lines shows that they have retained the 16 key *loci* they are expected to express, indicating that these cell lines have retained the characteristic genotype throughout the entire culture process (Figure 4.8).
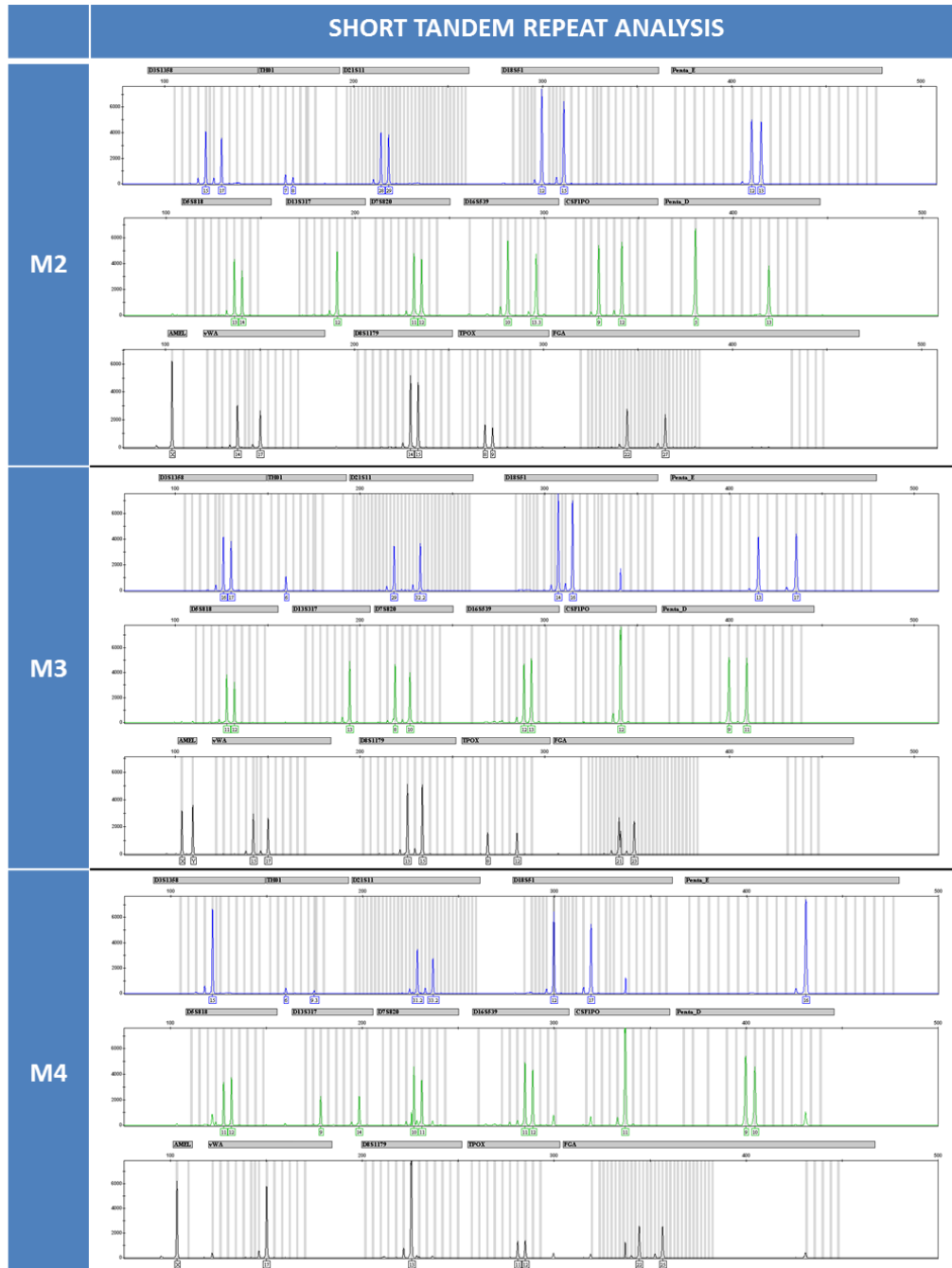
Figure 4.8. Short tandem repeat analysis of M2, M3 and M4 BM-hMSC lines at the end of the expansion process demonstrating retention of the 16 loci that are characteristic of BM-hMSCs.

4.4 Characterisation of BM-hMSCs from multiple donors

4.4.1 Experimental overview

As mentioned previously, the measurement of cellular characteristics is of critical importance for the successful development of BM-hMSC manufacturing processes. The M2, M3 and M4 BM-hMSC lines have been taken forward for further characterisation as M2 and M4 had similar growth characteristics from Section 4.2 and M3 had much lower growth potential over the five passages. To assess the colony forming unit fibroblast (CFU) potential, four T-75 flasks for each of these donor lines were taken through eight experimental passages and at the end of each of these passages remaining cellular material from each T-75 flask was plated into two T-25 flasks for CFU analysis as described in Section 3.4.9. In conjunction with this, at passages three, seven and ten, remaining cellular material from each of the four flasks was plated into three wells of a 12-well plate and quantitatively assessed for osteogenic potential as described in Section 3.4.8. The development and validation of this protocol can be found in Appendix A.

4.4.2 Colony forming unit-fibroblast potential of BM-hMSCs from multiple donors

It is widely acknowledged that a better understanding of the mechanism by which BM-hMSCs elicit their therapeutic action will be required before processes can be developed in order to preserve or potentially maximise it. Figure 4.9 shows the colony forming (CFU) efficiency of three of the BM-hMSC lines, M2, M3 and M4. Despite similarities in growth kinetics between M2 and M4 their ability to form colonies over ten passages in culture is very different, which would pose a challenge if the products were being assessed under the same QA guidelines. If the product does not meet the QA specification defined during clinical development, the product batch will be failed, creating significant consequences for both autologous and allogeneic processes. As allogeneic manufacturing processes are operated at larger batch sizes, the failure to meet the product release criteria will result in the loss of a large amount of invested capital, increasing the financial risk in the process. In contrast, the implications of a product batch failure during an autologous cell-based therapy process are that the patient will go untreated. Depending on the severity of the clinical indication targeted, this has the potential to be fatal, which will have severe implications for the health of the patient.

It can also be seen from Figure 4.9 that the CFU potential of M2, M3 and M4 decreases throughout the monolayer expansion process, which is particularly apparent for M3 and M4. This provides valuable information about the relative quality of the BM-hMSC lines as despite

demonstrating similar growth kinetics and net metabolite flux, M2 and M4 have shown very different colony forming characteristics. The trend of BM-hMSCs showing decreasing CFU potential through culture also has implications for the development of large-scale processes with a higher cell expansion ratio, as desired attributes must be maintained in the final product.
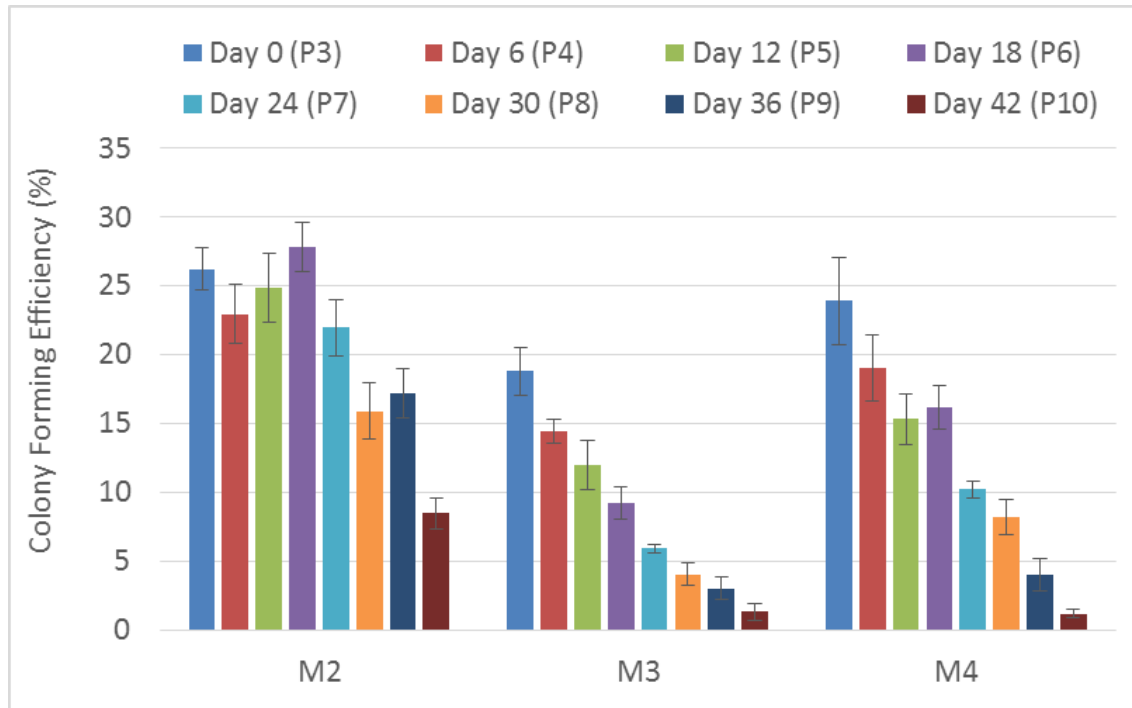
Figure 4.9. Further characterisation of three of the BM-hMSC lines throughout culture showing the differences in the colony forming unit fibroblast efficiency. (Data shows mean ± SD, n = 4)

4.4.3 Quantitative osteogenic potential of BM-hMSCs from multiple donors

The osteogenic potential of M2, M3 and M4 has also been quantified using collagen production under nine days of osteogenic differentiation (Figure 4.10). As with the colony forming unit fibroblast efficiency, the relative production of collagen under osteogenic conditions reduced significantly for M3 and M4 from passage three to passage ten, whilst the collagen production from the M2 cell line remained lower throughout culture. The loss in BM-hMSC multi-potency during *in vitro* expansion has previously been related to a loss of *in vivo* bone formation (Siddappa *et al.* 2007), which could be used as a critical-to-quality attribute (CQA) for a clinical

indication relating to bone tissue regeneration. Considering the rapid loss in activity after passage three, this would potentially limit the use of culture expanded BM-hMSCs for this type of clinical indication.
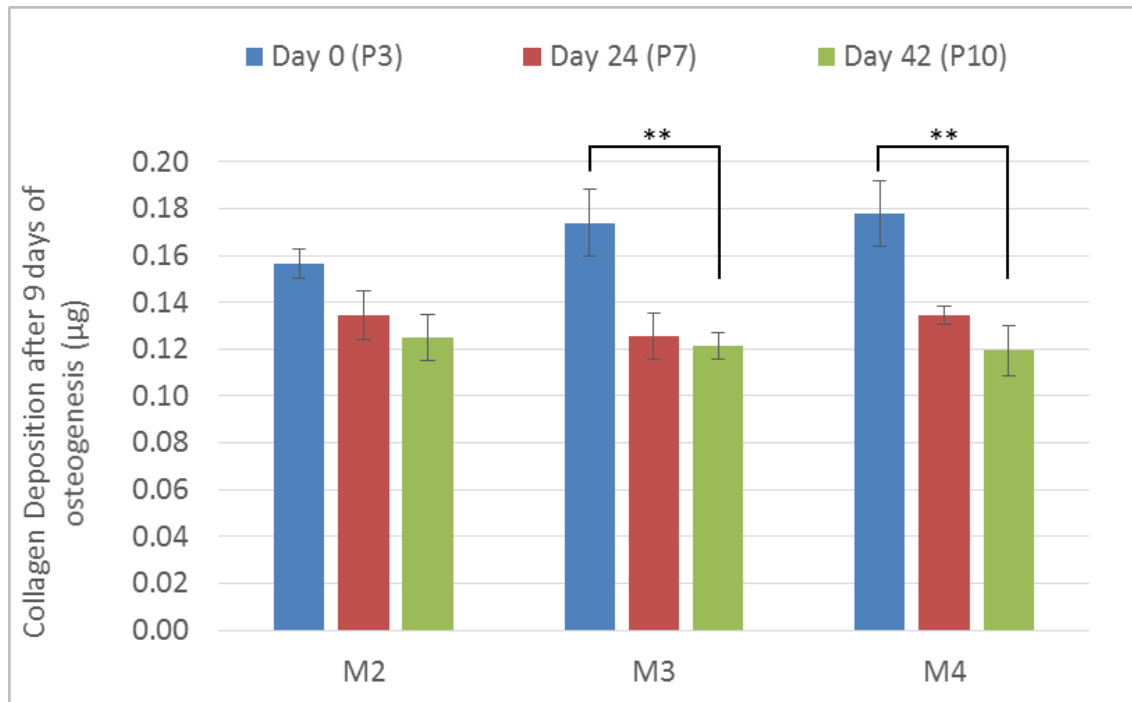
Figure 4.10. Further characterisation of three of the BM-hMSC lines throughout culture showing the differences in the quantification of the collagen deposition after nine days under osteogenic conditions. Data shows mean ± SD, n = 4, ** denotes p < 0.01.

It has been shown previously that donor age and gender has an effect on the function of BM-hMSCs (Siegel *et al.* 2013), particularly relating to their ability for immunoregulation *in vivo* (Galipeau 2013). With these intrinsic donor characteristics having such an effect on the functionality of the cell-based therapy products, it is important to understand how they will affect the final product. To maintain the consistency required within the process, it will likely be necessary to pre-screen donor material for both autologous and allogeneic products prior to the expansion process. By taking this approach it might be possible to reduce the impact of the variability in donor BM-hMSCs described, however, the ethical implication of pre-selecting patients for autologous cell-based therapies must be carefully considered.

4.5 Implications of multiple donors in bioprocess development

4.5.1 Demonstrating comparability

Any changes to the manufacturing process during clinical development will require validation of the process to ensure it remains comparable before and after the change. Validating process changes will require significant time and resource, as well as the development of functional assays to demonstrate that there has been no change to the safety or function of the cell-based therapy product. In addition to making process changes, comparability must also be demonstrated if a cell-based therapy product is to be manufactured at multiple facilities (Hourd *et al.* 2014b). Multisite manufacture has the advantage of reducing the capital cost for scaling out product manufacture to meet commercial demand as well as reducing the inherent risk of having a single manufacturing facility.

The process of demonstrating product comparability is not a trivial one and must go beyond the conventional in-process and product release characterisation, requiring a large amount of process and product data during development to act as a stable foundation from which to demonstrate product comparability. At the core of this dataset is the establishment of a set of product CQAs linked to the product mechanism of action for a specific clinical indication. Demonstrating this level of product comparability for a process that is expanding cells from multiple donors will be challenging, as variability in the input material will reduce the process consistency. In addition to this, with a divergence in BM-hMSC growth as seen in Figure 4.1b, increasing the number of product population doublings will make the process of demonstrating comparability more challenging still. Driving a consistent process will therefore be a logical first step towards developing these comparable processes, with reliable control strategies forming the basis for this consistency. Another aspect of ensuring consistency is sufficient control on the process input materials such as reagents, culture medium and disposables.

As can be seen from Figure 4.9 and Figure 4.10, the characteristics of each of these cell lines changes throughout the culture process. Depending on the target indication and the set of CQAs for the cell-based therapy product, this will make the demonstration of process comparability challenging for expanded cell-based therapy products. Each of the product characteristics monitored during this study have shown a reduction as the number of cell population doublings increases, a clear sign that reducing the expansion ratio of the product where possible will improve the chances of maintaining product functionality and demonstrating comparability.

Understanding these process changes could be greatly improved by a detailed analysis of the metabolic activity of these products. Figure 4.3 shows the net metabolite flux of glucose, lactate and ammonium, however, understanding the metabolic intermediates such as pyruvate would also aid in demonstrating that process changes have not inadvertently affected the product characteristics, an important aspect of process comparability.

4.5.2 Process analytical technology (PAT)

As highlighted above, defining and measuring relevant product characteristics forms a critical part of developing successful manufacturing processes for cell-based therapies. If these processes are to be successfully transferred to a scalable manufacturing platform, these parameters must not only be measured, but must be integrated into online monitoring and control strategies. Process analytical technology or PAT is a system for analysing and controlling manufacturing processes through measurement of product attributes to ensure final product quality, proposed by the Food and Drug Administration (FDA) (Services 2004).

This process can be broken down into three distinctive steps (S. Rathore *et al.* 2009):

1. Understanding of the product quality attributes and how process parameters affect them.
2. Ability to analyse quality attributes and monitor critical process parameters.
3. Control of the critical process parameters to achieve consistent product quality.

It will therefore be desirable to begin to measure online parameters in order to develop control systems to ensure that the product characteristics described in Section 4.4 remain consistent. These relevant process parameters are likely to include a combination of cell growth, medium temperature, pH, pO_2 and pCO_2, which are commonplace in current biopharmaceutical production processes (Cierpka *et al.* 2013). In addition to this, process parameters such as metabolite concentrations (glucose, lactate, ammonia and glutamine) can play a role in product understanding during the manufacturing process and should be controlled to ensure consistent product quality. The benefit of operating a production process under the guidance of PAT will likely be a reduction in product variability, which will reduce the likelihood of product batch failure. Having a detailed product understanding using online measurements also introduces the possibility for real-time release testing of product batches, which will reduce costs by reducing the quality test burden at the end of the process.

4.6 Chapter conclusions

Characterising input material from different BM-hMSC donors has allowed for an assessment of the effect of variation on developing cell-based therapy manufacturing processes. Identifying the divergent nature of the growth of multiple BM-hMSC donor lines has been identified as a potential issue for the development of both autologous and allogeneic processes where cell expansion is required. Furthermore, measuring multiple quality characteristics of these BM-hMSC lines throughout culture has demonstrated a reduction in quality as the population doubling level increases, which must be considered as these processes are scaled.

Developing manufacturing processes from multiple BM-hMSC donors will require an understanding of the effect of donor characteristics on expanded autologous and allogeneic cell-based therapy bioprocesses. Measuring informative product attributes that are characteristic of the desired therapeutic effect for each clinical indication will facilitate the development of consistent manufacturing processes and will play a key role in unlocking the value of demonstrating process comparability, allowing for any necessary process changes and multisite manufacturing models.

Having identified this variation between BM-hMSC donors and discussed the implications for patient specific and off-the-shelf manufacturing processes, steps must be taken to reduce this early in process development. With this in mind and considering the potential scalability issues associated with the use of FBS, altering the medium formulation for this monolayer expansion process prior to process transfer and scale-up will be an important step in limiting the impact of this donor variation. In addition to this, the growth medium is likely to have an influence on the growth and quality attributes of the BM-hMSCs, which will increase process yield and cost-effectiveness.

Publications arising from this Chapter:

Heathman TRJ, Rafiq QA, Chan AK, Coopman K, Nienow AW, Kara B, Hewitt CJ. Characterisation of human mesenchymal stem cells from multiple donors and the implications for large scale bioprocess development. Biochemical Engineering Journal, (2015) *(in press)*

Chan AK, **Heathman TRJ**, Coopman K, Hewitt CJ. Multiparameter flow cytometry for the characterisation of extracellular markers on human mesenchymal stem cells. Biotechnology letters, (2014) 36 (4): 731-41.

5 Improving the Yield and Consistency of BM-hMSC Expansion

5.1 Chapter introduction

Achieving the consistent manufacture of medicinal products is a key requirement for regulatory approval and begins with assessing and reducing process variation where possible (Williams *et al.* 2012). Driving a consistent process will demonstrate a state of control over the product and provides a foundation for comparability, whereby process changes during clinical development can be validated and the product can be manufactured at multiple sites.

A key aspect of these manufacturing processes is the culture medium in which the cells are to be expanded, which is typically supplemented with fetal bovine serum (FBS) (Wappler *et al.* 2013). In addition to lot-to-lot variability, there are further process constraints on the use of FBS such as limited supply (Brindley *et al.* 2012), potential for pathogen transmission and immunological reactions against bovine antigens (Kocaoemer *et al.* 2007). Human platelet lysate (HPL) has been proposed as a viable alternative, whereby blood platelets are lysed to release growth factors such as platelet-derived growth factor (PDGF), epidermal growth factor (EGF), transforming growth factor-β (TGF-β) and fibroblast growth factor (FGF) which then supplement the BM-hMSC growth medium (Lubkowska *et al.* 2012). This can be used as a patient specific supplement from their own blood plasma or pooled from multiple donors, for example Stemulate™ manufactured by Cook Regentec (USA). Furthermore, HPL has already been reported as a superior substitute to FBS for the *in vitro* expansion of BM-hMSCs (Schallmoser *et al.* 2010) and has been shown to maintain stem cell characteristics and multipotent capacity (Doucet *et al.* 2005).

Rather than simply replacing the serum source in culture medium, it is highly desirable to develop serum-free medium formulations and avoid a number of the aforementioned constraints on serum-based processes (Heathman *et al.* 2015d). Serum-free culture has also been previously shown to be amenable to scalable expansion technology such as microcarriers and stirred bioreactors, producing higher BM-hMSC yields per unit time than serum-based processes, which will be important for driving down the production cost of BM-hMSC therapies (dos Santos *et al.* 2011a). That said, the current cost of serum-free medium for research is generally higher than serum-based medium, however, as the demand increases and higher yield processes can be developed, these costs will likely be reduced over time.

Considering the innate biological variability that exists between donors and the importance of ensuring a consistent manufacturing process, driving this philosophy into process development at an early stage is critical. Therefore, the aim of this Chapter is to demonstrate how the development of a serum-free expansion process can drive increased consistency and yield of BM-hMSC manufacture between donors and explore the benefits this can bring as the process scale increases.

5.2 Growth characteristics of BM-hMSCs in different media

5.2.1 Experimental overview

Given the importance of the medium formulation on the expansion of BM-hMSCs and on the development of scalable processes, three different medium formulations have been assessed for their effect on the yield, quality and consistency of two BM-hMSC lines. From Chapter 4, the M2 BM-hMSC line has been selected for this study due to the higher growth and quality characteristics, as well as, M3 which displayed the lowest growth kinetics and a sharp reduction in cellular characteristics. The three medium formulations are as follows (see Section 3.2.1):

1. DMEM supplemented with 10% foetal bovine serum (FBS)
2. DMEM supplemented with 10% human platelet lysate (HPL)
3. Irvine Scientific PRIME-XV® MSC Serum-free medium (SFM)

Prior to this study, the concentration of HPL in DMEM was screened to assess the level required for similar growth characteristics to 10% FBS (found to be 10% HPL), the results of which can be found in Appendix B. The selection of PRIME-XV® SFM was made following a pre-screen of six commercially available serum-free media and the PRIME-XV® SFM was tested for compatibility with BM-hMSCs prior to these experiments, the results of which can be found in Appendix C. Four T-75 flasks were seeded for each BM-hMSC line, in each medium formulation giving a total of 24 flasks that were cultured for 36 days in accordance with the protocol described in Section 3.2.5. At passage the viable cell number, mean cell diameter and percentage cell aggregation was determined (Section 3.4.2) and the growth kinetics calculated (Equation 1). The culture medium supplemented with either FBS or HPL was exchanged after three days and SFM was exchanged every two days. Daily medium samples were taken and analysed for glucose, lactate, ammonia, lactate dehydrogenase (LDH) and total protein as in Section 3.4.6 on the Cedex Bio-HT. Metabolite analysis was transferred from the BioProfile FLEX to the Cedex Bio-HT as more medium components could be measured using the Cedex Bio-HT with increased accuracy and higher throughput. The metabolite concentrations and per cell metabolite flux was then calculated from these measurements (Equation 5 and 6).

5.2.2 Growth kinetics over multiple passages

Human mesenchymal stem cells are currently under clinical investigation for the treatment of many diseases, with the majority of these off-the-shelf therapies typically requiring more than one billion cells per patient (Prasad *et al.* 2011; Maziarz *et al.* 2015). In order for manufacturing processes to meet this demand, a large cell expansion ratio will be required to treat many patients from the same batch. Figure 5.1 shows the relative difference between a serum-free medium (SFM), PRIME-XV®, and medium supplemented with fetal bovine serum (FBS) or human platelet lysate (HPL) in terms of BM-hMSC growth. It is clear that the SFM offers a significantly higher proliferation rate over FBS and HPL ($p < 0.001$) with a maximum specific growth rate of 0.471 day^{-1} compared with 0.244 day^{-1} in FBS and 0.334 day^{-1} during the 36 day expansion process (Figure 5.2). This increased growth rate corresponds to a final median cumulative population doubling level of 18.15 in the SFM compared with 8.93 in FBS and 9.91 in HPL culture across the two donors at the end of the 36 day expansion process.
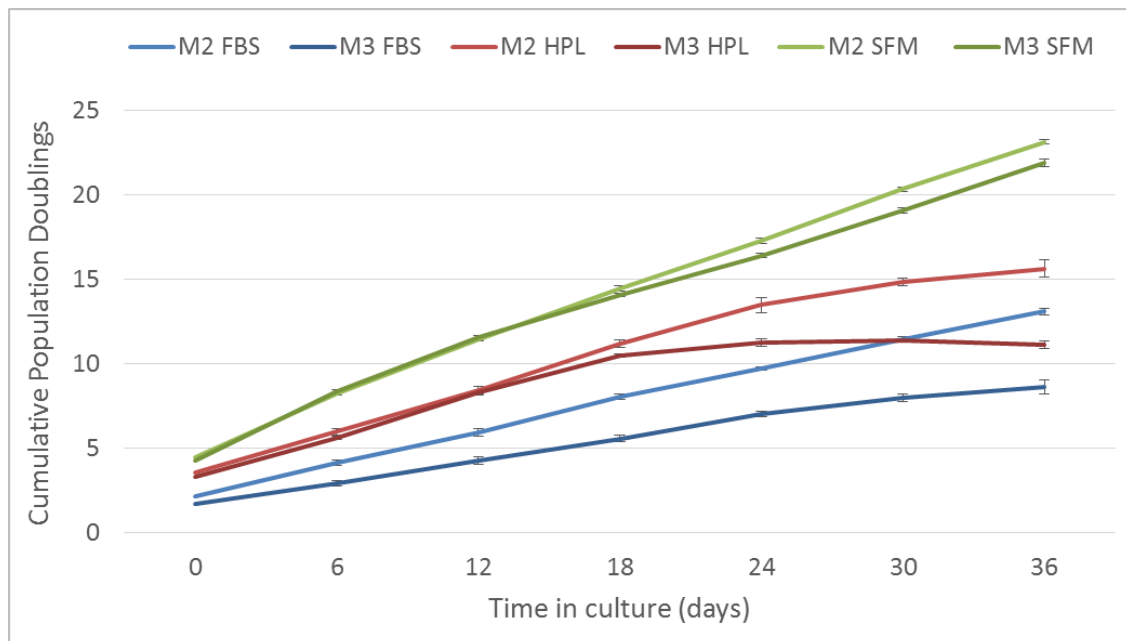
Figure 5.1. Cumulative population doublings of the two BM-hMSC lines over 36 days of expansion in FBS, HPL and SFM. Showing the increased consistency and yield in SFM over 36 days and increased consistency and yield in HPL over 18 days compared to FBS-containing medium. Data shows mean ± SD, n=4

This represents an increase of around 600 times the number of cells under the SFM culture compared with FBS culture over this expansion period, which dramatically increases the effective product yield and potential scalability of the SFM process to meet the needs of a large scale off-the-shelf cell-based therapy.

Cells that experience nutrient deprivation typically spend longer in the G1 phase of the cell cycle, resulting in slower proliferation (Jorgensen and Tyers 2004). The fact that the PRIME-XV® medium supported a more rapid cell growth therefore indicates that it may provide a better nutritional balance or activates growth regulation pathways such as the PI(3)K pathway, than the FBS-containing medium under the medium exchange regime employed here.
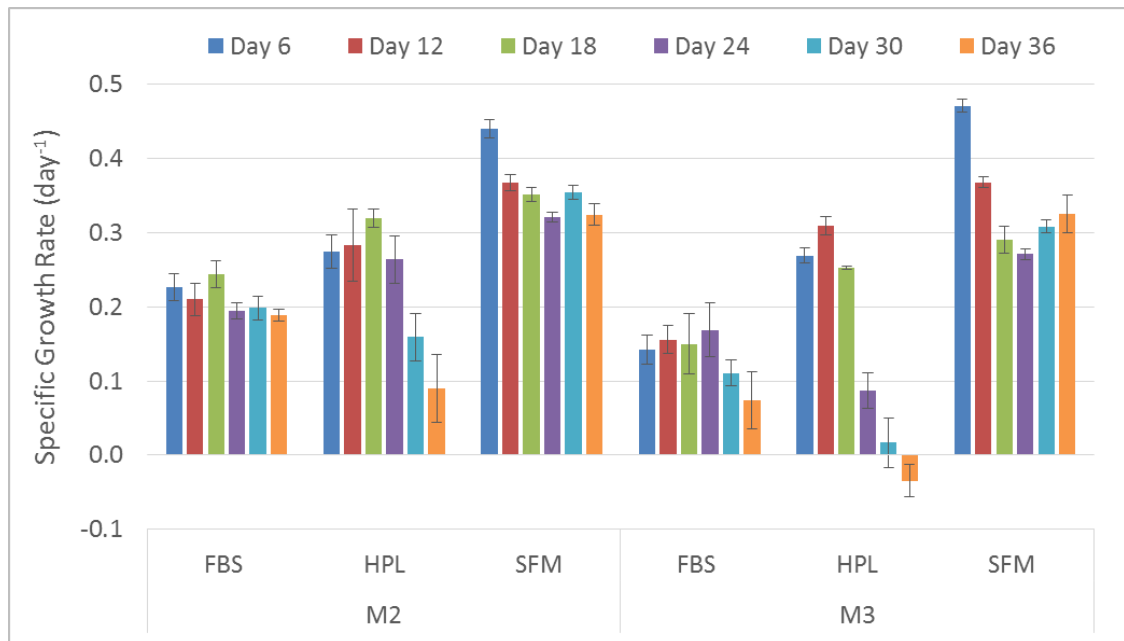
Figure 5.2. Specific growth rate of the two BM-hMSC lines over 36 days of expansion in FBS, HPL and SFM. Showing the increased consistency and yield in SFM and the decline in growth rate of BM-hMSCs in HPL culture. Data shows mean ± SD (n=4)

5.2.3 Mean cell diameter of BM-hMSCs over multiple passages

The cell diameter of the BM-hMSCs throughout the expansion process in FBS, HPL and the SFM culture has been measured to determine whether this attribute remains consistent. It can be seen from Figure 5.3 that the BM-hMSCs cultured in the SFM have a smaller diameter

throughout the expansion process compared to FBS and HPL, which in volumetric terms equates to around half the size (assuming complete sphericity). The increase in cell diameter of M2 and M3 towards the end of the culture process is associated with a reduction in growth rate (Figure 5.4) and therefore stability in cell diameter throughout culture will be important in order to maintain BM-hMSC growth kinetics. Figure 5.4 shows the relationship between the mean cell diameter of the BM-hMSC population against the growth kinetics of the subsequent passage. This demonstrates that the smaller BM-hMSCs generally have higher growth kinetics, which has been reported previously (Majore *et al.* 2009; Christodoulou *et al.* 2013). In addition to growth, BM-hMSC size is also linked to aging of BM-hMSCs and loss in differentiation potential (Stolzing and Scutt 2006; Wagner *et al.* 2010) and therefore increasing size can also be used as a surrogate marker of BM-hMSC senescence.
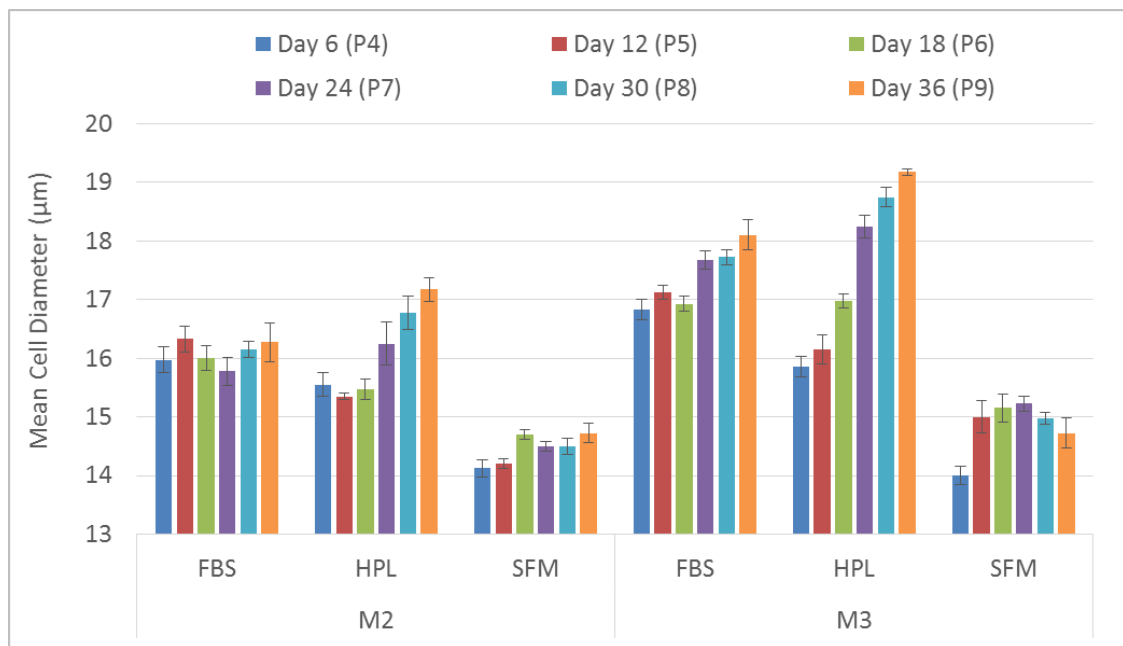
Figure 5.3. Mean cell diameter of the two BM-hMSC lines throughout 36 days of expansion in FBS, HPL and SFM. Showing the reduced mean cell diameter under SFM and an increase in HPL throughout culture. Data shows mean ± SD (n=4)

Importantly, the osmolality of the FBS-based, HPL-based and PRIME-XV® SFM are similar (0.31, 0.31 and 0.29 Osmol.kg^{-1}, respectively), further indicating that the difference in cell size noted in Figure 5.3 is not a simple matter of a change in osmotic balance, although it should be noted that the osmolality of the PRIME-XV® SFM is closer to human physiological conditions (Cheuvront *et al.* 2014). Although the reasons for this relationship are not clear, it can

nonetheless provide a basis for evaluating the stability of the BM-hMSCs throughout expansion and provide as an early indication that cell growth kinetics may begin to reduce. The smaller cell size experienced in the SFM will also allow for higher number of cells per area, an important attribute for adherent cell expansion, however, the implications of this smaller size on the functional properties must be assessed during product pre-clinical and subsequent clinical development.

$$y = -0.083x + 1.548$$
$$R^2 = 0.8705$$
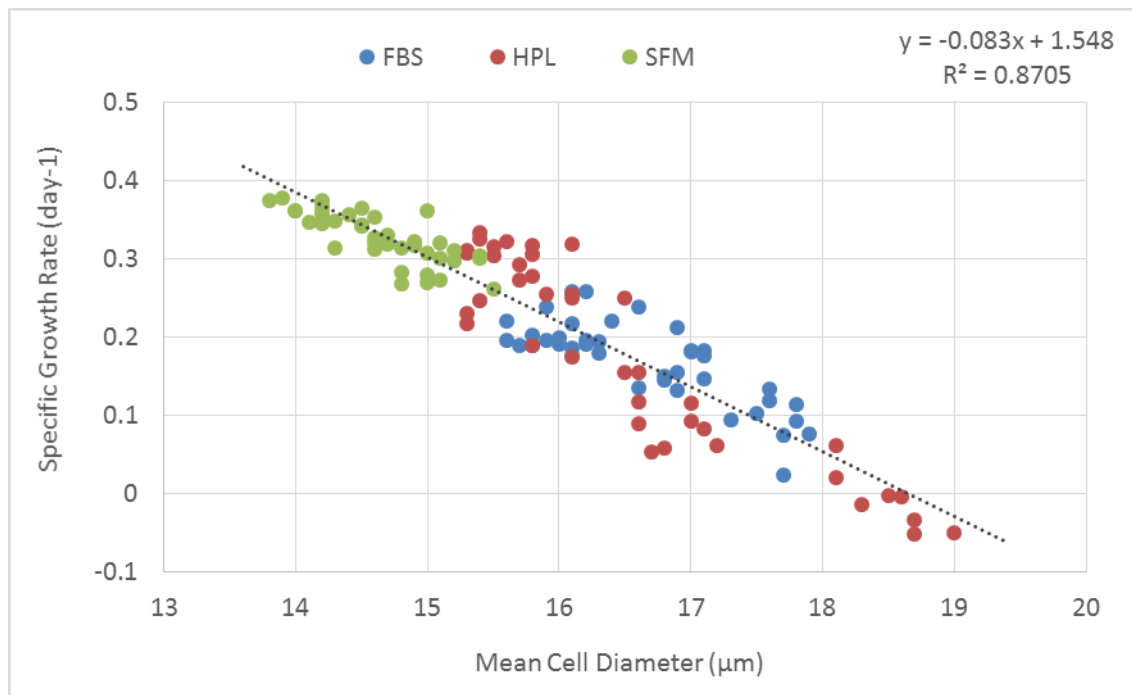
Figure 5.4. Correlation showing the relationship between mean cell diameter and specific growth rate of BM-hMSCs during the following passage, R^2=0.8705. Data shows (n=*144*)

The size of the BM-hMSC also has the potential to affect the post-transplant safety profile of the therapy and the impact of the process conditions on this attribute should be considered in relation to the delivery method (Ge *et al.* 2014). If the cell-based therapy is to be delivered by intra-arterial infusion, there is a potential risk of microembolisms and decreased cerebral blood flow which must be mitigated by altering the cell dose, infusion volume and velocity (Cui *et al.* 2015). The size of freshly isolated stem cells is ~11 µm and can be transported through capillaries, while expansion has previously been shown to increase the size to ~20 µm obstructing microvascular vessels after infusion (Moelker *et al.* 2007). Considering that BM-hMSCs cultured under FBS reached a maximum cell diameter of 18.4 µm compared with SFM

with a maximum cell diameter of 15.5 µm, the smaller cell diameter achieved under SFM would offer advantages of reduced risk of these complications. Cells of around 15 µm have previously been shown to carry reduced risk of restricting cerebral blood flow, with larger cells requiring a reduced dose and infusion rate (Janowski *et al.* 2013).

5.2.4 Net metabolite flux per BM-hMSC

The net metabolite flux of glucose and lactate has been measured in FBS, HPL and SFM culture over the expansion process to better understand the relative consistency between the donor BM-hMSCs with time in culture. Figure 5.5 shows the per cell flux of glucose for FBS, HPL and SFM culture, with a range of per cell glucose flux of 24.29, 28.77 and 8.81 $pmol.cell^{-1}.day^{-1}$ for FBS, HPL and SFM expansion, respectively. This is concurrent with the relative flux of lactate per cell (Figure 5.6), with a range of 22.47, 25.76 and 2.11 $pmol.cell^{-1}.day^{-1}$ for FBS, HPL and SFM expansion, respectively.
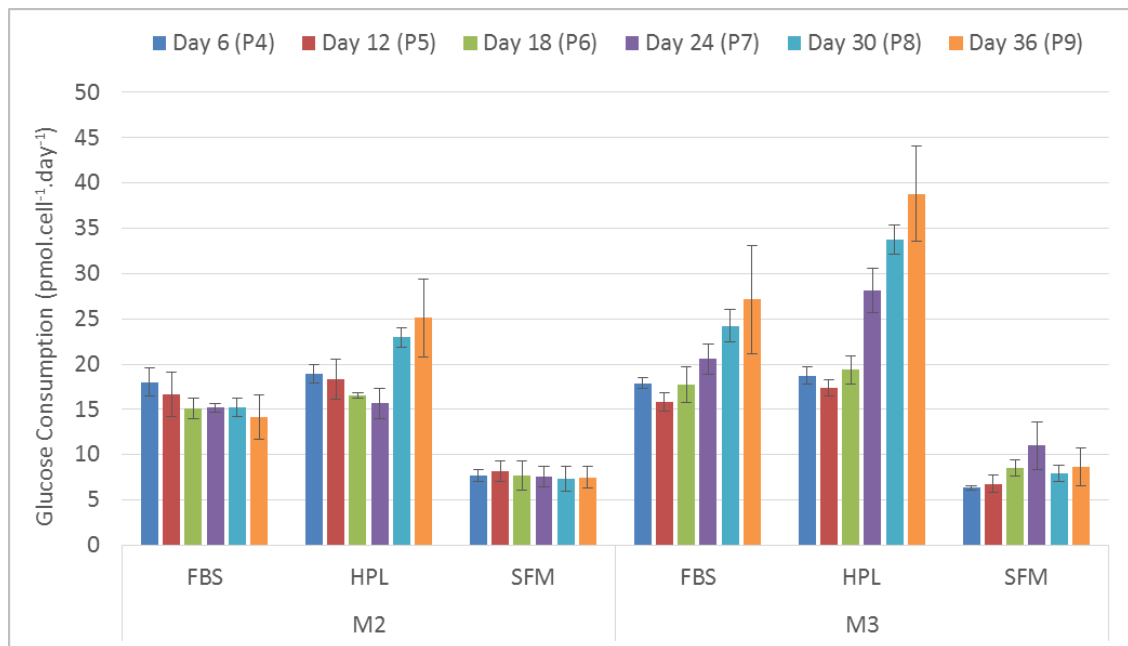
Figure 5.5. Per cell metabolite flux of two BM-hMSC lines over 36 days of monolayer expansion in FBS, HPL and SFM. Showing increasing per cell glucose consumption rate through culture in FBS and HPL. Data shows mean ± SD (*n=4)*

This increased range in per cell metabolite flux in FBS and HPL is primarily due to increased variability between donors at the end of the expansion process and is associated with a reduction in BM-hMSC growth and increase in cellular senescence that is not experienced in the SFM, despite the higher number of population doublings.
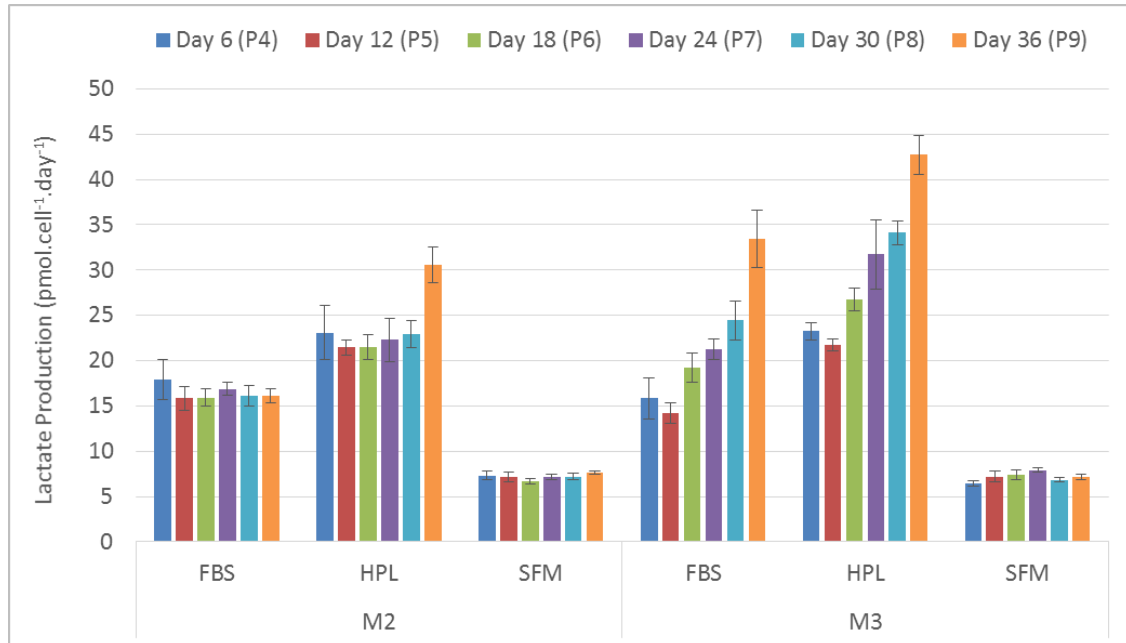
**Figure 5.6. Per cell metabolite flux of two BM-hMSC lines over 36 days of monolayer expansion in FBS, HPL and SFM. Showing increasing per cell lactate production rate through culture in FBS and HPL. Data shows mean ± SD (*n=4)*

Figure 5.7 shows the ammonia flux per cell of M2 and M3 in FBS, HPL and SFM. This shows a similar increase in the ammonia production rate towards the end of HPL expansion that was experienced with the glucose consumption and lactate production rates. This reaches a maximum of 6.92 ± 0.38 pmol.cell^{-1}.day^{-1} after 36 days expansion in M3, which is almost double the production rate measured in SFM. The yield of lactate from glucose (Figure 5.8) in SFM was typically below 1 mol.mol^{-1}, suggesting a combination of anaerobic glycolysis and oxidative phosphorylation to drive energy production (Ozturk and Palsson 1991; Cruz *et al.* 1999). The higher yield of lactate from glucose in FBS and HPL suggests increased utilisation of anaerobic glycolysis, suggesting that the BM-hMSC cultured in SFM more efficiently utilise glucose for energy production (Schop *et al.* 2008).
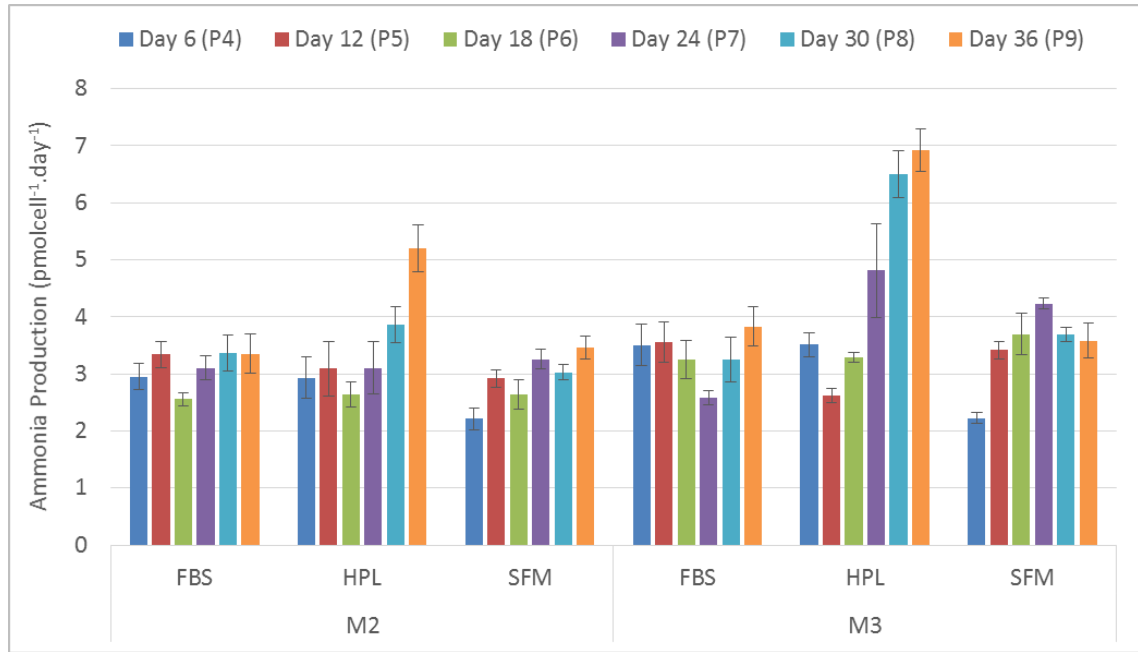
Figure 5.7. Per cell metabolite flux of two BM-hMSC lines over 36 days of monolayer expansion in FBS, HPL and SFM. Showing increasing per cell ammonia production rate through culture in HPL. Data shows mean ± SD (*n=4*)
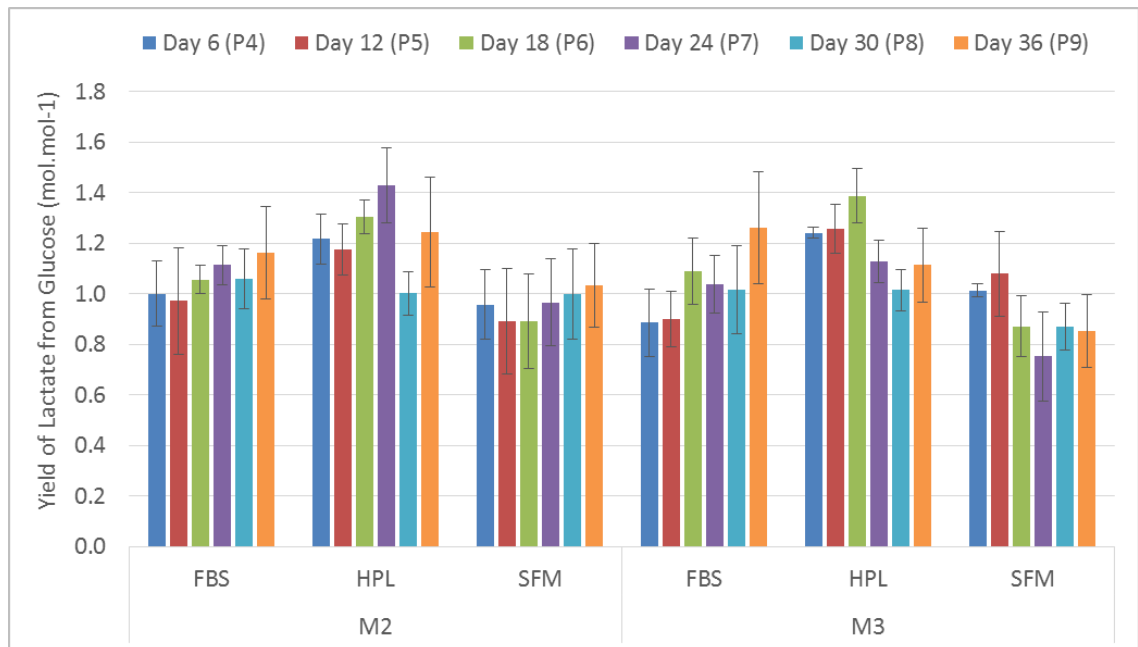
Figure 5.8. Yield of lactate from glucose of two BM-hMSC lines over 36 days of monolayer expansion in FBS, HPL and SFM. Demonstrating that BM-hMSCs use glucose *via* anaerobic glycolysis in all conditions. Data shows mean ± SD (*n=4*)

The net flux of metabolites has the potential to form part of a panel of measurements for the purposes of demonstrating comparability, whereby process changes can be evaluated for their impact on cellular characteristics. This understanding of the cell during the expansion process will also be a valuable tool during process scale-up to ensure that the interaction between the cell and its environment has not changed during technology transfer. This highlights the importance of process analytical technology (PAT), which can be employed to monitor and control process and product attributes to ensure consistency and quality in the final product. It can be seen from Figure 5.5 and Figure 5.6 that there is reduced per cell consumption of glucose and production of lactate in SFM culture, which is likely to be a beneficial product attribute as the process is scaled. This will be particularly apparent once suspension-based expansion processes routinely reach high cell densities (in excess of $1x10^6$ cell.mL^{-1}), where the buildup of waste products such as lactate have the potential to inhibit the expansion process. Considering that the culture medium is likely to contribute to a significant portion of the cost of goods for BM-hMSC production, product attributes that reduce the usage of culture medium will be increasingly beneficial at the large scale.

The increased consistency between donor BM-hMSC lines in terms of per cell metabolite flux is a further demonstration that the cells cultured in the SFM conditions show reduced inter-donor variation, an important consideration given the large amount of variation experienced in cell-based therapy manufacture. Although this has been demonstrated here for basic metabolites, there is scope to extend this analysis to a larger panel of metabolic intermediates to provide a detailed understanding of the impact of the process on the BM-hMSC metabolic characteristics during scale up. The reason for this increased consistency in the SFM has yet to be explored in the literature, however, the combination of BM-hMSCs cultured on fibronectin with serum-free growth medium has previously shown to activate the platelet-derived growth factor receptor, which is essential for cell migration (Veevers-Lowe *et al.* 2011). Activation of BM-hMSCs in this way provides a potential mechanism for the cell characteristics to converge, as the BM-hMSCs are actively forced to utilise specific cellular pathways, as opposed to serum-based culture where an abundance of various proteins are available to the cells. This combination of a fibronectin coating with growth medium supplemented with platelet-derived growth factor has been used previously to positively select for smaller, highly proliferative cell populations from bone-marrow, termed multipotent adult progenitor cells (MAPCs) (Breyer *et al.* 2006). This positive selection process could also be contributing to the increase in consistency measured in several different characteristics under serum-free conditions as discussed further below.

5.2.5 Live metabolite flux over multiple passages

The measurement of live metabolite concentrations throughout culture is important to ensure that the medium exchange regime employed is sufficient to supply the required nutrients and limit the concentrations of metabolites that have the potential to limit cell growth. Figure 5.9 show the concentration of glucose in each medium formulation for both BM-hMSC donors, demonstrating that the concentration of glucose did not fall below 2 mmol.L^{-1} at any point during the 36 days of expansion in FBS, HPL or SFM.
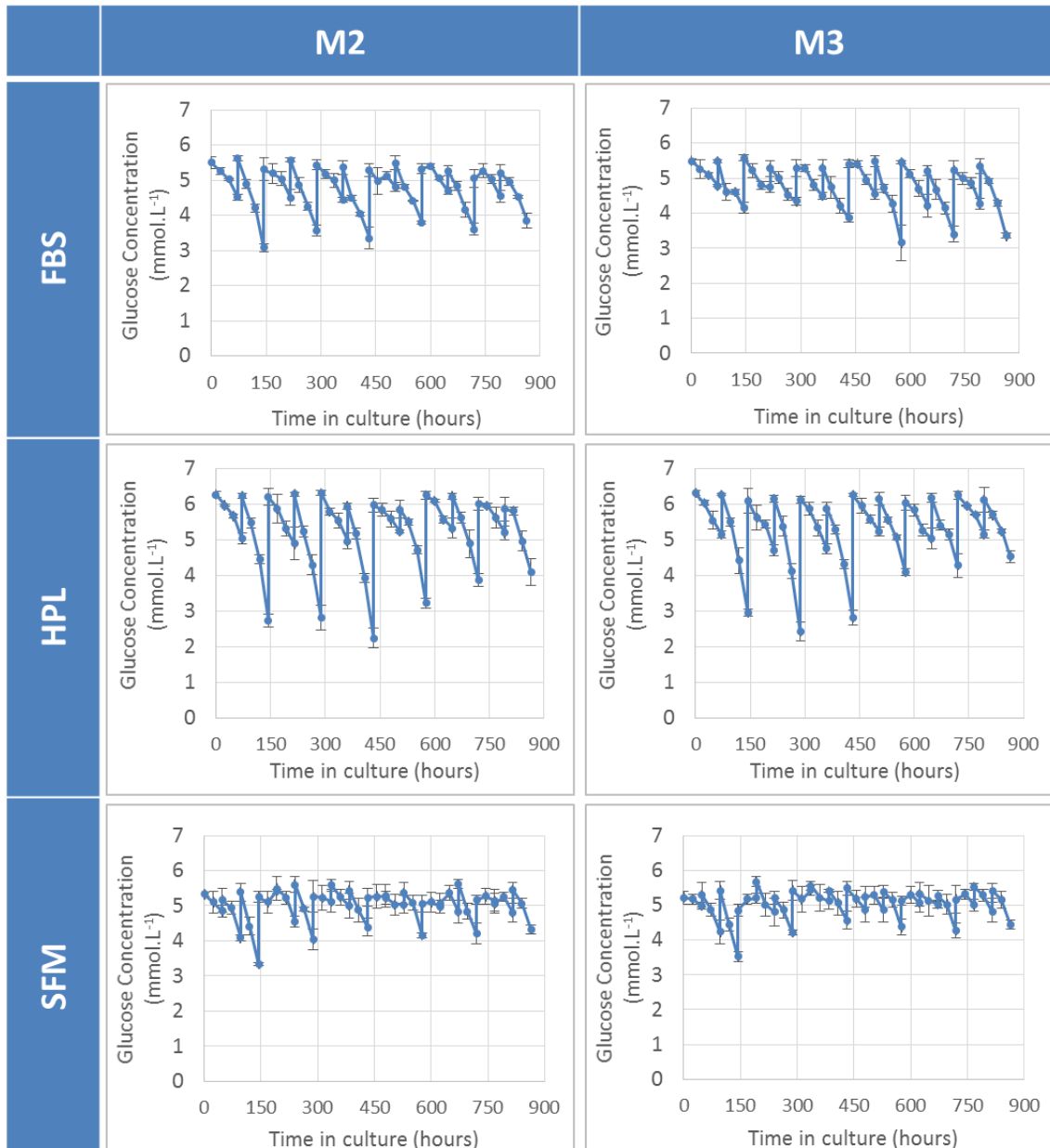
Figure 5.9. Live glucose concentration of two BM-hMSC lines over 36 days of monolayer expansion in FBS, HPL and SFM. Showing reduced glucose concentration in HPL and lower glucose utilisation of BM-hMSCs in SFM. Data shows mean ± SD (n=4)

Similarly, the concentration of lactate in the culture medium must be reduced to avoid inhibition of BM-hMSC growth and characteristics which has previously been determined to be 35.4 mmol.L^{-1} for BM-hMSCs (Schop *et al.* 2009b). It can be seen from Figure 5.10 that the maximum level of lactate for FBS and HPL culture was 6.67 ± 0.06 and 9.44 ± 0.66 mmol.L^{-1}, respectively. In contrast, the maximum level of lactate in SFM was far lower at 3.22 ± 0.19 mmol.L^{-1}, more than an order of magnitude lower than the previously determined inhibitory level.
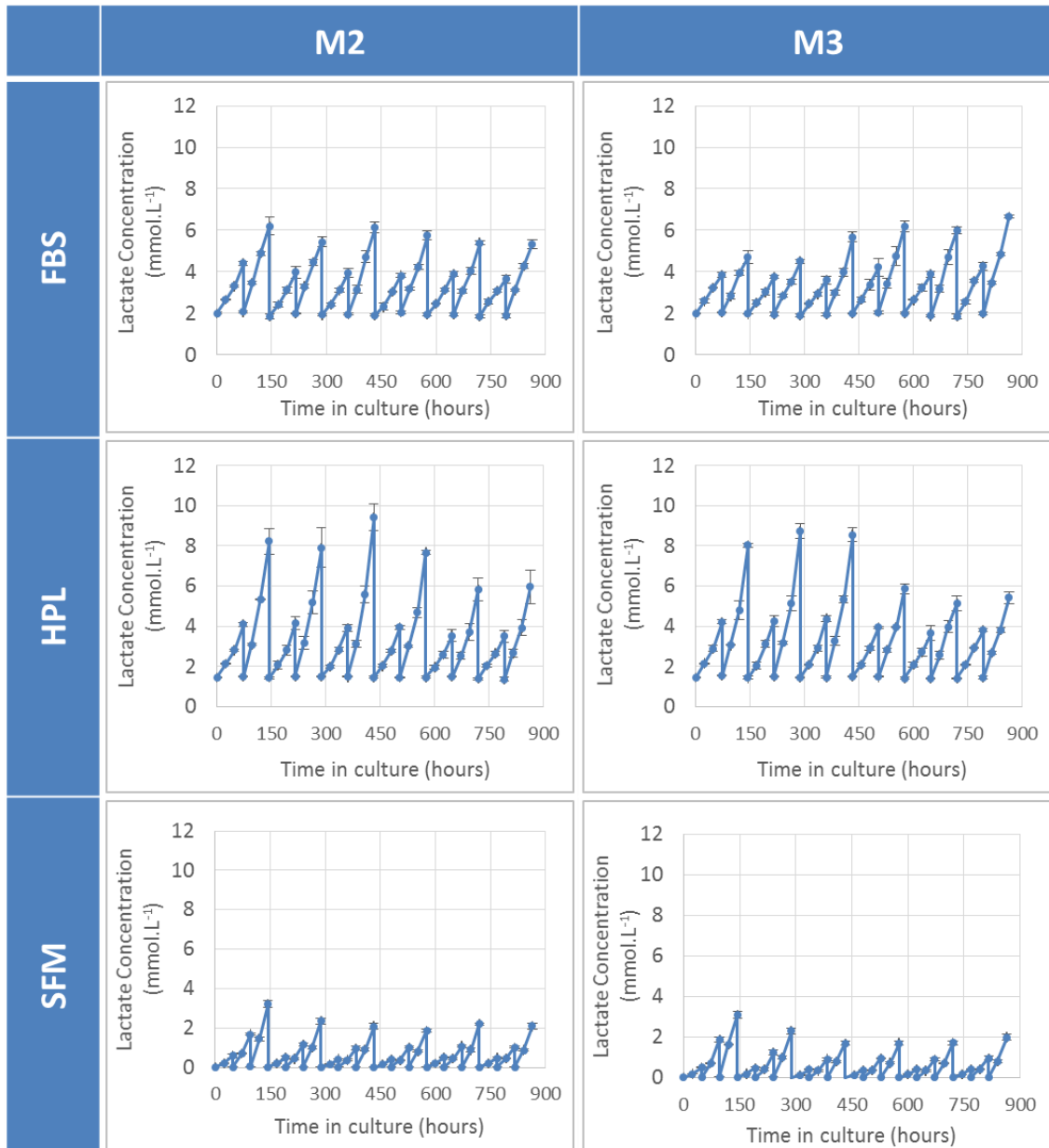
Figure 5.10. Live lactate concentration of two BM-hMSC lines over 36 days of monolayer expansion in FBS, HPL and SFM. Showing increased lactate concentration in HPL and lower lactate concentration in SFM. Data shows mean ± SD (n=4)

The concentration of ammonia in the culture medium must also be reduced to avoid inhibition of BM-hMSC growth and characteristics which has previously been determined to be 2.4 mmol.L^{-1} for BM-hMSCs (Schop *et al.* 2009b). It can be seen from Figure 5.11 that the maximum level of ammonia for FBS and HPL culture was 0.70 ± 0.05 and 0.87 ± 0.05 mmol.L^{-1}, respectively. In this instance, the maximum level of ammonia in SFM was higher at 0.90 ± 0.02 mmol.L^{-1}, however, still half the previously determined inhibitory ammonia level for BM-hMSCs.
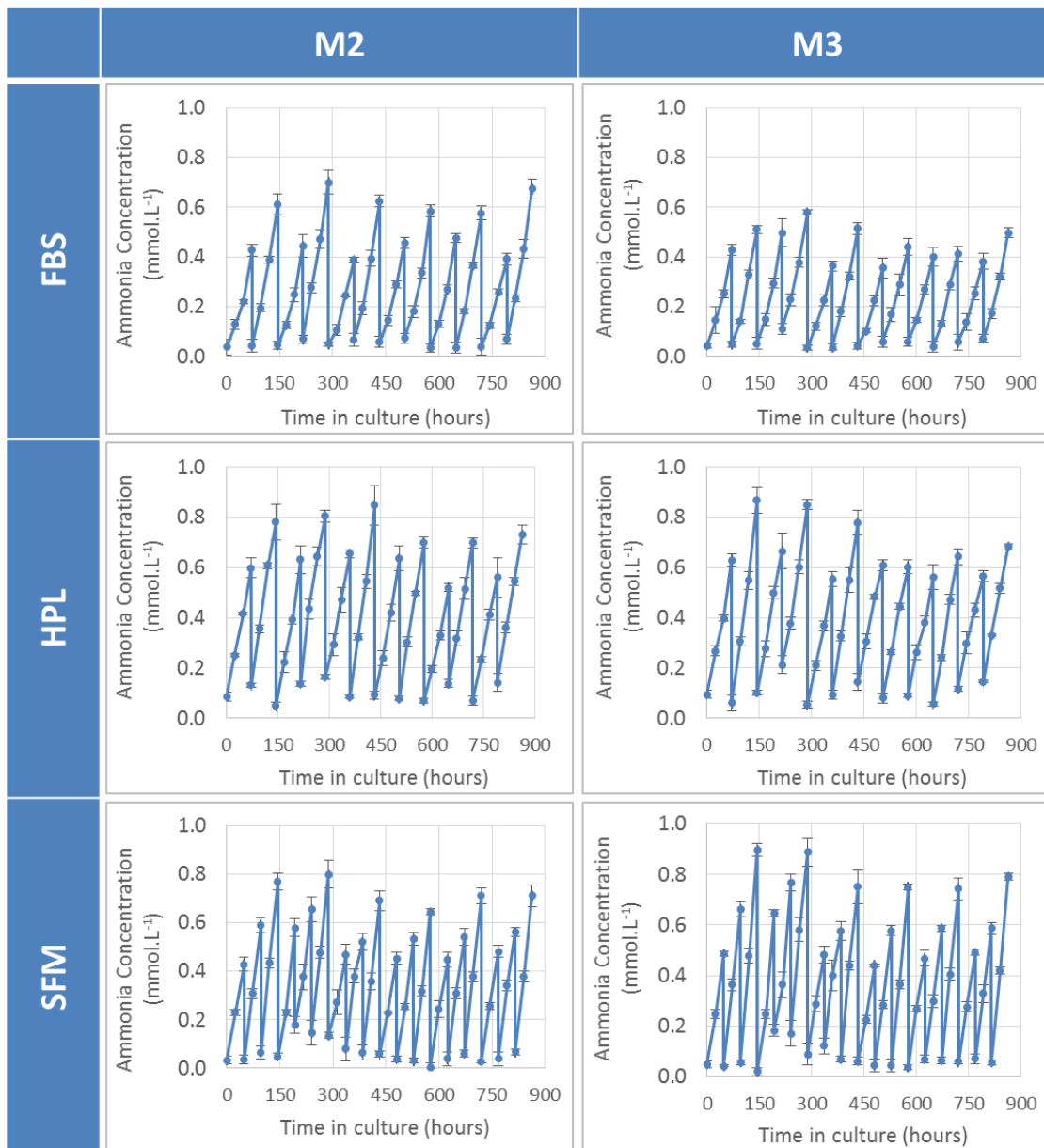
Figure 5.11. Live ammonia concentration of two BM-hMSC lines over 36 days of monolayer expansion in FBS, HPL and SFM. Showing similar levels of ammonia concentration in FBS, HPL and SFM. Data shows mean ± SD (n=4)

Cell damage was evaluated by measuring a combination of lactate dehydrogenase (LDH) (Lavrentieva *et al.* 2010a) and total protein released. Figure 5.12 and Figure 5.13 show these concentrations throughout culture, which indicate only a minimal increase in LDH and no change in the subsequent total protein concentration. The only appreciable increase in LDH concentration occurred in SFM at the first passage from the baseline of around 3 U.L^{-1} up to 10.13 ± 1.56 U.L^{-1}.
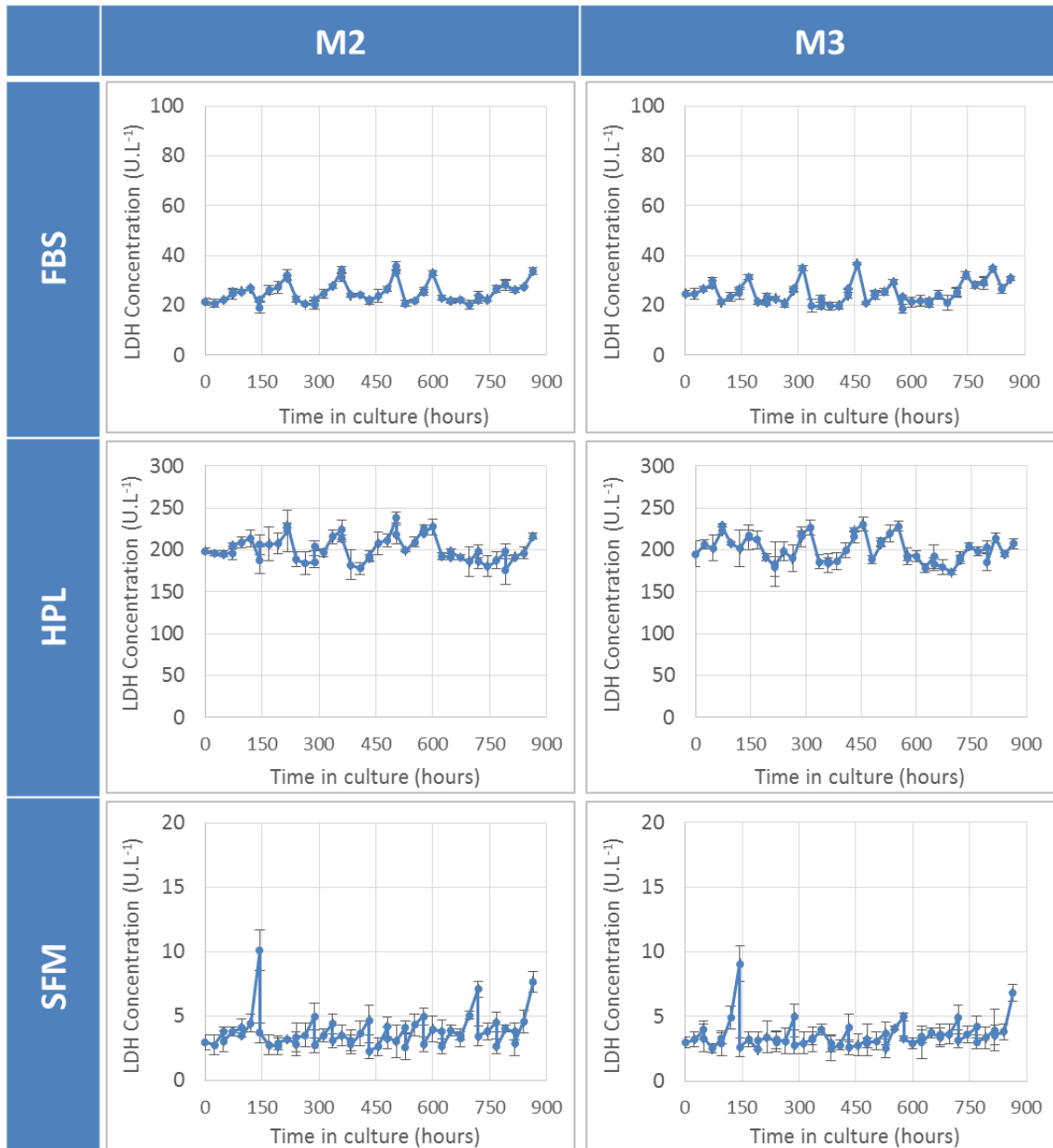
Figure 5.12. Live lactate dehydrogenase (LDH) concentration of two BM-hMSC lines over 36 days of monolayer expansion in FBS, HPL and SFM. Showing increased LDH concentration in SFM at increased cell densities. Data shows mean ± SD (n=4)

This is in conjunction with the highest cell density during the expansion process and therefore should be monitored, particularly during bioreactor culture where it is desirable to have high BM-hMSC densities to increase product yields. This combined measurement demonstrates that cell death was minimal throughout the expansion process, making the fold expansion data a reliable estimate of net proliferative rate.
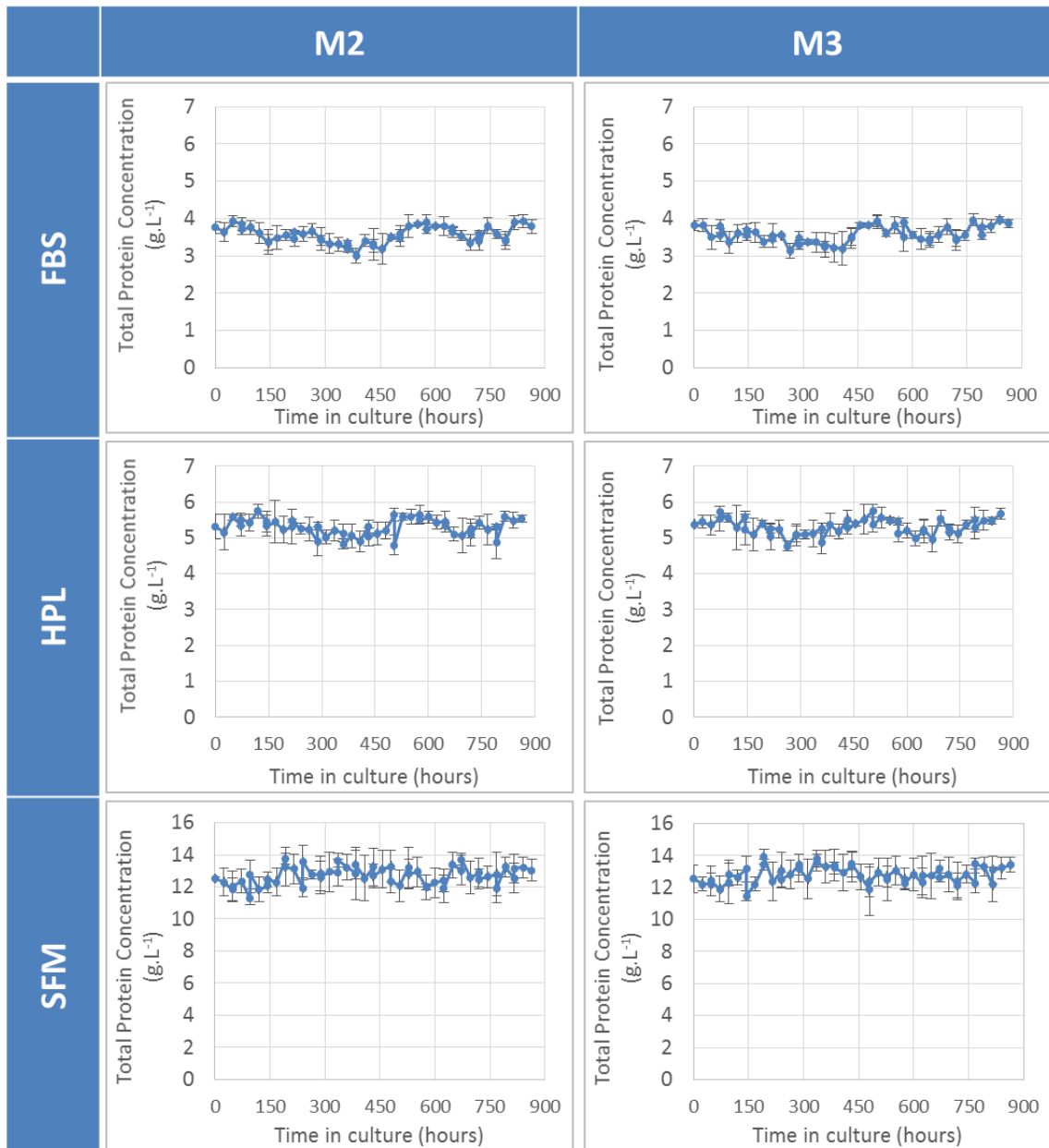
Figure 5.13. Live total protein concentration of two BM-hMSC lines over 36 days of monolayer expansion in FBS, HPL and SFM. Showing no increase in concentration throughout expansion, indicating a low amount of BM-hMSC death. Data shows mean ± SD (n=4)

5.3 Identity of BM-hMSCs in different medium formulations

5.3.1 Experimental overview

The identity of BM-hMSCs must be sustained throughout the expansion process and ensuring that this is the case for all potential culture media or changes to the process is important during process development. To achieve this, the tri-lineage differentiation potential of both BM-hMSC donors in each media condition has been assessed after six experimental passages using the protocol outlined in Section 3.4.4 with representative images taken in each condition. Multicolour flow cytometry has also been used to assess the co-expression of surface markers on the BM-hMSCs after six passages, using the protocol in Section 3.4.5. Finally, the genotype of three of the BM-hMSC donors has been verified by short tandem repeat (STR) analysis after six experimental passages to ensure the BM-hMSC cultures have remained genetically stable and have not become contaminated during subsequent culture.

5.3.2 Tri-lineage differentiation potential of BM-hMSCs in different formulations

As defined by the International Society of Cellular Therapy (ISCT) (Dominici *et al.* 2006), BM-hMSCs from both donors in each medium formulation must demonstrate the ability to differentiate down the osteogenic, chondrogenic and adipogenic lineages *in* vitro. This qualitative demonstration of tri-lineage differentiation potential for all donor BM-hMSCs can be seen in Figure 5.14. The BM-hMSCs cultured in chondrogenic medium as micromasses have stained positive for the presence of glycosaminoglycans (GAGs) with Alcian Blue, indicative of chondrogenic differentiation. In addition, BM-hMSCs cultured in adipogenic medium have formed lipid vacuoles (stained with Oil Red-O) and BM-hMSCs cultured in osteogenic medium have demonstrated the production of alkaline phosphatase and calcium, stained black with silver nitrate. Figure 5.14 shows that BM-hMSCs have demonstrated this potential for both of the BM-hMSC donors in all three medium formulations, which demonstrates that changing the medium formulation has not had an adverse impact on the *in vitro* differentiation potential of the BM-hMSCs.
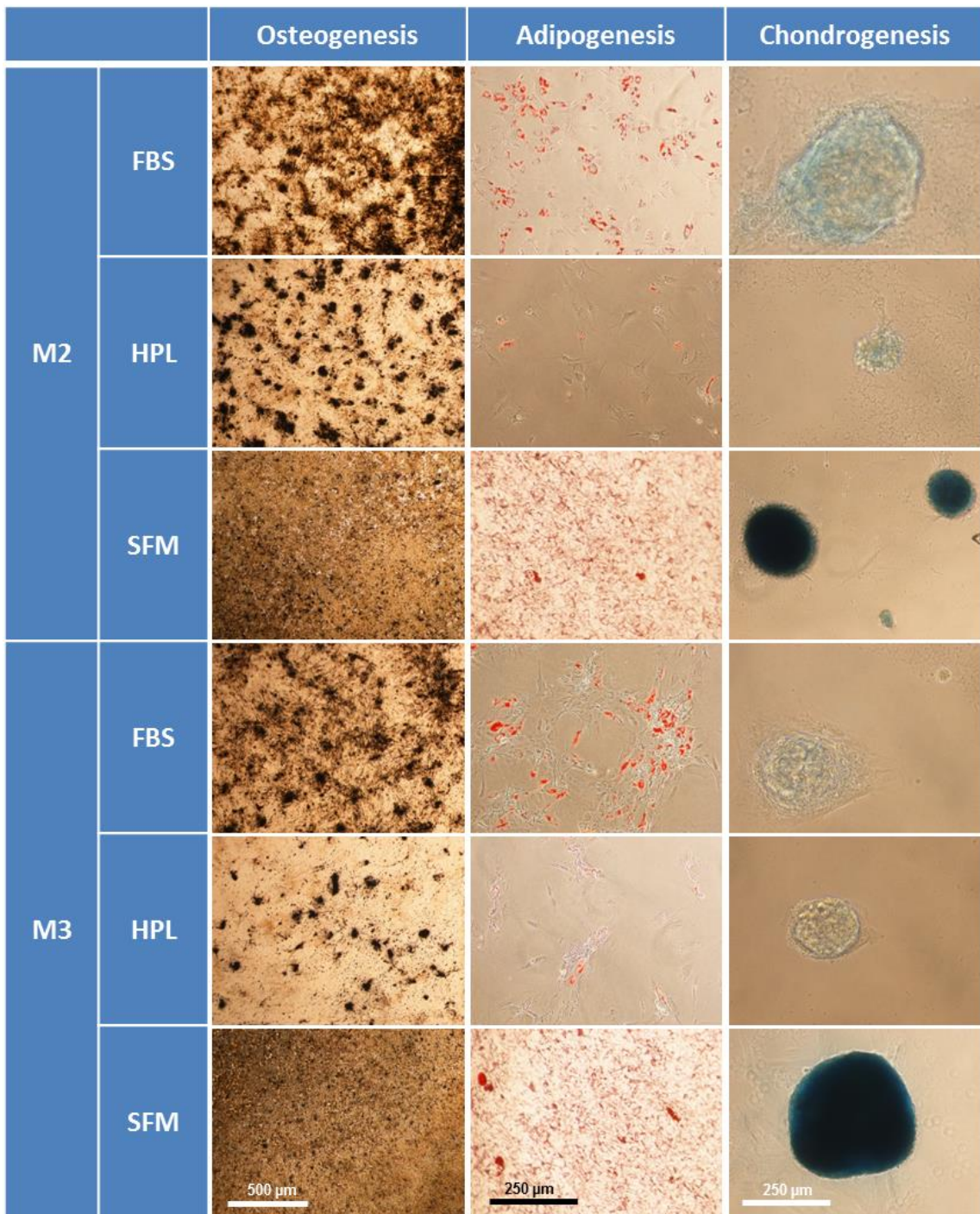
Figure 5.14. Tri-lineage differentiation potential of the two BM-hMSC lines in FBS, HPL and SFM using phase contrast microscopy. Showing osteogenic differentiation by staining for alkaline phosphatase and calcium deposition, adipogenic differentiation by staining with Oil Red O and chondrogenic differentiation by staining with Alcian Blue

5.3.3 Immunophenotype of BM-hMSCs in different medium formulations

In addition to the tri-lineage differentiation potential in Section 5.3.2, BM-hMSCs must also demonstrate the expression of both positive and negative surface markers in accordance with the ISCT criteria. Table 5.1 shows the percentage co-expression of CD90+, CD73+, CD105+, CD34- & HLA-DR- of the two BM-hMSC lines in FBS, HPL and SFM at the start and end of the expansion process.

Table 5.1. Multiparameter flow cytometry showing percentage co-expression of CD90+, CD73+, CD105+, CD34- & HLA-DR- of two BM-hMSC lines in FBS, HPL and SFM at day 0 (passage 3) and after day 36 (passage 9). Mean value ± SD, in all cases 10,000 events were measured

		Co-expression (%)	
		Passage 3 (day 0)	Passage 9 (day 36)
M2	**FBS**	94.72 ± 1.09	98.70 ± 1.16
	HPL	95.67 ± 0.74	93.70 ± 0.95
	SFM	98.88 ± 0.14	98.05 ± 0.39
M3	**FBS**	94.79 ± 0.79	98.40 ± 1.08
	HPL	95.15 ± 0.78	96.50 ± 0.93
	SFM	99.55 ± 0.16	98.53 ± 0.52

Despite the differences in cell growth and net metabolite flux described in Section 5.2, all of the BM-hMSC lines displayed the expected immunophenotype by the positive co-expression of CD73, 90 and 105 and negative co-expression of CD34 and HLA-DR at the start and end of the culture process. This level of expression has been maintained above 90% for all of the BM-hMSC donors across six experimental passages and 36 days in culture, demonstrating that cellular changes in growth kinetics and net metabolite flux do not have an effect on the expression of BM-hMSC surface markers. Further to this, the flow cytometry plots can be seen in Figure 5.15 for M2 and Figure 5.16 for M3 at the end of the expansion process. This confirms the co-expression of the required immunophenotype markers and also shows a difference in population distribution for the different conditions, with BM-hMSCs cultured in SFM displaying a tighter distribution of marker expression.
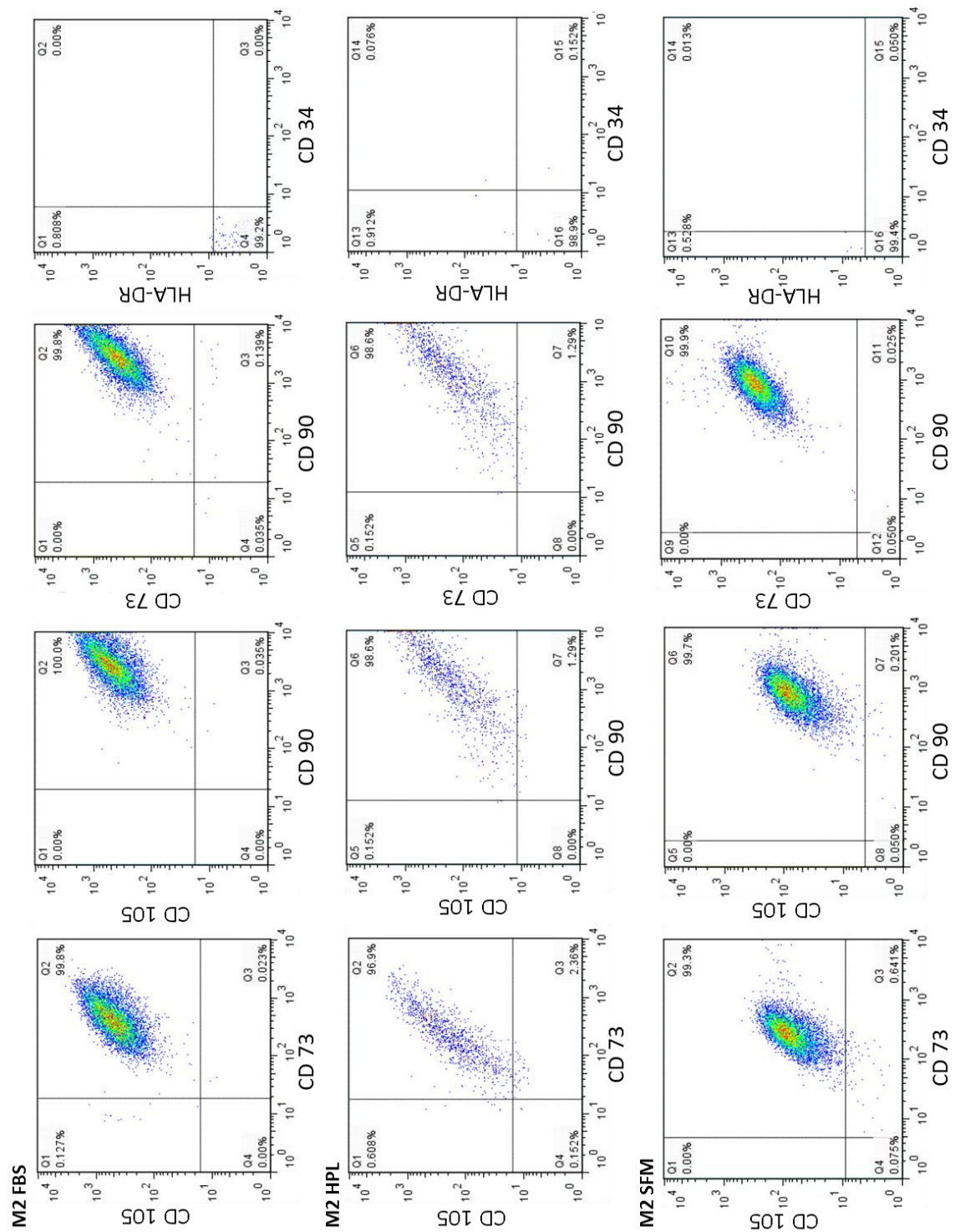
Figure 5.15. Multiparameter flow cytometry plots for M2 in FBS, HPL and SFM after 36 days of expansion showing co-expression of CD90+, CD73+, CD105+, CD34- & HLA-DR-
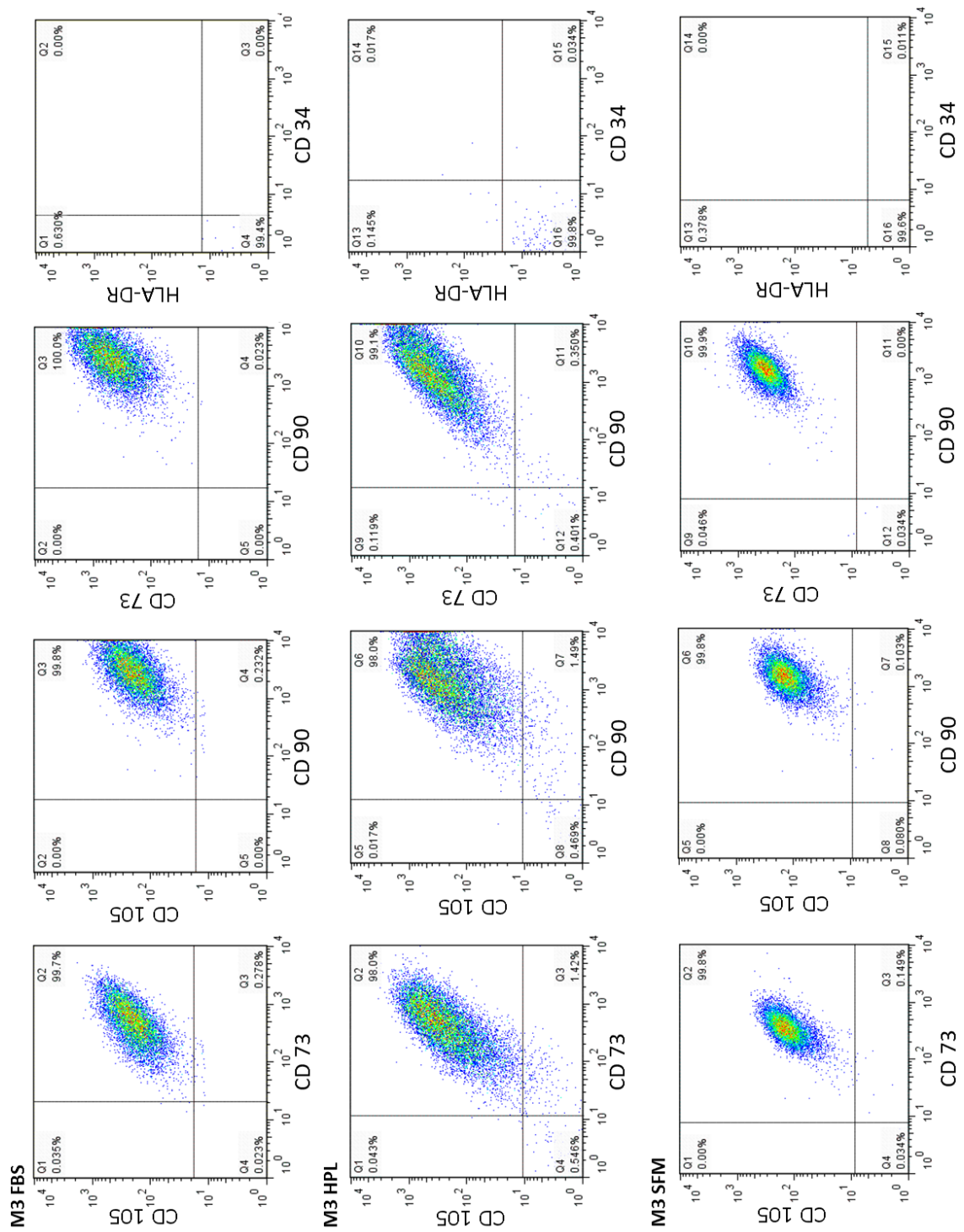
Figure 5.16. Multiparameter flow cytometry plots for M3 in FBS, HPL and SFM after 36 days of expansion showing co-expression of CD90+, CD73+, CD105+, CD34- & HLA-DR-

5.3.4 Short tandem repeat analysis of BM-hMSCs in different medium formulations

Short tandem repeat (STR) analysis of M2 and M3 BM-hMSC lines in FBS, HPL and SFM after 36 days culture can be seen in Figure 5.17. This shows that they have retained the 16 key *loci* they are expected to express, indicating that these cell lines have retained the characteristic genotype throughout the entire culture process in all conditions.
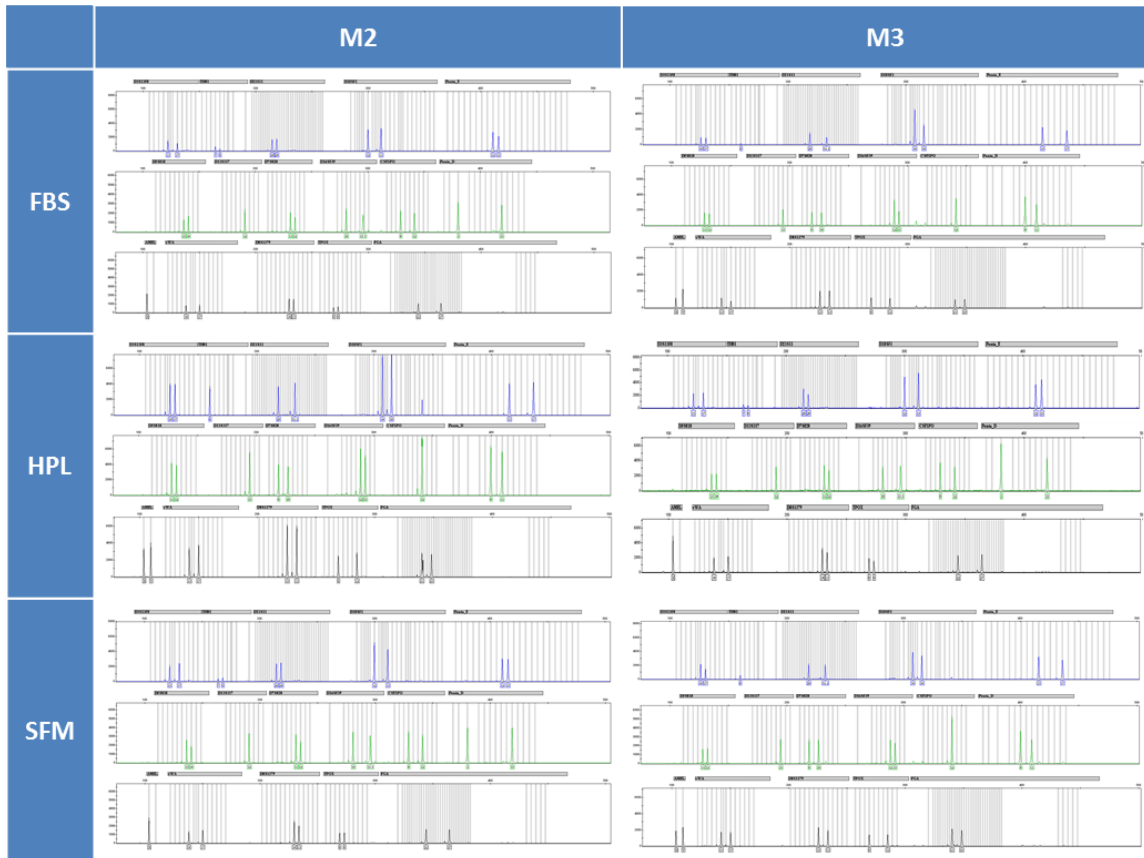
Figure 5.17. Short tandem repeat analysis of M2 and M3 BM-hMSC lines in FBS, HPL and SFM after 36 days of expansion demonstrating retention of the 16 loci that are characteristic of BM-hMSCs

5.4 Characterisation of BM-hMSCs in different medium formulations

5.4.1 Experimental overview

The measurement of cellular characteristics is of critical importance for the successful development of BM-hMSC manufacturing processes, particularly when assessing the impact of different process conditions such as medium formulations, on the product. The BM-hMSC morphology has been assessed in each medium formulation during the expansion process, using a representative phase contrast microscopy image of the BM-hMSCs adhered to the surface of a tissue culture flask. In addition to this, RNA expression of four key BM-hMSC genes were assessed at passage three, six and nine of culture for each BM-hMSC line in each medium formulation. The following primers for cell markers were used: CCL2 (recruits monocytes, memory T cells, and dendritic cells to the sites of inflammation produced by either tissue injury or infection, p21 (regulates the cell cycle and mediates cellular senescence), OCT4 (pluripotent marker associated with self-renewal of undifferentiated cells) and VEGF (associated with vascularization and growth of blood vessels). Expression was normalized to the reference gene 36B4 and plotted against the number of cumulative population doublings.

To assess the colony forming unit fibroblast (CFU) potential of M2 and M3 in each medium formulation, four T-75 flasks for each of these donor lines were taken through six experimental passages and at the end of passage three, six and nine remaining cellular material from each T-75 flask was plated into two T-25 flasks for CFU analysis as described in Section 3.4.9. In conjunction with this, remaining cellular material from each of the four flasks was plated into three wells of a 12-well plate and quantitatively assessed for osteogenic potential as described in Section 3.4.8. The output of each of these assays was plotted against cumulative population doublings to provide to normalised assessment of colony forming and osteogenic potential of each BM-hMSC line.

5.4.2 Morphology of BM-hMSCs in different medium formulations

Figure 5.18 shows the difference in BM-hMSC morphology between donor lines in FBS-based culture that is reduced in HPL and SFM culture, with smaller spindle-shaped cells. This increased consistency between donors in cellular morphology observed in HPL and SFM has benefits for the development of manufacturing processes based on a fixed surface area. This will be particularly apparent for patient specific therapies, where the number of obtainable cells per square centimeter will determine the final cell yield of the product batch.
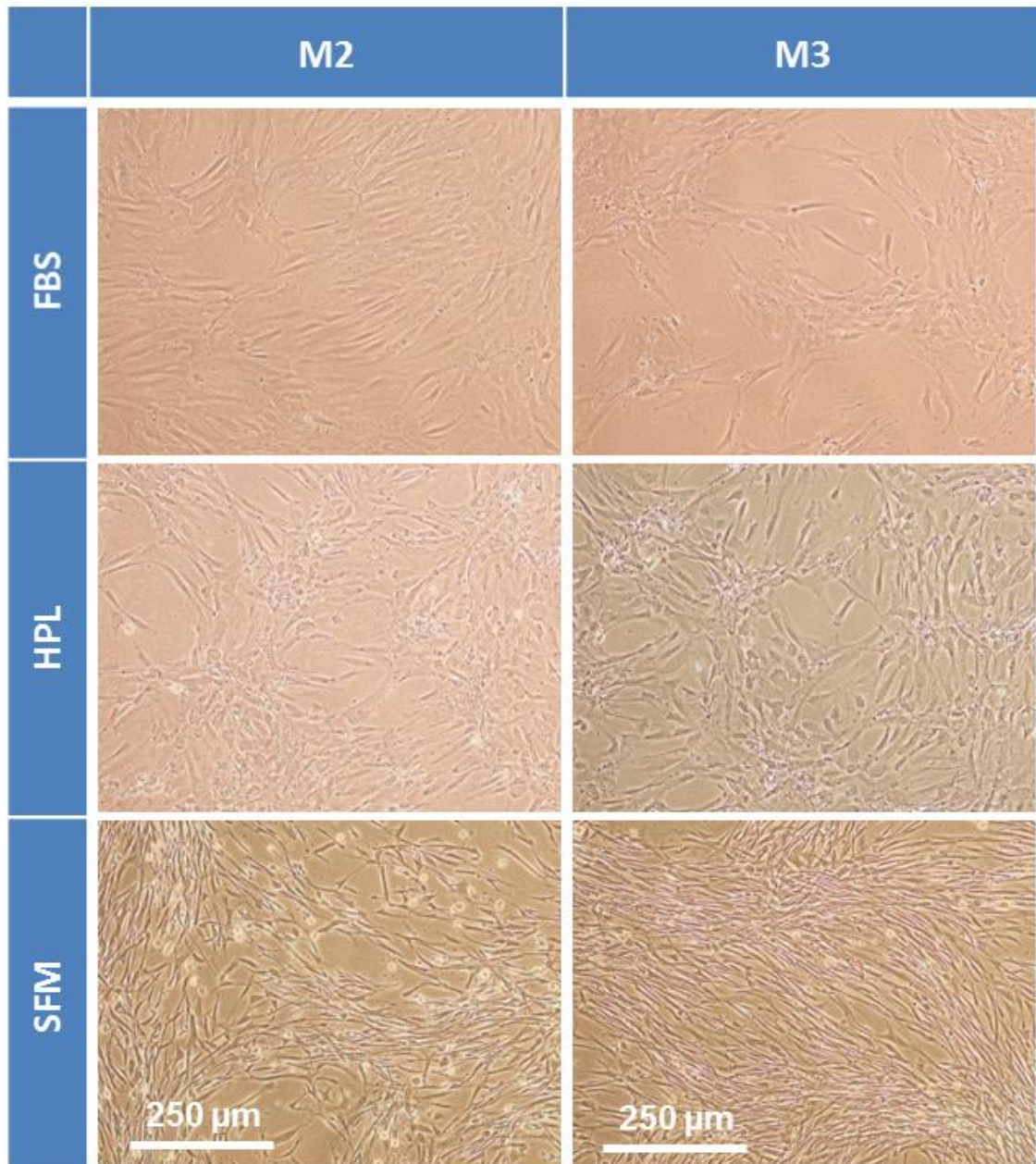
Figure 5.18. Day six phase contrast images showing the more consistent morphology between M2 and M3 in HPL and SFM compared to FBS expansion

Considering that manufacturing processes for these cell-based therapies will likely have a minimum number of cells per dose, this reduced variation under HPL and SFM will greatly reduce the risk of suffering a product batch failure, increasing the cost-efficiency of the process.

5.4.3 Genetic expression of BM-hMSCs in different medium formulations

It is also important that the BM-hMSCs retain the expression of key genes throughout the expansion process, as they are likely to play a key role in the product performing its function *in vivo*. In general, BM-hMSCs cultured under SFM conditions retained the expression of all four genes analysed, indicating that the believed positive selection occurring to generate the more homogenous population in SFM, is not impacting the expression of key genes.
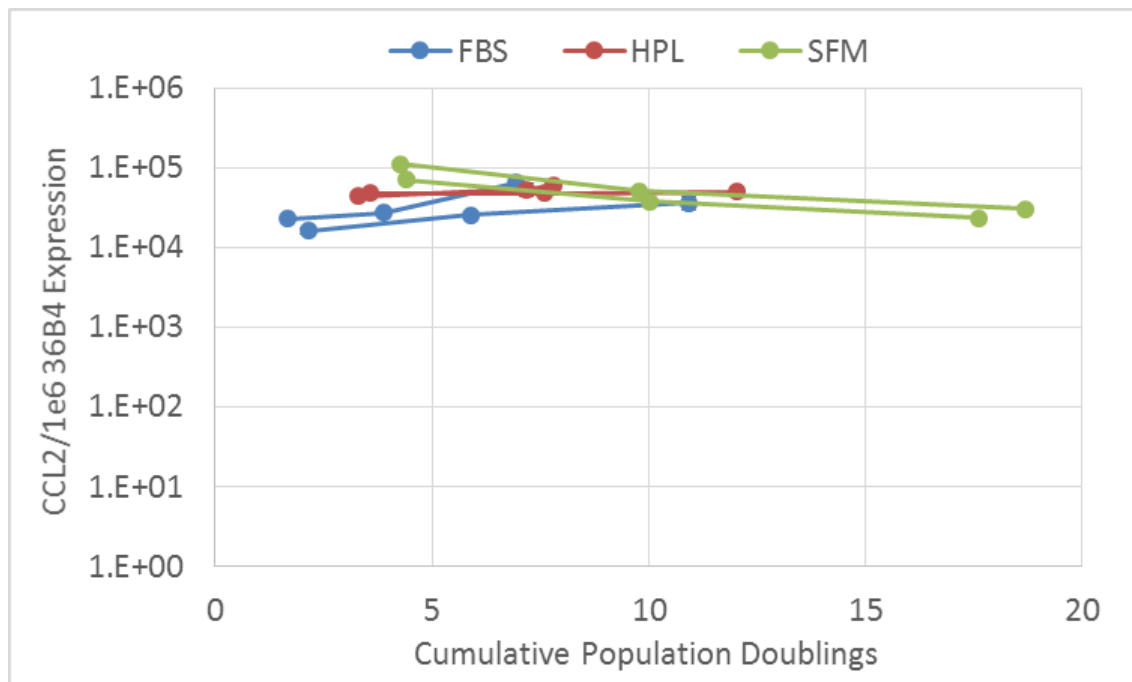
Figure 5.19. Quantitative RT-PCR analysis showing RNA expression of CCL2 gene in FBS, HPL and SFM expansion against cumulative population doublings for the two BM-hMSC lines. cDNA is normalized to housekeeping gene 36B4

The comparative analysis of the CCL2 gene for both BM-hMSC lines in FBS, HPL and SFM can be seen in Figure 5.19. This shows that the RNA expression of this gene has been maintained in all conditions despite the differences in the number of population doublings. The CCL2 gene has been implemented in the recruitment of T-cells, monocytes and dendritic cells to the sites of inflammation (Guilloton *et al.* 2012) and is therefore an important gene to maintain for clinical indications that require a level of immune modulation. Immunomodulatory properties of BM-hMSCs play a key role in their therapeutic potential (Le Blanc *et al.* 2004; Le Blanc *et al.* 2008),

suppressing tissue rejection by inhibiting the response of the patient's lymphatic cells. A number of companies such as Athersys Inc. (USA), Tigenix (Belgium), Pluristem Therapeutics Inc. (Israel) and Mesoblast Ltd (Australia) are developing BM-hMSC products to target clinical indication relating to immune modulation, demonstrating the increased emphasis that industry has placed on the immunomodulatory mechanism of action that BM-hMSCs have previously demonstrated.
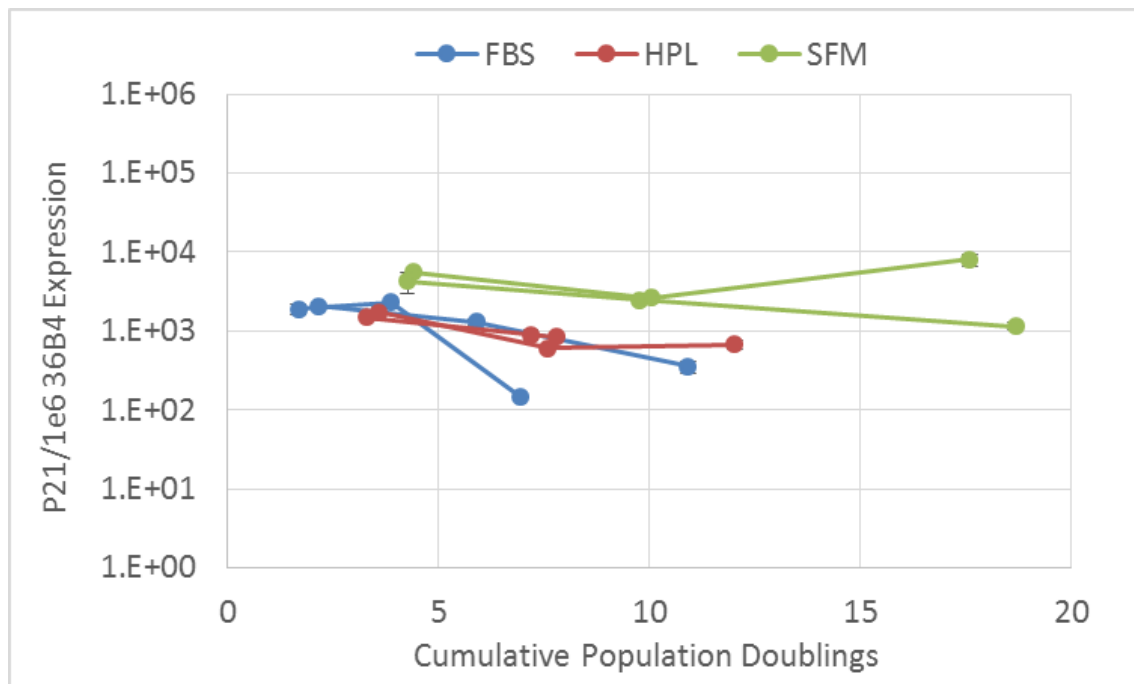
Figure 5.20. Quantitative RT-PCR analysis showing RNA expression of P21 gene in FBS, HPL and SFM expansion against cumulative population doublings for the two BM-hMSC lines. cDNA is normalized to housekeeping gene 36B4

Figure 5.20 shows the relative expression of P21, a gene relating to cellular aging and senescence (Chen *et al.* 2011) and has not unduly increased throughout the expansion process in SFM, HPL or FBS culture. This demonstrates that the onset of senescence toward the end of the expansion process in FBS and HPL in this instance did not occur in conjunction with the up-regulation of the P21 gene as has been demonstrated previously (Estrada *et al.* 2013).
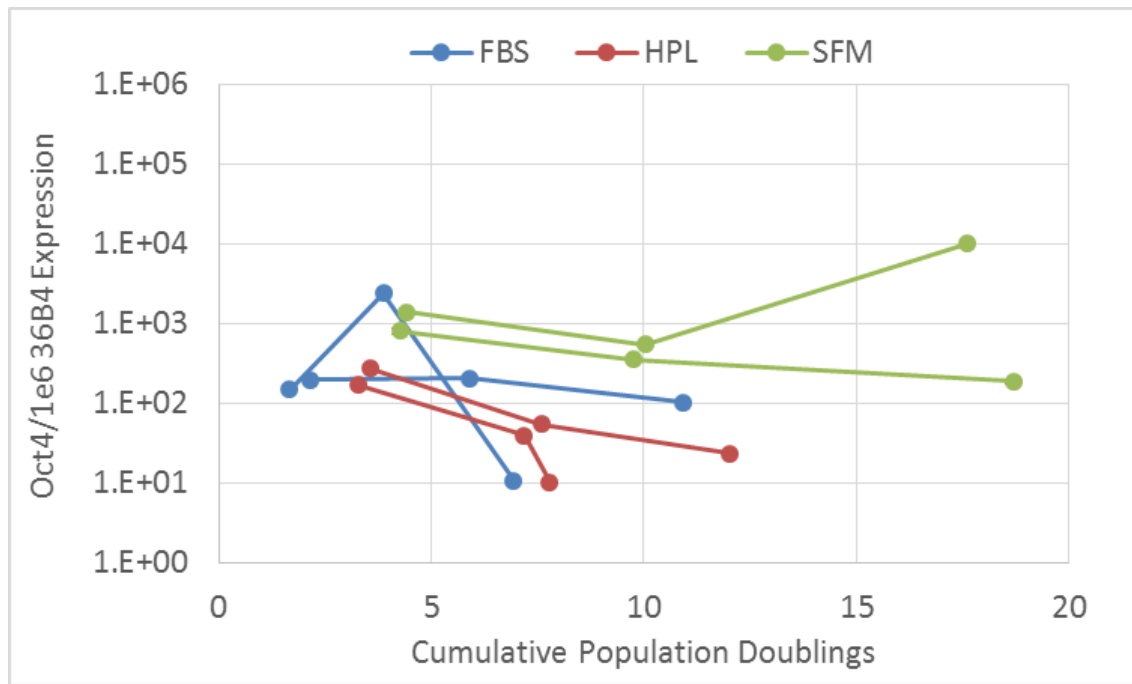
Figure 5.21. Quantitative RT-PCR analysis showing RNA expression of Oct4 gene in FBS, HPL and SFM expansion against cumulative population doublings for the two BM-hMSC lines. cDNA is normalized to housekeeping gene 36B4

Oct4 is a marker of pluripotency, mainly associated with embryonic stem cells, but has previously demonstrated expression in BM-hMSCs (Riekstina *et al.* 2009). Maintenance of Oct4 under SFM expansion (Figure 5.21) demonstrates the continued ability of the cells to self-proliferate at high population doubling. It has previously been demonstrated that BM-hMSCs selected by serum deprivation are a subpopulation of very early progenitor cells with enhanced expression of Oct4 and several other genes characteristically expressed in embryonic cells (Pochampally *et al.* 2004). This demonstrates an advantage of BM-hMSCs culture in SFM, with the expression of pluripotent markers being important for the clinical application of cell-based products that undergo cellular differentiation. It can also be seen from Figure 5.21 that the expression of Oct4 decreased in FBS and HPL for the BM-hMSC line that underwent senescence towards the end of the expansion process. This should be monitored during the expansion process to ensure that it does not affect the therapeutic potential of the BM-hMSC therapy, as the retention of functional material is vital for the development of successful expansion processes.
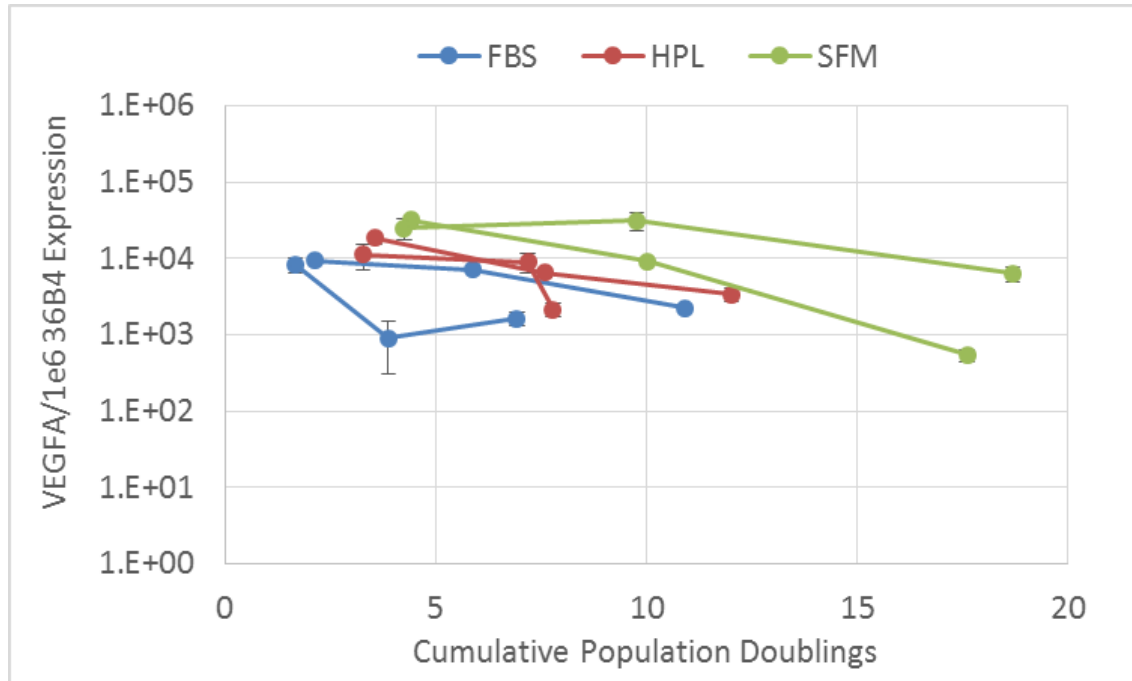
Figure 5.22. Quantitative RT-PCR analysis showing RNA expression of VEGFA gene in FBS, HPL and SFM expansion against cumulative population doublings for the two BM-hMSC lines. cDNA is normalized to housekeeping gene 36B4

Figure 5.22 shows the expression of VEGF across both BM-hMSC lines in all medium conditions over the monolayer expansion process. VEGF has been shown to be a highly important gene in the promotion of angiogenesis by BM-hMSCs (Beckermann *et al.* 2008), which will be important in a number of clinical indications, particularly for cardiac repair (Gao *et al.* 2007), a key target for a number of BM-hMSC-based therapies. Despite a higher relative expression of VEGF in BM-hMSCs cultured in SFM, there is a decrease in the expression of VEGF in FBS, HPL and SFM as the number of population doublings increases, which should be further investigated if the BM-hMSC product requires a high level of cumulative population doublings and is to be used for clinical indications requiring angiogenesis.

5.4.4 Colony forming potential of BM-hMSCs in different medium formulations

There is currently much discussion about the true identity and desired characteristics of BM-hMSCs for clinical applications and how they elicit their therapeutic mechanism of action (Bianco *et al.* 2013b). Despite this, some hints come from a Graft-versus-host disease (GVHD) study showing that just a few passages can make a significant difference to the product efficacy. Human MSCs from passages 1-2 compared to passages 3-4 showed a decrease in patient survival

and response while no *in vitro* differences were found (von Bahr *et al.* 2012). Despite this uncertainty in the application of BM-hMSCs, there is still a need to rigorously characterise the cellular product during the development of an expansion process to ensure the process itself is not having a detrimental impact on the product characteristics whilst yield is increased. It is important that assay development takes place in parallel with clinical development so that the prediction of clinical effect for a specific target indication can be correlated to process measurements *in vitro*.

As BM-hMSC expansion processes move through the development phase, there is an increasing need to assess the characteristics of the product in relation to the number of population doublings the cells have undergone and is favorable under the current regulatory guidelines. This has the benefit of normalizing cell expansion data as passage number does not take into account the seeding density of the cells or the relative expansion level of the product in each condition. Using population doubling level versus cellular characteristic in this way allows for a fair comparison between conditions and is also far more amenable to comparisons with scale-up technology such as bioreactors, when the term passage does not readily apply.
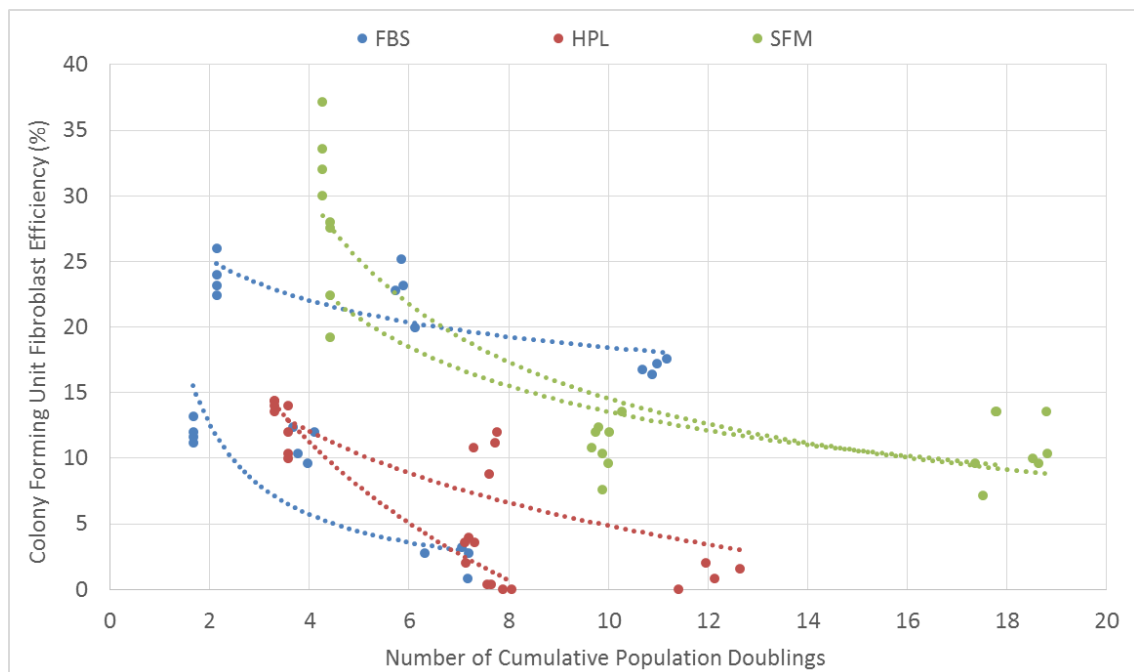
Figure 5.23. Colony forming efficiency of the two BM-hMSC lines against number of population doublings throughout the expansion process in FBS, HPL and SFM. Demonstrating the increased consistency between BM-hMSC lines in SFM compared to FBS and HPL-based medium

Figure 5.23 shows the colony forming potential of the BM-hMSC donor lines under FBS, HPL and SFM culture against the number of population doublings. This demonstrates that the colony forming potential decreases through the expansion process as the number of population doublings increases, which hints at the challenges that exist when developing large scale manufacturing processes, which are likely to require lot sizes in excess of a trillion cells (Rowley *et al.* 2012b).

Despite this, BM-hMSCs cultured in SFM retained a similar level of colony forming potential at a high number of population doublings and importantly, the consistency between the two BM-hMSC donor lines was far greater than in FBS and HPL. What our data therefore suggests is that the SFM condition used, PRIME-XV®, in conjunction with growth on fibronectin, is able to support the generation of a more homogenous cell population in terms of colony forming potential as well as cell size and growth rate, possibly through a positive selection process or the maintenance of asymmetric division. Indeed, an increased presence of CFU-Fs in an BM-hMSC population has previously been noted when using an optimized defined medium formulation as compared to DMEM supplemented with FBS (Jung *et al.* 2010). Furthermore, Wagner and colleagues (Wagner *et al.* 2006) compared two serum-containing media noted that one was able to support a more homogenous morphology than the other. This maintenance of consistency between donors will be important for both patient specific and off-the-shelf therapies and will reduce the likelihood of suffering product batch failure during quality testing. This will result in a reduced cost at the large scale, as the capital invested per batch will be high but more importantly for patient specific therapies, a batch failure would result in a patient going without treatment, which would be highly undesirable.

5.4.5 Quantitative osteogenic potential of BM-hMSCs in different formulations

As with the colony forming potential in Figure 5.23, the quantitative osteogenic potential of the BM-hMSCs in each medium formulation has been evaluated. Similarly, the same trend is also presented in Figure 5.24, which shows that the osteogenic potential of the BM-hMSCs decreasing as the number of population doublings increases. This is also supported by *in vivo* clinical data (Yamachika and Iida 2013) for these indications as well as for additional indications outside of the BM-hMSC niche (Moll *et al.* 2014a). It is important to assess the impact of the expansion process on quality attributes early in development, as it will determine the maximum

allowable expansion ratio of the product for each particular indication, which will in turn influence the overall cost and scale of the therapy.
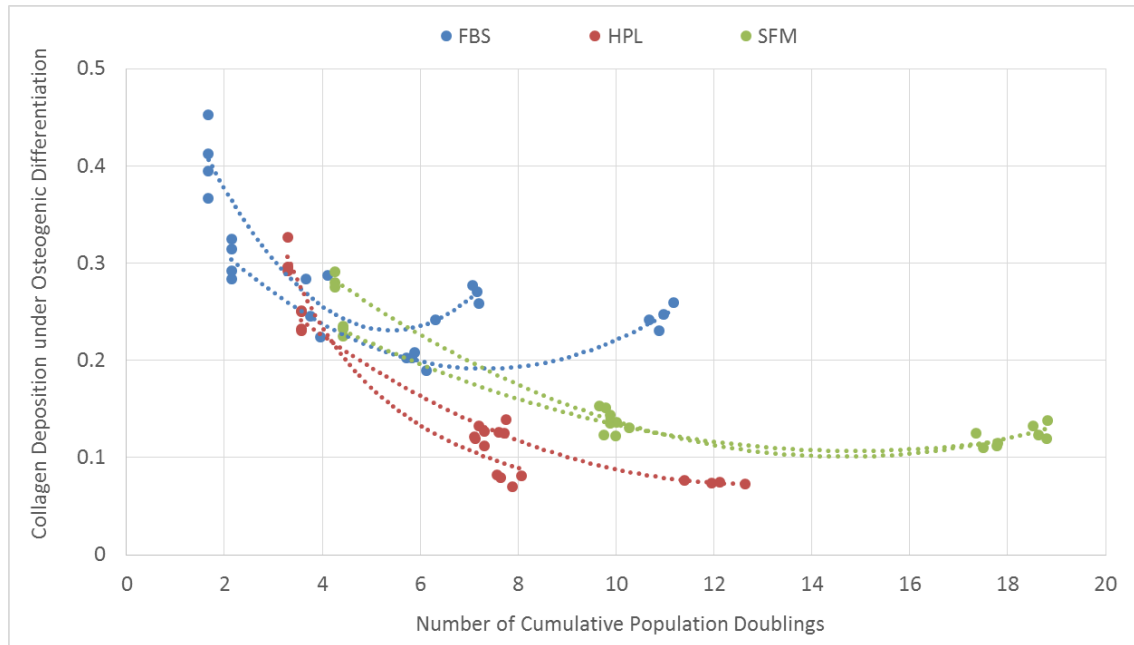
Figure 5.24. Osteogenic potential of two BM-hMSC lines against number of population doublings throughout the expansion process in FBS, HPL and SFM. Demonstrating the maintenance in osteogenic potential of both BM-hMSC lines in SFM at a high number of population doublings.

5.5 Considerations for consistency in bioprocess development

One of the key driving factors for the overall production cost of a BM-hMSC therapy, as well as medium cost, will likely be in the level of donor to donor variability experienced during the manufacturing process, leading to increased process time and risk of batch failure. The donor lines selected for this study had previously demonstrated large differences in cellular characteristics (Chapter 4), which will particularly impact the successful development of patient specific BM-hMSC therapies.
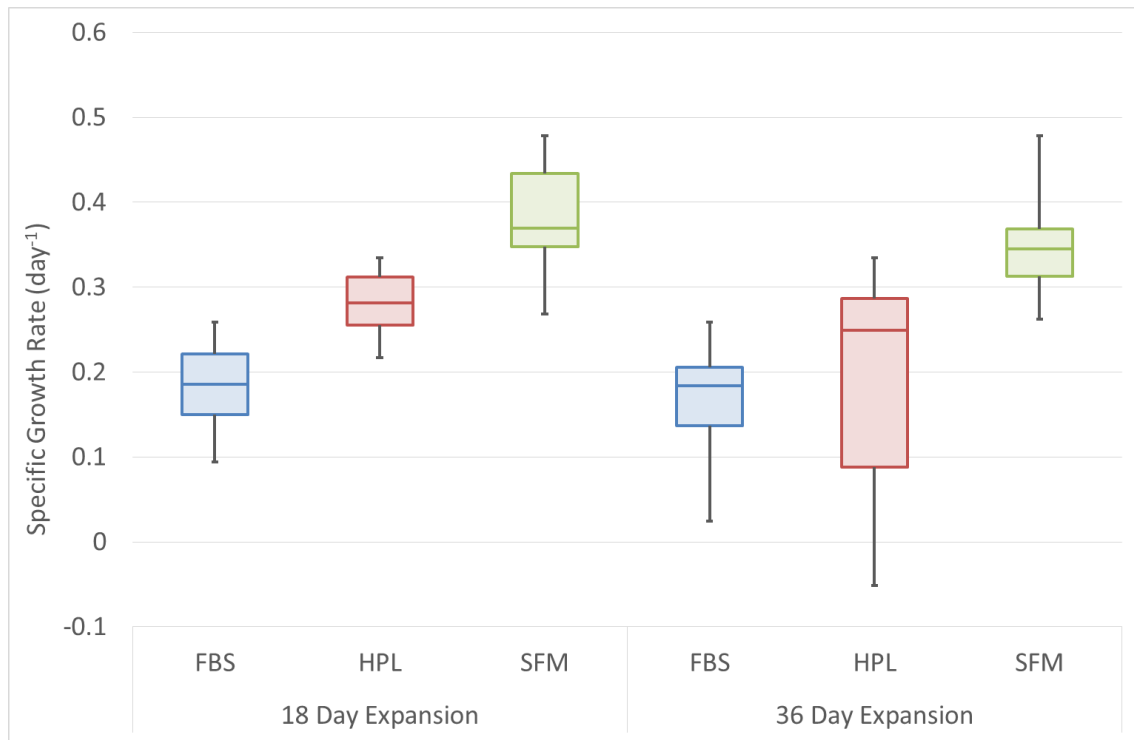
Figure 5.25. Box and whisker plots showing the consistency in growth kinetics of two BM-hMSC lines over 18 days and 36 days expansion in FBS, HPL and SFM. Demonstrating the increased variation in FBS and HPL over 36 days of expansion and the maintenance of consistency in SFM expansion.

Figure 5.25 shows the inconsistency between the growth characteristics of these BM-hMSC lines, with a range of 0.234 day^{-1} in FBS, 0.386 day^{-1} in HPL and 0.216 day^{-1} in SFM following the 36 day expansion process, demonstrating a diverging process occurring in HPL culture. In contrast to this variance experienced in HPL culture and despite a higher number of cumulative

population doublings, the SFM culture process had a corresponding range of only 1.45 population doublings between these donors and batch runs after 36 days in culture. This indicates that SFM is highly amenable to a large scale expansion process, where a high number of product population doublings are required. Further to this, HPL has demonstrated consistent BM-hMSC growth characteristics over 18 days of expansion, which indicates that is represents a viable alternative to FBS for patient specific manufacturing processes where a lower number of population doublings are required.

Table 5.2. Process time required to manufacture a theoretical batch of 350 million BM-hMSCs demonstrating variation in process time between and within donor material that is reduced in HPL and further reduced in SFM. (From 2 million BM-hMSCs starting material).

| Condition | hMSC line | Per Dose of 350 million hMSCs | | |
		Process Time (days)	Inter Batch Range (days)	Inter Donor Range (days)
FBS	M2	23.5	0.9	19.4
	M3	39.5	5.0	
HPL	M2	17.7	1.0	4.5
	M3	20.2	2.8	
SFM	M2	12.9	0.5	0.9
	M3	12.4	0.6	

For the development of a patient specific cell-based therapy, where the inter donor variability has to be accounted for during manufacture, this reduction in product variance offers a significant benefit to the process. Reducing the divergence in donor cell characteristics will alleviate potential bottlenecks in the isolation, expansion and delivery process, an important consideration for cell-based therapy process development. In conjunction with this, a more consistent expansion process will reduce the risk of suffering a product batch failure, which for a patient specific therapy will mean that the patient will fail to be treated. Table 5.2 shows the variability between the two BM-hMSC lines for a hypothetical process requiring a batch size of 350 million cells from a starting population of two million cells (Heathman *et al.* 2015b). This demonstrates the increased consistency that can be achieved in the SFM and HPL process

between production batches and between donors, with a reduction in range from 19.4 days in the FBS process to 4.5 days in the HPL process and 0.9 days in the serum free process. This also has advantages for off-the-shelf therapies, as it is possible to select material for the expansion process by pre-screening BM-hMSCs and discarding those that do not display sufficient growth kinetics. Under the SFM condition, both of the BM-hMSC lines displayed similar process times between donors and a reduced inter donor range. This has the potential to lead to reduced costs in the process development phase as fewer donor lines will be excluded (and therefore require testing) compared to FBS culture and will be available for the production process. The reduced process time to achieve this batch size in the serum free condition will also be advantageous for reducing the overall medium costs, as product batches can be manufactured in reduced time.
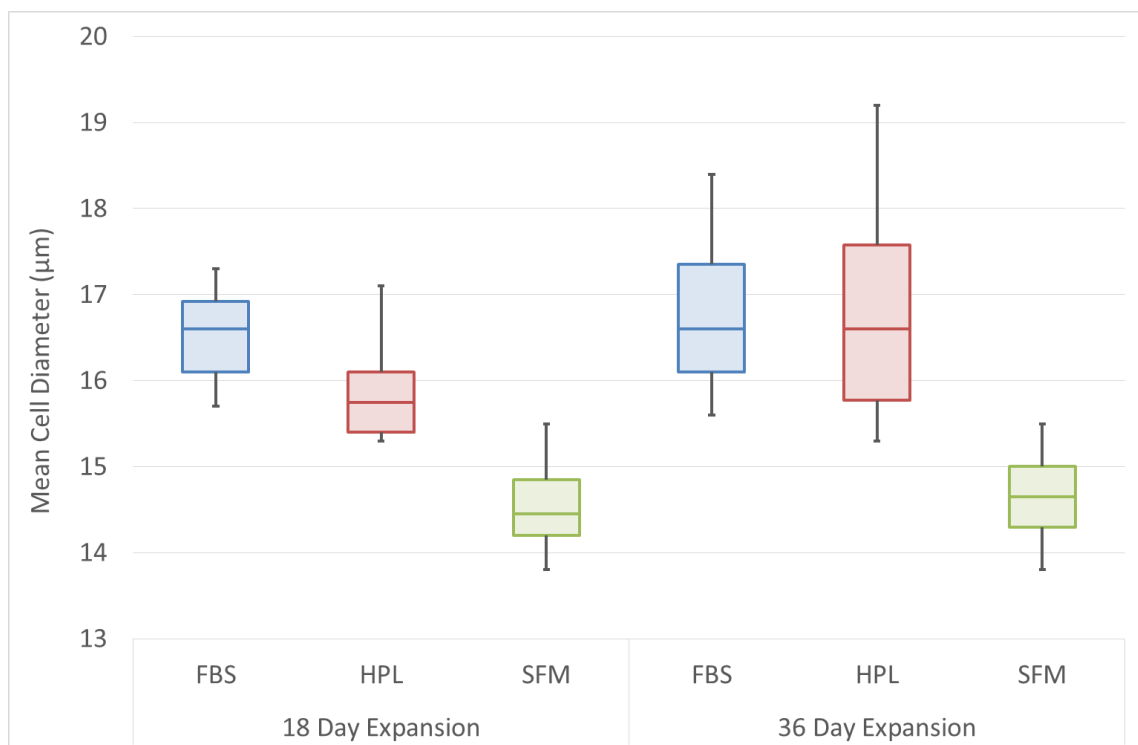
Figure 5.26. Box and whisker plots showing the consistency in mean cell diameter of two BM-hMSC lines over 18 days and 36 days expansion in FBS, HPL and SFM. Demonstrating the increased variation in FBS and HPL over 36 days of expansion and the maintenance of consistency in SFM expansion.

Furthermore, an increase in achievable cell number per batch will also increase the material available for quality release testing which is an important consideration of patient specific therapies as each patient batch must be independently tested prior to release. A study by Deskins and colleagues also demonstrated that three independent *in vitro* assays based on growth rate, proliferative potential and ATP content were able to predict *in vivo* performance, with BM-hMSCs performing above average in all three assays having increased *in vivo* regenerative abilities (Deskins *et al.* 2013).

Human MSCs cultured in SFM had a cell diameter of 14.65 ± 1.7 µm (median ± range) compared to FBS culture with a cell diameter of 16.6 ± 2.8 µm (median ± range) and HPL culture also at 16.6 ± 3.9 µm (median ± range). The variability in cell diameter throughout expansion in FBS and HPL-based medium (Figure 5.26) could have further implications for the delivery process in terms of cell concentration and infusion rate, which would likely have to be standardized during clinical development. As well as an increase in BM-hMSC productivity, this demonstrates a further advantage of SFM culture of BM-hMSCs in terms of cell size consistency over a 36 day expansion process. In addition to this, BM-hMSCs expanded in SFM demonstrated a reduction in post-harvest cell aggregation (Figure 5.27), which will be beneficial for the downstream and formulation process steps.
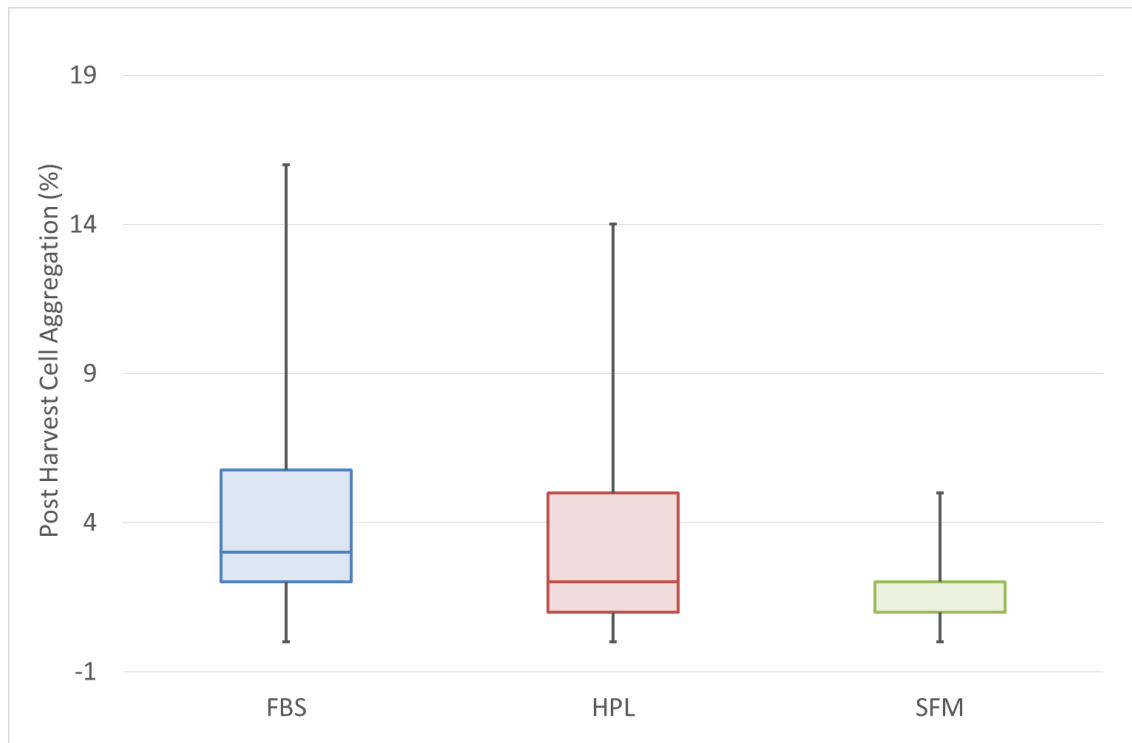
Figure 5.27. Box and whisker plots showing the post-harvest aggregation of five or more cells in FBS, HPL and SFM. Demonstrating the reduced BM-hMSC aggregation in SFM expansion compared to FBS and HPL. Data shows n = 144.

Associated with the reduction in inter-donor variability, further reductions in process input variability can be made by placing controls on the supply of raw materials. Considering the potential issues surrounding the limited availability and batch-to-batch variability of FBS (Brindley *et al.* 2012), the development of defined, serum-free medium formulations will further drive consistency into the manufacturing process. In this model, culture medium can be manufactured to a specific formulation, ensuring inter-batch consistency and reducing overall costs by scaling up the medium manufacturing process and benefitting from increasing economies of scale. This is in contrast to a manufacturing process based on FBS, where the cost of the culture medium will increase as the process is scaled through clinical development into commercial scale production. It should be said, however, that the development of a defined medium formulation should be based on a rigorous product understanding, so that desired product attributes are maximized and not impacted by the various medium components. These desired product attributes could range from growth kinetics all the way to functional attributes, which will depend on the target clinical indication.

5.6 Chapter conclusions

The development of consistent manufacturing processes remains a key challenge that must be overcome to ensure the successful translation of cell-based therapies. This serum-free medium has demonstrated the potential to reduce the variability of input material to these processes, which will allow for increased control over process consistency. By developing this serum-free process, the yield and consistency of BM-hMSC expansion has been increased between donors, which offers large advantages in the development of both off-the-shelf and patient specific cell-based therapies. The convergence of BM-hMSC characteristics throughout an expansion process demonstrates a level of control over the product manufacture, which has the potential to increase the cost effectiveness and reduce the risk in these processes.

Now that alternative medium formulations have been identified that have the potential to increase product yield and consistency, these can now be transferred to a scalable microcarrier based process. This will drive a level of scalability into the process, as a suspension based system can benefit from increasing economies of scale, whilst having the potential to meet the BM-hMSC lot-sizes required for the commercial production of an off-the-shelf therapy.

Publications arising from this Chapter:

Heathman TRJ, Stolzing A, Fabian C, Rafiq QA, Coopman K, Nienow AW, Kara B, Hewitt CJ. Serum-free process development: Improving the yield and consistency of human mesenchymal stem cell production. Cytotherapy, (2015) 17 (11): 1524-1535

Heathman TRJ, Stolzing A, Fabian C, Rafiq QA, Coopman K, Nienow AW, Kara B, Hewitt CJ. Scalability and process transfer of mesenchymal stem cell production from monolayer to microcarrier culture using human platelet lysate. Cytotherapy, (2015) (*in review*)

Rafiq QA, **Heathman TRJ**, Fonte G, Coopman K, Nienow AW, Hewitt CJ. Monolayer expansion of hMSCs in multiple brands of serum-free medium. Cytotherapy, (2015) (*in preparation*)

6 Transfer of the BM-hMSC Expansion Process into Suspension

6.1 Chapter introduction

The addition of microcarriers has been used to culture adherent cells such as BM-hMSCs in suspension (Schop *et al.* 2008; dos Santos *et al.* 2011a; Chen *et al.* 2013; Rafiq *et al.* 2013a) allowing for process scale up, where online monitoring and control systems can be used to deliver a consistent and cost-effective BM-hMSC product. Stirred-suspension bioreactors are currently employed for mammalian cell culture in biopharmaceutical production and therefore their design and operation are well-understood (Nienow 2006), with the potential to meet the expected manufacturing demands of large-scale BM-hMSC therapies.

A key aspect of reducing variation in the process will be reducing and eventually eliminating the use of fetal bovine serum (FBS) from the cell culture medium (Wappler *et al.* 2013). In addition to lot-to-lot variability, there are further process constraints on the use of FBS such as limited supply (Brindley *et al.* 2012), spiraling cost, potential for pathogen transmission, increased risk of recipient immune reaction (Spees *et al.* 2004) and reduced scope for process optimisation. Furthermore, FBS has been shown to contain immunogenic contaminants which have the potential to negatively impact post-transplant clinical results (Heiskanen *et al.* 2007), potentially increasing the regulatory burden placed upon these products. All of these considerations mean that moving towards a serum-free process would be beneficial in achieving scalable, tunable and consistent BM-hMSC manufacturing processes. In addition, BM-hMSCs grown in a serum-free medium have demonstrated increased proliferation rates, up-regulation of genes important in BM-hMSC function and down-regulation of genes involved in the production of proinflammatory cytokines (Crapnell *et al.* 2013).

Unlike traditional suspension-based bioprocesses, cell harvesting from the microcarrier surface is critically important as the quality characteristics of BM-hMSCs must be retained throughout this process. Harvesting involves two stages, detachment of BM-hMSCs from microcarriers followed by microcarrier separation from the BM-hMSC product (Nienow *et al.* 2014). After separation, cell-based products will undergo a holding time prior to downstream processing and formulation in order to pool the product. Product quality can deteriorate with prolonged holding time (Pal *et al.* 2008) and should be considered during process development. The large scale manufacture of an allogeneic BM-hMSC product will require long term product storage to decouple production from delivery, in a business model akin to current biopharmaceuticals.

Therefore, cryopreservation of BM-hMSCs must be carefully considered to ensure the therapeutic potential of the BM-hMSC product does not deteriorate prior to delivery (Moll *et al.* 2014b).

The aim of this Chapter therefore was to develop a microcarrier expansion process for BM-hMSCs in serum-based medium and to subsequently transfer this into a serum-free process. The integration of sequential unit operations for the serum-free BM-hMSC production process from expansion through to cryopreservation will also be evaluated to provide an important study in the development of a scalable end-to-end manufacturing process for BM-hMSC therapies.

6.2 Developing an agitated microcarrier process in serum-based medium

6.2.1 Experimental overview

Following the successful development of a monolayer expansion process in serum and serum-free medium, with increased consistency and yield between donor BM-hMSC lines M2 and M3, this process must be transferred to a scalable expansion process with the potential to meet the lot-sizes required for commercial production of an off-the-shelf therapy. The first stage of this will be to transfer the serum-based monolayer process to microcarrier culture in suspension. For this, four 100 mL spinner flasks were cultured in FBS and HPL-containing medium with BM-hMSC lines M2 and M3 for six days, to replicate a similar process to monolayer (Section 3.3). Daily medium samples were taken for analysis of glucose, lactate and ammonia, lactate dehydrogenase and total protein with cell counts performed on day three of culture (four samples were analysed per spinner flask as per Section 3.4.3). The culture medium was exchanged on day three for both FBS and HPL culture (Section 3.3.3). At harvest, the BM-hMSC were removed from the microcarriers and separated according to Section 3.3.4. The BM-hMSCs harvested from each condition were then assessed for mean cell diameter (3.4.2), tri-lineage differentiation potential (Section 3.4.4) and immunophenotype (Section 3.4.5). In addition to these identity measurements, BM-hMSC quality characteristics of colony forming efficiency (Section 3.4.9), osteogenic potential (Section 3.4.8) and outgrowth potential were also assessed post-harvest. Following this process, a comparison was made between these microcarrier and previous monolayer growth and post-harvest characteristics to assess the impact of transferring the BM-hMSC expansion process into suspension.

6.2.2 Growth kinetics of BM-hMSCs in agitated microcarrier culture

For a large number of clinical indications, BM-hMSCs will need to be manufactured on a large scale in order to reduce the cost of production and to meet the market need for the treatment. Microcarriers have previously been demonstrated to support the proliferation and harvest of BM-hMSCs in suspension (dos Santos *et al.* 2011a; Chen *et al.* 2013; Rafiq *et al.* 2013a) and therefore have the potential to be operated up to and beyond the thousand liter scale.

The growth kinetics of BM-hMSCs will also play a part in reducing costs, as accommodating BM-hMSCs with a lower expansion potential will reduce annual production rates (Heathman *et al.* 2015c; Naing *et al.* 2015a). Figure 6.1 shows the growth rate of the two BM-hMSC donors over six days in culture in both FBS and HPL-containing medium. The growth kinetics of the two donor

BM-hMSC lines in the HPL-based medium is significantly higher (p < 0.01) than the FBS-containing medium for both of the BM-hMSC lines, in particular M3 showed extremely low growth kinetics in FBS with 0.44 ± 0.18 population doublings over the six day growth period. This increase in growth kinetics for BM-hMSCs during microcarrier culture has also been demonstrated at 5% HPL compared with 10% FBS (Sunil *et al.* 2014).
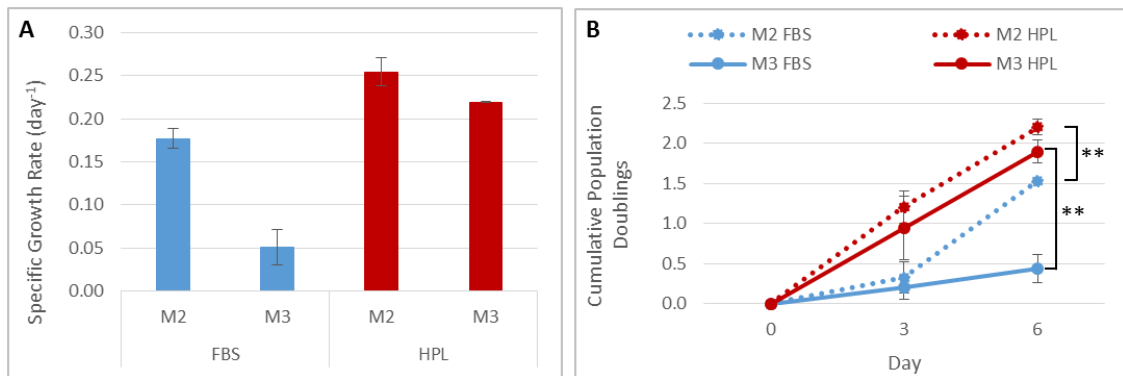
Figure 6.1. Growth kinetics of BM-hMSCs cultured on microcarriers in FBS-containing medium and HPL-containing medium for six days showing increased growth kinetics in HPL (p < 0.01). (A) Specific growth rate and (B) cumulative population doublings. Data shows mean ± SD *n=4*.

The increased consistency between donors gives significant advantages to the manufacturing process as increased production rates and reduced batch failure rates are likely to reduce the overall cost of the product. It can be seen from Figure 6.1 that the lag phase experienced by BM-hMSCs in FBS culture between day 0 and day 3 is not present when the cells are cultured in HPL, which is the likely cause of the difference in growth kinetics over the six day period. The reason for this may be due to an increase in the attachment rate of the cells which in turn shortens the lag phase prior to cell division taking place. This link between attachment efficiency and cell growth is well established (Mitchell *et al.* 2014) and the level of relevant attachment proteins present in HPL is typically higher than in FBS, which will contribute to this effect (Bieback 2013). The attachment of the BM-hMSCs to the culture surface is particularly important for suspension culture, where the cells and microcarriers are constantly agitated throughout the culture period.

6.2.3 Metabolite flux of BM-hMSCs in agitated microcarrier culture

The net metabolite flux of the cells in microcarrier culture has been measured for M2 and M3. Figure 6.2A shows the glucose consumption of BM-hMSCs in FBS and HPL culture, which was between $11.13 - 15.32$ pmol.cell^{-1}.day^{-1} with no significant difference measured across these conditions. The lactate production rate is shown in Figure 6.2B, which again shows a similar level of production between FBS and HPL. This suggests that the BM-hMSCs in both conditions are using similar metabolic pathways, as confirmed by the yield of lactate from glucose (Figure 6.2D). This is in contrast to previous studies using serum-free medium which demonstrated that BM-hMSCs tend to favor the relative production of ammonia over lactate during microcarrier culture under serum-free conditions (dos Santos *et al.* 2011a). There was however a reduction in the production of ammonia for M2 in HPL to 1.20 ± 0.03 pmol.cell^{-1}.day^{-1}, suggesting altered amino acid use, which may be related to the need for precursors (e.g. glutamine and asparagine) supporting purine and pyrimidine biosynthesis (Higuera *et al.* 2012).
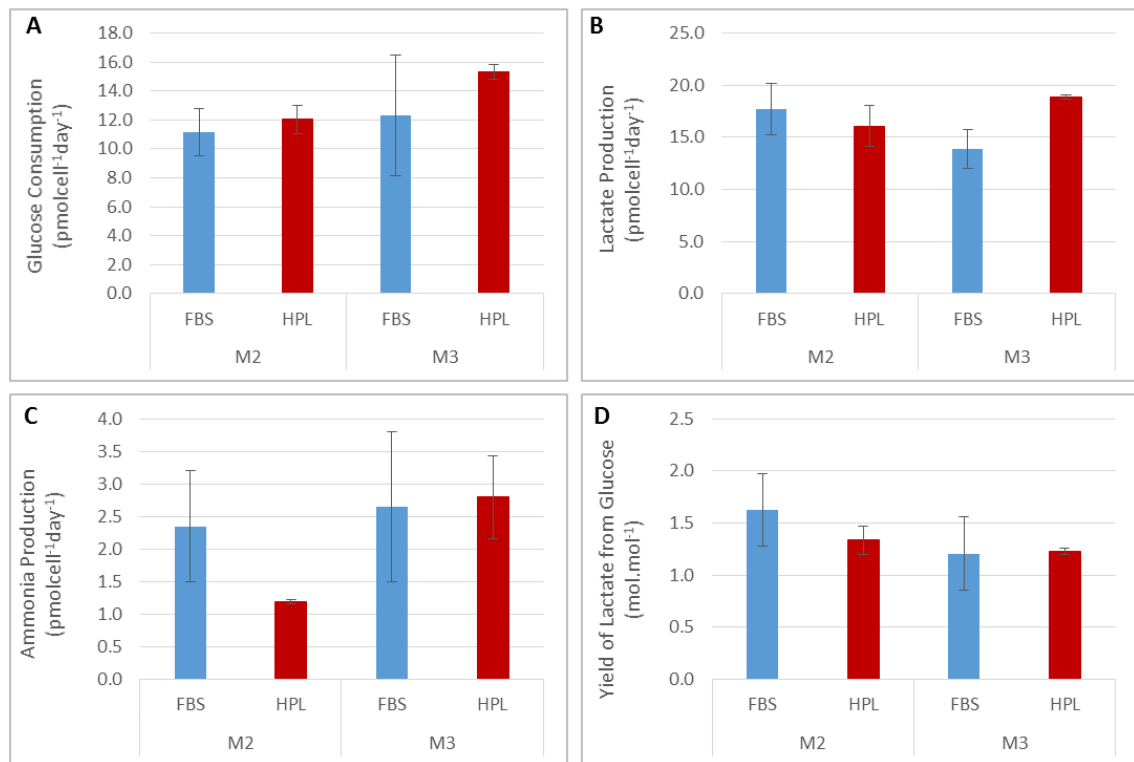
Figure 6.2. Per cell metabolite flux of two BM-hMSC lines over six days microcarrier expansion. Showing (A) per cell glucose consumption rate, (B) per cell lactate production rate, (C) per cell ammonia production rate and (D) Yield of lactate from glucose. Data shows mean ± SD (*n=4*).

Cell death was evaluated by measuring a combination of lactate dehydrogenase (LDH) (Lavrentieva *et al.* 2010a) and total protein released into the culture medium. Figure 6.3 shows these concentrations throughout culture, which show no increase in the LDH or total protein concentrations for both M2 and M3 in FBS and HPL-based culture. This demonstrates that cell damage was minimal throughout the microcarrier expansion process, despite the process change from static to agitated culture.
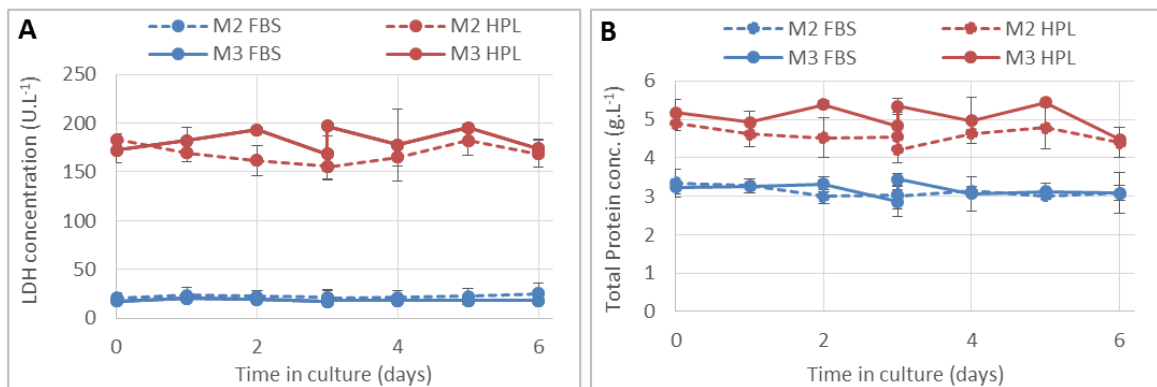
Figure 6.3. Nutrient and metabolite flux of BM-hMSC expansion on microcarriers. Total protein (A) and lactate dehydrogenase concentration (B) are shown for FBS and HPL-containing medium for M2 and M3. Data shows mean ± SD, n = 4

6.2.4 Post-harvest characterisation of BM-hMSCs from agitated microcarrier culture

The post-expansion detachment and separation of the BM-hMSCs from the microcarriers is of critical importance for a scalable production process, as cellular attributes must be maintained throughout the process (Nienow *et al.* 2014; Nienow *et al.* 2015b). A previously developed harvesting protocol (Nienow *et al.* 2014) was modified for this study by replacing trypsin-EDTA with TrypLE Express for the HPL culture to ensure the process was animal-component free. The post-harvest viability from both donor BM-hMSC lines in FBS and HPL was > 95%, demonstrating that this harvest process did not have a detrimental impact on the membrane integrity of the cells. It is important that BM-hMSC characteristics are also maintained following this detachment and separation process from the microcarriers.

Figure 6.4 shows the effect of the microcarrier process on BM-hMSC attributes compared to pre-expansion for colony forming efficiency, osteogenic potential, specific outgrowth rate and mean cell diameter. The colony forming efficiency of the BM-hMSCs following the microcarrier

expansion and harvest process generally saw an increase compared to pre-expansion, with a significant increase for M2 in HPL ($p < 0.05$). Similarly, the specific outgrowth rate and mean cell diameter have been maintained post-harvest, demonstrating that the microcarrier process has not affected these BM-hMSC characteristics. In contrast, the osteogenic potential of the BM-hMSC decreased for all conditions ($p < 0.01$), which should be further investigated if the BM-hMSCs are to be used for clinical indications relating to the production of collagen. There is the potential however, for this type of clinical indication, that biodegradable microcarriers could be directly implanted as a cell-scaffold construct to support the regeneration of bone tissue (Gao *et al.* 2015), removing the need for cell harvest altogether.
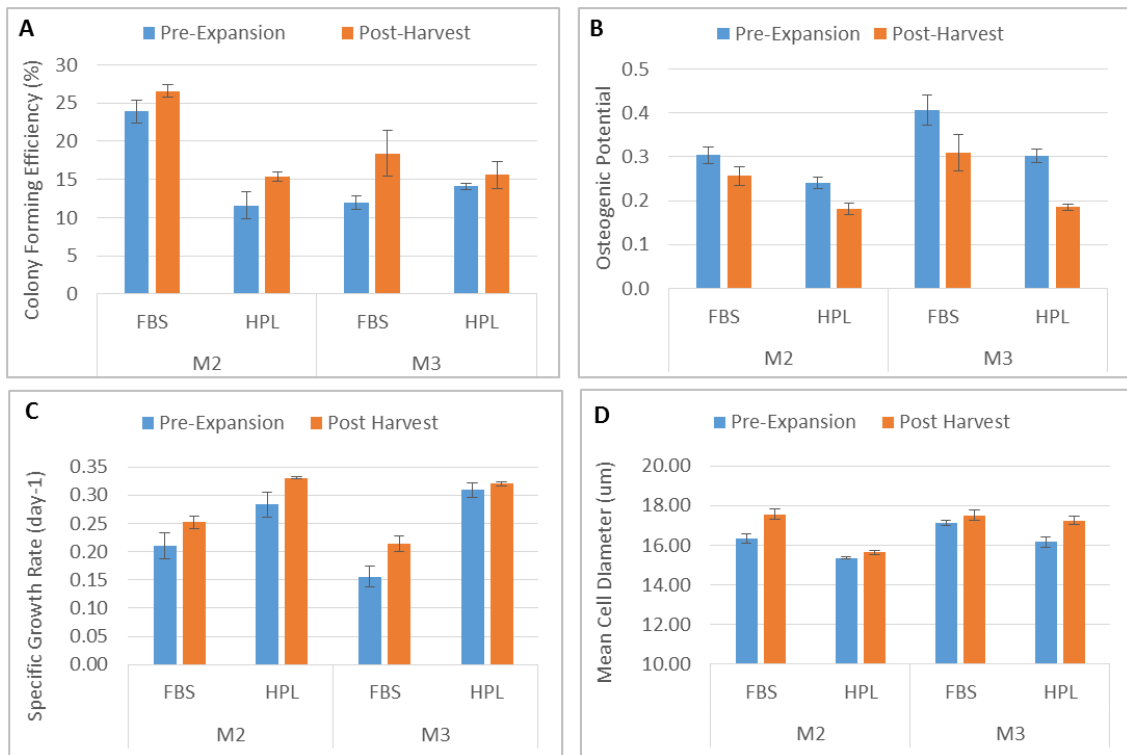
Figure 6.4. Post-harvest BM-hMSC quality compared to pre-expansion demonstrating retention of key attributes, showing (A) colony forming efficiency, (B) osteogenic potential, (C) specific outgrowth rate and (D) mean cell diameter. Data shows mean ± SD (*n=4*).

The BM-hMSCs harvested from the microcarrier process must also retain their identity in accordance with the ISCT criteria. Figure 6.5 shows the tri-lineage differentiation potential of the BM-hMSC following microcarrier expansion in HPL down the adipogenic, osteogenic and

chondrogenic lineages. This demonstrates that the BM-hMSCs have retained their tri-lineage differentiation potential following microcarrier expansion in HPL.
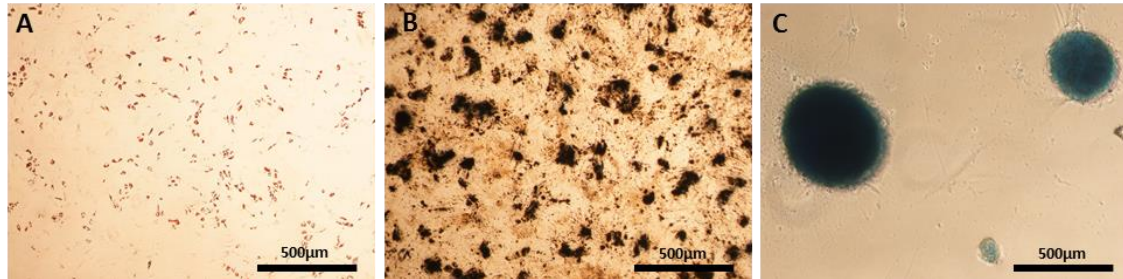
Figure 6.5. Tri-lineage differentiation potential of BM-hMSC lines using phase contrast microscopy. Showing adipogenic differentiation (A) by staining with Oil Red O, osteogenic differentiation (B) by staining for alkaline phosphatase and calcium deposition and chondrogenic differentiation (C) by staining with Alcian Blue

In addition to a demonstration of the tri-lineage differentiation potential, BM-hMSC harvested from the microcarrier process must also retain their immunophenotype. Figure 6.6 shows the multiparameter flow cytometry plots of post-harvest BM-hMSCs demonstrating the maintained positive co-expression of CD105, CD90 and CD73 throughout the microcarrier expansion process. Further to this, BM-hMSC have retained the negative co-expression of CD45, CD34, CD11b, CD19 and HLA-DR following the microcarrier expansion process. This demonstrates that the BM-hMSCs have retained the desired immunophenotype throughout the microcarrier process as has been demonstrated during the monolayer expansion process.
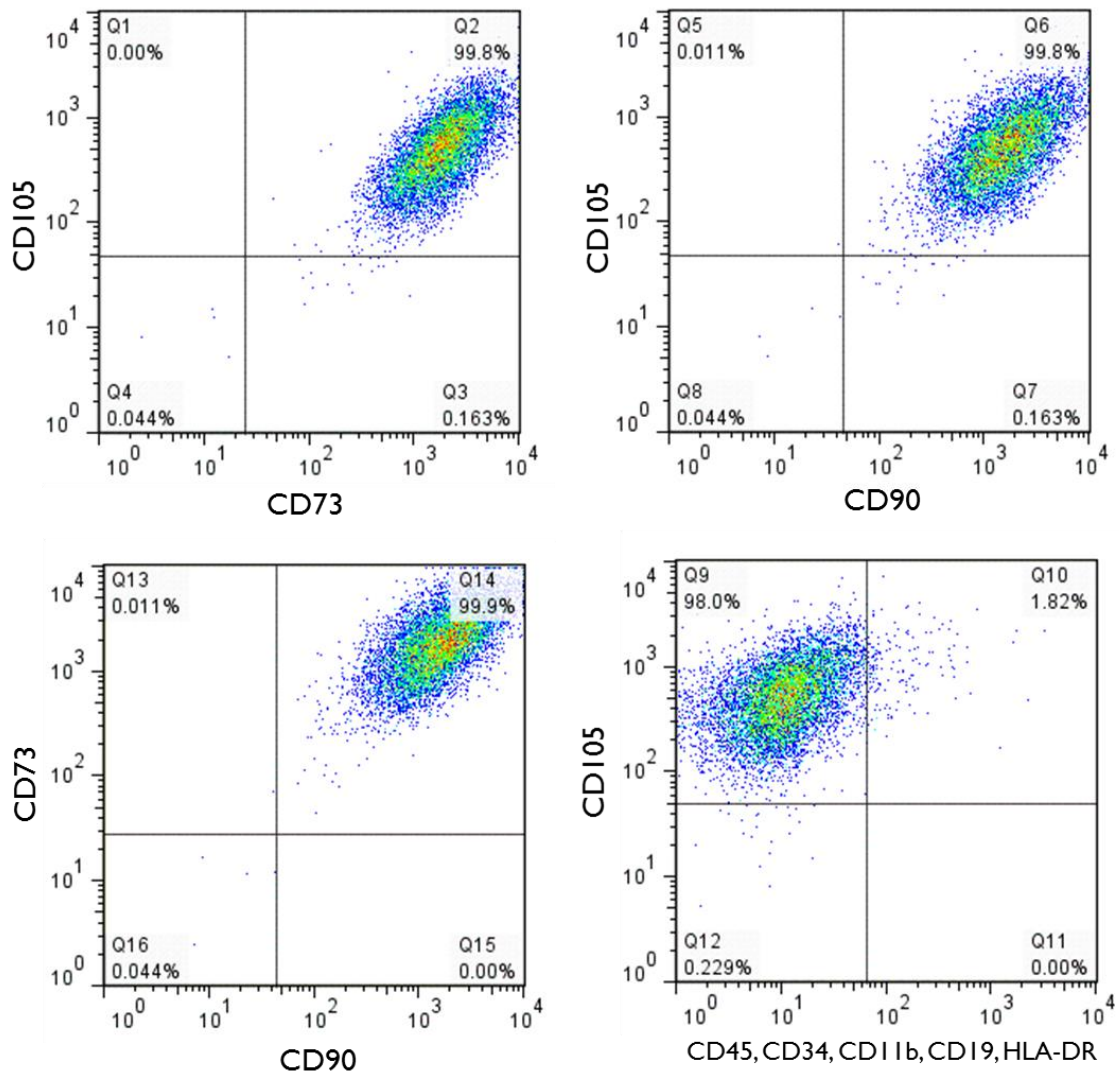
Figure 6.6. Post-harvest multiparameter flow cytometry plots showing co-expression of CD90+, CD73+, CD105+, CD44+, CD34-, CD45-, CD11b-, CD19- & HLA-DR- from microcarrier culture

This demonstrates that HPL is a viable alternative to FBS for the microcarrier culture of BM-hMSCs and has the potential to be taken forward to support further process development and scale-up. The increased consistency in growth between donors in HPL will also benefit the development of both patient specific and off-the-shelf BM-hMSC therapies, allowing for increased production rates and shorter processing times.

6.2.5 Comparison of BM-hMSCs in monolayer and agitated microcarrier culture

One of the key challenges in the successful development of scalable cell therapy manufacturing processes, is in the process transfer away from traditional manual monolayer processes. The decision of when in the development cycle to complete these bridging studies and move toward a scalable process should be carefully considered and many companies have suffered as a result of waiting until the end of clinical development, prior to commercial production. The advantages of automated and closed processing systems in driving scalable production by reducing costs should not be underestimated (Williams *et al.* 2012; Hampson 2014), with suspension based systems being a lead candidate, as they are routinely operated in this manner. This process transfer from monolayer to microcarrier culture will aim to assess the impact of the new process on the product attributes, to ensure they are comparable between the processes, avoiding the need to repeat clinical work, which will cost significant time and capital.

Table 6.1. Comparison of monolayer and microcarrier culture of BM-hMSCs in FBS and HPL-containing medium showing the improved process transfer under HPL. Statistics show significance between monolayer and microcarrier condition. * denotes p < 0.05 and ** denotes p < 0.01.

		Growth Rate (day^{-1})		Mean Cell Diameter (μm)		CFU Efficiency (%)		Osteogenic Potential		Outgrowth Rate (day^{-1})		Yield of lactate from glucose (mol.mol^{-1})	
		Mono-layer	Micro-carrier	Mono-layer	Micro-carrier	Mono-layer	Micro-carrier	Mono-layer	Micro-carrier	Mono-layer	Micro-carrier	Mono-layer	Micro-carrier
M2	FBS	*0.23 ±0.02	*0.18 ±0.01	16.33 ±0.22	14.93 ±1.27	23.90 ±1.54	26.60 ±0.85	**0.30 ±0.02	**0.26 ±0.02	*0.21 ±0.02	*0.25 ±0.01	*1.00 ±0.13	*1.63 ±0.35
	HPL	0.27 ±0.02	0.25 ±0.02	15.35 ±0.06	15.47 ±0.38	*11.60 ±1.82	*15.33 ±0.61	**0.24 ±0.01	**0.18 ±0.01	0.28 ±0.05	0.33 ±0.01	1.22 ±0.10	1.34 ±0.14
M3	FBS	**0.14 ±0.02	**0.05 ±0.02	**17.13 ±0.13	**15.23 ±0.46	12.00 ±0.86	18.40 ±3.02	**0.41 ±0.03	**0.31 ±0.04	**0.16 ±0.02	**0.21 ±0.01	0.89 ±0.13	1.20 ±0.35
	HPL	*0.27 ±0.01	*0.22 ±0.01	*16.15 ±0.25	*15.53 ±0.08	14.10 ±0.38	15.60 ±1.74	**0.30 ±0.02	**0.19 ±0.01	0.31 ±0.01	0.32 ±0.01	1.24 ±0.02	1.23 ±0.03

Obtaining similar growth kinetics of the BM-hMSCs from the monolayer and microcarrier processes is also important, as this will affect the number of BM-hMSCs that can be manufactured per unit time, which will reduce the number of batches produced per year. Table 6.1 shows the comparison of the monolayer and microcarrier process for M2 and M3 in FBS and

HPL-based culture. The growth rate of BM-hMSCs in FBS-based culture showed a significant reduction from monolayer to microcarrier culture for both BM-hMSC lines ($p < 0.05$ and $p < 0.01$), which is particularly apparent for M3, with a reduction from 0.14 ± 0.02 to 0.05 ± 0.02 day^{-1}. This would create challenges during process scale up within a suspension based system and would necessitate careful selection of donor material for master cell banks, to ensure it is amenable to this potential change in process conditions from static to agitated culture. It is likely that this widening of the gap in growth kinetics between the static monolayer process and agitated microcarrier culture is due to the efficiency of cell attachment, which becomes more important within the agitated environment.

In contrast to FBS-based culture, HPL proved more effective in supporting the transfer of the process from static to agitated conditions with only a slight reduction in the growth kinetics of M3 and no significant difference between the monolayer and microcarrier growth kinetics of M2. This demonstrates the potential of HPL to be used as a medium supplement within monolayer culture as well as for suspension culture of BM-hMSCs. Table 6.1 also shows that the colony forming efficiency, mean cell diameter and outgrowth rate have not been reduced for the microcarrier process which will be important during process transfer and scale up toward commercial production. It is also evident from Table 6.1 that the yield of lactate from glucose is more similar when comparing monolayer and microcarrier culture in HPL with FBS, which suggests a maintenance of the glycolytic pathway during microcarrier culture (Pattappa *et al.* 2011). All of this means that HPL represents a beneficial alternative to FBS for monolayer expansion processes and further process transfer into suspension based systems. This has implications for both patient specific and off-the-shelf BM-hMSC therapies in terms of increasing yield and reducing costs of therapies that are currently in development.

6.3 Development of a fibronectin coating process for microcarriers

6.3.1 Experimental overview

As has been discussed previously, the development of serum-free manufacturing processes will be important the drive the consistent and cost-effective production of BM-hMSC therapies. Considering the yield and consistency gains that have been achieved in serum-free monolayer culture and the successful process transfer of the serum-based process into suspension *via* the addition of microcarriers, it was important to also transfer the serum-free process into microcarrier culture. The key difference between the serum-based and the serum-free process for the culture of BM-hMSCs is in the fibronectin treatment of the tissue culture flask to provide the necessary attachment proteins to enable cell proliferation. This process is well established for monolayer culture, however, additional challenges to this coating process for microcarrier culture mean that a new process must be developed to ensure the adequate coating of the microcarriers and enable BM-hMSC expansion under serum-free conditions.

The first experiment in this process was to assess the impact of fibronectin coating in monolayer in FBS-based culture. This is to provide a baseline for microcarrier coating in FBS-based culture so that the initial microcarrier coating development can be completed in FBS-based medium as this provides a far more cost-effective process development pathway. Four T-75 flasks were coated with 0.4 $\mu g.cm^{-2}$ of PRIME-XV® Fibronectin and cultured in FBS-containing medium alongside four uncoated T-75 flasks for three passages. At the end of each passage, the viable cell number and mean cell diameter was determined and the growth kinetics were calculated. In addition, the three hour attachment efficiency was determined at the end of each passage for coated and uncoated T-25 flasks.

In order to determine the concentration of fibronectin to coat the microcarriers, an experiment was designed to compare different concentrations of fibronectin in PBS prior to culture. Table 6.2 shows the volume and concentrations of fibronectin used for each of the tested coating protocols for microcarriers. Four spinner flasks were cultured for each coating concentration for six days (see Section 3.3.3) and harvested according to Section 3.3.4 to determine the final cell number. Following this, post-harvest characterisation was completed to verify BM-hMSC immunophenotype and tri-lineage differentiation potential. In addition, an experiment was conducted to ensure that the fibronectin substrate did not coat the internal glass surface of the

spinner flask, which would allow BM-hMSCs to attach and proliferate on the internal surface of the flask. This was not found to be the case and these results can be found in Appendix D.

Table 6.2. Fibronectin coating protocol for microcarrier culture

Final coating concentration (μg.cm^{-2})	Microcarrier surface area (cm^2)	Concentration of fibronectin (μg.mL^{-1})	Volume of coating solution (mL)
0.4	500	5	40
0.2	500	2.5	40
0.1	500	1.25	40

The coating protocol was as follows:

1. Depending on microcarrier surface area required, the appropriate amount of polystyrene plastic microcarriers was weighed as per the manufacturer's instructions and transferred to a spinner flask vessel. (1.4 g provided 500 cm^2 of microcarrier growth area).
2. 25-30 mL of distilled water was added and the spinner flask was autoclaved.
3. After autoclaving, the water was aspirated from the spinner flask.
4. The appropriate amount of coating substrate was added according to Table 6.2 and the spinner flask was agitated at N_{JS} (30 rpm) for two hours at room temperature.
5. The microcarriers were washed once with PBS, 100 mL of SFM was added and the flask was transferred to in an incubator prior to BM-hMSC inoculation.

Following this initial screening study in FBS, the best performing fibronectin concentration was taken forward to assess the performance in serum-free culture, with both human fibronectin (FN) and recombinant fibronectin (MatrIS-F). In addition to the pre-coating protocol described above, the potential for a direct coating process was also assessed. The advantage of this would be that it would shorten the process time, as well as alleviating the need to validate the coating process which would need to be de-coupled from the expansion process to reduce the risk in suffering a quality assurance failure, which would impact the subsequent process operation. The protocol for this direct coating was as follows:

1. Depending on microcarrier surface area required, the appropriate amount of polystyrene plastic microcarriers were weighed as per manufacturer's instructions and transferred to a spinner flask vessel. (1.4 g provided 500 cm^2 of microcarrier growth area).

2. 25-30 mL of distilled water was added and the spinner flask was autoclaved.

3. After autoclaving, the water was aspirated from the spinner flask.

4. Fibronectin was added to 40 mL of SFM to give a final concentration of 1.25 $\mu g.mL^{-1}$, which was agitated at 30 rpm for two hours at room temperature.

5. Finally, 60 mL of fresh SFM was added and the flask was transferred to an incubator prior to BM-hMSC inoculation.

After six days of culture, the four spinner flasks for each condition were harvested according to Section 3.3.4 and the cell number determined prior to post-harvest BM-hMSC characterisation.

6.3.2 Fibronectin coating of FBS culture in monolayer

The first part of developing a microcarrier coating process for serum-free culture was to assess the effect of culturing BM-hMSCs on fibronectin in FBS-containing medium in monolayer. This is because the initial development of a microcarrier coating process took place in FBS-based culture and it is important to obtain a baseline in monolayer to compare these results to the microcarrier coating protocol. Figure 6.7 shows the results of the monolayer fibronectin coating protocol in FBS-based medium. It can be seen from Figure 6.7 that the fibronectin coating of the tissue culture flasks led to a significantly increased growth rate of the BM-hMSCs at passage four ($p < 0.01$), passage five ($p < 0.05$) and passage six ($p < 0.01$). The specific growth rate of BM-hMSCs at passage five was 0.258 ± 0.034 day^{-1} for non-coated and 0.316 ± 0.018 day^{-1} in fibronectin coated flasks, which can be used for comparison against the microcarrier coating, following an adaption passage.

It has previously been shown that BM-hMSCs adhered to fibronectin strongly potentiate platelet-derived growth factor receptor (PDGFR)-β phosphorylation and focal adhesion kinase (FAK) activity. This leads to the regulation of actin reorganisation and increased cell migration, which is important during culture as well as therapeutically, for the remodelling of vasculature (Veevers-Lowe *et al.* 2011) and has been shown to enhance osteogenesis (Li *et al.* 2013). In addition to the increased growth characteristics of BM-hMSCs, the mean cell diameter of the

BM-hMSCs cultured on fibronectin was also significantly reduced for the first two passages ($p < 0.05$), which is in accordance with the previous findings in Section 5.2.3, which showed that a reduced cell diameter was associated with increased growth kinetics.

An indication that fibronectin enhances the attachment of BM-hMSCs can be seen in Figure 6.7, which is significantly higher for the first two passages ($p < 0.05$) compared to uncoated tissue culture plastic. It is also evident that the consistency in BM-hMSC attachment is improved when cultured on fibronectin, which will be important for the development of BM-hMSC manufacturing processes, particularly on microcarriers, where the cell attachment is particularly important under agitated conditions (Rafiq *et al.* 2015b).
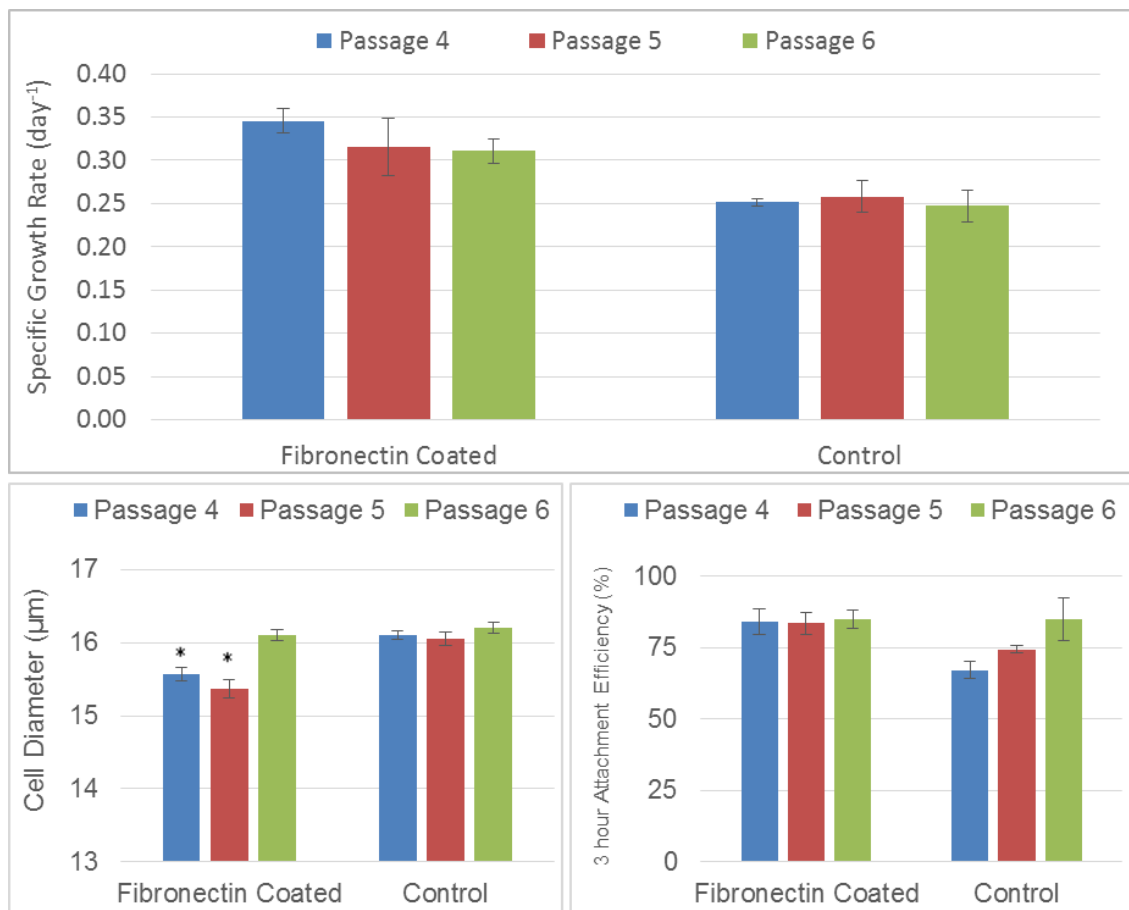
Figure 6.7. Fibronectin coating in FBS monolayer culture at a concentration of 0.4 μg.cm^{-2} showing the specific growth rate, cell diameter and attachment efficiency of BM-hMSCs over three passages. Demonstrating the increased attachment and growth kinetics of BM-hMSCs cultured on fibronectin. Data shows mean ± SD, n=4. * denotes p < 0.05

6.3.3 Fibronectin coating of microcarriers in FBS culture

Now that a baseline for fibronectin coating has been established in monolayer culture, a comparison of coating concentrations can be evaluated in microcarrier culture using FBS-containing medium. The results of this study can be seen in Figure 6.8, which shows the fold increase in BM-hMSCs at fibronectin concentrations of 0, 0.1, 0.2 and 0.4 $\mu g.cm^{-2}$, demonstrating an increase in growth rate at lower concentrations of fibronectin. As with the monolayer culture previously, coating the microcarriers in fibronectin produced a significant increase in growth kinetics ($p < 0.05$), demonstrating that the microcarriers are being successfully coated with the fibronectin substrate at all concentrations.

Part of the reason for the improved growth kinetics at lower fibronectin concentrations can be seen in Figure 6.9, which shows the high level of microcarrier aggregation that occurs, particularly at a fibronectin coating concentration of 0.4 $\mu g.cm^{-2}$. The consequence of increase microcarrier aggregation is that the available surface area for BM-hMSCs to expand on is reduced, resulting in a lower cell number at the end of six days in culture. In contrast, the level of microcarrier aggregation at 0.1 $\mu g.cm^{-2}$ was comparable to the level of aggregation observed in the uncoated control.
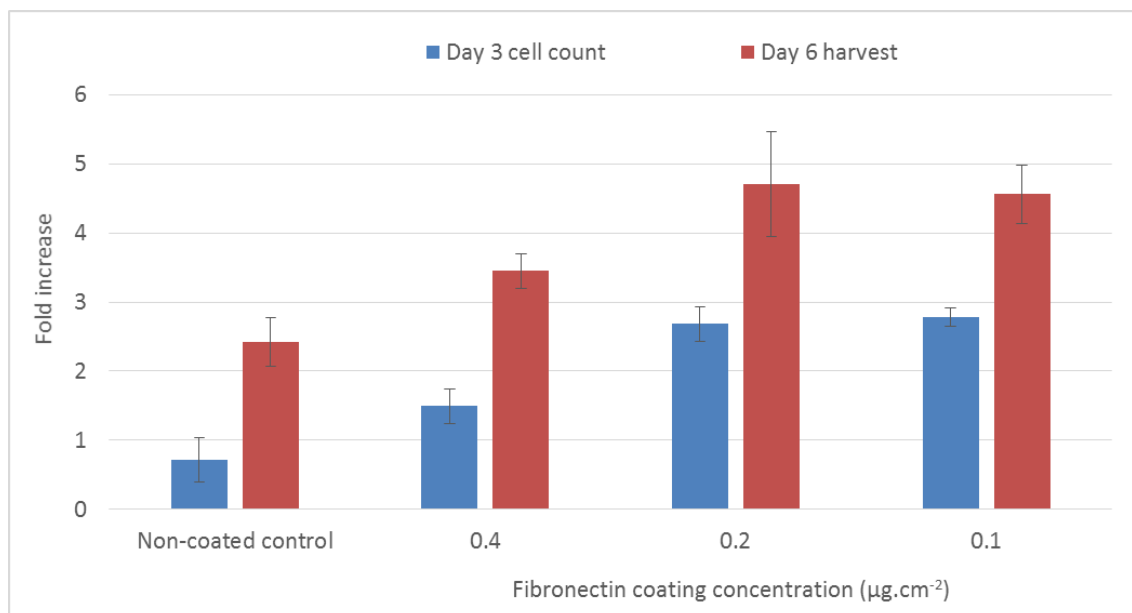
Figure 6.8. Fibronectin coating of microcarriers at different concentrations in FBS showing the increased BM-hMSC expansion rate at reduced fibronectin concentrations. Data shows mean ± SD, n=4

In terms of a direct comparison between monolayer and microcarrier culture of BM-hMSCs, the uncoated monolayer condition had a growth rate of 0.258 ± 0.034 day^{-1}, compared to 0.147 ± 0.2 day^{-1} in microcarrier culture, a reduction of 0.111 day^{-1}. In contrast, the difference in growth kinetics between monolayer and microcarrier culture for the fibronectin coated condition was 0.059 day^{-1}. This increased comparability in BM-hMSC growth kinetics between monolayer and microcarrier culture for fibronectin coated surfaces is likely a result of the improve attachment efficiency seen in Figure 6.7, as effective cell attachment becomes increasing important on microcarriers under agitated conditions. This characteristic of fibronectin coated microcarrier culture makes developing a serum-free microcarrier process a highly attractive proposition, considering the improved BM-hMSC growth and quality characteristics seen for monolayer culture in Chapter 5.
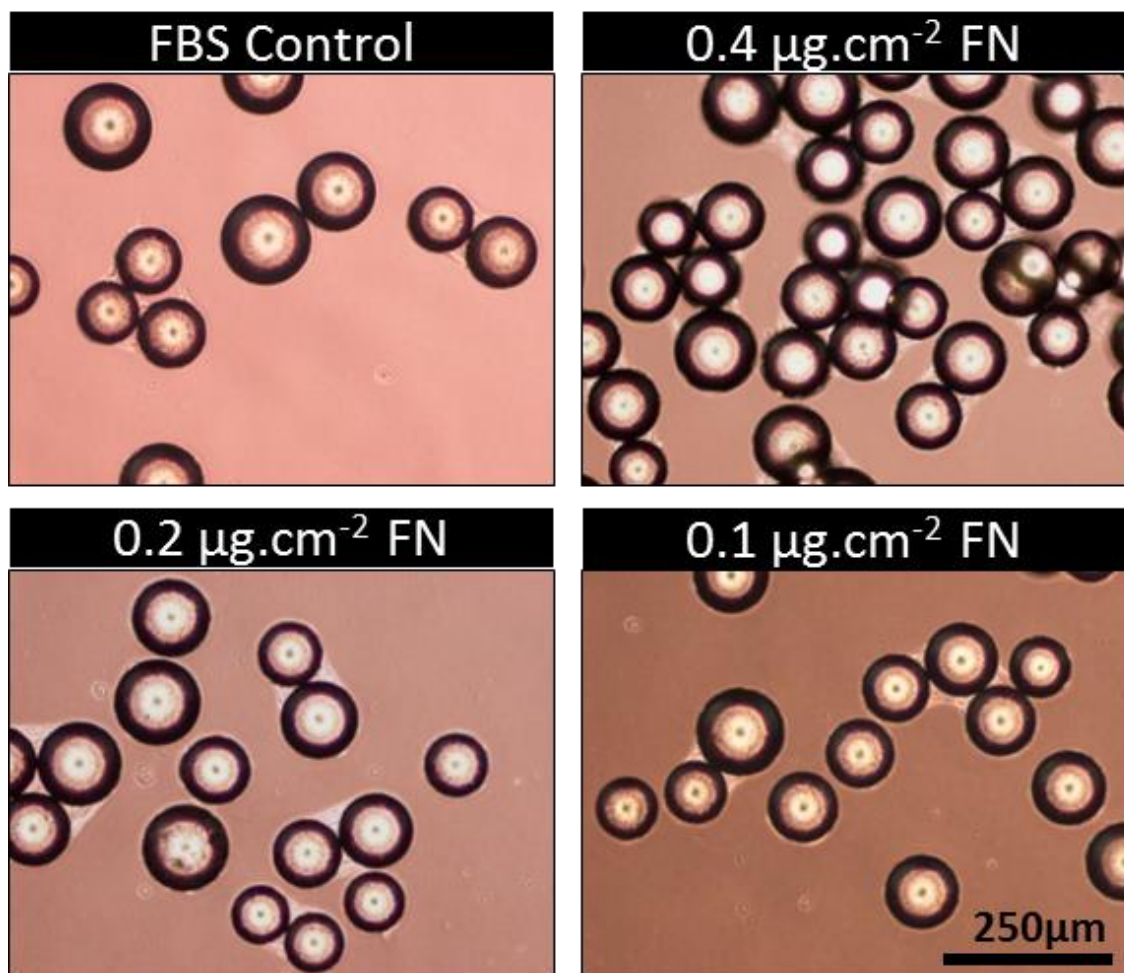
Figure 6.9. Phase contrast images showing the aggregation of BM-hMSCs and microcarriers with fibronectin coating at different concentrations in FBS

To ensure that the fibronectin coating of microcarrier does not affect the identity characteristics of the BM-hMSC, immunophenotype, tri-lineage differentiation and morphology have been assessed in accordance with the International Society for Cellular Therapy (ISCT) criteria (Dominici *et al.* 2006). Figure 6.10 shows the compliance of the BM-hMSCs with the ISCT criteria, by adherence to tissue culture plastic, demonstrating the same morphology post-harvest in fibronectin coated and uncoated culture and differentiation down the osteogenic, adipogenic and chondrogenic lineages. The post-harvest BM-hMSC immunophenotype can be seen in Figure 6.10 which shows the co-expression of positive markers CD73, 90 and 105 as well as the expression of CD34 and HLA-DR at less than 2 % (Chan *et al.* 2014b).
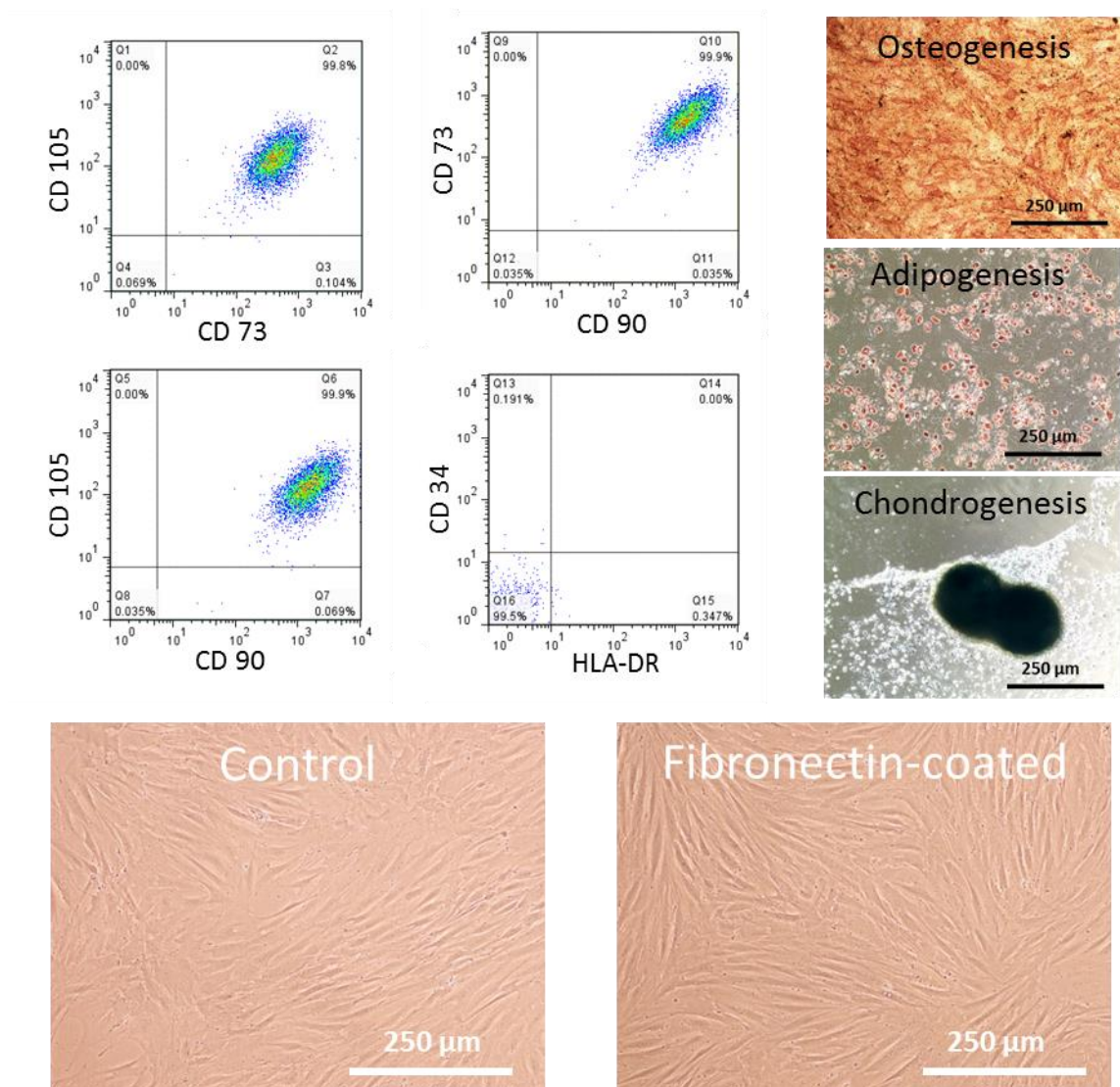
Figure 6.10. Post-harvest characterisation showing retention of BM-hMSC morphology, immunophenotype and tri-lineage differentiation potential for fibronectin coated microcarrier culture in FBS-based medium

6.3.4 Fibronectin coating strategy for microcarriers in SFM

Following the successful demonstration of fibronectin coating of microcarriers in FBS-containing medium, the process was validated for serum-free culture using the lowest fibronectin concentration of 0.1 µg.cm^{-2}. The reason for this was because it demonstrated similar growth characteristics to 0.2 µg.cm^{-2} ($p > 0.05$) whilst requiring half the amount of fibronectin, representing a significant cost saving for the process. For the development of the fibronectin coating process for microcarriers in SFM, human derived fibronectin (FN) will be used in conjunction with recombinant fibronectin (MatrIS-F) to assess the relative performance of the two fibronectin sources. The reason for this is that the development of defined manufacturing processes will require the use of non-animal and non-human derived components to reduce the risk of pathogen transmission as well as reducing the variability between batches of substrates (Unger *et al.* 2008). This means that the use of recombinant proteins, such as fibronectin in future BM-hMSC processes will be favourable and therefore it is important to assess whether they are amenable to the microcarrier process at an early stage in development. Further to this, if a similar performance can be demonstrated between human-derived fibronectin and recombinant fibronectin, then the rest of this development can be carried out using the more cost-effective fibronectin source, with the knowledge that if future development requires a recombinant protein source, the process can be successfully transferred in a timely fashion.
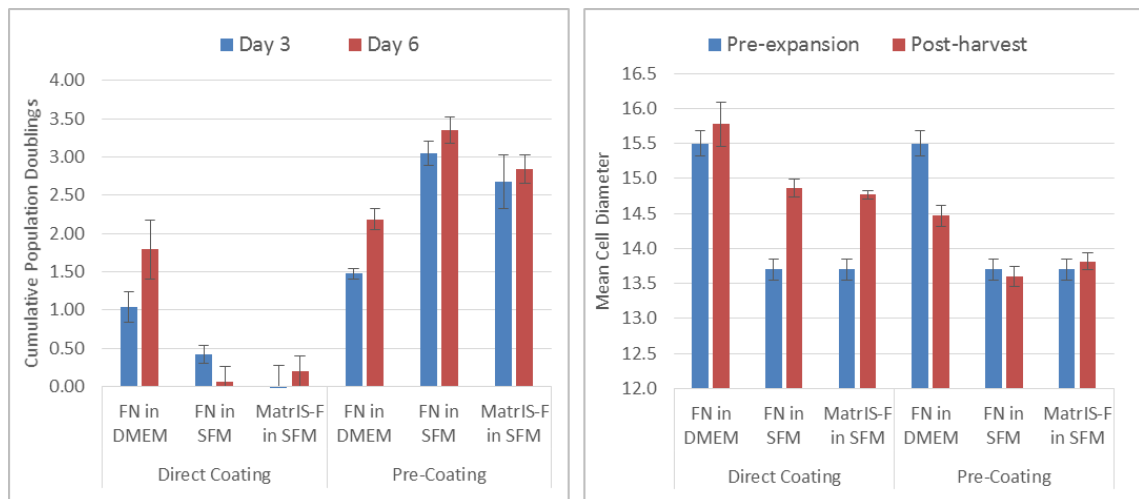
Figure 6.11. The effect on BM-hMSC growth and cell diameter of pre-coating microcarriers versus directly adding the coating substrate into the medium for FBS and SFM-based expansion. Coating at 0.1 µg.cm^{-2} using human-derived (FN) and recombinant (MatrIS-F) fibronectin. Data shows mean ± SD, n=4

Figure 6.11 shows the results for this development using PRIME-XV® SFM with pre-coating of the microcarriers in PBS and directly adding the fibronectin into the culture medium to avoid the additional process of coating the microcarriers. It can be seen from Figure 6.11, however, that directly adding the attachment substrate into the culture medium does not effectively support the proliferation of BM-hMSCs, with almost no growth over the six days of culture in SFM. This means that despite the advantages of eliminating the need to pre-coat the microcarriers, it is necessary to do so when expanding BM-hMSCs in SFM. The contrast between FBS and SFM in this instance is due to the increased presence of attachment proteins in FBS, which are able to support the attachment and proliferation of BM-hMSCs even when ineffective microcarrier coating occurs when the fibronectin is directly added to the culture medium.
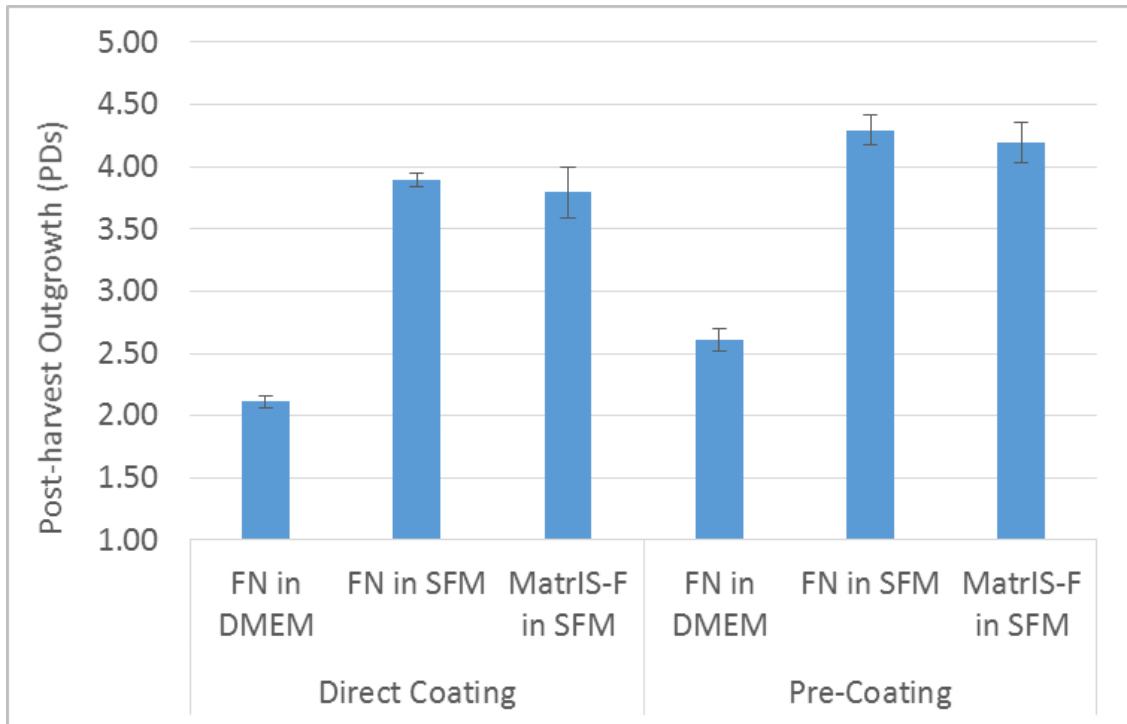
Figure 6.12. Post-harvest outgrowth showing the reduced outgrowth rate of cells cultured on microcarriers with attachment substrate added into the medium. Data shows mean ± SD, n=4

It was also evident from Figure 6.11 that the growth kinetics of BM-hMSCs in SFM were drastically enhanced compared to FBS in microcarrier culture, as was seen in monolayer culture in Chapter 5. The mean cell diameter of BM-hMSCs in SFM was also lower than BM-hMSCs in

FBS culture, which was particularly evident for the BM-hMSCs cultured on pre-coated microcarriers (Figure 6.11). The fact that the post-harvest mean cell diameter of BM-hMSCs in the direct coating condition was significantly higher (p < 0.01) than in the pre-coating condition is further evidence that the BM-hMSCs in this condition were not able to successfully attach to the microcarriers.

Figure 6.12 shows the post-harvest outgrowth kinetics of BM-hMSCs from each of the microcarrier conditions, which shows the reduced outgrowth kinetics of BM-hMSCs cultured on microcarriers that were directly coated from the culture medium. This is a further indication that the direct coating method for the microcarriers is having a detrimental impact on the BM-hMSCs, which should be avoided during the manufacturing process. All of this evidence shows that for the successful expansion of BM-hMSCs in SFM, that pre-coating the microcarriers with fibronectin will be required at a concentration of 0.1 μg.cm^{-2}, which can now be taken forward to develop a serum-free microcarrier process for the expansion of BM-hMSCs.

6.4 Development of a serum-free microcarrier process for BM-hMSCs

6.4.1 Experimental overview

Following the successful development of a fibronectin coating protocol for microcarriers in SFM, a full investigation of the serum-free culture of BM-hMSCs on microcarriers was completed. For this, four 100 mL spinner flasks were cultured in FBS-containing medium with BM-hMSC line M2 and four were cultured in SFM following the microcarrier coating protocol described in Section 6.3 for six days. Daily medium samples were taken for analysis of glucose, lactate, ammonia, lactate dehydrogenase and total protein with cell counts performed on day three of culture (four samples were analysed per spinner flask as per Section 3.4.3). The culture medium was exchanged on day three for FBS culture and every two days for SFM culture (Section 3.3.3). At harvest, the BM-hMSCs were removed from the microcarriers and separated according to Section 3.3.4. The BM-hMSCs harvested from each condition were then assessed for mean cell diameter (3.4.2), tri-lineage differentiation potential (Section 3.4.4) and immunophenotype (Section 3.4.5). In addition to these identity measurements, BM-hMSC quality characteristics of colony forming efficiency (Section 3.4.9) and outgrowth potential were also assessed post-harvest.

It is important that the development of BM-hMSC production processes also consider the downstream implications of the process and in particular the cryopreservation of the product, as many of these off-the-shelf therapies will require long term storage. Part of this was considering the time it will take to process bioreactor material on a large scale and integrating these realistic downstream processing times into the process prior to cryopreservation. With this in mind, a four hour holding time was incorporated into the SFM process post-harvest, with this BM-hMSC product taken forward into a serum-free cryopreservation process (Section 3.3.6). Following this cryopreservation process, BM-hMSCs were thawed and assessed for adhesion and F-actin content (Section 3.4.13).

6.4.2 Process map of the serum-free BM-hMSC microcarrier process

Process mapping is a key part of systematic process development and allows for a structured development methodology centered on the concept of integrated unit operations and is being adopted in current biopharmaceutical manufacture (ICH 2005). Breaking a process down into unit operations allows for the detailed analysis of each process sub-unit, which can be assessed in terms of its impact on the product characteristics. This flags potential issues or bottlenecks in

the process which can then be systematically resolved. Figure 6.13 shows our simplified process map, which forms the basis for our integrated serum-free BM-hMSC production process, allowing us to develop individual unit operations to eventually achieve a larger yield of high quality product. The timing of the microcarrier-fibronectin coating step has been highlighted as a potential bottleneck, which cannot take place immediately prior to the expansion step. A quality risk management approach has highlighted that the quality assurance of the microcarrier coating could not take place in-process, as a failure event would severely impact subsequent unit operations. This will be addressed during future process development as this unit operation would have to take place in advance to decouple the coating step from the BM-hMSC expansion, reducing the inherent risk in the process.

hMSC Bank	Pre-Expansion	Expansion	Downstream	Preservation
Thaw	Monolayer Expansion	Microcarrier Harvest	Filtration	Thaw
	Monolayer Harvest	Microcarrier Expansion	Centrifugation	Product Cell Bank
	FN Coating Microcarriers	Microcarrier Cell Seed	4 Hour Hold Time	Cryo-preservation
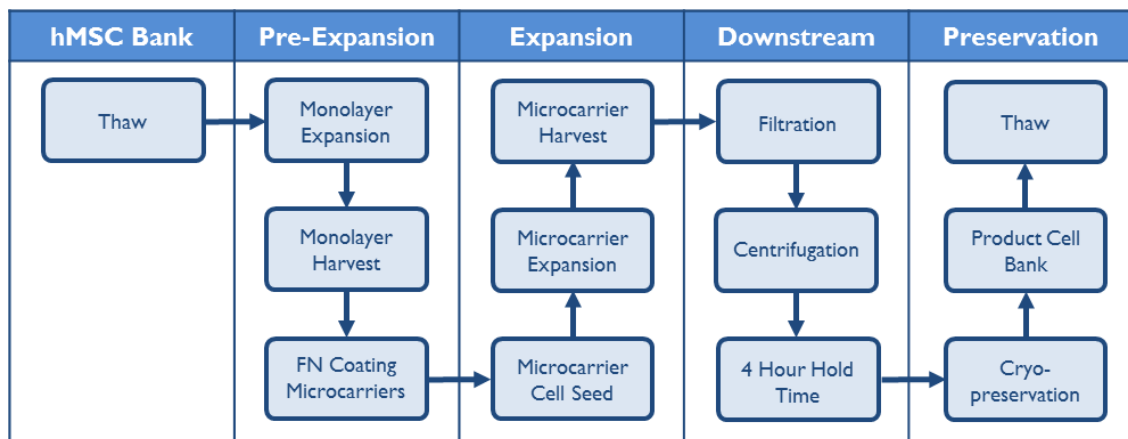
Figure 6.13. Process map for the serum-free expansion, harvest, downstream processing and preservation of BM-hMSCs on microcarriers.

A further benefit of the process map is that it allows for interchangeability of unit operations that may not be sufficiently scalable for future product requirements. An example of this in the current process is the use of vacuum filtration and centrifugation to separate the BM-hMSCs from the microcarriers, which would be a challenge to operate at large scale. Therefore, during future development, scalable technology would be assessed for the separation and concentration step such as tangential-flow filtration. The effect of this unit operation must be assessed in terms of the impact on the product characteristics, to ensure product quality is not compromised. This assessment should be done in a timely manner, as the implications of changing process unit operations late in clinical development can be prohibitive. Therefore by taking this systematic development methodology and utilising process mapping, potential

bottlenecks and scalability issues can be alleviated at an early stage of development, avoiding costly changes as processes move through clinical development.

6.4.3 Growth kinetics of BM-hMSCs in serum-free microcarrier culture

As described previously, intensive process scale-up will be required to meet the clinical and commercial need for these large-scale allogeneic therapies. For instance, for a typical clinical indication like myocardial infarction, the dose requirements will be in the range of 35 – 350 million BM-hMSCs per patient (Hare *et al.* 2009).
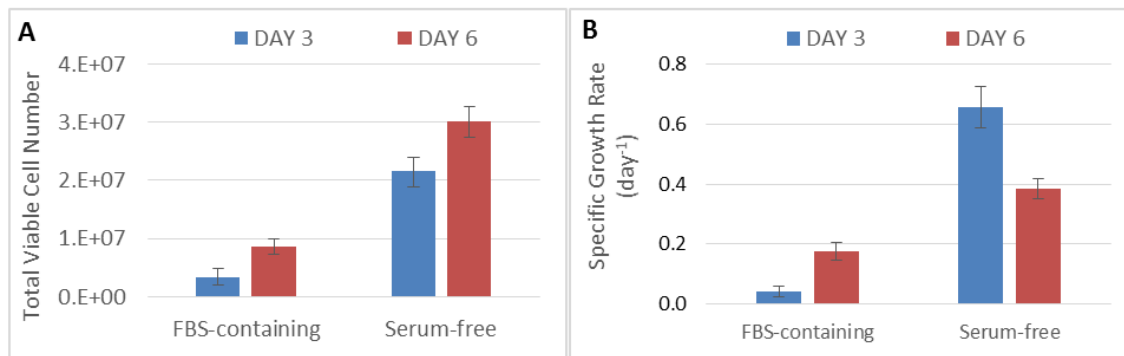
Figure 6.14. Growth kinetics of BM-hMSCs cultured on microcarriers in FBS-containing medium and serum-free medium. Showing (A) Total viable cell number and (B) Specific growth rate. Data shows mean ± SD N=3

The BM-hMSCs were expanded on non-porous plastic microcarriers in 100 mL spinner flasks over six days in FBS-containing medium and PRIME-XV SFM®. To facilitate cell attachment without the presence of serum (Hayman *et al.* 1985), plastic microcarriers were pre-coated with fibronectin before expansion under serum-free conditions. For BM-hMSCs expanded in spinner culture with FBS-containing medium, a final cell density of $(8.58 \pm 1.37) \times 10^4$ cells.mL^{-1} (mean ± SD, n=3) was reached, corresponding to a fold expansion of 2.86 ± 0.46 (Figure 6.14). In contrast, BM-hMSCs expanded in serum-free medium reached a final cell density of $(3.01 \pm 0.27) \times 10^5$ cells.mL^{-1}, corresponding to a fold increase of 10.04 ± 0.88 over the same time period (Figure 6.15). Operating under serum-free conditions gave a 350% increase in BM-hMSC yield, which is significantly higher than serum-based culture ($P < 1 \cdot 10^{-6}$). This difference represents a significant

step forward in increasing the lot-size of BM-hMSC expansion and is comparable to studies which have achieved a BM-hMSCs density on microcarriers of $1 - 2$ x 10^5 cells.mL^{-1}, also under serum-free conditions (Santos *et al.* 2011; dos Santos *et al.* 2014). It was also observed that the BM-hMSC growth kinetics under serum-free microcarrier culture (0.384 ± 0.014 day^{-1}) were significantly higher (p < 0.0001) than serum-free monolayer culture (0.323 ± 0.011 day^{-1}). This increase could also be improved further by adding more surface area during the microcarrier culture, reducing the surface area limitation experienced under serum-free conditions.
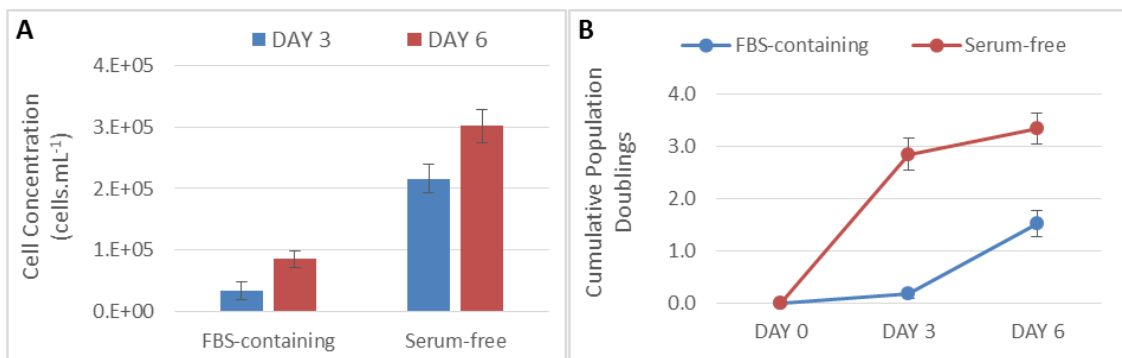
Figure 6.15. Growth kinetics of BM-hMSCs cultured on microcarriers in FBS-containing medium and serum-free medium. Showing (A) Cell concentration and (B) cumulative population doublings. Data shows mean ± SD N=3

Despite this improvement in BM-hMSC yield under serum-free conditions, the expansion unit operation is clearly far from optimal. Figure 6.16 shows the large amount of microcarrier aggregation that occurred in serum-free culture, which limited the effective surface area available for expansion. The growth kinetics in Figure 6.14B and Figure 6.15B, where the BM-hMSC growth between days 3 to 6 was reduced compared to day 0 to 3 in serum-free culture, is also suggestive of surface area limitation. It is likely that microcarrier aggregation is caused by a combination of accelerated cell growth, the microcarriers reaching effective confluence and the medium sampling process which requires the microcarriers to settle. These potential mechanisms will need to be addressed moving forward as aggregation not only has the potential to reduce cell yield but can also accentuate cell microenvironment heterogeneity (Baraniak *et al.* 2012) resulting in a cell product of inconsistent quality, although this did not occur here.
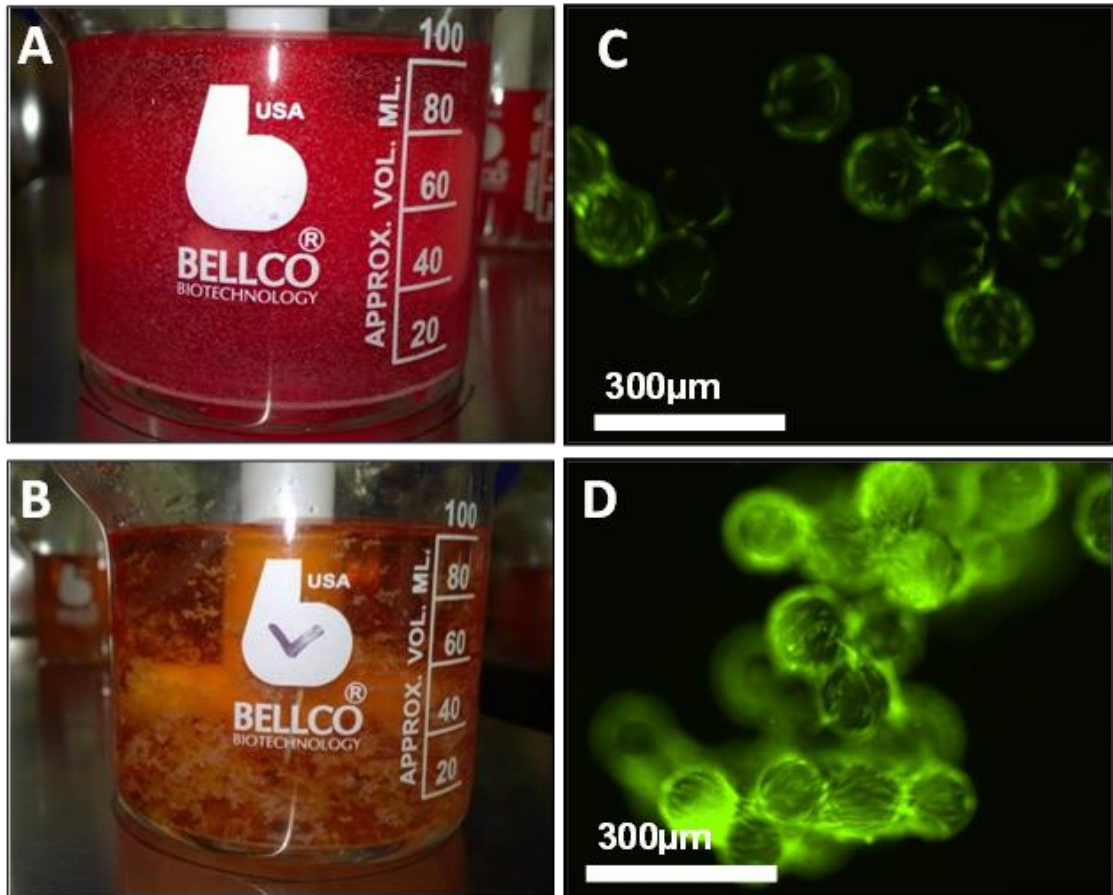
Figure 6.16. Microcarrier culture of BM-hMSCs on day 5 showing representative images of cell-microcarrier aggregation. Image of microcarriers in spinner flask with FBS-containing medium (A) and serum-free medium (B). Live/dead cell stain of BM-hMSCs on microcarriers in FBS-containing medium (C) and serum-free medium (D). Live cells stained with Calcein AM fluorophore (GREEN) and dead cells are stained with ethidium homodimer (RED).

6.4.4 Metabolite flux of BM-hMSCs in serum-free microcarrier culture

Metabolite analysis of microcarrier-based suspension culture of BM-hMSCs showed differences in the metabolic pathway usage relating to lactate and ammonia production between FBS-containing and serum-free cultures. In FBS-containing medium, BM-hMSCs favoured the relative production of lactate over ammonia, whereas the relative production of ammonia over lactate was favoured with BM-hMSCs cultured in serum-free conditions (Figure 6.17). This finding is consistent with the monolayer process evaluated in Chapter 5.
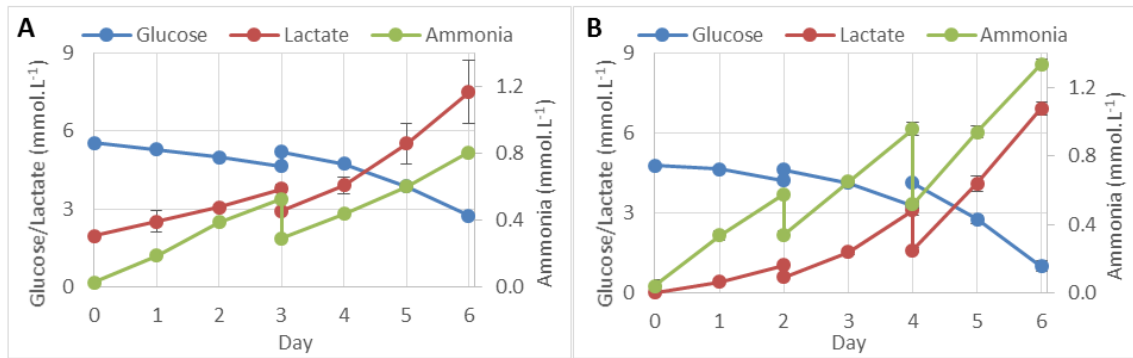
Figure 6.17. Nutrient and metabolite flux of BM-hMSC expansion on microcarriers. Glucose, lactate and ammonia concentrations in FBS-containing medium (A) and serum-free medium (B). Data shows mean ± SD, N=3

Figure 6.18 shows that the per cell production of lactate was lower in serum-free culture at 12.63 ± 0.59 pmol.cell^{-1}.day^{-1} (mean ± SD, n=3) compared with 20.81 ± 4.88 pmol.cell^{-1}.day^{-1}, whereas the production of ammonia was 2.82 ± 0.15 pmol.cell^{-1}.day^{-1} in serum-free, compared to 3.31 ± 0.10 pmol.cell^{-1}.day^{-1} in FBS-containing culture. The estimated yield of lactate from glucose over the entire culture period was 1.91 ± 0.03 and 1.76 ± 0.04 mol.mol^{-1} for FBS-containing and serum-free culture, respectively. It is considered that the observed differences in these metabolic profiles are predominantly related to proliferative rate in this instance. The increased proliferative rate coupled with the smaller cell size makes DNA a larger proportion of the total cell biomass under serum-free conditions. Increased ammonia production suggests altered amino acid utilisation, which may be related to the increased need for precursors (e.g. glutamine and asparagine) supporting purine and pyrimidine biosynthesis (Higuera *et al.* 2012).
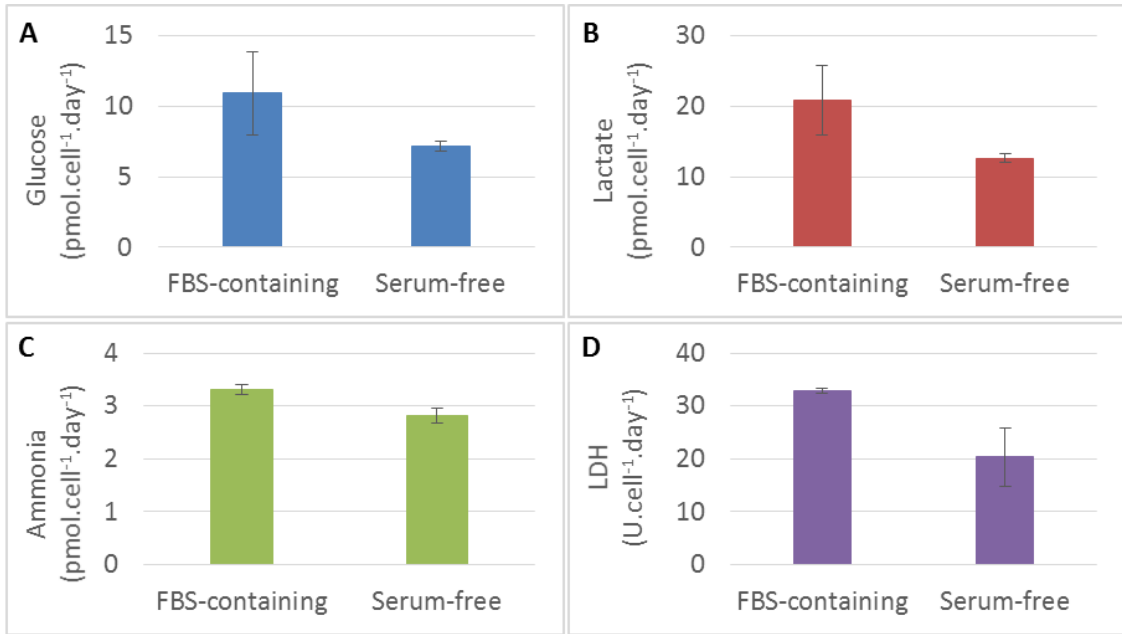
Figure 6.18. Specific consumption rate per cell of glucose (A) and production rate per cell of lactate (B), ammonia (C) and lactate dehydrogenase (D) for FBS-containing medium and serum-free medium. Data shows mean ± SD (N=3).

It is clear that a more detailed metabolic analysis is required and the development of culture medium should consider the impact of these metabolic pathways on cell characteristics. The reduced consumption of glucose and production of lactate per cell under serum-free conditions does however provide an advantage over serum-based culture, as the usage and build-up of metabolites has the potential to inhibit cell growth as the yield and scale increases.
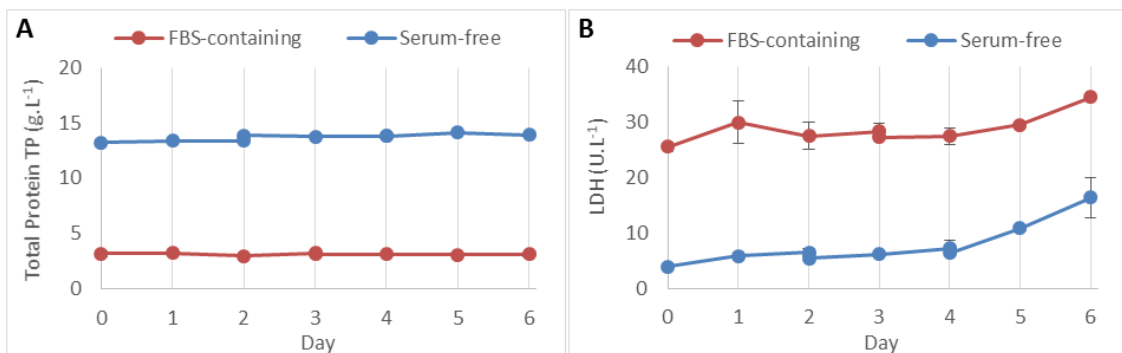
Figure 6.19. Nutrient and metabolite flux of BM-hMSC expansion on microcarriers. Total protein (A) and lactate dehydrogenase concentration (B) are shown for FBS-containing and serum-free medium. Data shows mean ± SD, N=3

Growth limiting concentrations of lactate and ammonia for BM-hMSCs, reported as 35.4 mM and 2.4 mM, respectively (Schop *et al.* 2009a), were not reached in any of our microcarrier cultures. Cell death was evaluated by measuring a combination of lactate dehydrogenase (LDH) (Lavrentieva *et al.* 2010a) and total protein released. Figure 6.19 shows these concentrations throughout culture, which indicate only a minimal increase in LDH and no change in the total protein released. This demonstrates that cell death was minimal throughout the expansion process, despite the increase in microcarrier aggregation, making the fold expansion data a reliable estimate of net proliferative rate.

6.4.5 Harvest of BM-hMSCs from serum-free microcarrier culture

The post-expansion detachment and separation of the BM-hMSC product from the microcarrier surface, whilst retaining the cell quality, is of critical importance for a scalable production process. The sequential expansion and harvest of BM-hMSCs represents an important step in the successful integration of these unit operations and has been demonstrated previously in FBS-based culture (Nienow *et al.* 2014). The same harvest protocol was modified for this study by replacing trypsin-EDTA with TrypLE Express for the serum-free culture to ensure the process was animal-component free. It was also observed that though microcarrier aggregation and cell number in the serum-free process was significantly greater than FBS-based culture, this difference did not limit the effectiveness of the harvest protocol and the BM-hMSCs were successfully detached from the microcarrier surface (Figure 6.20), with post-harvest cell viability (based on membrane integrity) of 99.63 ± 0.03 % (mean ± SD, n=3).

Expansion Condition	Post-Harvest Viability (%)
FBS-containing medium	99.45 ± 0.57
Serum-free medium	99.63 ± 0.03
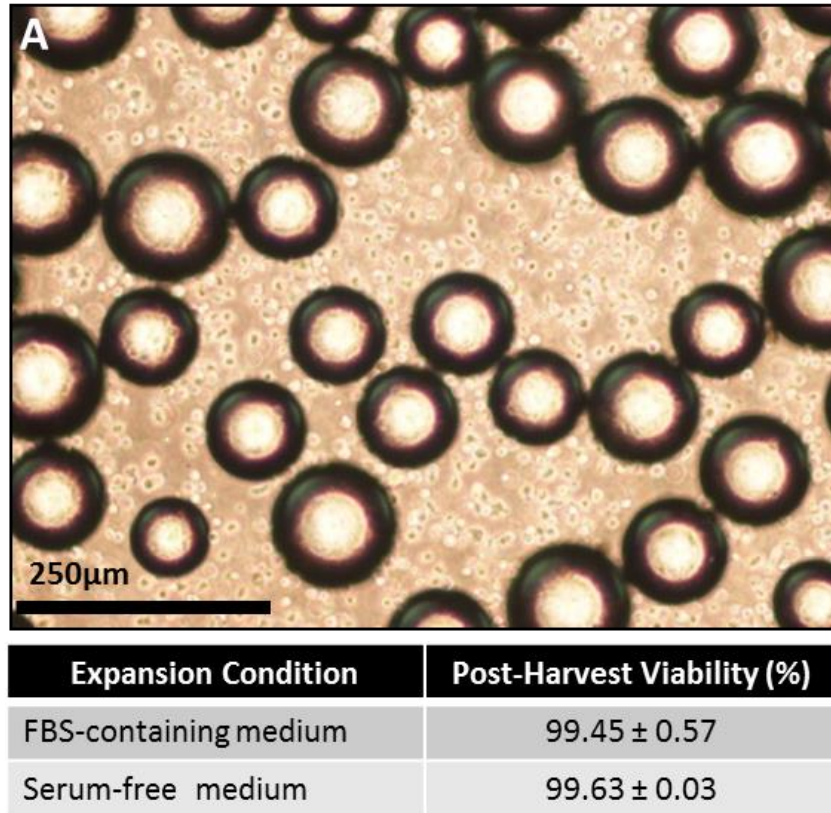
Figure 6.20. Post-expansion harvest of BM-hMSCs from microcarriers showing successful BM-hMSC detachment from microcarriers (A). Post-harvest viability shows high number of intact BM-hMSCs for FBS-containing medium and serum-free medium. Data shows mean ± SD, N=3.

After separating the cells from the microcarriers by vacuum filtration, the BM-hMSCs were held in culture medium at room temperature to simulate a potential large-scale batch pooling time before centrifugation, freezing medium equilibration and cryopreservation. This holding step was considered important for a cell-based product, as a BM-hMSC holding time of greater than six hours has been shown to negatively impact cellular quality (Pal *et al.* 2008), which could impose limits on the potential scalability of the bioprocess, depending on the sensitivity of the cell-based product. This holding process can be broken down into the microcarrier harvest (two hour process) and microcarrier-cell separation with an ambient hold in culture medium (two hour process). These steps are followed by suspension and equilibration of the cell product in freeze medium for up to one hour at 4°C prior to cryopreservation, which should be an acceptable exposure time for mixing and dosing thousands of vials or bags with suitable

manifold filling systems (Rowley *et al.* 2012a). Tangential-flow filtration has the potential to wash and concentrate cell products at the large scale within this two hour window (Pattasseril *et al.* 2013), meaning that the combined harvest, downstream and preservation timings in this study would still be relevant as the process is scaled-up further.

6.4.6 Post-harvest identity of BM-hMSCs from serum-free microcarrier culture

To ensure that the microcarrier-based expansion and harvest unit operations have not had a detrimental effect on identity and quality, BM-hMSC characteristics have been evaluated immediately post-harvest. The primary objective for this is to demonstrate that the BM-hMSCs conform to the International Society for Cellular Therapy (ISCT) criteria (Dominici *et al.* 2006). Figure 6.21 shows the compliance of the BM-hMSCs with the ISCT criteria, by adherence to tissue culture plastic, demonstrating the same morphology post-harvest as was demonstrated pre-expansion and differentiation down the osteogenic (Figure 6.21E), adipogenic (Figure 6.21F) and chondrogenic (Figure 6.21G) lineages. The post-harvest BM-hMSC immunophenotype can be seen in Figure 6.21H which shows the co-expression of positive markers CD73, 90 and 105 at greater than 99 % as well as the expression of HLA-DR at less than 2 % (Chan *et al.* 2014b). There was an increase in the positive expression of CD34 above the 2% positive threshold, which can be attributed to an increase in non-specific antibody binding caused by the culture of BM-hMSCs on a fibronectin substrate and has previously been reported to be positive for adipose derived BM-hMSCs (Wagner *et al.* 2005).
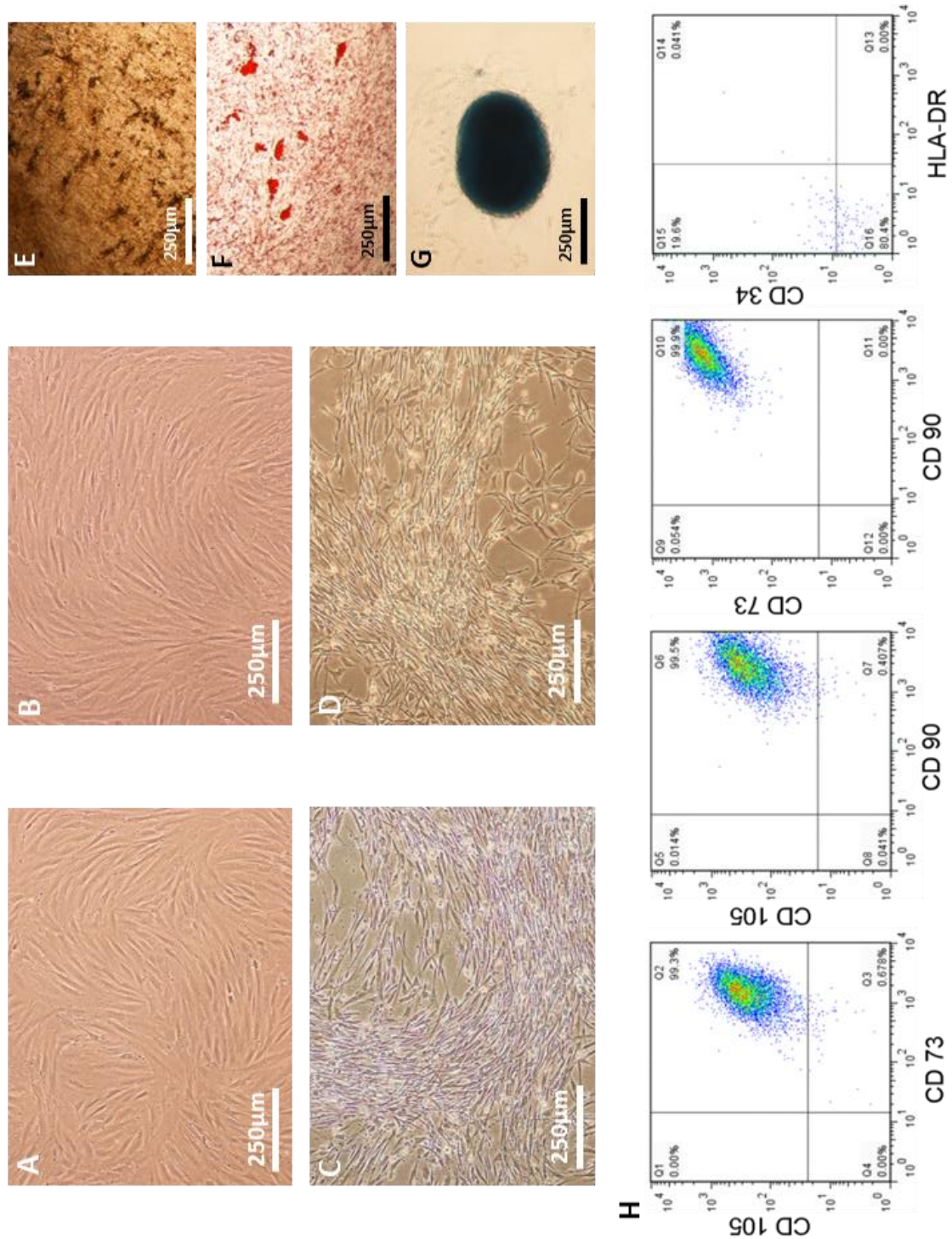
Figure 6.21. Post-harvest BM-hMSC characterisation. (A) pre-expansion and (B) post-harvest BM-hMSC morphology in FBS-containing medium. (C) pre-expansion and (D) post-harvest BM-hMSC morphology in serum-free medium. Tri-lineage differentiation of BM-hMSCs showing (E) osteogenic, (F) adipogenic and (G) chondrogenic potential post-harvest in serum-free medium. Multiparameter flow cytometry showing dual gating of CD73, 90, 105, 34 and HLA-DR for BM-hMSCs post-harvest from serum-free microcarrier culture (H).

6.4.7 Post-harvest characterisation of BM-hMSCs from agitated microcarrier culture

The successful development of a BM-hMSC manufacturing process relies on the characterisation of product identity and quality at each unit operation (Carmen *et al.* 2012a). The development of clinical indication specific BM-hMSC quality assays has proved to be complex, owing to their unique and multifactorial putative mechanism of action. Without definitive quality assays, the field relies on surrogate assays to measure cell attributes that are known to be related to aspects of BM-hMSC quality. Figure 6.22A shows the outgrowth of BM-hMSCs before, during and after expansion, with no decline in the proliferative potential observed across these unit operations. This suggests that BM-hMSCs have not experienced detrimental conditions during the microcarrier expansion and harvest process that could have affected their proliferation potential (Sethe *et al.* 2006).
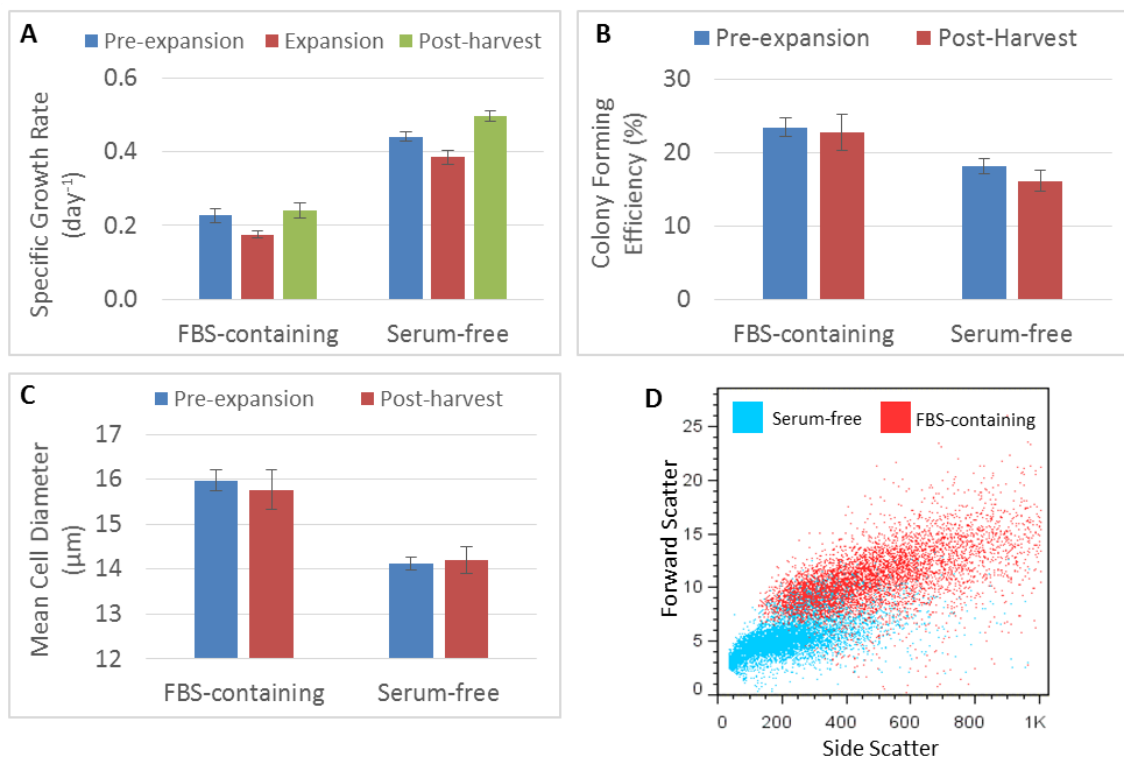
Figure 6.22. Post-harvest BM-hMSC quality compared to pre-expansion demonstrating retention of key attributes, showing (A) specific growth rate, (B) colony forming efficiency, (C) mean cell diameter and (D) forward/side scatter of cell populations confirming difference in mean cell diameter.

Colony forming potential has been highlighted as an important assay for the quality of BM-hMSC preparations (Pochampally 2008) and is known to deteriorate during culture (Schellenberg *et al.* 2012). Figure 6.22B shows the maintenance of colony forming potential from pre-expansion to post harvest for both conditions, which further demonstrates that the BM-hMSCs have not been damaged during the harvest and separation process.

The size of BM-hMSCs in culture is known to increase as they undergo cellular senescence (Wuchter *et al.* 2014), and should therefore be tracked throughout expansion and harvest to ensure it remains stable. Figure 6.22C demonstrates that the mean cell diameter remained stable throughout culture, with significantly smaller BM-hMSCs produced under serum-free culture ($p < 0.05$). Without the availability of a robust potency assay to determine the implications of a smaller cell size in serum-free culture, it is not known how this will affect *in vivo* BM-hMSC quality attributes. Despite this, clinical work has demonstrated that smaller BM-hMSCs reduce the potential for vascular obstructions and stroke following the intra-artery injection of cells (Ge *et al.* 2014), as well as reducing capillary entrapment (Dreher *et al.* 2013). These observations suggest that a smaller cell size may not only be beneficial in terms of obtaining a higher number of cells per area for expansion, but might also be advantageous in product delivery. This possibility raises a question of whether the therapeutic potential of the cell is related to size and whether we need to think not only in terms of cell number but also in terms of product biomass for production and delivery of cell therapies. Cellular enlargement has been associated with the development of professional secretory cells such as plasma cells (Shaffer *et al.* 2004), with more organelles and increased protein synthesis. Considering that protein secretion is a putative mechanism of action of BM-hMSCs *in vivo*, the relation of cell size to secretory capability of BM-hMSCs should be clinically evaluated post-delivery.

6.4.8 Downstream and preservation from a serum-free microcarrier process

The BM-hMSCs harvested from serum-free spinner cultures were preserved using a serum-free freezing medium and a slow-freezing cryopreservation process. After thawing, cell viability (by membrane integrity) decreased to 75.8 ± 1.4% as a consequence of the cryopreservation process (Figure 6.23A). However, this value remains above the FDA guideline for cell-based therapies of 70% (FDA 2008a). A similar number of cells were recovered after three hours in culture, based on their sustained adherence to fibronectin without loss of membrane integrity (Figure 6.23A). It is important to note that this post-thaw recovery is comparable to studies

where BM-hMSCs have been immediately processed from monolayer culture (Liu *et al.* 2010), without the microcarrier harvest, filtration and holding time steps.
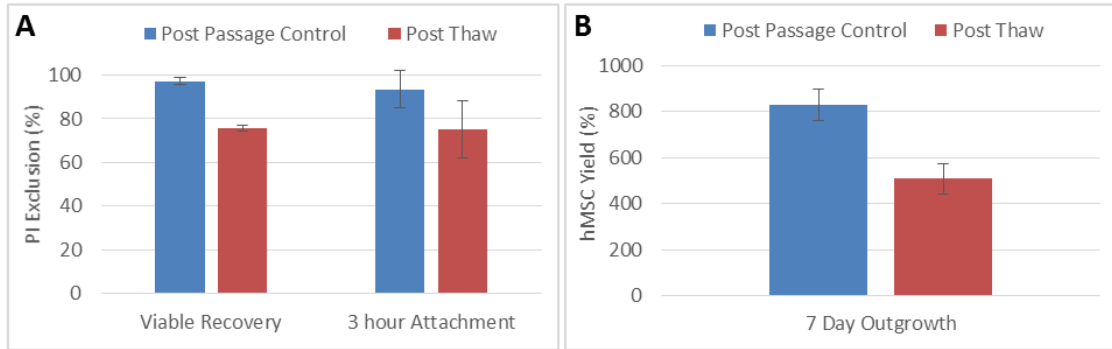
Figure 6.23. Post-thaw BM-hMSC recovery following serum-free cryopreservation, showing (A) post-thaw recovery and 3 hour cell attachment based on PI exclusion. Post-thaw BM-hMSC outgrowth (B) following serum-free cryopreservation. Data shows mean ± SD (N=3).

Despite the initial cell loss post-thaw, a 500 % increase in cell yield was obtained after 7 days in monolayer culture (compared with 800 % for unpreserved post-passage control), demonstrating that recovered cells were able to proliferate normally (Figure 6.23B). Recovered cells also displayed comparable morphology to unpreserved cells after 3 hours and 24 hours of culture on fibronectin, with signs of matured cell-matrix interactions, cell elongation (indicative of motility) (Huttenlocher and Horwitz 2011) and recovery of F-actin networks (Figure 6.24). These observations demonstrate that BM-hMSCs can be cryopreserved and recovered from a microcarrier expansion, harvest and holding process, with comparable cell yields to traditional monolayer harvest and immediate cell preservation.
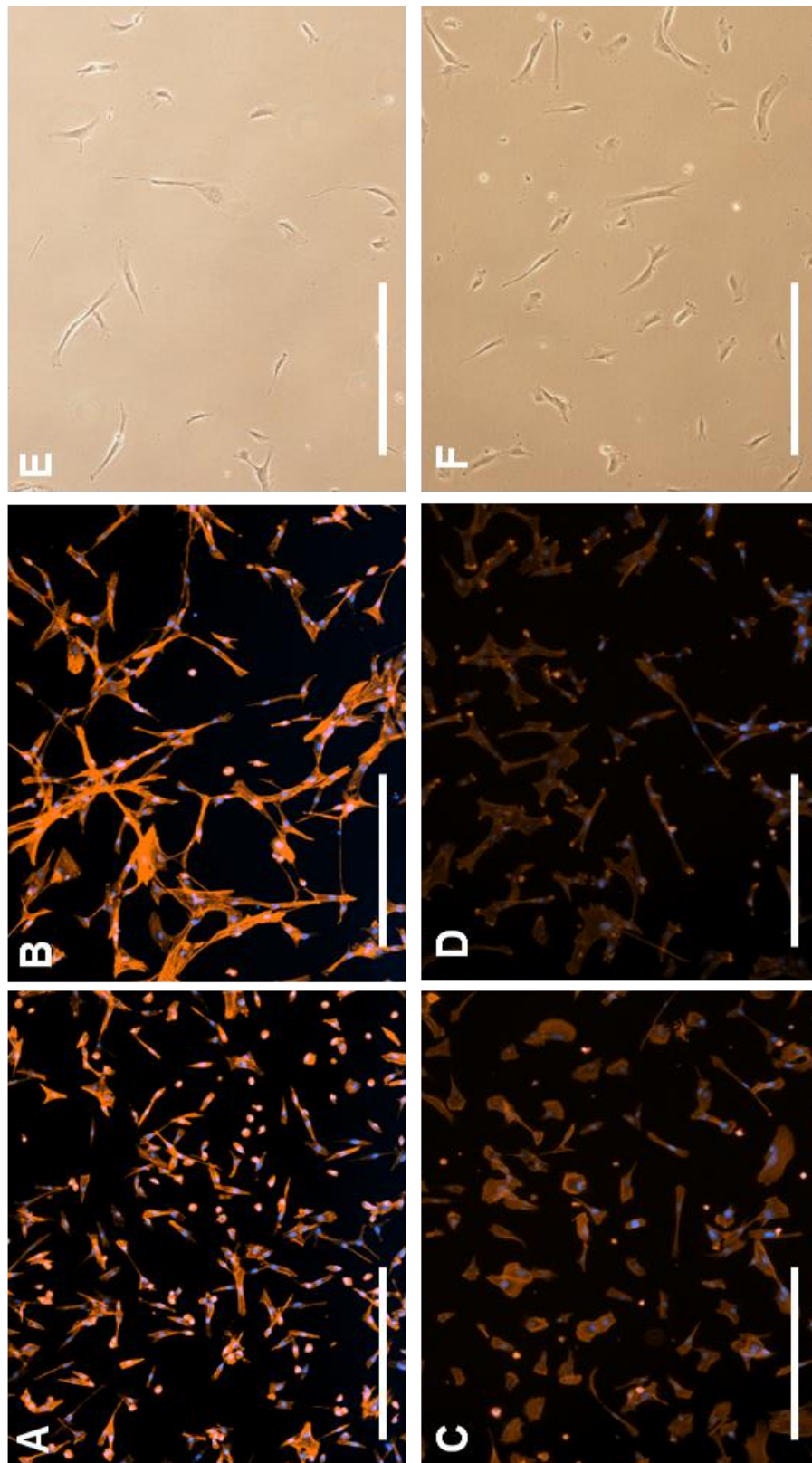
Figure 6.24. Post-thaw BM-hMSC recovery following serum-free cryopreservation, showing formation of F-Actin cytoskeleton (A) 3 hours, (B) 24 hours post thaw (C) 3 hours post-passage control and (D) 24 hours post-passage control. Phase contrast images show day 2 BM-hMSC morphology post-thaw (E) and post passage control (F). Scale bar = 250 μm.

6.5 Chapter conclusions

This Chapter has demonstrated that the serum-based monolayer BM-hMSC expansion process developed in Chapter five can be directly transferred into suspension *via* the introduction of microcarriers. This is an important process transfer step as the development of a scalable microcarrier expansion process has the potential to take advantage of increasing economies of scale to cost-effectively manufacture BM-hMSCs at the lot-sizes required for commercial production. Furthermore, the increased yield and donor consistency that was experienced for the monolayer process in HPL, has also directly transferred to the microcarrier process, indicated that this improved efficiency has the potential to be carried through increasing process scales, with preliminary process development and BM-hMSC donor screening taking place in small scale monolayer processes. In order for this microcarrier process to be operated under serum-free conditions, a fibronectin coating process has been developed for microcarrier culture. This has revealed that a lower concentration of fibronectin is more advantageous for microcarrier process which will be important to reduce the cost of goods in BM-hMSC manufacturing processes. It has been identified that the microcarriers must be pre-coated with fibronectin prior to the expansion process which will necessitate the validation and potential storage conditions for fibronectin coated microcarriers, to ensure the process is compatible with critical manufacturing principles.

This Chapter has also demonstrated the feasibility of a serum-free microcarrier process for the expansion, harvest and preservation of BM-hMSCs. The integration of multiple process unit operations is an important step in developing a microcarrier-based expansion process capable of meeting the lot sizes required for clinical applications. The BM-hMSC identity and quality have been maintained throughout every unit operation of this integrated process, culminating with the successful recovery of BM-hMSCs from the cryopreservation step. Mapping has provided a robust process understanding from end-to-end, which can be broken down into individual unit operations and optimised for BM-hMSC yield, quality and consistency.

The systematic development of a process control strategy for the expansion unit operation will form a key part of driving increased yield and consistency into the process, as well as the identification and mitigation of bottlenecks to further streamline the process. The focus of the following Chapter therefore, will be the development of a process control strategy for the microcarrier expansion of BM-hMSCs that can be integrated into this serum-free production process.

Publications arising from this Chapter:

Heathman TRJ, Glyn VAM, Picken A, Rafiq QA, Coopman K, Nienow AW, Kara B, Hewitt CJ. Expansion, harvest and cryopreservation of human mesenchymal stem cells in a serum-free microcarrier process. <u>Biotechnology & Bioengineering</u>, (2015) 112 (8): 1696-1707

Heathman TRJ, Stolzing A, Fabian C, Rafiq QA, Coopman K, Nienow AW, Kara B, Hewitt CJ. Scalability and process transfer of mesenchymal stem cell production from monolayer to microcarrier culture using human platelet lysate. <u>Cytotherapy</u>, (2015) (*in review*)

Nienow AW, Hewitt CJ, **Heathman TRJ**, Glyn VAM, Fonte G, Hanga MP, Coopman K, Rafiq QA. Agitation Conditions for the Culture and Detachment of hMSCs from Microcarriers in Multiple Bioreactor Platforms. <u>Biochemical Engineering Journal</u>, (2015) *(in press)*

7 Process Control Strategy for BM-hMSC Microcarrier Culture

7.1 Chapter introduction

The addition of microcarriers has been used to culture adherent cells such as BM-hMSCs in suspension (Chapter 6) allowing for process scale-up, where online monitoring and control systems can be used to deliver a consistent and cost-effective BM-hMSC therapy. Further to this, stirred-suspension bioreactors are currently employed in biopharmaceutical production and therefore their design and operation are well-understood (Nienow 2006), with the potential to meet the expected manufacturing demands of large-scale BM-hMSC therapies (Heathman *et al.* 2015b). The supply of oxygen to the BM-hMSCs in these microcarrier suspension processes is essential and is typically achieved by headspace aeration as the oxygen uptake rate of BM-hMSCs is relatively low (Rafiq *et al.* 2013a; Heathman 2015). That said, however, as the volume of the bioreactors and cell densities increase, it is likely that the sufficient supply of oxygen will require aeration directly into the culture medium *via* a sparger, which could be potentially detrimental to the BM-hMSCs (Nienow *et al.* 1996; Nienow *et al.* 2015a).

One of the key aspects of a successful manufacturing process is in the reduction of product variation, which is particularly challenging when the cell is the final product. Variation can be introduced into the product by both the process input material and the process conditions (Williams *et al.* 2012). The input to the process must be controlled by strict BM-hMSC isolation techniques and potentially cell selection steps to improve product input consistency (Naing *et al.* 2015b), although these are typically poorly defined for BM-hMSCs. Additionally, the raw materials, such as the culture medium, must be controlled to further reduce variation and the development of defined medium formulations without the use of animal serum has been proposed as a mechanism to achieve this (Heathman *et al.* 2015e). The use of serum-free medium with microcarriers for the expansion of BM-hMSCs has previously been demonstrated for uncontrolled processes (dos Santos *et al.* 2011a; Heathman *et al.* 2015a; Tan *et al.* 2015) and therefore represents a viable alternative for large-scale serum free manufacture of BM-hMSCs. The monitoring and control of process parameters such as pH and dissolved oxygen for these suspension bioreactor systems will be important to reduce the variation introduced by the process conditions. This will be critical in order to drive consistent and cost-effective manufacturing processes for BM-hMSC therapies and therefore should be integrated into early bioprocess development.

The US Food and Drug Administration (FDA) has released guidance documents on the use of process control and real time release testing for pharmaceutical manufacturing (FDA 2009). This guidance has highlighted the importance regulators are placing on continual process improvement and enhanced understanding as a fundamental aspect of process development and control. Process analytical technology or PAT is a system for analysing and controlling manufacturing processes through measurement of product attributes to ensure final product quality, proposed by the FDA (FDA 2004). It will therefore be desirable to utilise these PAT technologies and measure online parameters in order to develop control systems to ensure that the product characteristics remain consistent. These relevant process parameters are likely to include a combination of cell growth, medium temperature, pH, pO_2 and pCO_2, which are commonplace in current biopharmaceutical production processes (Cierpka *et al.* 2013).

The aim of this Chapter therefore, is to develop a process control strategy for the microcarrier culture of BM-hMSCs in suspension in order to drive increased consistency and yield into the process. The impact of this process control strategy on process economics and product consistency will be assessed for two BM-hMSC donors in both FBS-based and serum-free medium and compared to previously uncontrolled monolayer and microcarrier-based suspension BM-hMSC expansion processes in Chapter 5 and Chapter 6.

7.2 Effect of agitation rate on BM-hMSC expansion

7.2.1 Experimental overview

Following the successful development of a suspension-based microcarrier process for the expansion of BM-hMSCs, a control strategy should be developed to increase the yield and consistency in the process. The first step in this is to investigate the effect of the impeller speed on BM-hMSC growth and characteristics in order to determine the optimum agitation strategy for the microcarrier culture process. For this, three DASbox culture vessels per condition were cultured for six days in FBS-based medium (see Section 3.3.5) at 80, 115, 150 and 225 rpm in accordance with Table 7.1, which shows the characterisation of the bioreactor system at each impeller speed. It is important to note that the DASbox culture vessels do not contain baffles, however, the bioreactor system was assumed to be baffled due to the number of probes in the vessel in relation to the culture volume. The pH control set-point was 7.4, the dissolved oxygen concentration was controlled to 100 % and the temperature was controlled to 37 °C. Prior to all experiments, the control system on the DASGIP DASbox bioreactor platform was adjusted to ensure it remained stable, the process of which can be seen in Appendix E.

During culture, daily medium samples were taken for analysis of glucose, lactate, ammonia, lactate dehydrogenase and total protein with cell counts performed each day (four samples were analysed per bioreactor as per Section 3.4.3). The culture medium was exchanged on day three of culture. At harvest, the BM-hMSCs were removed from the microcarriers and separated according to Section 3.3.6. The BM-hMSCs harvested from each condition were then assessed for mean cell diameter (Section 3.4.2), tri-lineage differentiation potential (Section 3.4.4) and immunophenotype (Section 3.4.5). In addition to these identity measurements, BM-hMSC quality characteristics of colony forming efficiency (Section 3.4.9) and outgrowth potential were also assessed post-harvest.

Table 7.1. Physical characterisation of the DASGIP DASbox bioreactor platform at the various impeller speeds used in this study. For an impeller diameter of 0.03 m and a bioreactor diameter of 0.063 m. 1) from reference (Nienow *et al.* 2015b)

Impeller rate (rpm)	Culture volume (ml)	Power number[1]	Max dissipation rate/average dissipation rate[1]	Reynolds number	Impeller speed (s^{-1})	Max specific energy dissipation rate (W/kg)	Kolmogorov scale of turbulence (µm)
80	100	1.5	18	1439	1.33	0.016	90
115	100	1.5	18	2068	1.92	0.046	68
150	100	1.5	18	2697	2.50	0.103	56
225	100	1.5	18	4046	3.75	0.346	41

7.2.2 Human MSC growth kinetics on microcarriers

In order to support the successful expansion of BM-hMSCs on microcarriers in suspension bioreactors, it will be critically important to employ an agitation strategy that suspends the microcarriers without causing damage to the cells throughout scale-up. In order to quantify this, the impact of different impeller speeds on the growth of BM-hMSCs on microcarriers has been assessed. In conjunction with this, the physical parameter of the bioreactor system have been calculated to provide a strong theoretical basis for this comparison, which can be seen in Table 7.1. The controlled bioreactor system was operated at 100 % dissolved oxygen for each impeller rate, with the pH maintained at 7.4, which is commonly used for BM-hMSC culture (Wuertz *et al.* 2009).

Figure 7.1 shows the effect of the various impeller speeds on BM-hMSC growth from daily samples over six days, with the highest impeller speed of 225 rpm leading to the lowest BM-hMSC growth. This is confirmed by the post-harvest cell counts in Figure 7.2, which shows that there is significantly increased ($p < 0.05$) BM-hMSC growth at lower impeller speeds. The minimum impeller speed to suspend the microcarriers (N_{JS}) was visually determined to be 115 rpm, which explains why the daily cell counts at 80 rpm were lower than expected, as the microcarriers and cells were not entirely suspended. Maintaining the microcarriers and cells in suspension is critical to ensure that the effective mass and heat transfer can take place (Nienow 1997) and therefore the impeller speed in this microcarrier-based bioreactor system should be at least 115 rpm.
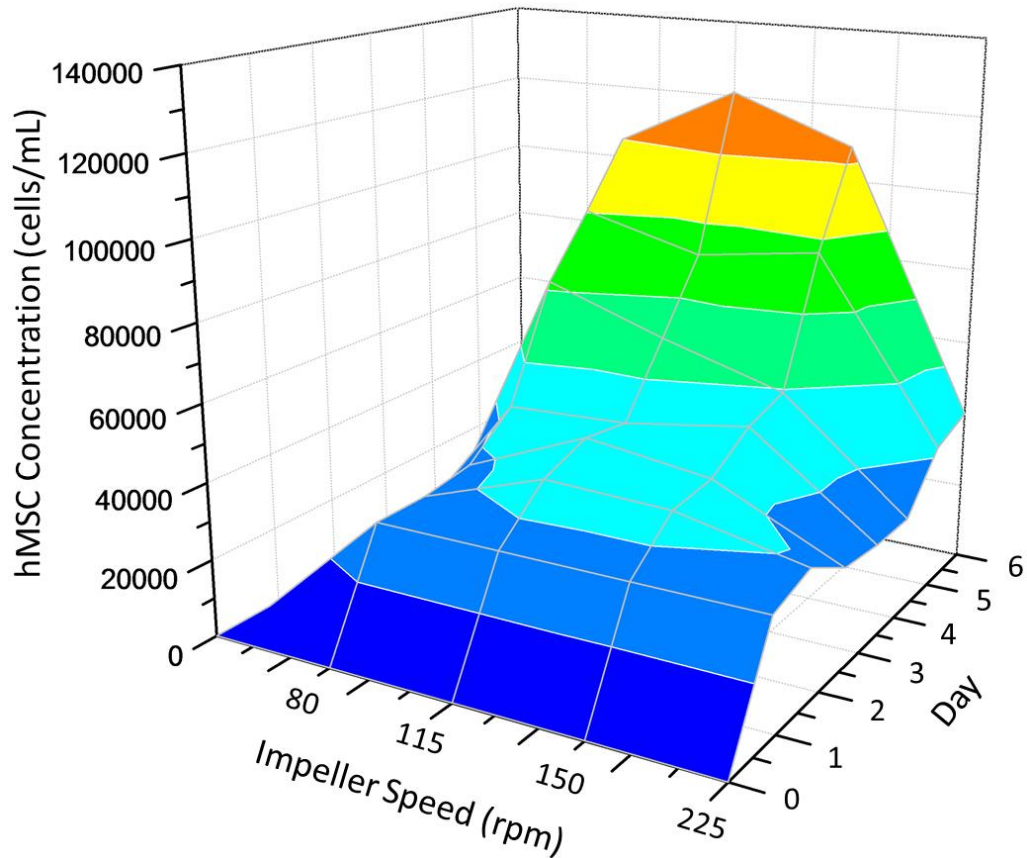
Figure 7.1. Effect of bioreactor impeller speed on BM-hMSC growth over six days of culture in the DASbox controlled bioreactor, showing the increased growth kinetics at N_{JS}. Control set-points are 100% dissolved oxygen tension and pH 7.4 with headspace aeration. Data shows mean of n = 3

Table 7.1 shows the characterisation of the bioreactor system at different impeller speeds with a calculation of the Kolmogorov microscale of turbulence for each impeller speed. Considering that the size of the microcarriers used in this study are in the range of 125-212 μm, Table 7.1 shows that the Kolmogorov scale turbulent eddies at each of the investigated impeller speeds is much less than the size of the microcarriers but bigger than a cell. Kolmogorov theory suggests that the eddies most likely to cause damage are those of the size of the suspended entity i.e. eddies which are the same size as the microcarriers (Cherry and Papoutsakis 1986), with the energy of the eddies being transferred to the surface of the microcarriers. This results in high local velocity gradients between the microcarriers and the fluid, and the highest shear rates on the cells. Work by Croughan *et al* (1987) has investigated the impact of this microscale of

turbulence on cells grown on microcarriers, with cell damage becoming significant when the microscale was less than or equal to about two-thirds the size of the microcarriers (Croughan *et al.* 1987). Based on the minimum microcarrier size used in this study it would suggest that the BM-hMSC growth kinetics would be affected at a turbulent eddy size of < 83 µm, which is the eddy size calculated for impeller speeds of 115 – 225 rpm, where the BM-hMSC growth kinetics were reduced compared with 80 rpm where the eddy size was 90 µm. However, in the latter case, the cells and microcarriers were not fully suspended at this impeller speed. This drop in growth rate clearly suggests that the impact of poor mass transfer to the cells due to the lack of suspension is more damaging than that due to fluid dynamic stress even though the microscale is only ~ 55 % of the size of the microcarrier at 115 rpm.
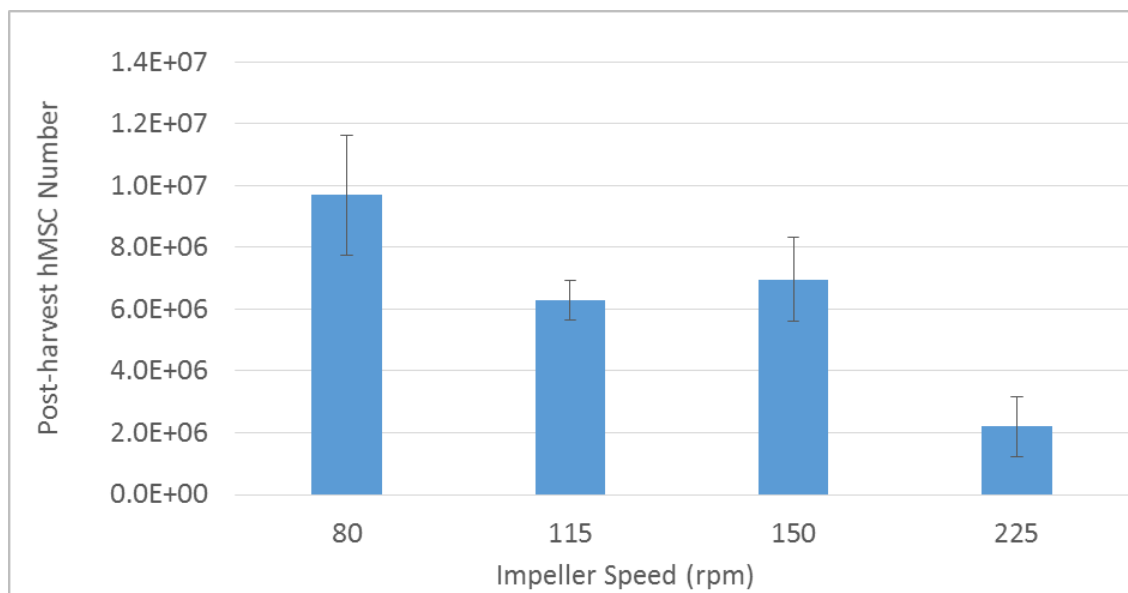
Figure 7.2. Effect of bioreactor impeller speed on post-harvest BM-hMSC number after six days of culture in the DASbox controlled bioreactor, showing the increased BM-hMSC number at lower impeller speeds. Data shows mean ± SD, n = 3

The spinner flask process employed an agitation strategy that gave a Kolmogorov microscale of 183 µm (Hewitt *et al.* 2011), representing double the eddy size calculated for the culture process at 80 rpm here. A key difference between the spinner flask process and the DASbox process is that the DO and pH are controlled in the DASbox rather than simply relying on a buffer in the culture medium and environment regulation in an incubator. The control of the medium pH will

be important during manufacture, particularly as the cell densities and metabolite concentrations increase. Despite the much higher eddy size in the spinner flask process, the post-harvest BM-hMSC number was similar at $8.69 \pm 0.58 \cdot 10^6$ (Chapter 6) compared to an impeller speed of 80 rpm which had a post-harvest cell number of $9.68 \pm 1.94 \cdot 10^6$ under a similar culture process. It should also be noted that the growth kinetics at an impeller speed of 150 rpm was similar ($p > 0.05$) to that measured at N_{JS}, which is beneficial as it allows for similar BM-hMSC growth kinetics at an increased energy dissipation rate of 0.103 W.kg^{-1} compared with 0.046 W.kg^{-1} at an impeller speed of 115 rpm (N_{JS}), allowing for increased process flexibility during scale-up.

7.2.3 Human MSC metabolite flux on microcarriers

The relative flux of metabolites is an important parameter to measure and understand during the expansion process as it has the potential to form part of a process control system, based upon BM-hMSC characteristics. Figure 7.3 shows the lactate dehydrogenase (LDH) and total protein concentration at the various impeller speeds throughout the culture process, which do not increase as the impeller speed in changed. If cell damage was occurring during the culture process, the levels of LDH and total protein would increase as the cell cytoplasmic membrane rupture and release protein and LDH into the culture medium (Lavrentieva *et al.* 2010b). The differences in BM-hMSC growth kinetics discussed in Section 7.2.2 due to changes in impeller speed are therefore not attributed to cellular damage by membrane disruption in this instance.
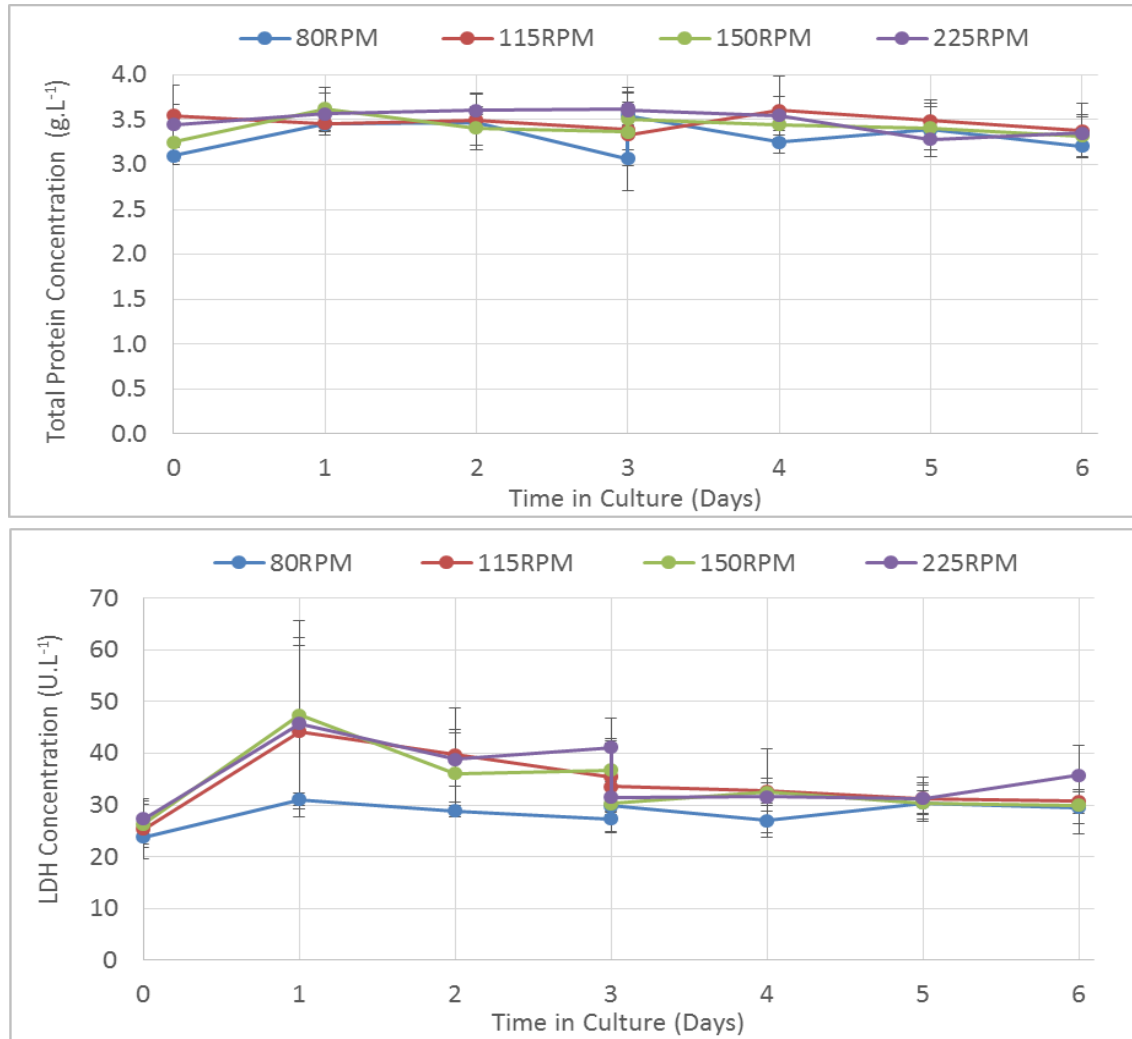
Figure 7.3. Live metabolite concentrations of lactate dehydrogenase (LDH) and total protein at various impeller speeds demonstrating little increase in concentrations throughout expansion indicating a low level of cellular damage. Data shows mean ± SD, n = 3

It has been demonstrated previously however, that increasing the shear stress in flow chambers during BM-hMSC culture leads to the inhibition of proliferation, in association with maintaining cells in G0/G1 phase of the cell cycle (Luo *et al.* 2011). Additionally, the reduction in growth kinetics at higher impeller speeds could be caused by an inhibition of BM-hMSC attachment and re-attachment to the microcarriers during the growth phase. Whatever the mechanism for the reduced growth rate of BM-hMSCs on microcarriers at increased impeller speeds, it is not caused by direct cell damage as is commonly assumed.

In addition to LDH and total protein concentration, the glucose, lactate and ammonia concentrations have been measured daily during the culture process for each impeller speed (Figure 7.4). The glucose concentration decreased to a minimum of 2.06 ± 0.45 mmol.L^{-1} at an impeller rate of 80 rpm, supporting that the post-harvest cell number was highest in this condition. The lowest reduction in glucose concentration was for 225 rpm, with a day six concentration of 4.08 ± 0.43 mmol.L^{-1} demonstrating a reduced glucose uptake at lower BM-hMSC growth rates. In addition to this, the lactate concentration reach a maximum of 7.73 ± 0.57 mmol.L^{-1} on day six of culture at an impeller speed of 80 rpm, with a similar trend for each impeller rate as for the glucose concentration. In contrast to this, the change in ammonia concentration was more similar across all of the impeller speeds, suggesting that ammonia production was less dependent on BM-hMSC growth than glucose and lactate during the culture process.

The net flux of each metabolite can be seen in Figure 7.5, which shows a similar level of per cell glucose consumption and lactate production across each impeller speed. This is an indication that the low BM-hMSC growth at an impeller speed of 225 rpm is not a result of cellular senescence, as the glucose consumption and lactate production per cell has previously been shown to increase if this is the case (Heathman *et al.* 2015c). The increased ammonia production at an impeller speed suggests altered amino acid utilisation, which may be related to the increased need for precursors (e.g., glutamine and asparagine) supporting purine, and pyrimidine biosynthesis (Higuera *et al.* 2012). The yield of lactate from glucose for impeller speeds of 80, 115 and 150 rpm was around 2 mol.mol^{-1} which indicates that the cells mainly metabolise glucose *via* the inefficient glycolytic pathway instead of the energy efficient oxidative phosphorylation pathway (Higuera-Sierra *et al.* 2009).
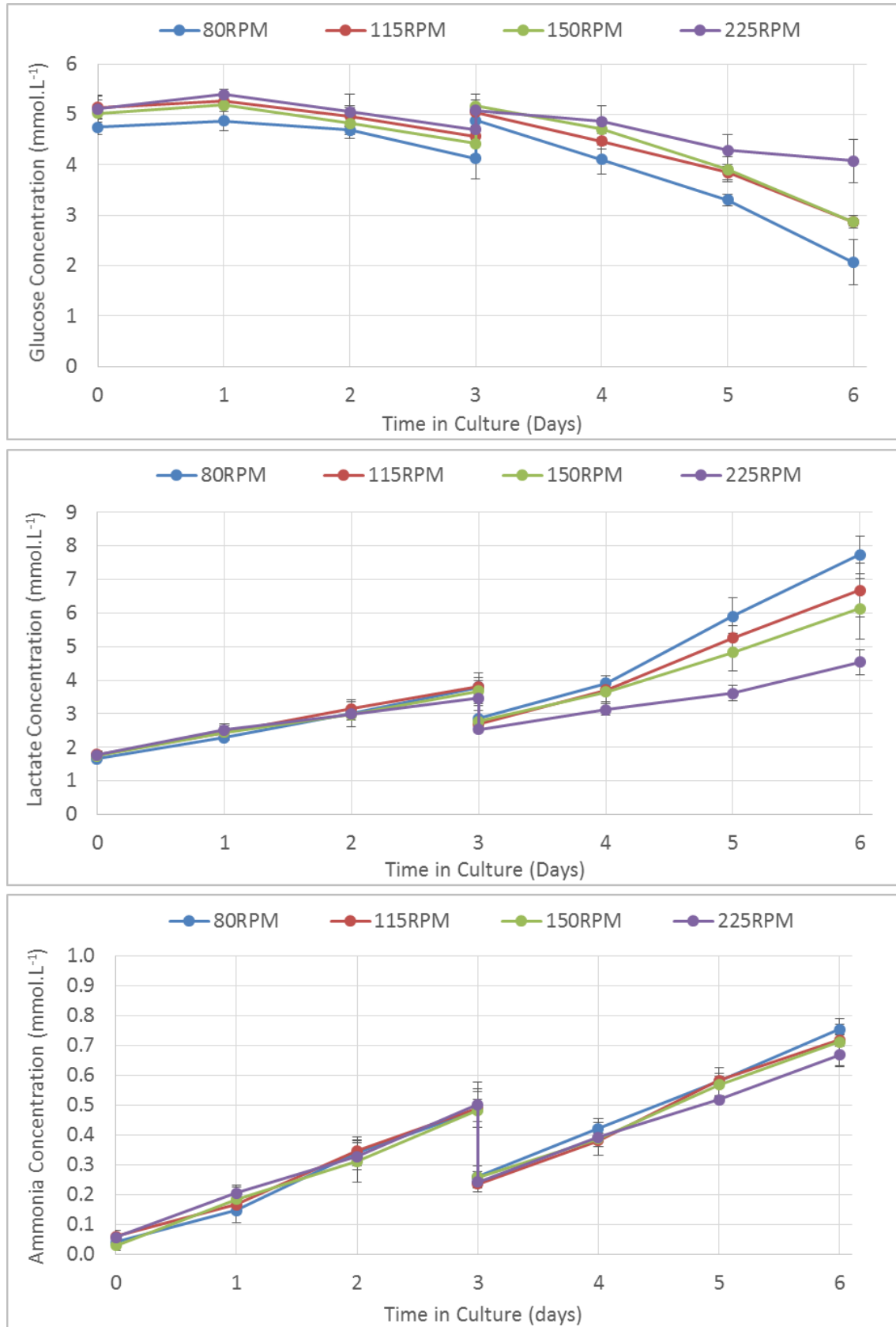
Figure 7.4. Live metabolite concentrations of glucose, lactate and ammonium for various impeller speeds showing the increased metabolic activity at lower agitation rates. Data shows mean ± SD, n = 3

The impeller speed of 225 rpm had a yield of lactate from glucose of 2.70 ± 0.73 mol.mol^{-1} which is above the theoretical maximum yield of 2 mol.mol^{-1} (Glacken 1988). This suggests that an additional carbon source, most likely glutamine, is being metabolised to produce lactate and ammonia, resulting in higher lactate yields and an increase in the per cell ammonia flux (Rafiq *et al.* 2013a) seen in Figure 7.5.
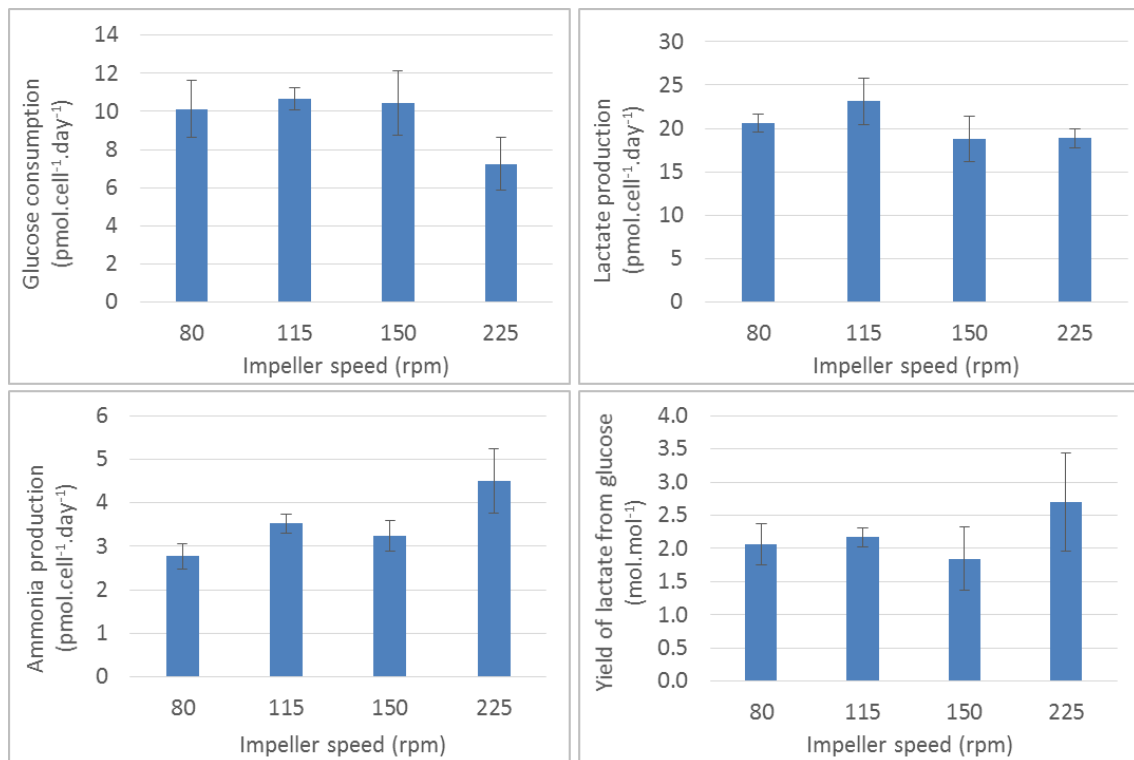
Figure 7.5. Metabolite consumption and production rate of BM-hMSCs at various impeller speeds. Showing glucose consumption, lactate production, ammonia production and the yield of lactate from glucose. Data shows mean ± SD, n = 3

7.2.4 Post-harvest characterisation of BM-hMSCs

In addition to the growth kinetics and metabolite flux, it is important to assess the post-harvest BM-hMSC characteristics to ensure that the process and harvest conditions have not had a detrimental impact on the quality of the cell (Nienow *et al.* 2014). The BM-hMSCs were

harvested from the microcarrier surface and separated prior to characterisation according to a previously published protocol for the DASGIP DASbox bioreactor platform (Nienow *et al.* 2015b).
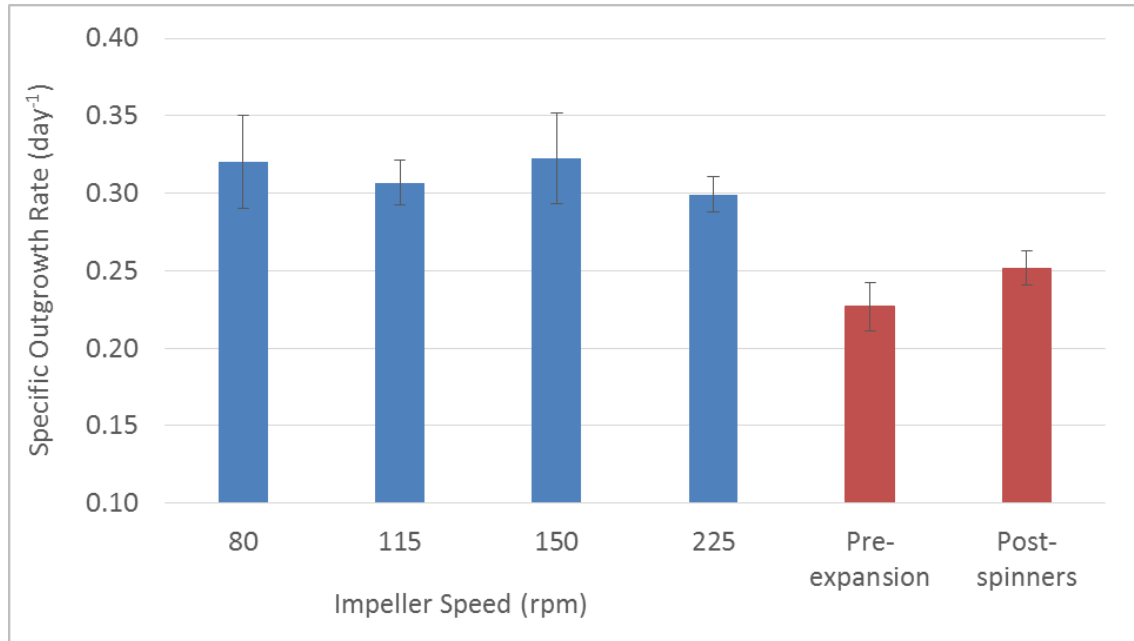
Figure 7.6. Post-harvest outgrowth rate of BM-hMSCs at various impeller speeds showing the increased outgrowth kinetics of BM-hMSCs from the controlled bioreactor compared to pre-expansion and post-spinner culture. Data shows mean ± SD, n = 3

The specific outgrowth rate can be seen in Figure 7.6 which shows that the BM-hMSC post-harvest outgrowth rate was similar across all of the impeller speeds investigated. Similarly, this suggests that the impeller speed of 225 rpm has not triggered a senescent state in the BM-hMSCs or caused detriment to their outgrowth potential. This is further evidence to support the hypothesis that the reduction of BM-hMSC growth kinetics on microcarriers at high impeller rates is due to inefficient cell-microcarrier attachment, rather than cell damage due to increasing shear forces. It can also be seen from Figure 7.6 that the post-harvest outgrowth kinetics of BM-hMSCs from the controlled DASbox bioreactor system at all impeller speeds were higher than either before expansion and post-harvest from the uncontrolled spinner flask process. This is an indication of the positive impact the controlled bioreactor process is having on the BM-hMSC characteristics which will be important for future bioprocess scale-up and development.
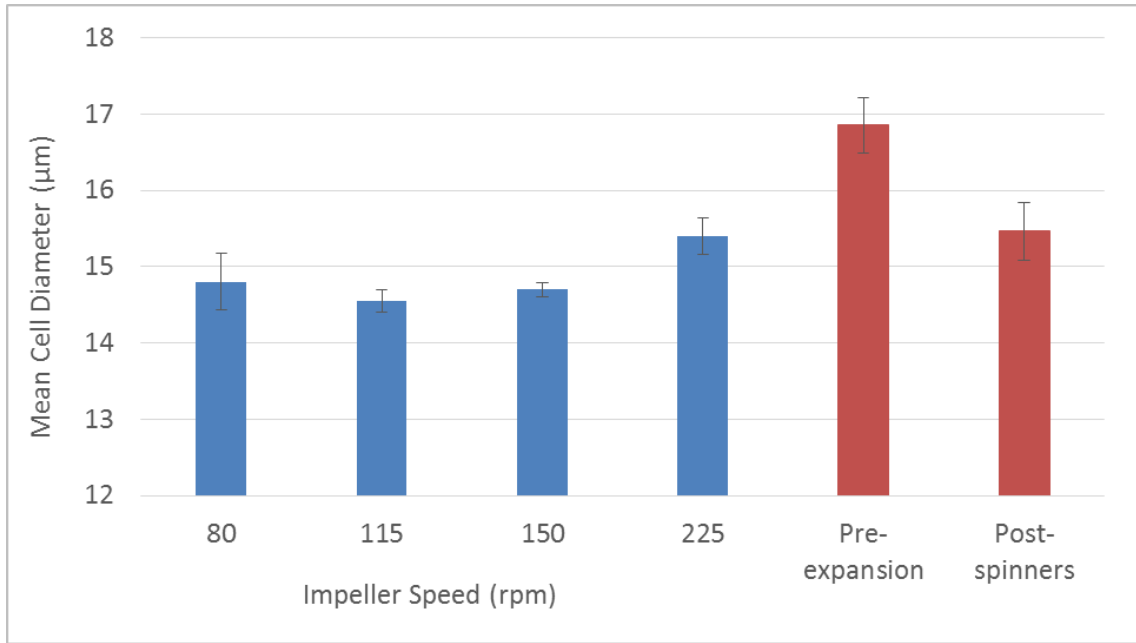
Figure 7.7. Post-harvest mean diameter of BM-hMSCs at various impeller speeds showing the reduced mean BM-hMSC diameter of BM-hMSCs from the controlled bioreactor compared to pre-expansion. Data shows mean ± SD, n = 3

Associated with the increase in post-harvest outgrowth, the BM-hMSCs cultured in the DASbox bioreactor platform had a reduced mean cell diameter for all impeller speeds compared to pre-expansion and post-harvest from uncontrolled spinner flasks. As well as being associated with a decrease in BM-hMSC growth rate, an increase in cell size has been linked to aging of BM-hMSCs and loss in differentiation potential (Stolzing and Scutt 2006; Wagner *et al.* 2010) and therefore a reduction in BM-hMSC size through controlled microcarrier expansion will be beneficial to the manufacturing process.

Colony forming potential has been highlighted as an important assay for the quality of BM-hMSC preparations (Pochampally 2008) and is known to deteriorate during culture (Schellenberg *et al.* 2012; Heathman *et al.* 2015c). Figure 7.8 shows the maintenance of colony forming potential from pre-expansion to post-harvest at all impeller speeds, which further demonstrates that the BM-hMSCs have not been damaged during the expansion and harvest process.
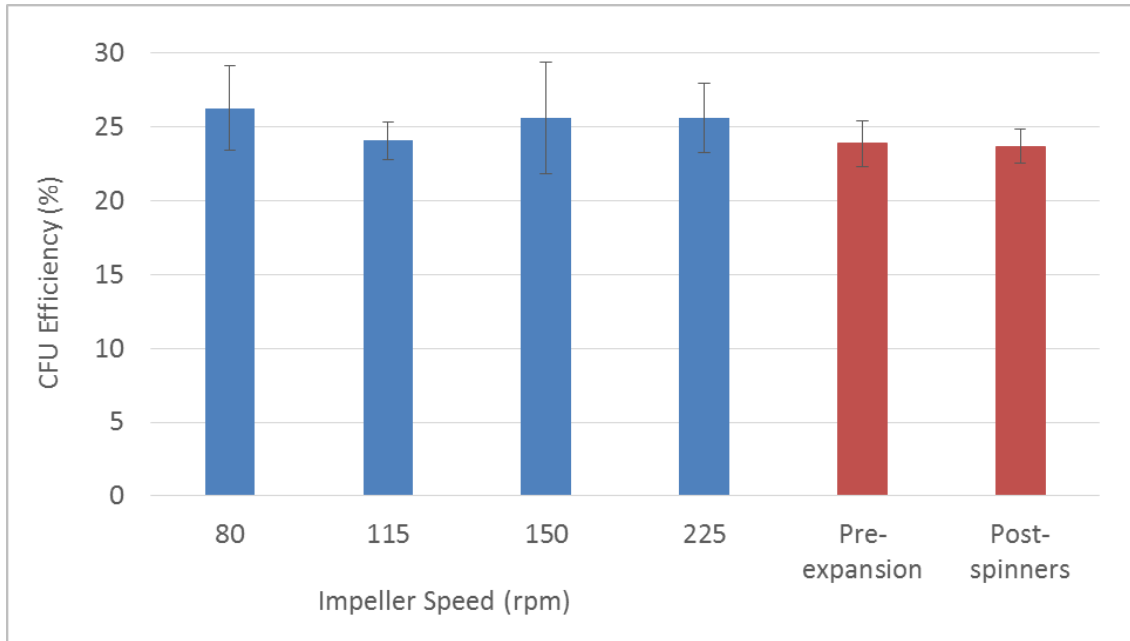
Figure 7.8. Post-harvest colony forming efficiency of BM-hMSCs at various impeller speeds showing a similar colony forming potential of BM-hMSCs across all conditions. Data shows mean ± SD, n = 3

To ensure that the microcarrier-based expansion and harvest unit operations have not had a detrimental effect on BM-hMSC identity, the immunophenotype has been evaluated immediately post-harvest. The primary objective for this is to demonstrate that the BM-hMSCs conform to the International Society for Cellular Therapy (ISCT) criteria (Dominici *et al.* 2006). The post-harvest BM-hMSC immunophenotype for an impeller speed of 225 rpm can be seen in Figure 7.9 which shows the co-expression of positive markers CD73, 90 and 105 as well as the negative expression of HLA-DR and CD34 (Chan *et al.* 2014b). Table 7.2 shows the percentage co-expression of each of these markers, which is greater than 95% for impeller speeds of 80, 150 and 225 rpm, confirming maintenance of BM-hMSC immunophenotype.
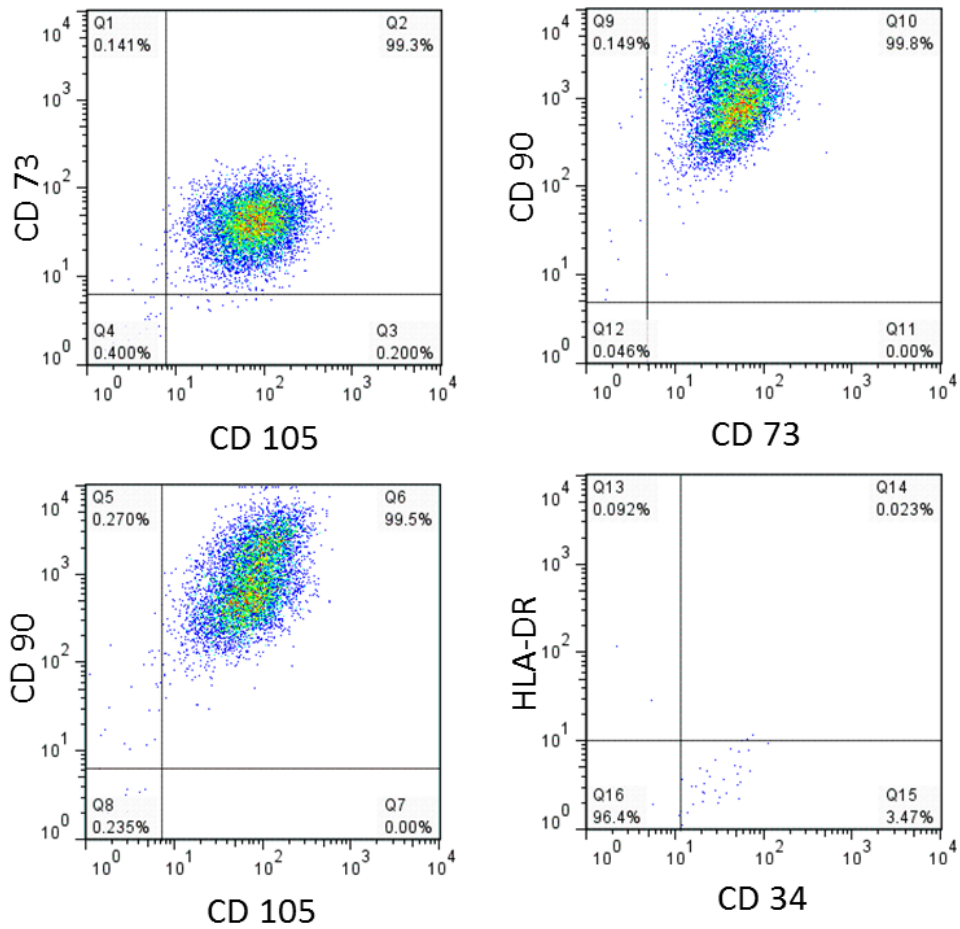
Figure 7.9. Exemplar multiparameter flow cytometry plots showing co-expression of CD90+, CD73+, CD105+, CD34- & HLA-DR- for an impeller speed of 225rpm

Table 7.2. Post-harvest multiparameter flow cytometry showing percentage co-expression of CD90+, CD73+, CD105+, CD34- & HLA-DR- at various impeller speeds. Mean value ± SD, in all cases 10,000 events were measured

Impeller speed (rpm)	% co-expression of CD73+, 90+, 105+, 34- and HLA-DR-
80	96.50 ± 0.14
150	96.80 ± 0.28
225	95.80 ± 0.14

7.3 Effect of dissolved oxygen concentration on BM-hMSC expansion

7.3.1 Experimental overview

In addition to the bioreactor impeller speed, the optimum dissolved oxygen (DO) concentration control set-point must be determined for BM-hMSC expansion on microcarriers. For this, three DASbox culture vessels per condition were cultured for six days (see Section 3.3.5) at 100, 75, 50, 25 and 10 % dissolved oxygen in FBS-based medium. The pH control set-point was 7.4, the impeller speed was controlled to 115 rpm and the temperature was controlled to 37 °C. Prior to all experiments, the control system settings on the DASGIP DASbox bioreactor platform were adjusted to ensure it remained stable, the process of which can be seen in Appendix E.

During culture, daily medium samples were taken for analysis of glucose, lactate, ammonia, lactate dehydrogenase and total protein with cell counts performed each day (four samples were analysed per bioreactor as per Section 3.4.3). The culture medium was exchanged on day three of culture. At harvest, the BM-hMSCs were removed from the microcarriers and separated according to Section 3.3.6. The BM-hMSCs harvested from each condition were then assessed for mean cell diameter (Section 3.4.2), tri-lineage differentiation potential (Section 3.4.4) and immunophenotype (Section 3.4.5). In addition to these identity measurements, BM-hMSC quality characteristics of colony forming efficiency (Section 3.4.9) and outgrowth potential were also assessed post-harvest.

7.3.2 The importance of dissolved oxygen control in bioreactor operation

Almost all of the current technology for BM-hMSC expansion utilise open, laboratory scale processes such as T-flasks wherein controlling, monitoring, and evaluating the impact of key parameters on target cell output and productivity is difficult (Kirouac and Zandstra 2008). Control of process parameters such as dissolved oxygen during the manufacturing process will be vital in maximising product consistency and ensuring that the process is scalable. A large part of this ability to control the process conditions is in maintaining a closed process during expansion, which not only reduces contamination risk but is vital in maintaining the desired culture environment of the BM-hMSCs and avoid fluctuations in these critical process parameters. Much of the current literature on low oxygen concentration or hypoxia (Table 7.3) culture of BM-hMSC use hypoxic incubators that maintain a low oxygen environment (an oxygen concentration in the gas phase lower than that found in atmospheric air) rather than controlling

the process conditions, with process manipulations taking place at atmospheric oxygen concentrations.

Table 7.3. Definitions of culture and physiological oxygen concentrations in relation to atmospheric and dissolved oxygen concentrations.

Atmospheric Oxygen Concentration (v/v)	Dissolved Oxygen Concentration (%)	*In vitro* Nomenclature	*In vivo* nomenclature
20 − 21	100	Normoxia	Hyperoxia
2 -5	10 - 25	Hypoxia	Normoxia

Figure 7.10 shows the impact of exposing low oxygen experiments to atmospheric oxygen within an agitated bioreactor process. This demonstrates that for a DO set-point of 5 % (1.05 % atmospheric oxygen), after a one hour exposure of the culture to atmospheric conditions (21 % atmospheric oxygen equivalent at saturation to 100 % dissolved oxygen), creates a deviation to a maximum DO concentration of 77.9 %, which takes a further 294 minutes to return back to 5 % DO with continual headspace aeration with 1.05% atmospheric oxygen. Considering the number of manipulations that occur during culture, for example, daily sampling and medium exchange, this mode of operation causes large and prolonged fluctuations in dissolved oxygen concentrations experienced by the BM-hMSCs. Considering that this study has taken place in agitated conditions with headspace aeration, it represents a best case scenario, as in static monolayer culture without headspace gassing these deviations in DO would be larger with an increased set-point recovery time. This is a potential reason why there is so much discrepancy within the published literature of BM-hMSCs cultured in low oxygen concentration atmospheres.
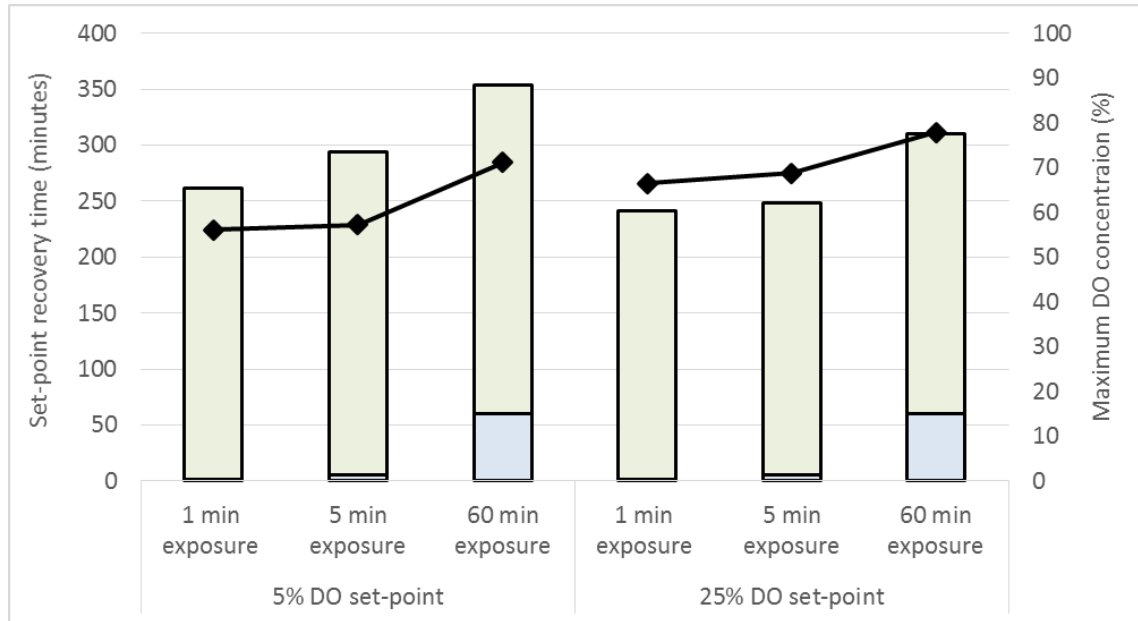
Figure 7.10. Implications of exposing low dissolved oxygen (DO) experiments (5 and 25%) to atmospheric conditions in a biological safety cabinet for 1, 5 and 60 minutes. Demonstrating the importance of continuous closed process control during bioreactor culture. Bars represent the set-point recovery time to 5 or 25% DO and diamonds represent the maximum DO concentration reached during each exposure and recovery period.

7.3.3 Human MSC growth kinetics on microcarriers

Following the initial experiment to assess the effect of the bioreactor impeller rate on BM-hMSC expansion on microcarriers, the impeller speed of 115 rpm has been selected for future bioreactor experiments. This speed was chosen because it allowed for the suspension of the microcarriers, without causing detriment to the BM-hMSC growth kinetics or post-harvest characteristics.
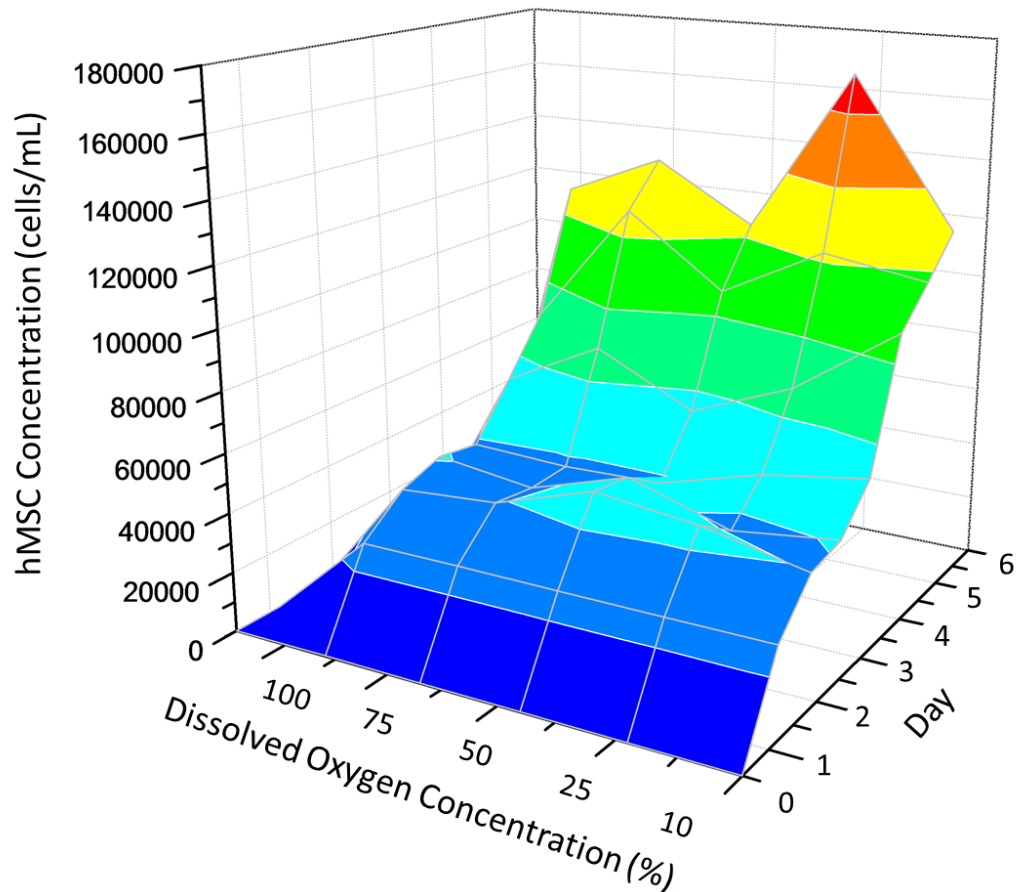
Figure 7.11. Effect of dissolved oxygen concentration on BM-hMSC growth over six days of culture in the DASbox controlled bioreactor, showing the increased growth kinetics at lower dissolved oxygen concentrations. Control set-points are 115rpm impeller speed and pH 7.4 with headspace aeration. Data shows mean of n = 3

Dissolved oxygen concentration has been previously shown to have an impact on BM-hMSC growth and cell characteristics (Grayson *et al.* 2006), with much debate around the use of the terms "normoxia" (100 % DO) and "hypoxia" (typically < 25 % DO) (Rafiq *et al.* 2013c). Figure 7.11 shows the effect of various controlled dissolved oxygen concentrations on BM-hMSC growth on microcarriers over six days of culture, with increased growth kinetics at lower dissolved oxygen concentrations. This is confirmed by Figure 7.12 , which shows the post-harvest cell number in each dissolved oxygen concentration, with significantly higher BM-hMSC numbers (p < 0.05) at 10 and 25 % DO compared with 100 % DO. There is currently no common consensus on whether low oxygen concentrations are beneficial for BM-hMSCs, with some studies demonstrating improved growth (Dos Santos *et al.* 2010) and function (Basciano *et al.*

2011), whilst others demonstrate diminished BM-hMSC characteristics (Rafiq *et al.* 2013c) in monolayer culture. This data therefore, provides an indication that BM-hMSC growth characteristics are improved at low dissolved oxygen concentrations, in a controlled microcarrier expansion process.
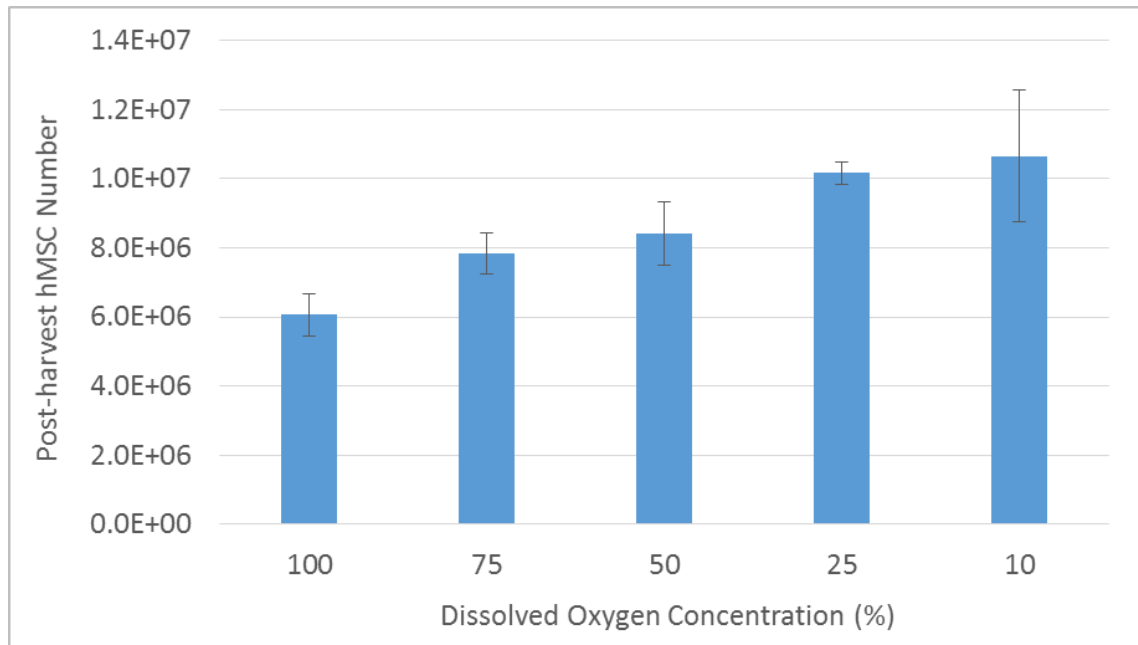
Figure 7.12. Effect of dissolved oxygen concentration on post-harvest BM-hMSC number after six days of culture in the DASbox controlled bioreactor, showing the increased BM-hMSC number at lower dissolved oxygen concentrations. Data shows mean ± SD, n = 3

7.3.4 Human MSC metabolite flux on microcarriers

It is again important to assess the effect of changing DO concentrations on the relative metabolite flux of the BM-hMSC during microcarrier expansion. Figure 7.13 shows the live concentrations of glucose, lactate and ammonia over the six days of expansion, with increased consumption of glucose and production of lactate in low dissolved oxygen concentrations, in accordance with the increased BM-hMSC growth rate in Section 7.3.3. In contrast, Figure 7.13 shows that the production of ammonia in 10 and 25 % DO was reduced compared with higher DO concentrations, despite the increased BM-hMSC number at the lower dissolved oxygen concentration. As with the impeller speed experiment, the LDH and total protein concentrations have been measured to assess whether any BM-hMSC stress or damage has been caused by the

different DO concentrations. Figure 7.14 shows these concentrations throughout culture, which have not unduly increased over the six day period, although the 100 % DO condition has demonstrated the highest level of total protein and LDH, despite having the lowest number of BM-hMSC through culture. This reduction in the release of LDH has previously been associated with a reduction in cell necrosis for a DO concertation of 7 %, compared to BM-hMSCs cultured at 100 % DO (Lavrentieva *et al.* 2010b). A reduction in cell necrosis at low dissolved oxygen concentrations would be beneficial for BM-hMSC manufacturing processes, as cell death has the potential to activate a cascade of negative cell responses that would reduce the purity of the final product and would therefore be undesirable (Festjens *et al.* 2006).

The per cell flux of glucose, lactate, ammonia and the yield of lactate from glucose can be seen in Figure 7.15 for BM-hMSC culture on microcarriers at various controlled DO concentrations. This shows a significantly higher glucose and lactate production rate (P < 0.05) for a dissolved oxygen concentration of 10 %. This is in agreement with previous studies for BM-hMSCs cultured in monolayer conditions at reduced DO concentrations (Brown *et al.* 2007; Dos Santos *et al.* 2010; Rafiq *et al.* 2013c), which demonstrates that the cell metabolism is switching from oxidative phosphorylation to anaerobic glycolysis (likely due to oxygen limitation in the culture medium) as well as an up-regulation of the glucose transport into the cells in low DO culture. Furthermore, the level of glucose consumption and lactate production for BM-BM-hMSCs is also comparable to these studies with around 15 $pmol.cell^{-1}.day^{-1}$ and 30 $pmol.cell^{-1}.day^{-1}$, respectively. It is important to note that this result for controlled microcarrier culture is consistent with the literature on the monolayer expansion of BM-hMSCs at low DO concentrations, demonstrating that despite the change in process conditions from monolayer to microcarrier culture, the metabolite flux of BM-hMSC remains comparable which is important during process development (Archibald *et al.* 2015).
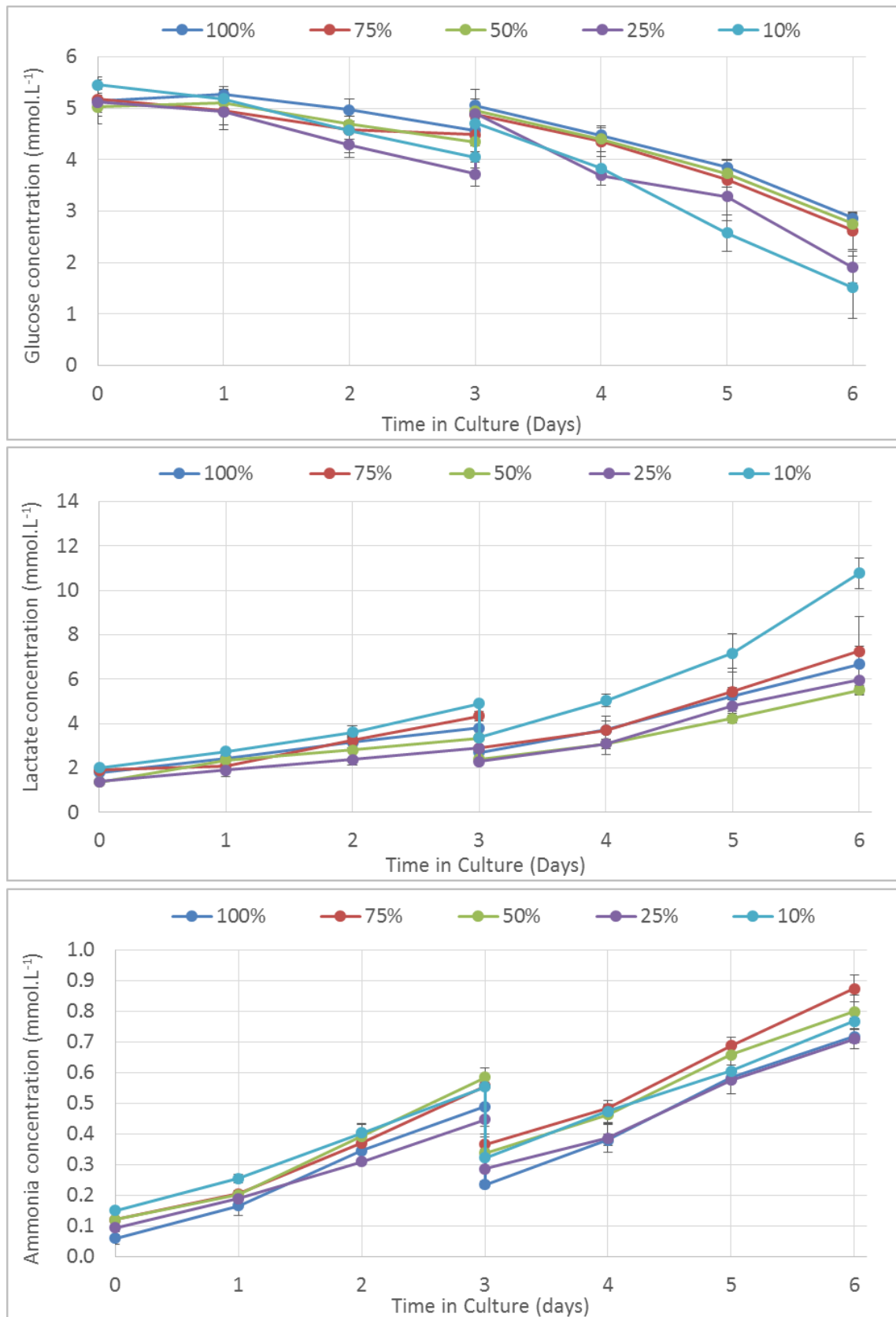
Figure 7.13. Live metabolite concentrations of glucose, lactate and ammonium for various dissolved oxygen concentrations showing the increased metabolic activity at lower dissolved oxygen concentrations. Data shows mean ± SD, n = 3

The flux of ammonia can also be seen in Figure 7.15, which shows a significant reduction ($p < 0.05$) for both 25 and 10 % DO to around 2.5 pmol.cell^{-1}.day^{-1}, compared to 100 % DO. This is again in agreement with previous studies (Dos Santos *et al.* 2010) and supports a more efficient cell metabolism under low DO culture conditions. A reduction in the production in ammonia at low DO concentrations for microcarrier culture is also advantageous for process operation, as the build-up of toxic compounds to inhibitory levels will become less of an issue (Schop *et al.* 2009b).
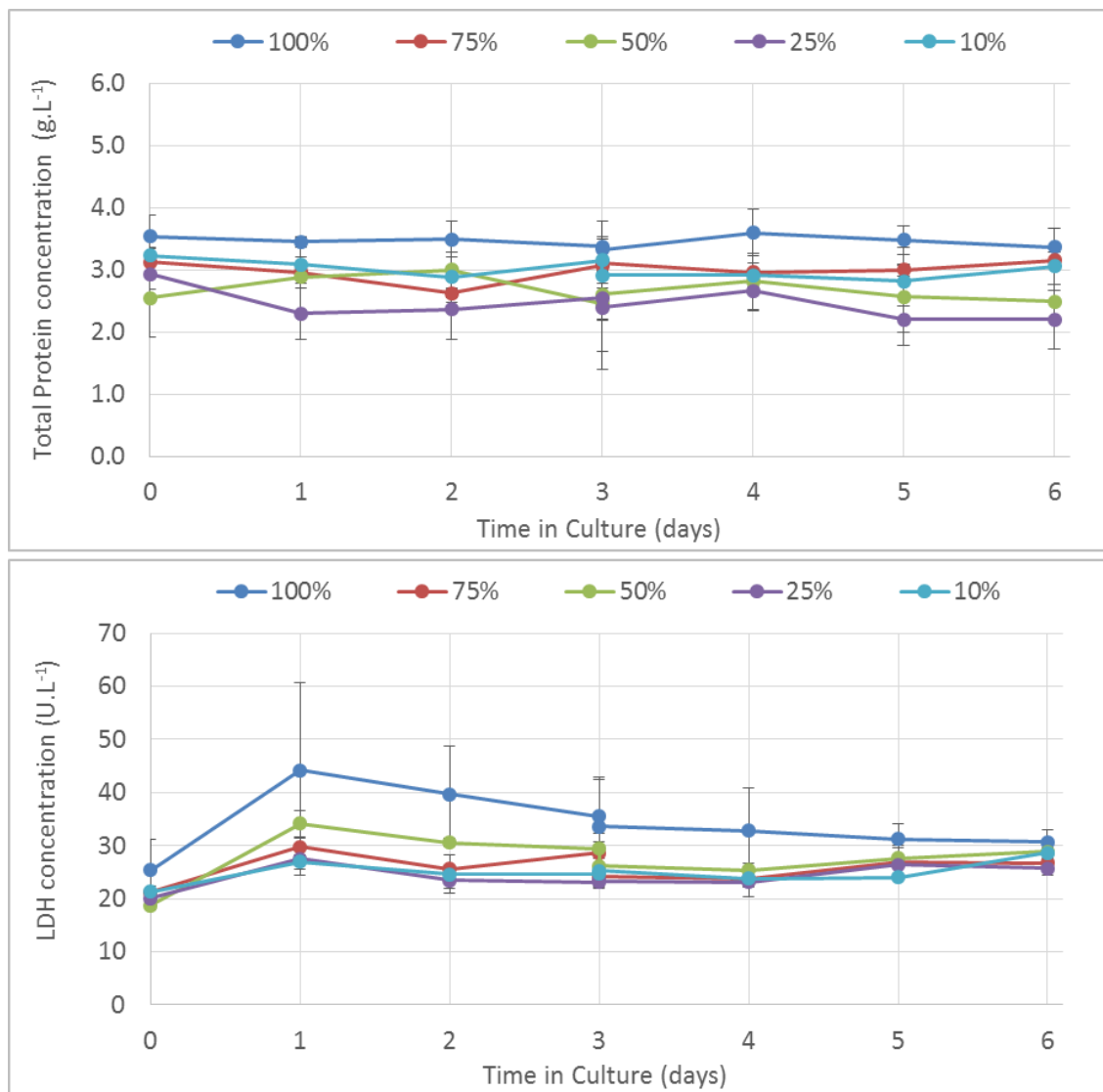
Figure 7.14. Live metabolite concentrations of lactate dehydrogenase (LDH) and total protein at various dissolved oxygen concentrations demonstrating little increase in concentrations throughout expansion indicating a low level of cellular damage. Data shows mean ± SD, n = 3

The yield of lactate production from glucose can also be seen in Figure 7.15, which shows a reduction in yield to 1.21 ± 0.37 mol.mol^{-1} at 25% DO, but a subsequent increase at 10 % DO to 2.27 ± 0.26 mol.mol^{-1} compared with 100 % DO. This is once again in agreement with studies of BM-hMSC culture at low oxygen concentrations in monolayer involving BM-hMSCs (Dos Santos *et al.* 2010; Rafiq *et al.* 2013c) but is significantly higher than BM-hMSCs derived from the umbilical cord at both high and low DO concentrations (Lavrentieva *et al.* 2010b). Considering the importance of the *in vivo* niche environment on hMSC characteristics, it is possible that this difference in cell metabolism at different dissolved oxygen concentrations is due to relative differences in the *in vivo* oxygen concentrations in the bone-marrow and umbilical cord tissues (Mohyeldin *et al.* 2010).
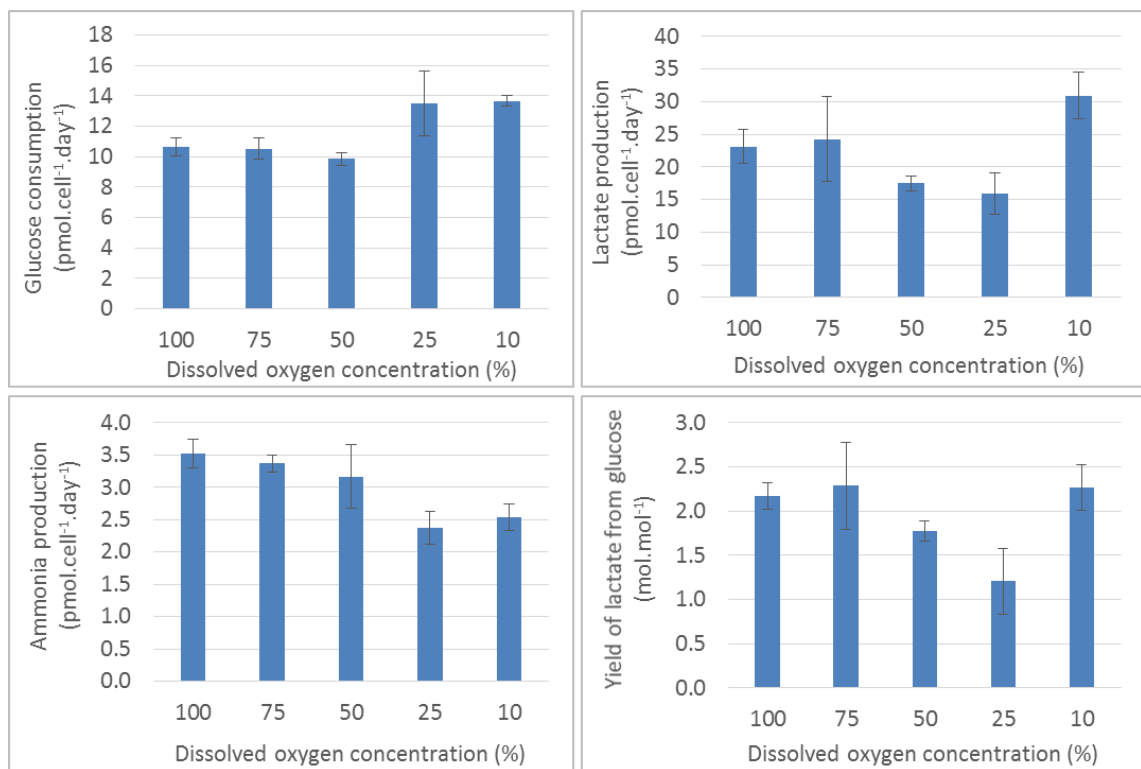
Figure 7.15. Metabolite consumption and production rate of BM-hMSCs at various dissolved oxygen concentrations. Showing glucose consumption, lactate production, ammonia production and the yield of lactate from glucose. Data shows mean ± SD, n = 3

7.3.5 Post-harvest characterisation of BM-hMSCs

As with the investigation of the effect of various impeller speeds, it is important to assess whether microcarrier expansion at reduced DO concentrations is not unduly effecting the post-harvest BM-hMSC characteristics, despite the improved growth kinetics seen in section 7.3.3. Figure 7.16 shows the outgrowth rate of BM-hMSCs harvested from microcarrier culture at the various DO concentrations compared to pre-expansion and post-harvest from uncontrolled spinner flasks at 100 % DO. This shows significantly higher ($p < 0.05$) outgrowth kinetics for BM-hMSCs across all controlled bioreactor expansion conditions compared to pre-expansion and post-harvest from the spinner flasks. In addition to this, BM-hMSCs cultured at 10 % DO demonstrated significantly higher ($p < 0.05$) outgrowth kinetics compared to all other controlled DO concentrations. This suggests that the controlled expansion of BM-hMSCs on microcarriers, particularly at low dissolved oxygen concentrations, is having a positive impact on the outgrowth kinetics of BM-hMSCs.
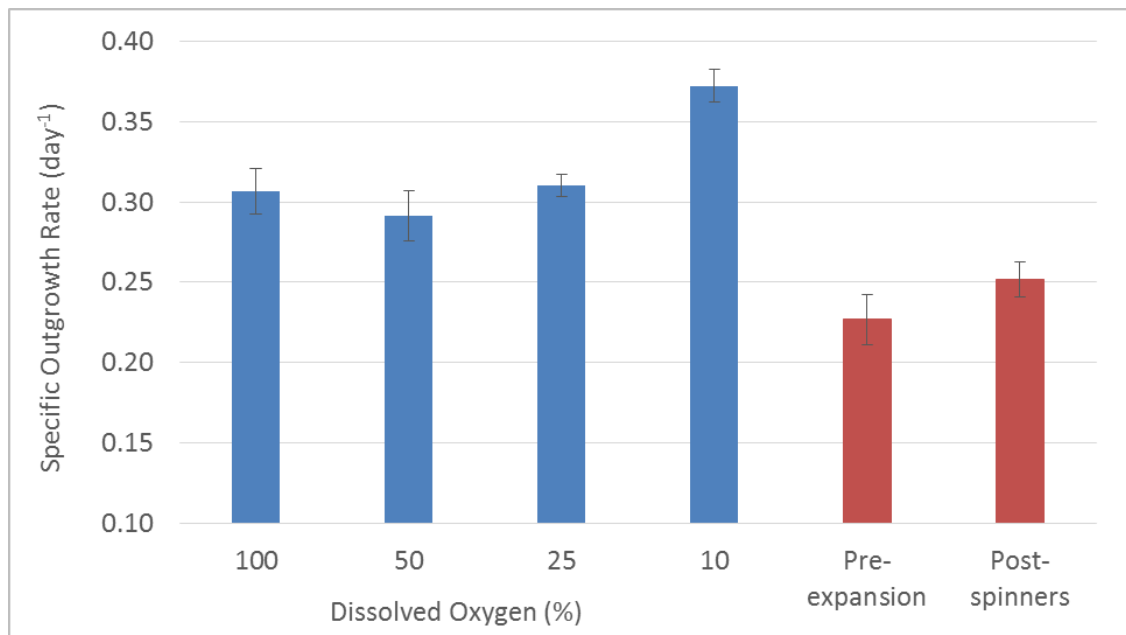
Figure 7.16. Post-harvest outgrowth rate of BM-hMSCs at various dissolved oxygen concentrations showing the increased outgrowth kinetics of BM-hMSCs from the controlled bioreactor particularly at low dissolved oxygen compared to pre-expansion and post-spinner culture. Data shows mean ± SD, n = 3

In accordance with the increase in outgrowth kinetics, the mean cell diameter of BM-hMSCs cultured in controlled bioreactor conditions in Figure 7.17 is significantly ($p < 0.05$) lower than pre-expansion and post-harvest from uncontrolled spinner flasks. The benefits to the manufacturing process of producing smaller BM-hMSCs has previously been discussed (Heathman *et al.* 2015e) and smaller cells are commonly associated with increased proliferation, greater colony-forming efficiency and longer telomeres (Samsonraj *et al.* 2015). Likewise, BM-hMSC culture at low DO from different sources may also display different functional characteristics and can modulate the autocrine or paracrine activity of a variety of cytokines and growth factors in BM-hMSCs (Das *et al.* 2010).
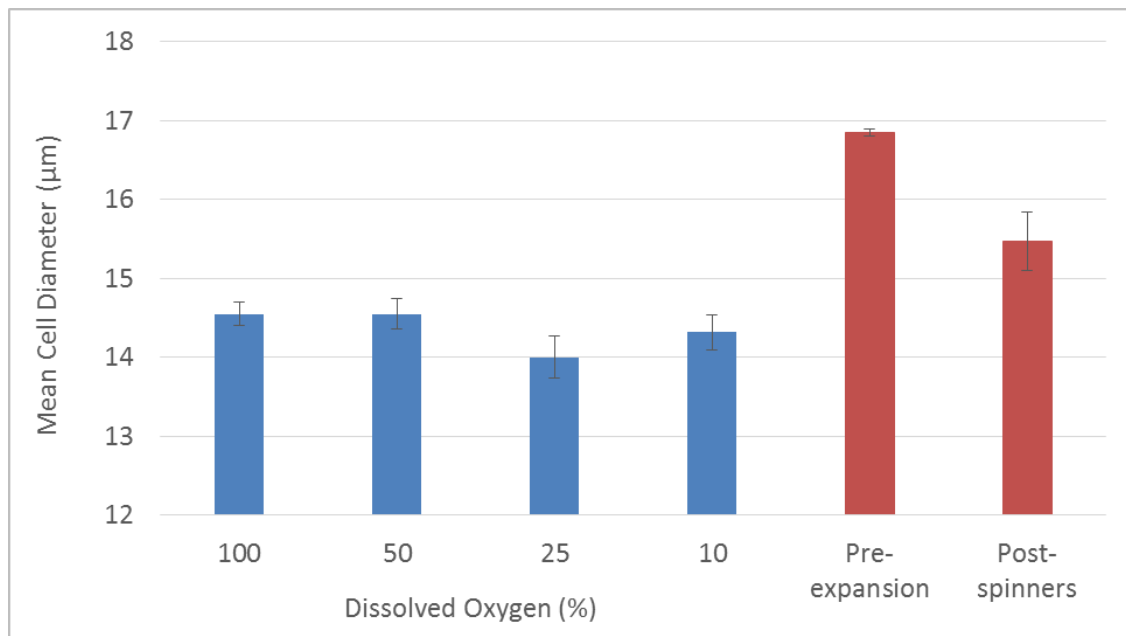
Figure 7.17. Post-harvest mean diameter of BM-hMSCs at various dissolved oxygen concentrations showing the reduced mean BM-hMSC diameter of BM-hMSCs from the controlled bioreactor compared to pre-expansion and post-spinner culture. Data shows mean ± SD, n = 3

The post-harvest colony-forming (CFU) efficiency of BM-hMSCs from the controlled bioreactor process at various DO concentrations can be seen in Figure 7.18, which shows a similar level of CFU efficiency for BM-hMSC harvested form 50 and 100 % DO conditions, compared with pre-

expansion and post-spinner culture. In contrast, the post-harvest CFU efficiency of BM-hMSC from 10 and 25 % DO was significantly higher ($p < 0.05$) than pre-expansion and post-harvest from spinner flasks. An increase in CFU efficiency of BM-hMSCs at low dissolved oxygen is widely reported and has been shown to be independent of hypoxia inducible factor (HIF) expression in BM-hMSCs (Tamama *et al.* 2011).
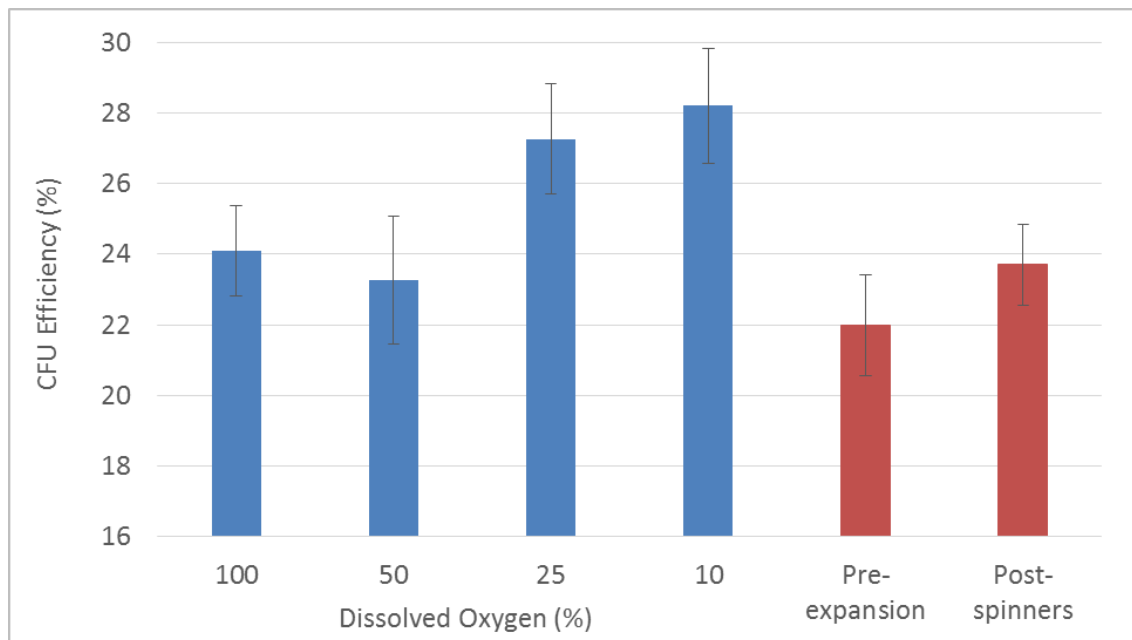
Figure 7.18. Post-harvest colony forming efficiency of BM-hMSCs at various dissolved oxygen concentrations showing an increased colony forming potential of BM-hMSCs at reduced dissolved oxygen concentrations. Data shows mean ± SD, n = 3

To ensure that the microcarrier-based expansion and harvest unit operations have not had a detrimental effect on BM-hMSC identity, the immunophenotype has been evaluated immediately post-harvest. The primary objective for this is to demonstrate that the BM-hMSCs conform to the International Society for Cellular Therapy (ISCT) criteria (Dominici *et al.* 2006). The post-harvest BM-hMSC immunophenotype for a dissolved oxygen concentration of 10% can be seen in Figure 7.19 which shows the co-expression of positive markers CD73, 90, 44 and 105 as well as the negative expression of CD45, 34, 11b, 19 and HLA-DR, demonstrating that low

oxygen culture of BM-hMSCs in a controlled microcarrier process does not affect the immunophenotype of the BM-hMSCs.
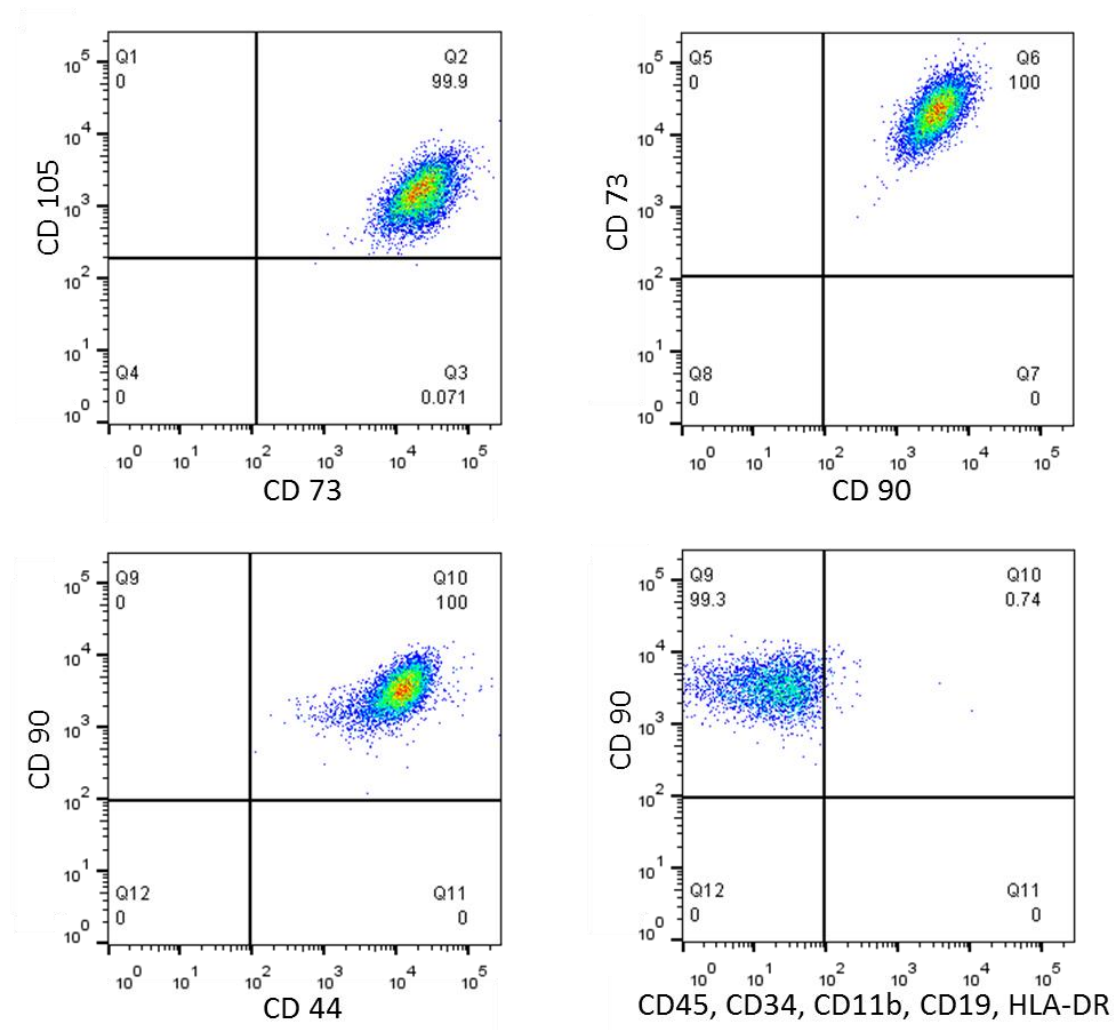
Figure 7.19. Exemplar multiparameter flow cytometry plots showing co-expression of CD90+, CD73+, CD105+, CD44+, CD34-, CD45-, CD11b-, CD19- & HLA-DR- for a dissolved oxygen concentration of 10%

7.4 Effect of sparging on BM-hMSC expansion

7.4.1 Experimental overview

Despite that fact that sufficient oxygen can be supplied to the culture medium by headspace aeration at the 100 mL volume and cell densities investigated here, it is acknowledged that this may not be the case as the bioreactor process is scaled-up and cell-densities increase. In order to address this early in process development, the effect of aeration *via* a sparger in the culture medium has been investigated with and without Pluronic™ F68, a commonly used cell protectant in suspension-based mammalian cell culture. Evidence suggests that Pluronic™ F68 has the potential to accumulate in mammalian cells during culture (Gigout *et al.* 2008), which would be undesirable for cell-based therapy applications and therefore its use should be limited where possible. For this investigation, three DASbox culture vessels per condition were cultured for six days (see Section 3.3.5) with an aeration rate of 0.1 VVM (gas volume flow per unit of liquid volume per minute). The dissolved oxygen was controlled to 100 %, the pH control set-point was 7.4, the impeller speed was set to 115 rpm and the temperature was controlled to 37 °C.

During culture, daily medium samples were taken for analysis of glucose, lactate, ammonia, lactate dehydrogenase and total protein with cell counts performed each day (four samples were analysed per bioreactor as per Section 3.4.3). The culture medium was exchanged on day three of culture. At harvest, the BM-hMSC were removed from the microcarriers and separated according to Section 3.3.6. The BM-hMSCs harvested from each condition were then assessed for mean cell diameter (3.4.2), colony forming efficiency (Section 3.4.9) and outgrowth potential.

7.4.2 Aeration strategies in BM-hMSC bioreactor process development

Agitation and aeration strategies will play a key role in the successful development of microcarrier based bioreactor processes for BM-hMSC manufacture, particularly as the scale of operation increases. Due to the fact that the specific oxygen demand and the cell densities achieved so far in BM-hMSC microcarrier culture are low, the oxygen demand of the cells in current benchtop bioreactors can be met by passing gas mixtures through the headspace. At the bench scale the relatively large surface area to volume ratio means that headspace aeration alone is sufficient to meet this demand, however on the commercial scale, as the available gas-

liquid interface area is inversely proportional to scale, this will become more of a challenge (Nienow 2006).

In order to address the oxygen supply issue, aeration directly into the culture medium *via* the incorporation of a sparger has been used for large scale mammalian cell culture, where the cell oxygen demand is an order of magnitude higher than BM-hMSCs (Rafiq *et al.* 2013a) and cell densities are greater than $5 \cdot 10^6$ ml^{-1} (Nienow 2003). The introduction of sparging into bioreactor culture also creates new challenges such as the addition of antifoam (Mostafa and Gu 2003) into the medium, which has been previously shown to significantly reduce the mass transfer properties of the system (Lavery and Nienow 1987). It is also widely accepted that cell damage due to sparging is primarily a result of bubbles bursting at the medium-air interface, where the local energy release is sufficient to damage the cell. Polymers such as Pluronic^{TM} F68 are widely used to decrease this cell damage and improve bioreactor performance in traditional mammalian cell suspension processes (Oh *et al.* 1989; Kilburn and Webb 2000). This improvement in performance by the addition of Pluronic^{TM} F68 is a result of its ability to reduce the hydrophobicity of the cell surface, preventing cell-bubble attachment and subsequent damage due to these bubbles bursting at the surface (Meier *et al.* 1999).

It is likely that the microcarrier culture of BM-hMSCs will encounter a number of these issues as the bioreactor scale and cell densities achieved increase throughout development. Therefore investigating the potential consequences will be important early in development. Furthermore, considering that the use of protective components, such as Pluronic^{TM} F68 have been successful for free suspension cell culture, it is possible that they will not be appropriate for the suspension culture of BM-hMSCs attached to microcarriers, as in this case the cells are administered directly to the patient and are subject to increased regulation.

7.4.3 Human MSC growth kinetics on microcarriers

The growth rate of BM-hMSC on microcarriers in a controlled bioreactor process has been assessed in order to compare the effect of sparging at 0.1VVM with and without Pluronic^{TM} F68 to headspace aeration. Figure 7.20 shows this BM-hMSC growth rate over six days of bioreactor expansion, demonstrating that headspace aeration ($1.70 \pm 0.45 \cdot 10^5$ cell.mL^{-1}) supports significantly higher ($p < 0.05$) growth kinetics compared to sparged culture with ($0.52 \pm 0.15 \cdot 10^5$ cell.mL^{-1}) and without ($0.84 \pm 0.18 \cdot 10^5$ cell.mL^{-1}) Pluronic^{TM} F68. This is the first indication that aeration directly into the culture medium *via* a sparger has a detrimental impact on the

expansion of BM-hMSCs on microcarriers. Furthermore, the improved performance experience by free suspension cell culture due to the addition of Pluronic™ F68 does not apply to the microcarrier system investigated here, which has also been demonstrated for an alternative cell type (Liu *et al.* 2004).
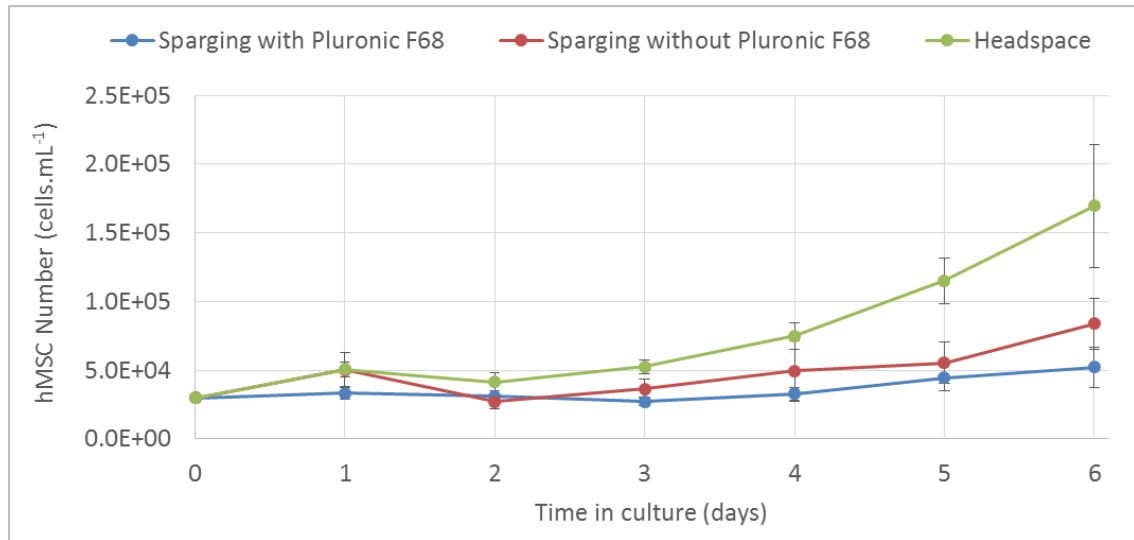
Figure 7.20. Effect of sparging with and without Pluronic™ F68 on BM-hMSC growth over six days of culture in the DASbox controlled bioreactor, showing the reduced growth kinetics when sparging. Control set-points are 115rpm impeller speed, 25% dissolved oxygen and pH 7.4. Data shows mean ± SD, n = 3

This results suggests that the detrimental impact of sparging on the microcarrier culture of BM-hMSCs is not due to cell-bubble attachment, with cell damage caused by subsequent bubble bursting at the gas-liquid interface as is the case with free suspension cell culture (Meier *et al.* 1999). The key difference with the microcarrier culture of BM-hMSCs compared to free suspension cell culture is that the cells must adhere to the microcarrier surface prior to growth. The addition of Pluronic™ F68 into the culture medium in this system is in fact having a detrimental impact on the growth of BM-hMSCs (Figure 7.20), which perhaps is not surprising given that the mechanism of Pluronic™ F68 is to reduce the cell hydrophobicity, thus reducing the affinity of the BM-hMSCs to attach to surfaces. Further evidence of this can be seen in Figure

7.21, which shows the attachment rate of the BM-hMSCs to the microcarriers during the six days of culture. This figure shows that the attachment rate of the BM-hMSCs is reduced in sparged culture compared to headspace aeration, suggesting that introducing bubbles into the bioreactor system is disrupting the BM-hMSC attachment process. Additionally, the inclusion of Pluronic™ F68 in the culture medium is further reducing the attachment rate of the BM-hMSCs to the microcarriers in suspension, in accordance with the mechanism described above. This reduced attachment rate of BM-hMSCs is likely to be contributing to the reduced growth kinetics seen under sparged conditions for BM-hMSCs culture on microcarriers. There is potential however, that headspace aeration could be used for the initial attachment phase and sparged aeration could then be used as the BM-hMSC density and subsequent oxygen demand increases throughout the process.
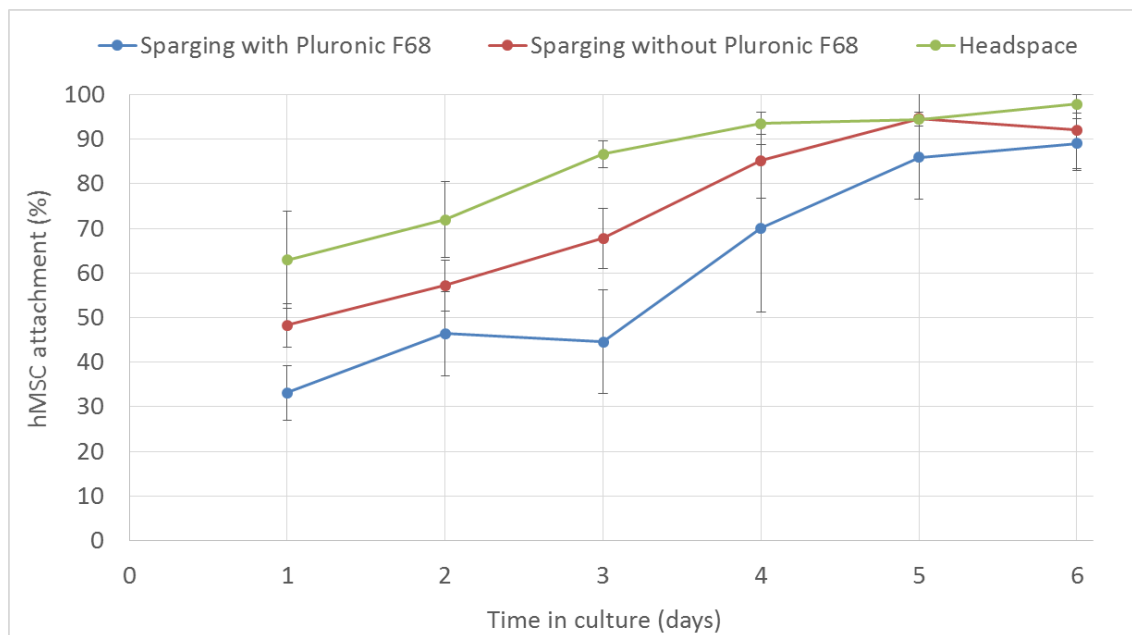
Figure 7.21. Attachment efficiency of BM-hMSC on microcarriers in the DASbox bioreactor system during sparger and headspace aeration strategies. Showing the reduced attachment rate of BM-hMSCs under sparged conditions. Data shows mean ± SD, n = 3

7.4.4 Human MSC metabolite flux on microcarriers

In addition to growth kinetics, the metabolite flux has been monitored throughout culture to assess the impact that sparging is having on the consumption and production of metabolites throughout microcarrier culture. Figure 7.22 show the concentrations of glucose, lactate and ammonia throughout the six days of expansion for sparged and headspace aeration culture. This shows that despite the reduced growth kinetics seen in sparged culture in Section 7.4.3, the net flux of glucose, lactate and ammonia is similar for all conditions and did not reach previously determined inhibitory levels at any point (Schop *et al.* 2009b).
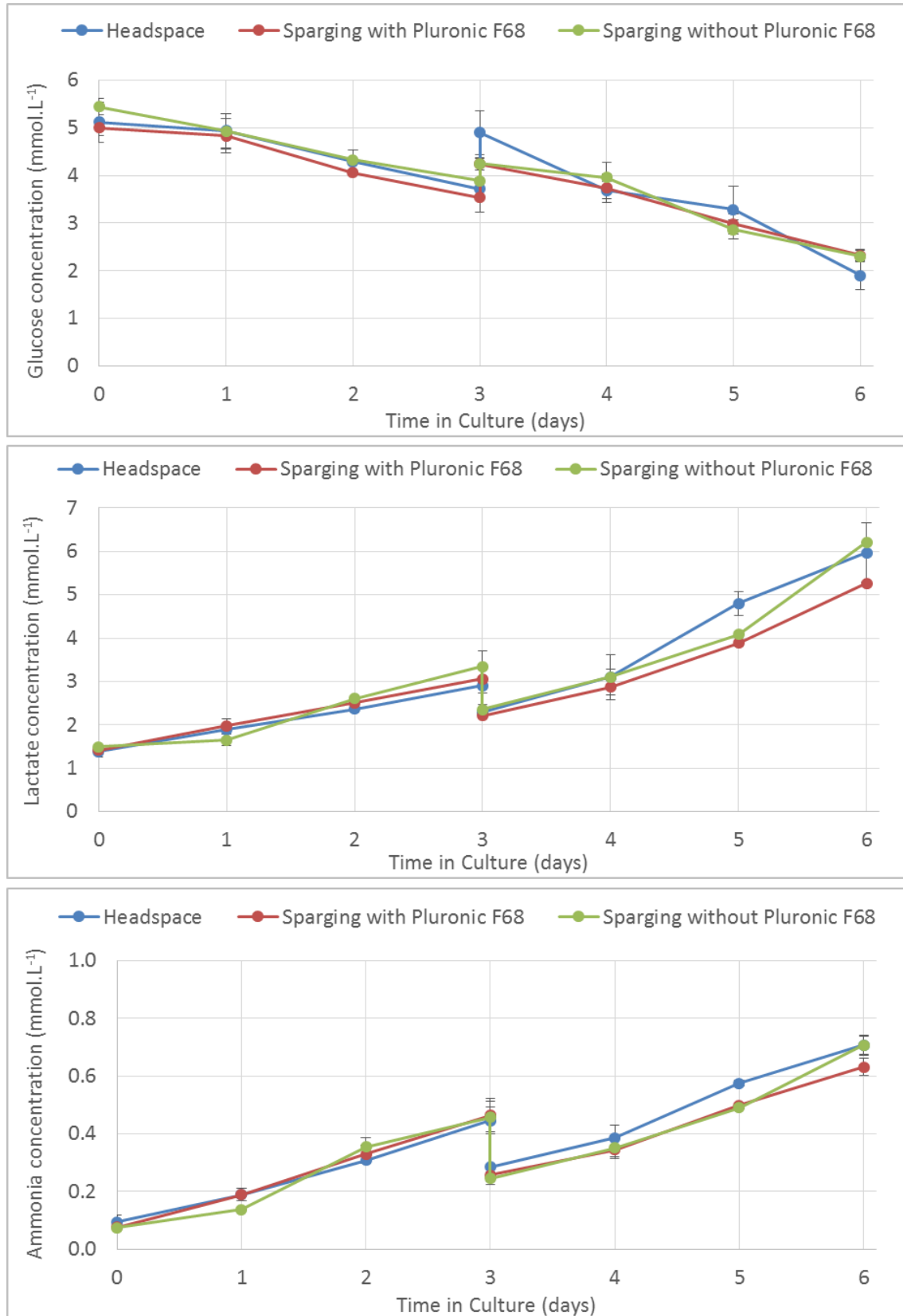
Figure 7.22. Live metabolite concentrations of glucose, lactate and ammonium at the different aeration strategies demonstrating a similar level of metabolic activity. Data shows mean ± SD, n = 3
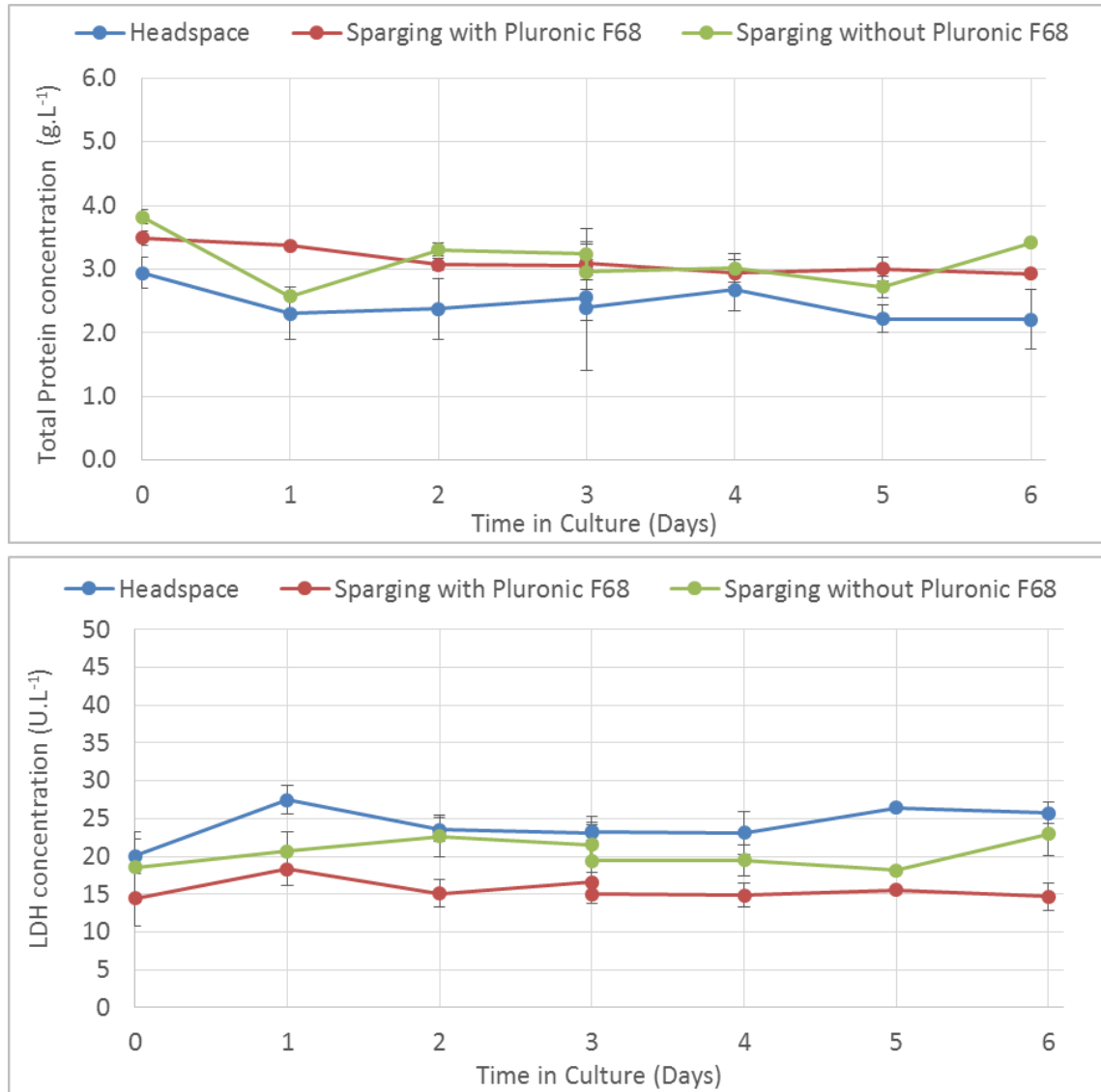
Figure 7.23. Live metabolite concentrations of lactate dehydrogenase (LDH) and total protein at the different aeration strategies demonstrating little increase in concentrations throughout expansion indicating a low level of cellular damage. Data shows mean ± SD, n = 3

As with the previous experiments, the LDH and total protein concentrations have been measured to assess whether any BM-hMSC stress or damage has been caused by sparged aeration. Figure 7.23 shows these concentrations throughout culture, which have not increased over the six day period in any condition. This is further evidence to suggest that introducing sparged aeration into the culture is not causing cell damage by bubble bursting, as the level of LDH and total protein would be increasing throughout culture if cell damage was occurring, which is the likely reason why the addition of Pluronic™ F68 into sparged culture is not

improving the BM-hMSC growth kinetics on microcarriers. Considering that cell damage is not occurring during sparged aeration, it seems that the reduction in growth kinetics during sparging is caused by the reduction in attachment rate seen in Section 7.4.3.
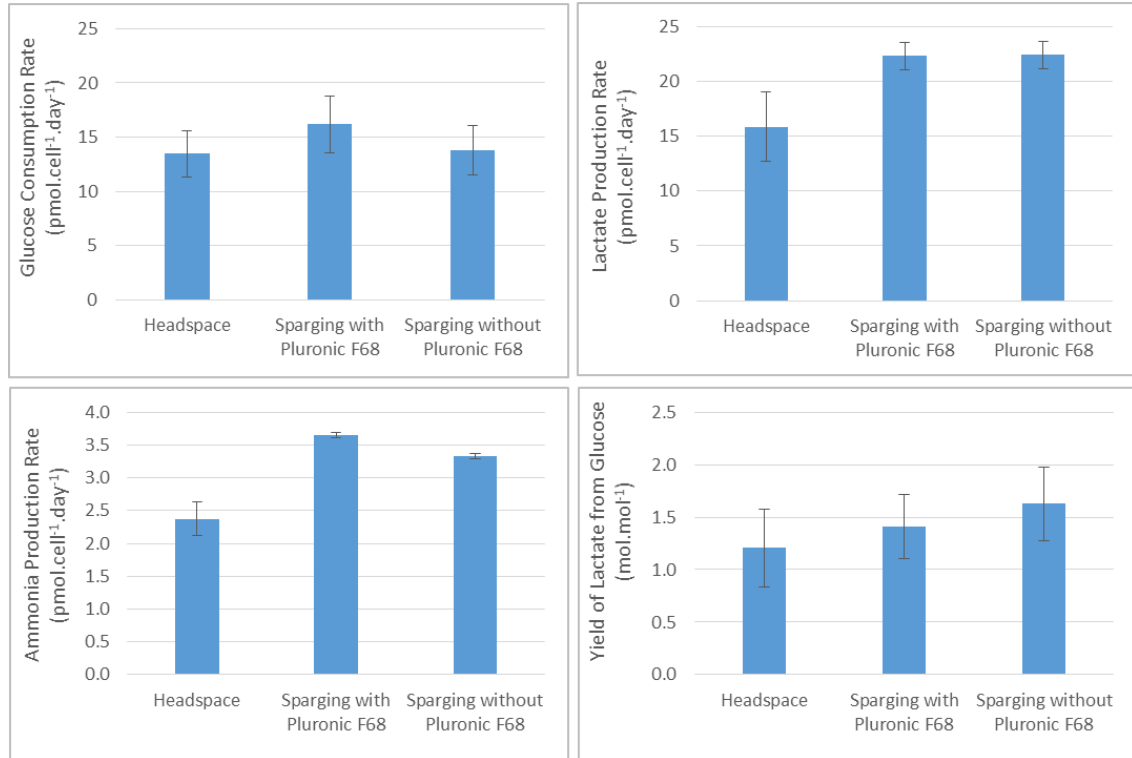
Figure 7.24. Metabolite consumption and production rate of BM-hMSCs at different sparging strategies. Showing the increased lactate and ammonia production for sparged culture. Data shows mean ± SD, n = 3

The per cell flux of each metabolite can be seen in Figure 7.24, which shows a similar level of net glucose consumption per cell in headspace and sparged aeration during culture. In contrast, the production of ammonia to above 3 pmol.cell^{-1}.day^{-1} and lactate to above 20 pmol.cell^{-1}.day^{-1} in sparged culture was significantly higher ($p < 0.05$) than from headspace aeration. The increase in the per cell production of lactate and ammonia has previously been associated with a reduction in growth kinetics of BM-hMSCs throughout an expansion process (Heathman *et al.* 2015c).

7.4.5 Post-harvest characterisation of BM-hMSCs

As with the previous experiments, it is important to assess whether the reduced growth characteristics of BM-hMSC in sparged aeration culture is also resulting in detrimental post-harvest BM-hMSC characteristics, as this will be critical for successful development of commercial BM-hMSC manufacturing processes. The post-harvest characteristics of the BM-hMSCs from the sparged and headspace aeration strategies can be seen in Figure 7.25, showing the relative post-harvest cell number, outgrowth rate, colony-forming potential and mean cell diameter.
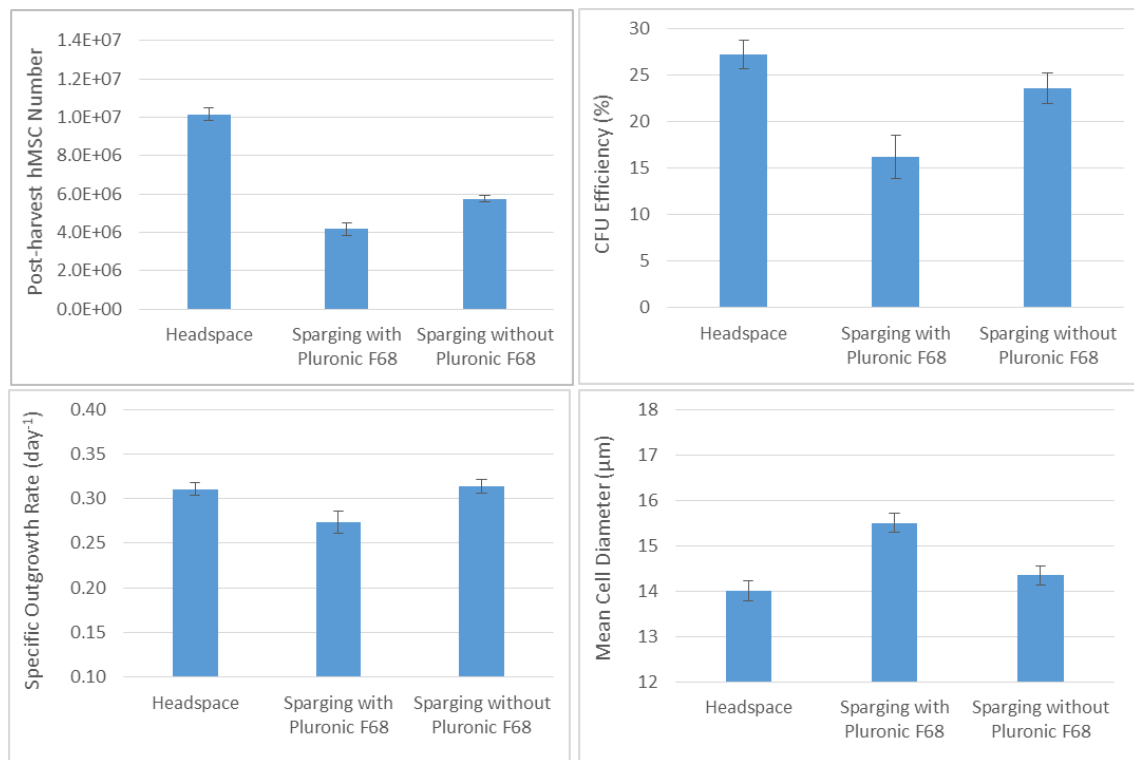
Figure 7.25. Post-harvest BM-hMSCs number, colony forming efficiency, outgrowth rate and mean cell diameter in different aeration strategies. Showing the reduced harvest cell number, mean BM-hMSC diameter and colony forming potential of BM-hMSCs from sparged culture. Data shows mean ± SD, n = 3

The post-harvest BM-hMSC number confirms the findings in Section 7.4.3, that a significantly higher ($p < 0.05$) number of BM-hMSCs were produced under headspace aeration, compared to

sparged aeration in the controlled bioreactor process. Figure 7.25 shows that the post-harvest BM-hMSC mean diameter is increased for sparged culture, with a significant increase ($p < 0.05$) seen for sparged aeration with the addition of Pluronic[TM] F68. This increase in post-harvest cell size is associated with a reduction in BM-hMSC attachment and subsequent growth rate with the addition of Pluronic[TM] F68, as was seen in Section 7.2.4 for an impeller speed of 225 rpm. In addition to the increased post-harvest BM-hMSC diameter, the addition of Pluronic[TM] F68 into the sparged culture lead to a reduction in BM-hMSC outgrowth kinetics as well as a significant reduction ($p < 0.05$) in the CFU potential of the BM-hMSCs. This reduction raises concerns about the use of Pluronic[TM] F68 in the culture of BM-hMSCs on microcarriers and its inclusion in cell-based therapy manufacturing processes should be carefully considered to ensure it is not having a detrimental impact on the growth or quality of the cell product.

7.5 Controlled expansion of BM-hMSCs in serum-free

7.5.1 Experimental overview

Now that a process control strategy has been developed for the microcarrier culture of BM-hMSCs, this can be transferred to the serum-free microcarrier process developed in Chapter 6. For this, three DASbox culture vessels per condition were cultured for six days (see Section 3.3.5) for BM-hMSC donors M2 and M3 in SFM and FBS-based medium. From the previous studies in this Chapter, the pH control set-point was 7.4, the dissolved oxygen was controlled at 10%, the impeller speed was controlled to 115 rpm and the temperature was controlled to 37 °C.

During culture, daily medium samples were taken for analysis of glucose, lactate, ammonia, lactate dehydrogenase and total protein with cell counts performed each day (four samples were analysed per bioreactor as per Section 3.4.3). The culture medium was exchanged on day three of culture for FBS and every two days for SFM. At harvest, the BM-hMSC were removed from the microcarriers and separated according to Section 3.3.6. The BM-hMSCs harvested from each condition were then assessed for mean cell diameter (Section 3.4.2), tri-lineage differentiation potential (Section 3.4.4) and immunophenotype (Section 3.4.5). In addition to these identity measurements, BM-hMSC quality characteristics of colony forming efficiency (Section 3.4.9) and outgrowth potential were also assessed post-harvest. In addition to this, the effective yield was calculated in terms of cells per volume of medium used per day, to determine the efficiency of the controlled process compared to uncontrolled in both FBS and SFM for the two donor BM-hMSC lines. The consistency between the BM-hMSC donors was also assessed by calculating the coefficient of variation for the controlled and uncontrolled processes.

7.5.2 Human MSC growth kinetics on microcarriers

Following the successful development of a process control strategy in FBS-based culture, it is important to assess the effect of this new control strategy on the serum-free (SFM) microcarrier expansion of the two BM-hMSC donors developed in Chapter 6. Figure 7.26 shows the growth kinetics of the two donor BM-hMSC lines in controlled bioreactors in FBS and SFM, with significantly increased growth kinetics for both BM-hMSC donors in SFM to a final cell concentration of $7.11 \pm 0.90 \cdot 10^5$ cell.mL^{-1} for M2 and $6.13 \pm 1.82 \cdot 10^5$ cell.mL^{-1} for M3. This represents a 300 % increase in the BM-hMSC yield across the two donors in SFM, which will be advantageous in driving cost-effective BM-hMSC manufacturing processes. The increase in growth kinetics in a controlled SFM microcarrier process presented here is in accordance with

previously published data for monolayer culture in Chapter 5 (Heathman *et al.* 2015e) and uncontrolled spinner flask culture in Chapter 6 (Heathman *et al.* 2015a).
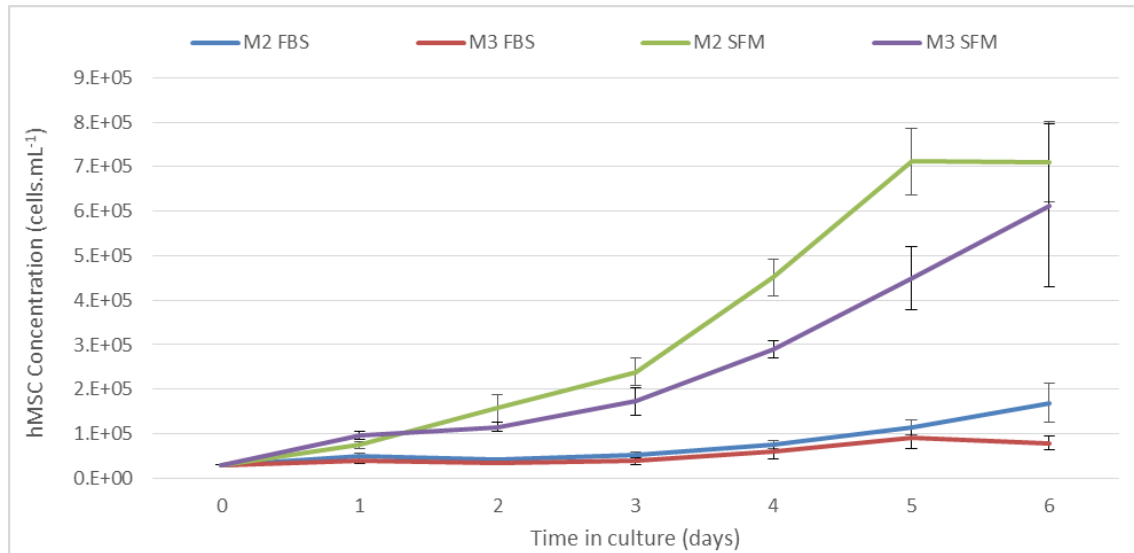
Figure 7.26. Serum-free and FBS expansion of two BM-hMSC donors over six days in the DASbox controlled bioreactor, showing the increased growth kinetics under serum-free. Control set-points are 115rpm impeller speed, 10% dissolved oxygen and pH 7.4. Data shows mean ± SD, n = 3

The harvest efficiency of BM-hMSC from the FBS-based process was 91.5 ± 8.9 % across both donors, which is comparable to previous studies which demonstrated > 95% harvest efficiency for a spinner flask based harvesting process (Nienow *et al.* 2014). This also demonstrates the effectiveness of the scalable harvesting method developed on sound engineering principles, as despite the change in bioreactor platform, maintaining the same specific energy dissipation rate and Kolmogorov microscale of turbulence in the DASbox bioreactor platform has yielded a similar BM-hMSC harvest efficiency (Nienow *et al.* 2015b). The overall harvest efficiency of the BM-hMSCs from the SFM process, however, was 76.5 ± 2.9 %, significantly lower than the previous FBS-based microcarrier processes. This is most likely due to the significantly increased BM-hMSC densities achieved under serum-free conditions, reducing the effectiveness of the separation process. Figure 7.27 shows that the harvest procedure employed has successfully removed the BM-hMSCs from the microcarriers in the SFM process. Therefore, the reduction in

harvest efficiency can be attributed to losses during the subsequent cell-microcarrier separation step and cell concentration. This separation problem will clearly have to be addressed moving forward, as increased cell densities will be required in order to drive cost-effective manufacturing processes and harvesting efficiencies will have fundamental impact on final product yields. Part of this success will be in developing scalable downstream technology, capable of reducing losses in the process step of separating the BM-hMSCs from the microcarriers after detachment.
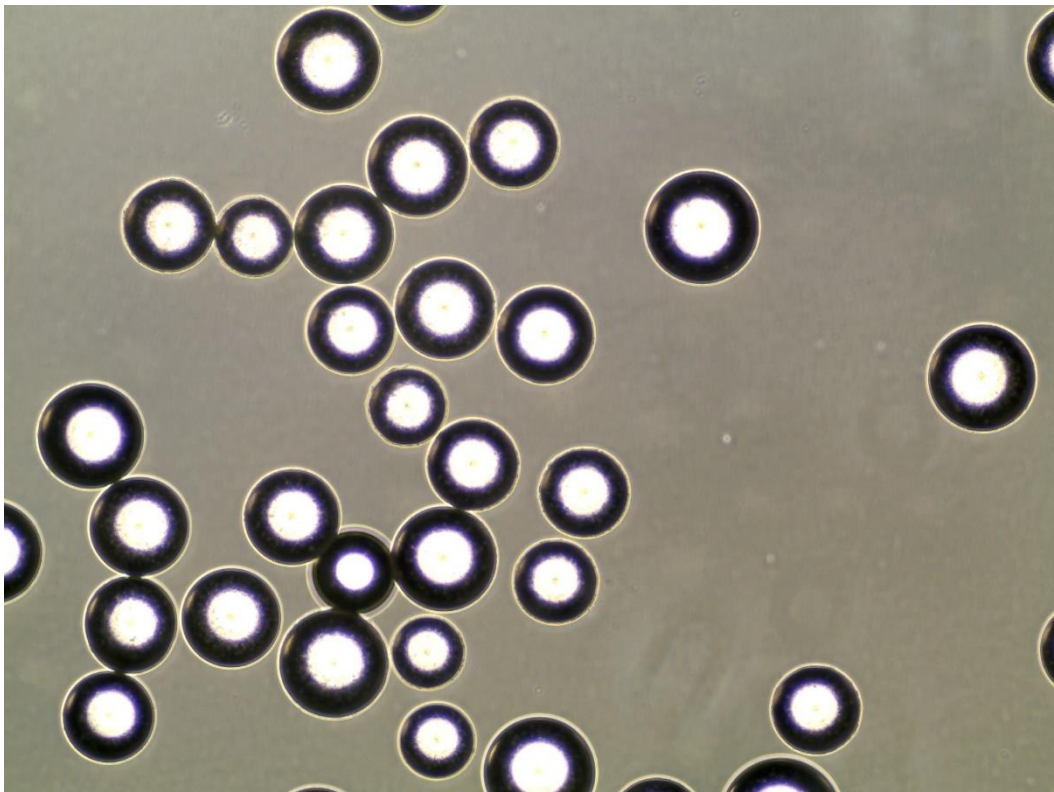
Figure 7.27. Phase contrast image of microcarriers post-harvest from the SFM process. Demonstrating that the BM-hMSCs have been successfully removed from the microcarriers during the harvesting process.

It is evident from Figure 7.28 that the attachment efficiency of BM-hMSCs to the microcarriers is improved for both donors in the SFM expansion process, with > 75 % attachment efficiency after one day. In contrast, the controlled FBS-based process had an attachment efficiency of <

70 % for both donors after one day, with a reduced attachment in the subsequent four days of expansion. Given the implications of poor cell-microcarrier attachment described above, particularly as the process increases in scale, this higher level of attachment represents a key advantage of the SFM process compared to the FBS-based microcarrier process.
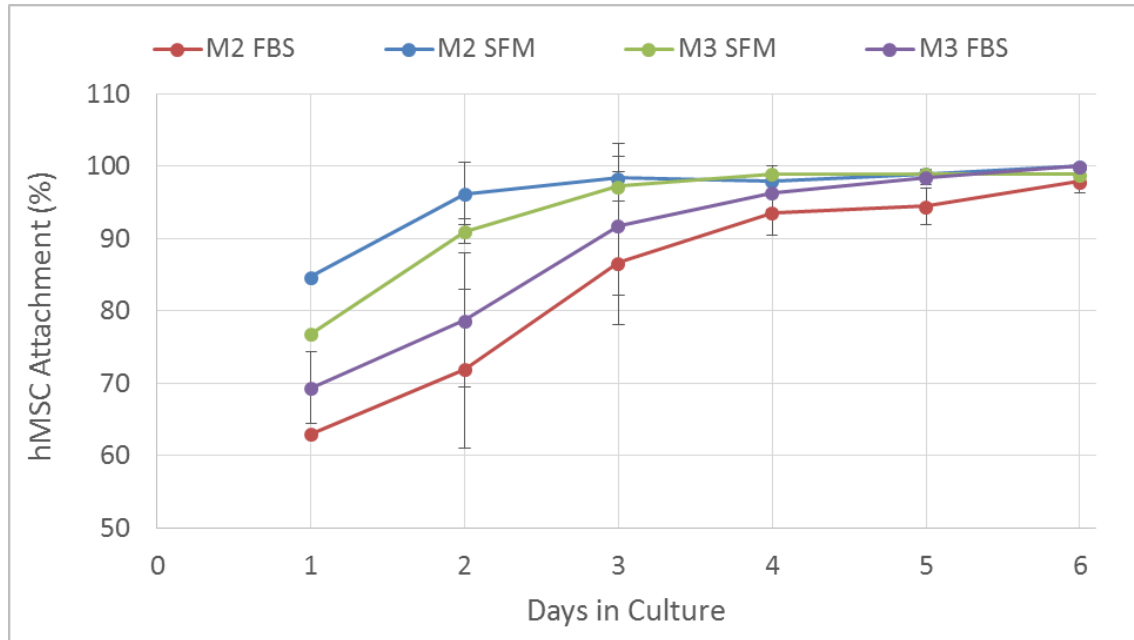
Figure 7.28. Attachment efficiency of two BM-hMSC donors on microcarriers in the DASbox bioreactor system in FBS and SFM expansion. Showing the increased attachment rate of BM-hMSCs in SFM. Data shows mean ± SD, n = 3

7.5.3 Human MSC metabolite flux on microcarriers

Metabolite analysis of the controlled microcarrier culture of BM-hMSCs showed differences in the metabolic pathway usage relating to lactate and ammonia production between FBS-containing and serum-free cultures. Figure 7.29 shows the relative consumption of glucose, production of lactate and ammonia, as well as the yield of lactate from glucose in FBS and SFM for two donor BM-hMSC lines. In FBS-based expansion the consumption of glucose was 9.86 ± 1.49 pmol.cell^{-1}.day^{-1} for M2 and 8.37 ± 1.94 pmol.cell^{-1}.day^{-1} for M3, whereas for SFM expansion the consumption of glucose was significantly lower (p < 0.05) for both BM-hMSC donors with 4.41 ± 0.14 pmol.cell^{-1}.day^{-1} for M2 and 3.54 ± 1.40 pmol.cell^{-1}.day^{-1} for M3. Similarly, the

production of lactate in the controlled microcarrier process was significantly lower (p <0.05) in the SFM process compared to the FBS-based process for both donor BM-hMSC lines. This result is once again comparable to the levels of glucose and lactate flux measured during monolayer (Heathman *et al.* 2015e) and uncontrolled microcarrier culture (Heathman *et al.* 2015a) using the same donor BM-hMSCs. As with these previous studies, the production of ammonia is more similar between the FBS and SFM conditions indicating that the metabolite utilisation under SFM conditions is more efficient, with a switch from energy production predominantly *via* anaerobic glycolysis in FBS culture to utilisation of the oxidative phosphorylation pathway under SFM.
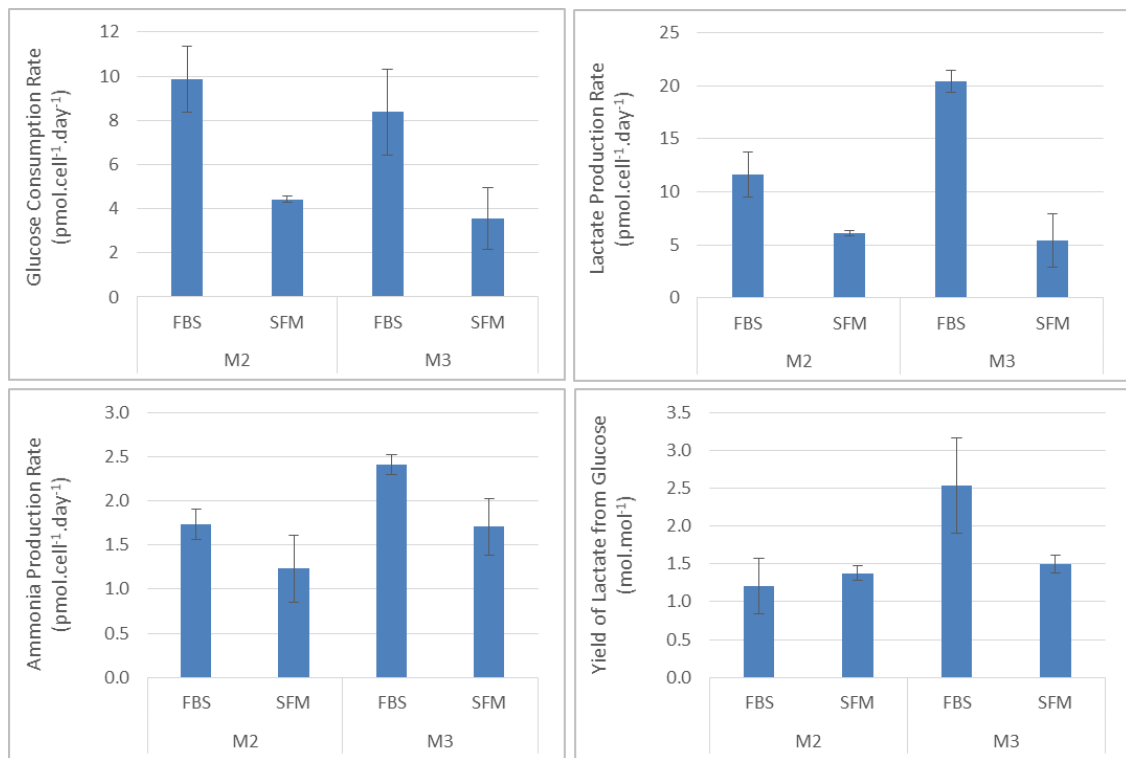
Figure 7.29. Metabolite consumption and production rate of two BM-hMSC donors in FBS and SFM. Showing the increased lactate and ammonia production for sparged culture. Data shows mean ± SD, n = 3

The metabolite utilisation between BM-hMSC donors is also more consistent in controlled SFM microcarrier culture, with a range in the yield of lactate from glucose between M2 and M3 of 0.12 mol.mol^{-1}. In contrast, the yield of lactate from glucose in controlled FBS culture between

donors showed a range of 1.32 mol.mol^{-1}. This increase in consistency of BM-hMSC characteristics between donors in controlled SFM culture offers significant advantages for bioprocess development and has been maintained from monolayer culture of BM-hMSCs, demonstrating comparable process transfer throughout development.
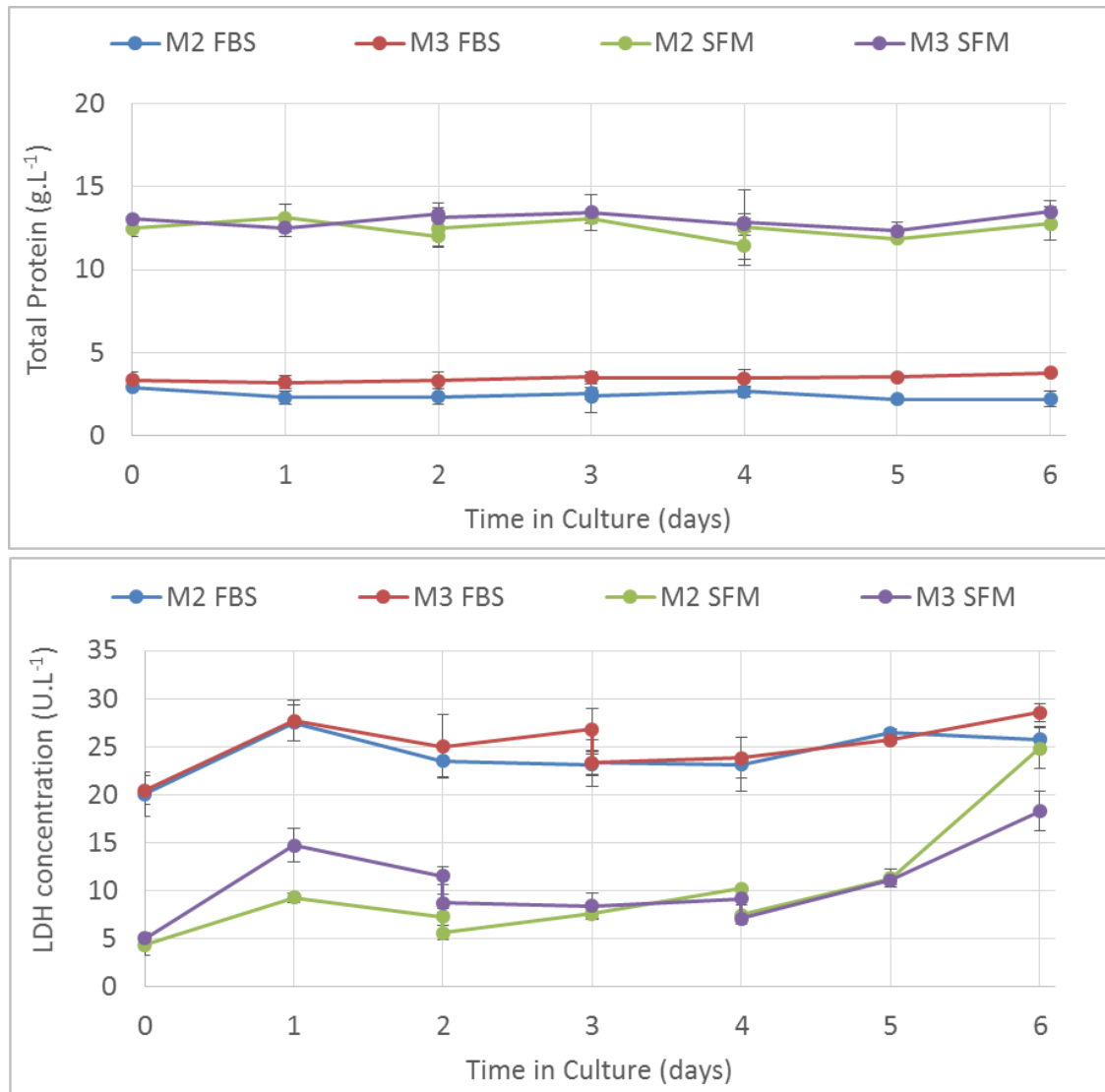
Figure 7.30. Live metabolite concentrations of lactate dehydrogenase (LDH) and total protein for two BM-hMSC donors in FBS and SFM showing an increase in LDH in SFM but no increase in total protein. Data shows mean ± SD, n = 3

The live concentrations of LDH and total protein for controlled FBS and SFM microcarrier culture for two BM-hMSC donors can be seen in Figure 7.30. The FBS-based controlled bioreactor

process demonstrated little increase in LDH or total protein over the six days of culture, suggesting no significant cell damage is occurring during the expansion process. The total protein concentration in controlled SFM expansion also showed no significant increase over the six days of culture, however, the LDH concentration did see a slight increase on day six, when the cell density is at a maximum, up to the baseline level during FBS culture. Considering that this occurs at increased BM-hMSC densities, this should be evaluated as the final cell density of BM-hMSC bioreactor processes increase, to ensure that increasing the yield does not impact the quality of the product.

7.5.4 Post-harvest characterisation of BM-hMSCs

The post-harvest characteristics from the controlled microcarrier expansion process in FBS and SFM have been assessed to ensure that the expansion process is not having a detrimental impact on the BM-hMSC characteristics. The specific outgrowth rate of BM-hMSCs from both the FBS and SFM controlled bioreactor processes can be seen in Figure 7.31 which shows that the post-harvest outgrowth kinetics of BM-hMSC have been maintained.
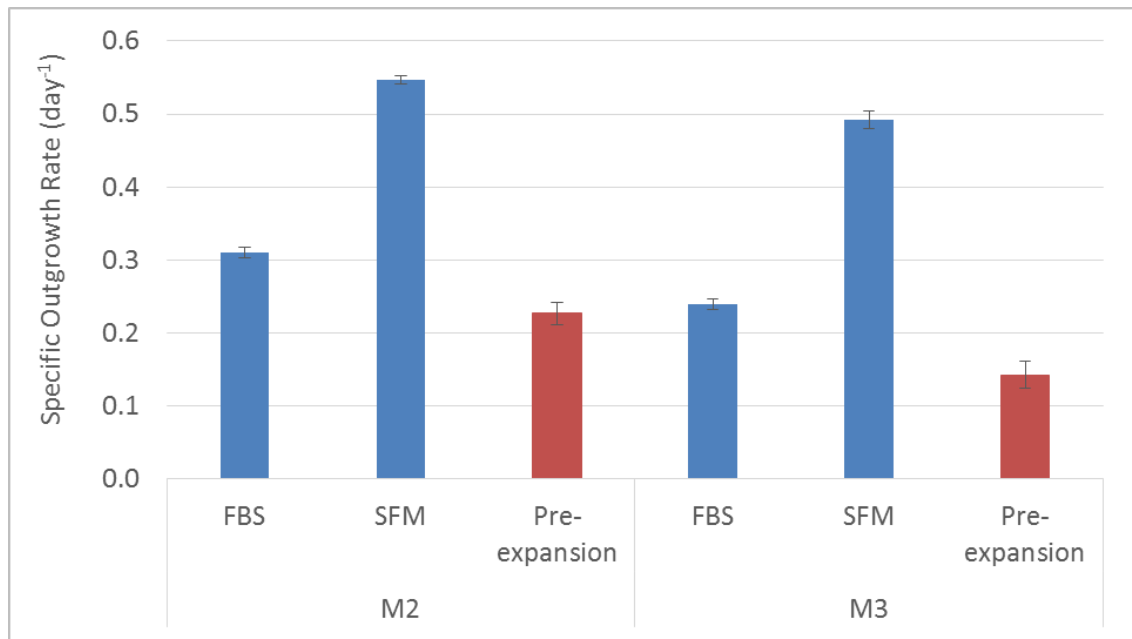
Figure 7.31. Post-harvest outgrowth rate of two BM-hMSC donors in FBS and SFM expansion showing the increased outgrowth kinetics of BM-hMSCs from the controlled bioreactor particularly under SFM. Data shows mean ± SD, n = 3

Figure 7.32 shows the post-harvest BM-hMSC diameter which has been significantly reduced ($p < 0.05$) compared to pre-expansion, which for the FBS process was 2.1 µm for M2 and 2.2 µm for M3. This is in contrast to the uncontrolled spinner flask process presented in Chapter 6 which demonstrated a slight increase in mean cell diameter of M2 (1.2 µM) and M3 (0.4 µm) between post-harvest and pre-expansion.
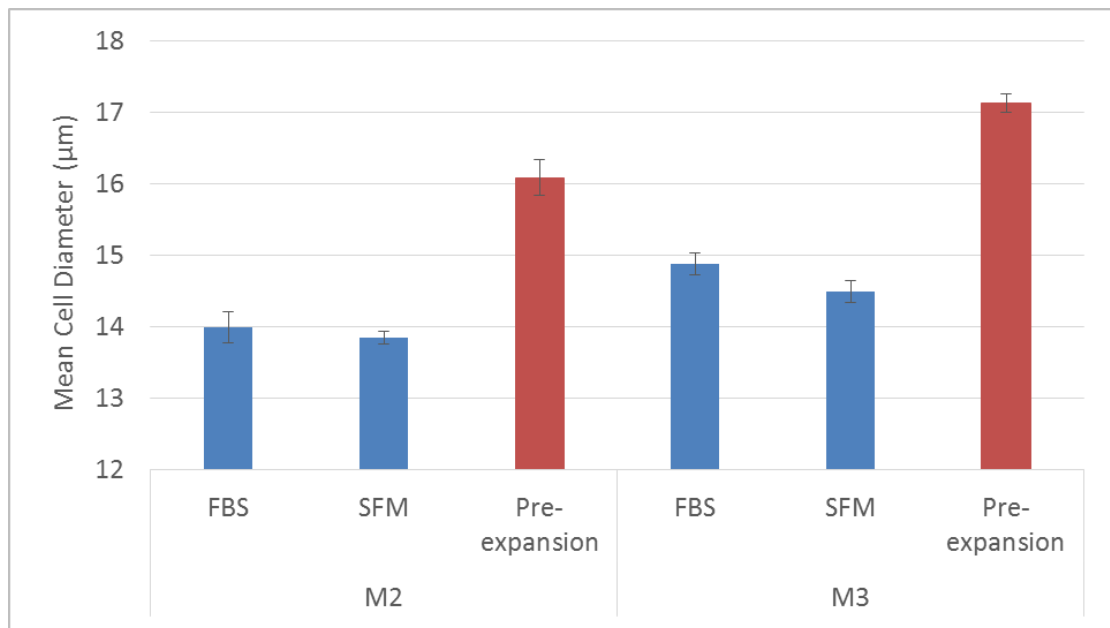
Figure 7.32. Post-harvest mean cell diameter of two BM-hMSC donors in FBS and SFM expansion showing the decrease in mean cell diameter from the controlled bioreactor process. Data shows mean ± SD, n = 3

The benefits to the manufacturing process of producing smaller BM-hMSCs has previously been discussed (Heathman *et al.* 2015e) and smaller cells are commonly associated with increased proliferation, greater colony-forming efficiency and longer telomeres (Samsonraj *et al.* 2015). This highlights a key advantage of the controlled bioreactor process, which is having a beneficial impact on the post-harvest characteristics of the BM-hMSCs, critical for process development and scale up.

The post-harvest colony-forming potential of the BM-hMSCs can be seen in Figure 7.33, which shows that the CFU potential has either increased or been maintained compared to pre-expansion. This is particularly apparent for the controlled FBS-based process, which showed a significant increase ($p < 0.05$) in the post-harvest CFU potential for both BM-hMSC donor lines. This is again an indication of the beneficial impact of the controlled low DO process for the two BM-hMSC donors in terms of CFU potential, as the uncontrolled spinner flask process presented in Chapter 6 did not demonstrate this increase post-harvest CFU potential.
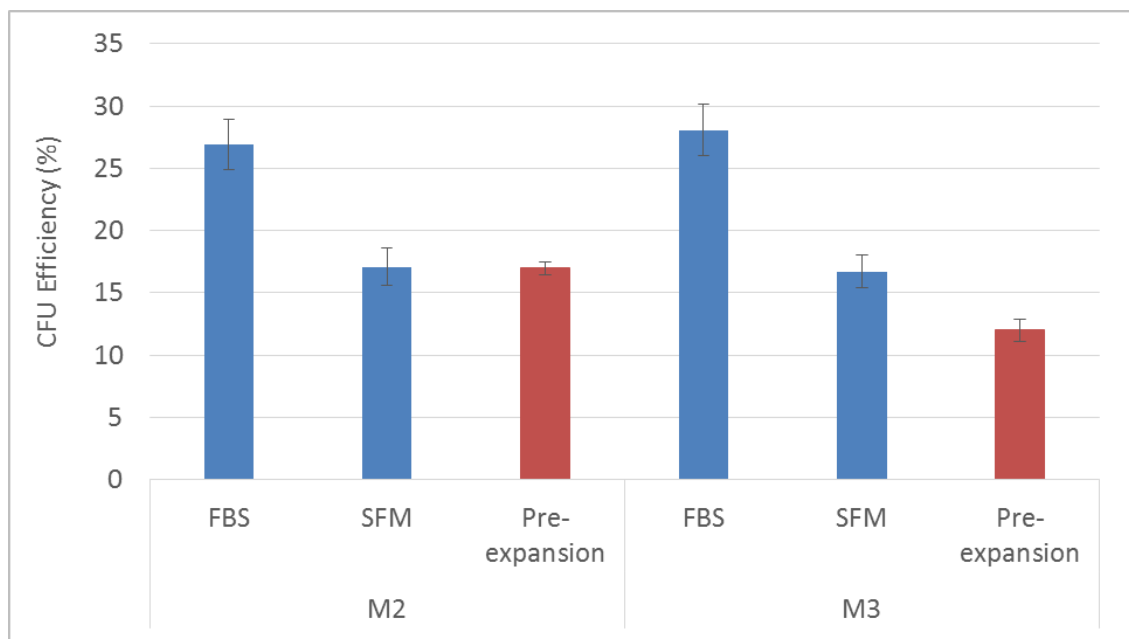
Figure 7.33. Post-harvest colony forming efficiency of two BM-hMSC donors in FBS and SFM expansion showing the increase in colony forming efficiency from the controlled bioreactor process in FBS. Data shows mean ± SD, n = 3

The BM-hMSCs harvested from the microcarrier process must also retain their identity in accordance with the ISCT criteria. Figure 7.34 shows the tri-lineage differentiation potential of the BM-hMSC following microcarrier expansion in SFM down the adipogenic, osteogenic and chondrogenic lineages. This demonstrates that the BM-hMSCs have retained their tri-lineage differentiation potential following controlled microcarrier expansion in SFM.
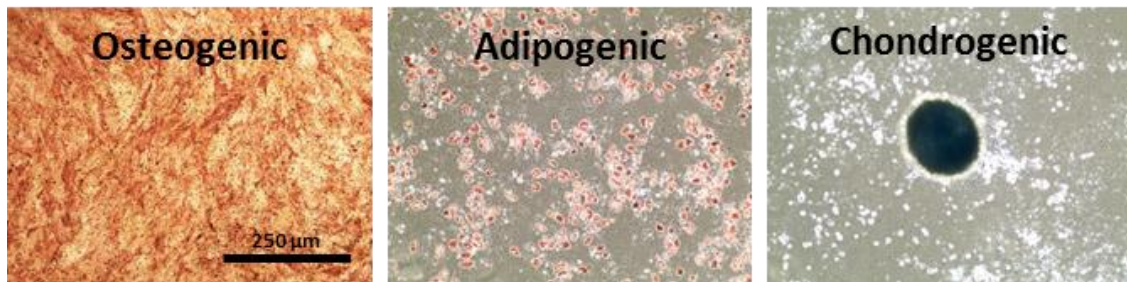
Figure 7.34. Post-harvest tri-lineage differentiation potential of BM-hMSCs using phase contrast microscopy. Showing osteogenic differentiation by staining for alkaline phosphatase and calcium deposition, adipogenic differentiation by staining with Oil Red O and chondrogenic differentiation by staining with Alcian Blue.

In addition to demonstration of tri-lineage differentiation potential, BM-hMSC harvested from the microcarrier process must also retain their immunophenotype. Figure 7.35 shows the multiparameter flow cytometry plots of post-harvest BM-hMSCs demonstrating the maintained positive co-expression of CD105, 90, 44 and 73 throughout the microcarrier expansion process. Further to this, BM-hMSC have retained the negative co-expression of CD45, CD34, CD11b, CD19 and HLA-DR following the controlled microcarrier expansion process in SFM.
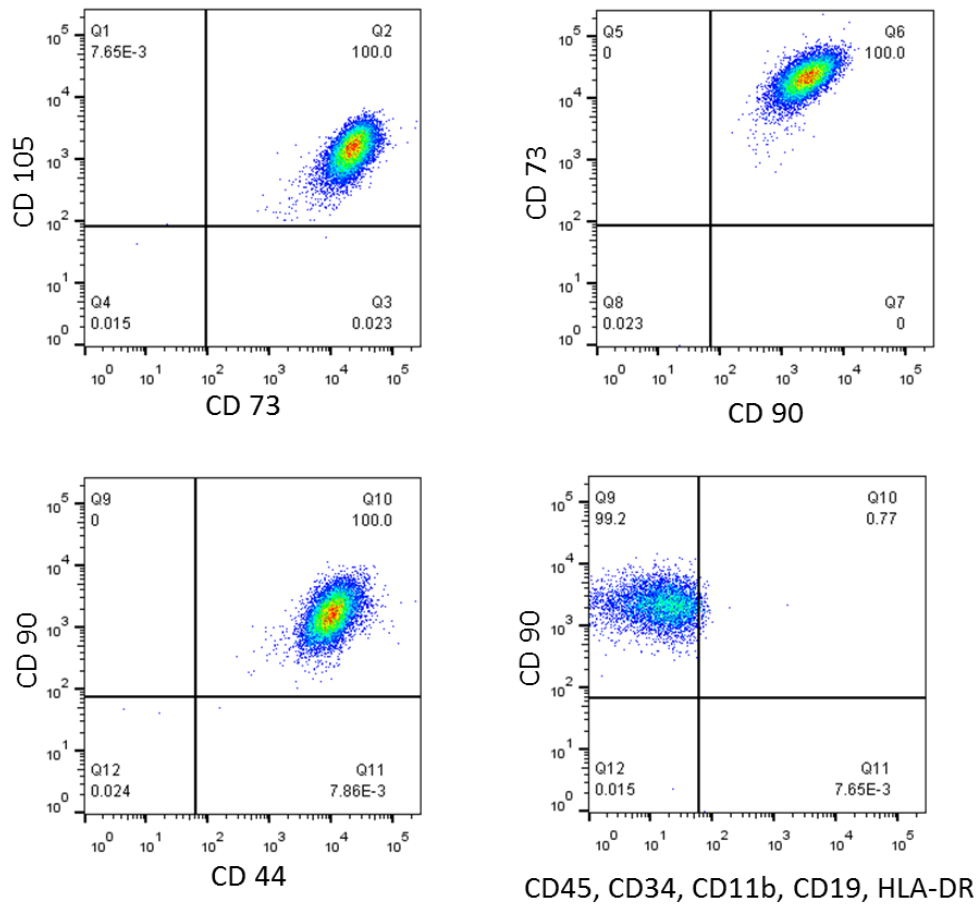
Figure 7.35. Exemplar multiparameter flow cytometry plots showing co-expression of CD90+, CD73+, CD105+, CD44+, CD34-, CD45-, CD11b-, CD19- & HLA-DR- for M2 expanded in SFM

7.5.5 Process control to drive yield and consistency

In order for these BM-hMSC therapies to successfully progress through to commercial production, the process cost of goods should be minimised throughout development. Driving yield and consistency into the BM-hMSC manufacturing process at an early stage of development will be critical in order to reduce the overall cost of goods and increase the cost-effectiveness of the final BM-hMSC product. Increasing the consistency of the final product will reduce process costs by demonstrating a level of control over the product and reducing the risk of batch failure. For large-scale off the shelf processes where the capital invested per batch is high, increasing the consistency of product quality will reduce the risk of product batch failures and significantly reduce the overall production costs. For patient specific therapies where there is a manufacturing batch per patient, increased inter-donor consistency will again reduce the

probability of batch failure, increasing overall costs and would mean that a patient would go without treatment. All of this means that assessing the final BM-hMSC yield and donor consistency for various process iterations, would be highly information on the direction of future process development to reduce overall production costs.

Currently, two of the key cost drivers for the production of cell-based therapies are in the culture medium and the time it takes to manufacture a product batch (Simaria *et al.* 2014). Therefore to make a basic yield comparison of each of the processes developed, the relative process yield in terms of number of BM-hMSCs produced as a function of the volume of culture medium and process time has been calculated for each of the controlled and uncontrolled systems for a theoretical process. In addition to this process yield estimation, a combination of the inter- and intra-donor variation has been assessed to get an understanding of the relative consistency within each process.
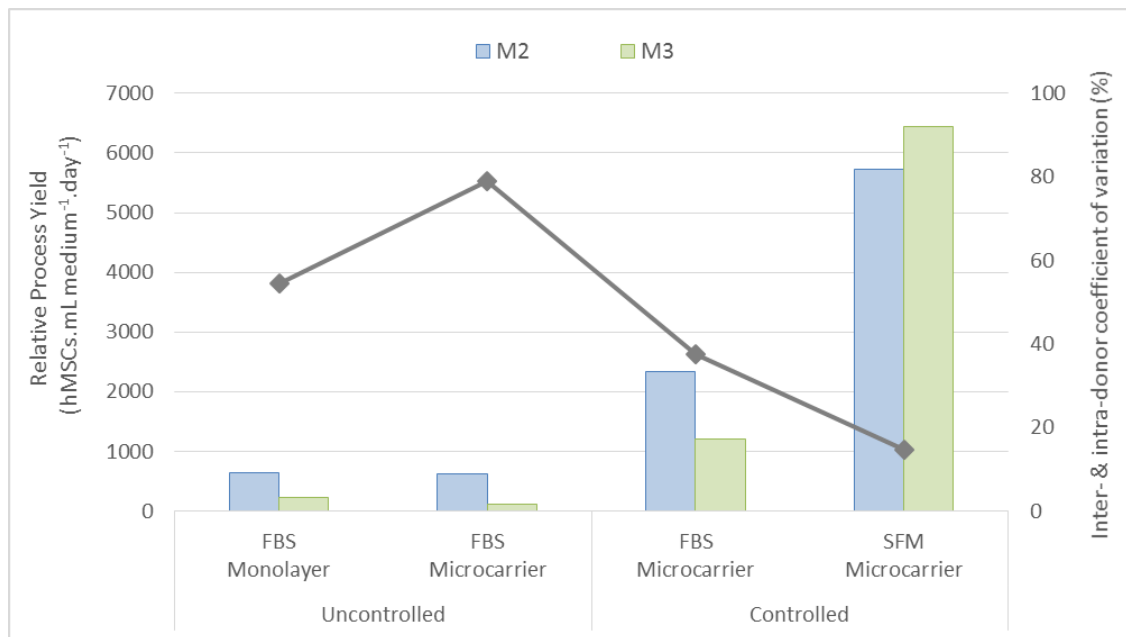
Figure 7.36. Impact of a process control strategy on the process yield from a microcarrier expansion process. Showing that controlled bioreactor processes under serum-free conditions provide much higher yield and consistency between donors. Bars denote process yield in terms of number of cells produced per volume of medium per unit time and the line chart denotes the coefficient of variation between and within donors.

The results of this can be seen in Figure 7.36, which demonstrates the increased process yield that is achieved in controlled SFM microcarrier culture. This improvement represents an increase in process yield of over 300 % for the controlled SFM process compared to the controlled FBS based process. As the process scale increases and the manufacturing costs of the SFM are reduced, this improvement is likely to increase further, due to the issues associated with serum supply at a large-scale (Brindley *et al.* 2012). It can also be seen from Figure 7.36 that the process yield is also increased by an average of around 500% for both donors under controlled conditions compared to uncontrolled expansion, highlighting the importance of systematically developing a process control strategy to increase the yield of BM-hMSC production on microcarriers. It is important to note that the large difference in process yield between monolayer and microcarrier culture at the bench-scale evaluated here, will increase as the scale increases, due to the improved economies of scale achievable in a suspension bioreactor based process.

The percentage coefficient of variation has been calculated for each of the expansion processes in order to assess the relative amount of variation between each condition. This parameter is a combination of inter-donor variation, (the variation between each donor) and intra-donor variation (the variation between batch runs of each donor). This can also be seen in Figure 7.36, which shows the lowest coefficient of variation for the controlled SFM microcarrier process with 14.7 %. A coefficient of variation of 15 % or less is in compliance with the established regulatory requirements (FDA 2011a; Streitz *et al.* 2013), demonstrating control over the product. There is also a clear difference between the controlled and uncontrolled processes in FBS, with process control reducing the coefficient of variation from 79.1 to 37.5 %. This outcome represents a significant reduction in process variation, *via* the introduction of a process control system, once again demonstrating the importance of developing a process control strategy for BM-hMSC production.

7.6 Chapter conclusions

This Chapter has demonstrated that the systematic development of a process control strategy for the microcarrier expansion of BM-hMSCs has significantly increased the yield and consistency achievable in the process. Unnecessarily increasing the impeller agitation speed during the microcarrier expansion of BM-hMSCs decreased the growth kinetics, however, did not have a detrimental impact on the BM-hMSC post-harvest characteristics. Direct aeration of the culture medium *via* a sparger has also been shown to be detrimental to BM-hMSC growth and post-harvest quality characteristics. Sparging of the medium during bioreactor culture is likely to be required at the large-scale to supply oxygen to the cells and remove carbon dioxide and is currently the preferred method of aeration in large scale bioreactors. It will be important during process scale-up, therefore, to ensure that bioreactor parameters such as energy dissipation and sparging rates are not increased above levels which might affect the growth characteristics of the BM-hMSC product.

Studies looking at the effect of exposing low oxygen bioreactor culture to atmospheric conditions during the culture period has highlighted the importance of operating closed and controlled processes to avoid large fluctuation of the dissolved oxygen concentration of the medium. Operating the microcarrier expansion process for BM-hMSCs in closed and controlled manner, has demonstrated improved growth and post-harvest BM-hMSC quality characteristics at 10 and 25 % dissolved oxygen in FBS-based medium. The introduction of serum-free medium into this low dissolved oxygen controlled bioreactor process has further increased the yield across two BM-hMSC donors, however, with reduced harvest efficiency compared to the FBS-based process that has lower cell numbers at harvest. Considering that this was primarily due to cell losses in the cell-microcarrier separation step, it will be imperative to develop specific downstream technology to effectively separate the cells from the microcarriers, even as the number of BM-hMSCs per volume is increased under serum-free conditions.

The development of a process control strategy has significantly increased the yield and consistency between BM-hMSC donors with a coefficient of variance between and within these donors under serum-free conditions of less than 15 %. This is in conjunction with a significant increase in the BM-hMSCs produced per volume of medium per unit time under serum-free conditions, which will be critical in increasing the economies of scale and reducing the cost of BM-hMSC therapies. Furthermore, the introduction of the process control strategy has significantly reduced the BM-hMSC inter- and intra-donor variation in FBS-based culture from

79.1 to 37.5 %, which will be critical for the future development of both patient specific and off-the-shelf BM-hMSC manufacturing processes.

The subsequent downstream and cryopreservation processes following the bioreactor expansion and harvest unit operations will have a profound impact on the scalability of the BM-hMSC manufacturing process. This is because as the scale and BM-hMSC yield increases, the time required to process and formulate the additional product will also increase, which has the potential to negatively impact the functionality of the final product. In order to assess this, the focus of the next Chapter will be to determine the impact of these subsequent unit operations on critical BM-hMSC characteristics through the downstream and cryopreservation processes.

8 Downstream Processing and Cryopreservation of BM-hMSCs

8.1 Chapter introduction

The successful development of a controlled serum-free microcarrier expansion and harvest process for BM-hMSCs in Chapter 7 has provided a consistent and potentially scalable upstream process for BM-hMSC production. Given the importance of maintaining critical product characteristics for cell-based therapies throughout the entire process (Carmen *et al.* 2012a; Heathman *et al.* 2015b), it is vital that the downstream process is also considered during development. This is because the BM-hMSCs, once harvested from the bioreactor, must be further processed and cryopreserved in order to decouple the manufacture from delivery and maximise the potential of this off-the-shelf business model. To achieve this, the downstream and cryopreservation process must be developed in conjunction with the upstream microcarrier process, taking a holistic process approach, considering the entire process from end-to-end (Heathman *et al.* 2015a). This is because any changes to the upstream process will have a direct impact on the downstream and cryopreservation processes and therefore must be developed in parallel, so that it remains cost-effective as the process scale increases (Hassan *et al.* 2015).

Increasing the volumetric yield of BM-hMSC therapies will also be important moving forward as significant economic gains can be made by increasing the cell densities of microcarrier processes (Simaria *et al.* 2014). In conjunction with this, scalability in the downstream and cryopreservation process must be maintained, to ensure that harvested material from the bioreactors can be processed without impacting cell quality, as the timing of process steps increases. Considering process timings that would be realistic as the process scale increases will be important to facilitate systematic process development and highlight potential challenges at an early stage of development. The precise timings of these downstream processes for BM-hMSC therapies are process specific and currently undefined, however, post-harvest washing and concentration is likely to be in the order of hours (Pattasseril *et al.* 2013), with subsequent manifold filling systems capable of formulating thousands of vials or bags within an hour (Rowley *et al.* 2012b). Future process development to reduce these downstream processing times by integrating up- and downstream unit operations and create functionally closed processes will also be critical, increasing the operability and scalability of BM-hMSC manufacturing (Cunha *et al.* 2015).

The preservation of therapeutically active cells as part of the manufacturing process is unique to the cell therapy industry (Rafiq *et al.* 2015a). This process step is necessary to decouple the production from the storage, shipment and delivery of cell product to the clinic. It also allows for time to validate the product and complete quality assurance tests, prior to delivery. Considering that a number of target clinical indications for cell therapy products will be emergency treatments, the long term storage of these products is vital to their success. The cryopreservation of cell therapy products has undergone much development, with an overview of 66 FDA submissions for BM-hMSC products showing that > 80% considered the use of cryopreservation prior to product storage and transportation (Mendicino *et al.* 2014). Despite this progress much work is still required to ensure that the cryopreservation process does not have a detrimental impact on the cell, with some clinical studies demonstrating reduced product efficacy following cryopreservation (Moll *et al.* 2014b).

This cryopreservation process is typically based on a combination of FBS and dimethylsulfoxide (DMSO), which acts as a cryoprotective agent (CPA) to stabilise cellular proteins (Buchanan *et al.* 2004) and the plasma membrane of the cell (Anchordoguy *et al.* 1991). Despite the use of DMSO at the laboratory scale, there are potential issues with its use for clinical delivery and it has been associated with the denaturation of certain proteins (Arakawa *et al.* 1990) as well as neurological toxicity when delivered to patients at high concentrations (Rodrigues *et al.* 2008). The use of FBS in cryopreservation is widespread, however should be minimised due to its limited supply (Brindley *et al.* 2012), potential for pathogen transmission and adverse immune response (Tuschong *et al.* 2002). This means that eliminating the use of FBS and reducing the concentration of DMSO during the BM-hMSC cryopreservation process, will be highly beneficial during process development (Liu *et al.* 2010) and therefore should be considered in conjunction with the downstream process following BM-hMSC expansion on microcarriers.

The aim of this Chapter therefore, is to evaluate a scalable serum-free downstream and cryopreservation process for BM-hMSCs (Figure 8.1), following the previously developed controlled expansion process on microcarriers. This will evaluate the effect of relevant and scalable process times on BM-hMSC quality throughout the downstream process and determine whether the previously observed donor variation has an impact on the future development of BM-hMSC downstream processes. In addition, the impact of increasing process yields towards commercially viable cell densities on the characteristics of BM-hMSCs will be evaluated in order to facilitate future process development.
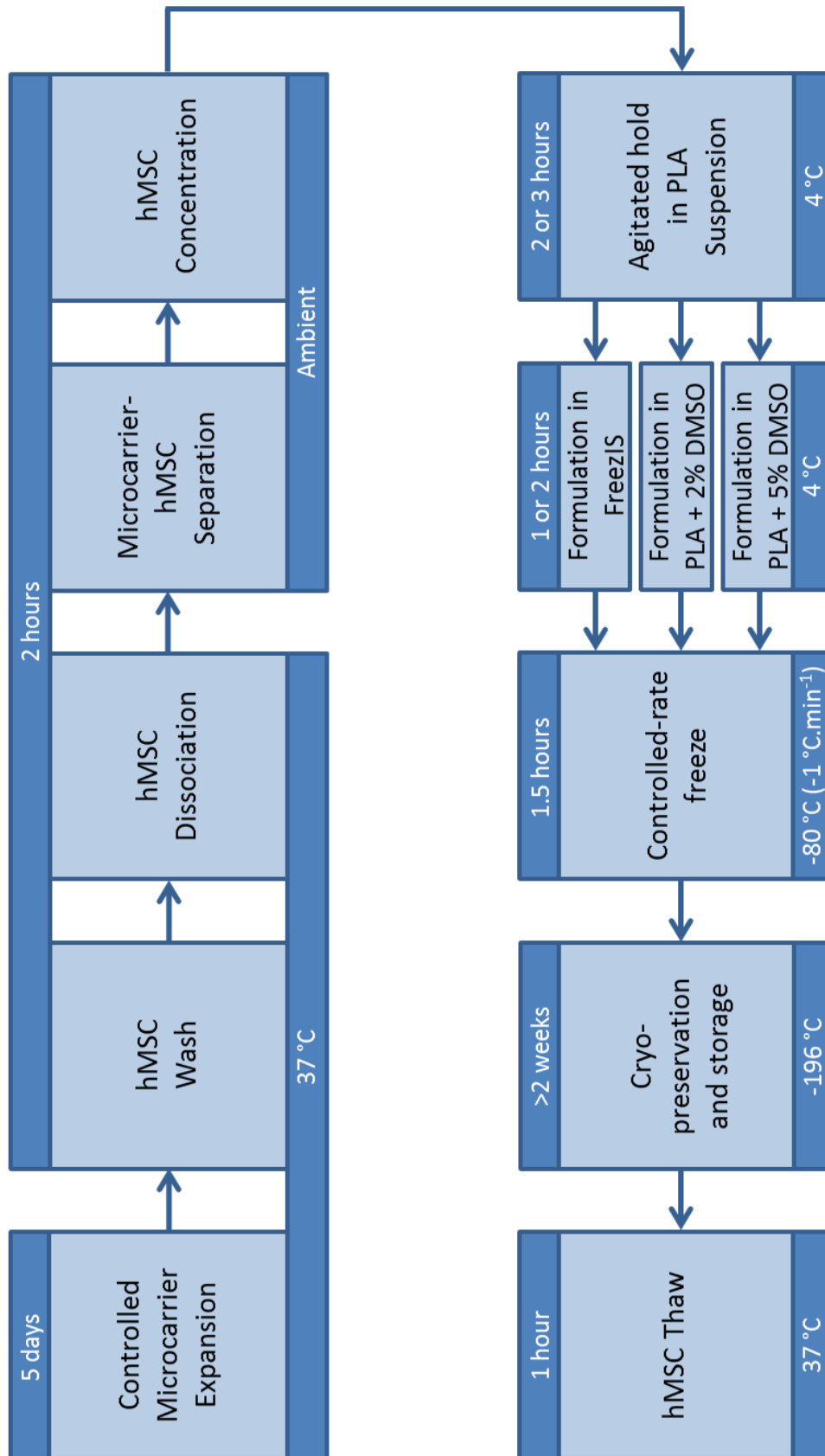
Figure 8.1. Process map for the controlled serum-free expansion, harvest, downstream and cryopreservation of BM-hMSC, including process timings and operating temperatures used here.

8.2 High density culture of BM-hMSCs in a controlled serum-free process

8.2.1 Experimental overview

Following the successful development of a controlled serum-free microcarrier process for the expansion and harvest of BM-hMSCs, the potential to increase the product yield has been investigated. For this, three DASbox culture vessels of 100 mL working volume per condition were cultured for five days (see Section 3.3.5) using BM-hMSC donor M2 with growth area of 500 or 1000 cm^2 and a constant BM-hMSC seeding density of 6000 cells.cm^{-2}. The pH control set-point was 7.4, the impeller speed was controlled to 115 rpm, the temperature was controlled to 37 °C and the dissolved oxygen concentration was controlled to 10 %. Prior to all experiments, the control system on the DASGIP DASbox bioreactor platform was adjusted to ensure it remained stable, the process of which can be seen in Appendix E.

During culture, daily medium samples were taken for analysis of glucose, lactate, ammonia, lactate dehydrogenase and total protein with cell counts performed each day (four samples were analysed per bioreactor as per Section 3.4.3) to determine cell number and attachment efficiency. The culture medium was supplemented with glucose for a surface area of 1000 cm^{-2} up to 20 mmol.L^{-1}, with medium exchange taking place every two days. The purpose of the glucose supplementation was to ensure that the culture did not deplete the available glucose when reaching higher cell densities. At harvest, the BM-hMSC were removed from the microcarriers and separated according to Section 3.3.6. The BM-hMSCs harvested from each condition were then assessed for mean cell diameter (Section 3.4.2), tri-lineage differentiation potential (Section 3.4.4) and immunophenotype (Section 3.4.5). In addition to these identity measurements, BM-hMSC quality characteristics of colony forming efficiency (Section 3.4.9) and outgrowth potential were also assessed post-harvest.

8.2.2 Growth kinetics of BM-hMSCs at increased yield

As mentioned previously, it will be important to increase the volumetric yield of BM-hMSC manufacturing processes, to reduce the number of batch runs required to meet the commercial demand of the product. This will likely reduce the cost of production and drive the development of cost-effective and reimbursable BM-hMSC therapies (Simaria *et al.* 2014). The final BM-hMSC yield can be seen in Figure 8.2 for the two processes following five days of culture, which show a final BM-hMSC density of $0.71 \pm 0.07 \cdot 10^6$ cells.mL^{-1} and $1.04 \pm 0.07 \cdot 10^6$ cells.mL^{-1} for the low yield and high yield processes, respectively. This represents a significant increase (p < 0.05) of

almost 50 % in the volumetric yield obtained after five days. Despite this however, the growth rate in the low yield process was higher, at 0.61 ± 0.16 day^{-1} compared with 0.55 ± 0.02 day^{-1} in the high yield process. This is mainly due to the increased BM-hMSC seeding density in the high yield process, with the increasing number of microcarriers and cells per volume, reducing the overall growth kinetics of the BM-hMSCs.
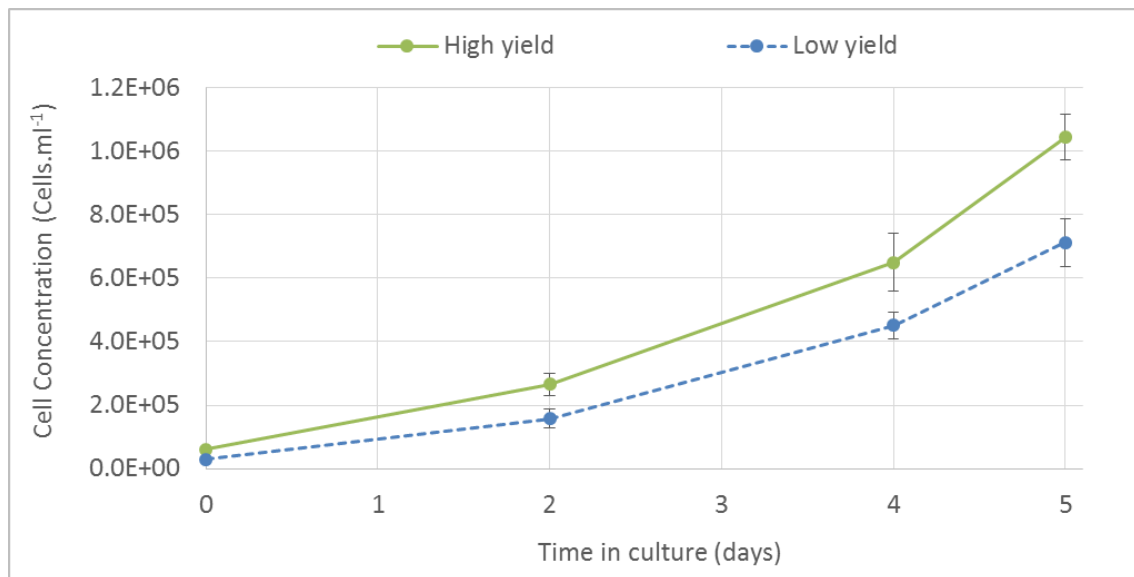
Figure 8.2. Growth kinetics of BM-hMSCs in a controlled bioreactor process showing the increased cell density that can be achieved in SFM. Bioreactor control conditions: pH = 7.4, DO = 10% and impeller speed = 115 rpm. Data shows mean ± SD, n = 3

It is clear that for the suspension culture of adherent cell-based therapies, the initial attachment of the BM-hMSCs to the microcarriers will be critical for successful expansion. Figure 8.3 shows the attachment efficiency of the BM-hMSCs in the high and low yield processes, with greater than 80 % BM-hMSC attachment after the first day of culture. The subsequent attachment rate of the BM-hMSC in both processes reaches almost 100 % attachment after the second day of culture, prior to the first medium exchange. It is important for the BM-hMSCs to be attached to the microcarriers before the medium exchange takes place, so that they are not removed in this process.
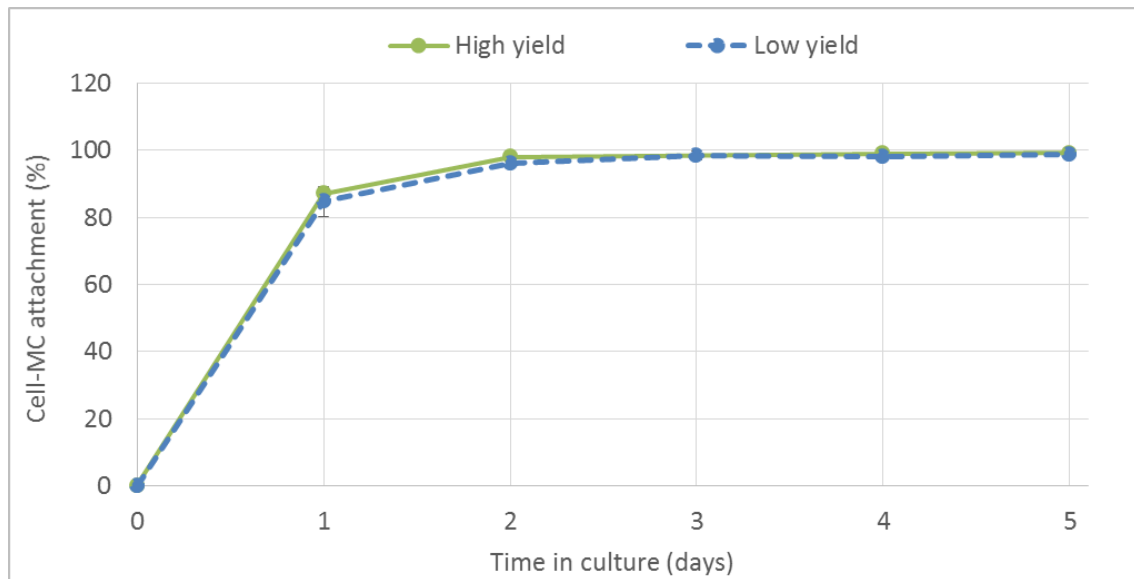
Figure 8.3. Cell attachment to microcarriers in a controlled bioreactor process showing the high BM-hMSC attachment rate in both serum-free conditions. Bioreactor control conditions: pH = 7.4, DO = 10% and impeller speed = 115 rpm. Data shows mean ± SD, n = 3

Following the five days of culture, the BM-hMSCs were harvested from the reactors by detachment from the microcarriers and separation of the cell from the microcarriers following the previously described protocol (Nienow *et al.* 2014; Nienow *et al.* 2015b). The harvest efficiencies were calculated following this process to be 72.9 ± 7.5 % and 76.5 ± 2.9 % for the high yield and low yield processes, respectively. As with in Chapter 7, the BM-hMSCs were successfully detached from the microcarriers using the developed protocol, however cell losses were experienced during the microcarrier-cell separation and concentration phase. This unit operation requires further development to not only integrate it as a closed process (Cunha *et al.* 2015), but to also ensure that it is able to support an expansion process that is yielding significantly higher cell numbers under serum-free conditions.

8.2.3 Metabolite flux of BM-hMSCs at increased yield

As the density of BM-hMSC suspension culture is increased, the availability of nutrients and removal of waste products will become increasingly important, to ensure that the BM-hMSC expansion does not become inhibited (Schop *et al.* 2009b). The concentration of glucose throughout the culture process can be seen in Figure 8.4, which shows that the level remained

above 2 mmol.L^{-1} in both conditions. The initial concentration of glucose in the high yield process was increased from 5 to 20 mmol.L^{-1} to ensure that there was sufficient supply of glucose at increasing cell densities for the fed-bath process. Although this meant that the glucose concentration did not become limiting, it would be more desirable to control the glucose level during culture rather than starting with a high concentration, which is depleted throughout expansion. This is because maintaining stability in process parameters will be important in driving further consistency into the process.
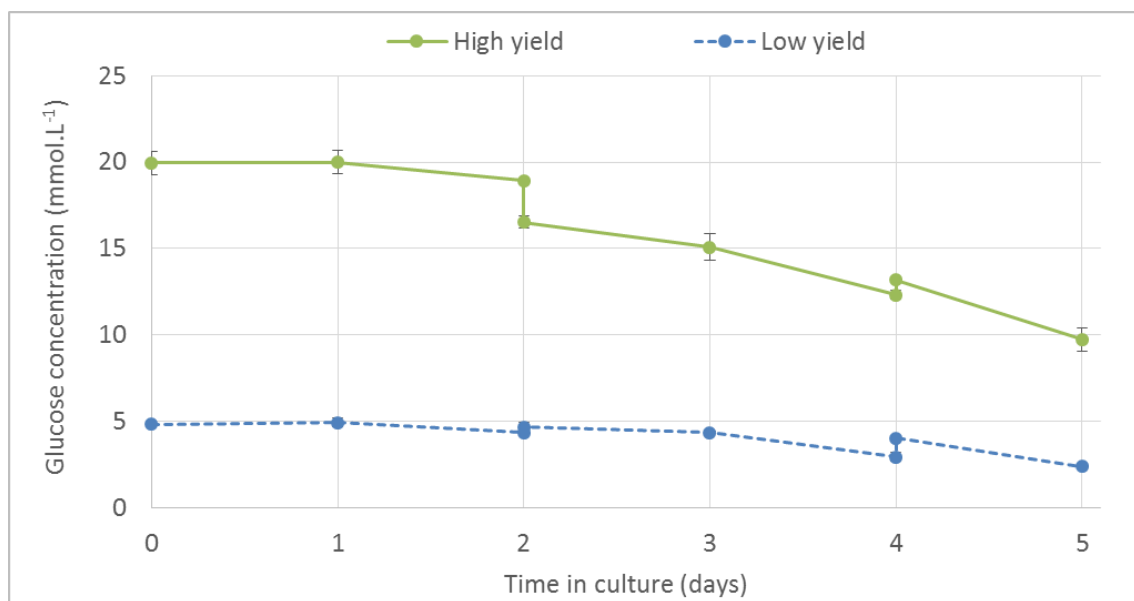
Figure 8.4. Glucose concentration of BM-hMSCs in a controlled bioreactor process at low and high yield showing the higher initial concentration and increased consumption in high yield culture. Data shows mean ± SD, n = 3

The effect or increased glucose concentration has been previously investigated, which demonstrates that a reduction in glucose concentrations leads to decreased apoptosis, an increased rate of BM-hMSC proliferation and increased colony forming potential in monolayer (Stolzing *et al.* 2006) and suspension (Stolzing *et al.* 2012) culture. It has been suggested that the mechanism for this detrimental effect of high glucose may be due to the aggravation of oxidative stress triggered by the presence of high glucose concentrations (> 25 mmol.L^{-1}) (Saki *et al.* 2013). Despite this, it has been shown that high glucose did not affect the secretory profile

of BM-hMSCs, with glucose concentrations of 20 and 30 mmol.L^{-1} not affecting the production of VEGF, HGF, or FGF2 by untreated BM-hMSCs or those treated with TNF-alpha, LPS, or hypoxia (Weil *et al.* 2009). Human MSCs have also demonstrated remarkable resistance against glucose concentrations as high as 40 mmol.L^{-1}, although over time this did create a proapoptotic environment, which has the potential to reduce BM-hMSC functionality after chronic exposure during culture (Li *et al.* 2007). The normal physiological concentration of glucose in the blood is typically between 4 - 6 mmol.L^{-1}, although patients with diabetes can experience an increase to levels as high as 10 mmol.L^{-1} (The Emerging Risk Factors 2010). Considering that BM-hMSCs would not typically experience glucose concentrations of 20 mmol.L^{-1} *in vivo*, a better manufacturing strategy might be to continuously control the glucose levels in the bioreactor to lower concentrations. This would form the following part of the process control strategy development after the DO, impeller speed and pH levels in Chapter 7, as this will be likely to drive further consistency, yield and potentially function into the BM-hMSC product.
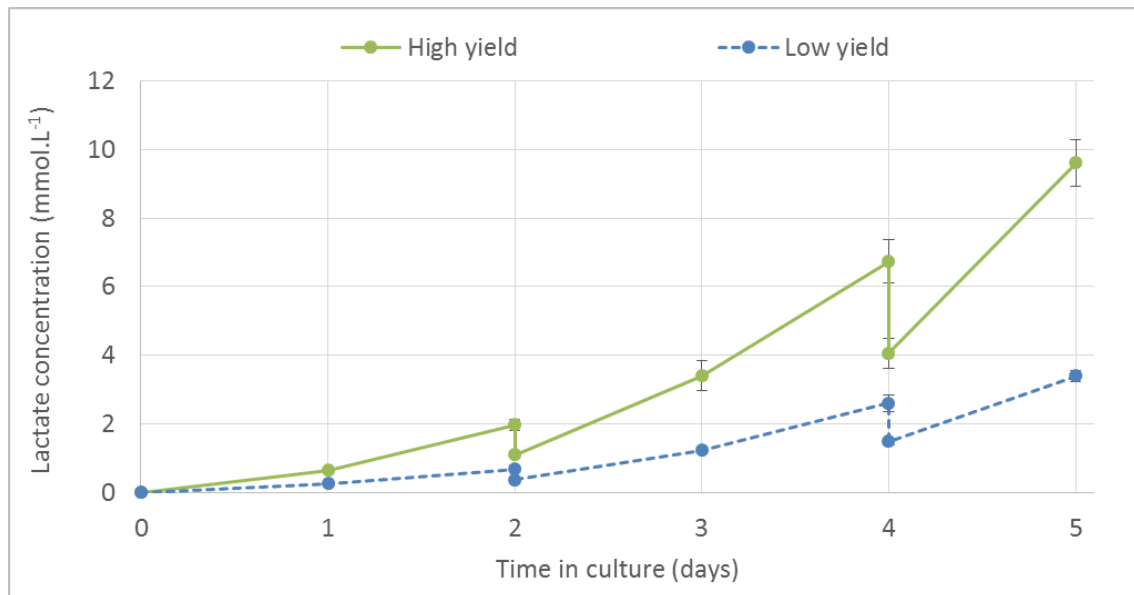
Figure 8.5. Lactate concentration of BM-hMSCs in a controlled bioreactor process at low and high yield showing the increased production in high yield culture. Data shows mean ± SD, n = 3

The concentration of lactate during the five days of culture in the high and low yield processes can be seen in Figure 8.5. As expected, the level of lactate in the high yield culture has increased more rapidly, reaching a final concentration of 9.62 ± 0.68 mmol.L^{-1}. Despite the increase in BM-hMSC density to above $1 \cdot 10^6$ cells.mL^{-1} the level of lactate remained far below previously determined inhibitory levels of lactate at 35.4 mmol.L^{-1} (Schop *et al.* 2009b). Despite the levels of lactate not reaching these inhibitory levels in culture, the concentration of lactate during high yield expansion is still in excess of typical levels *in vivo* (Bakker *et al.* 1991) and therefore the effect of this on BM-hMSC functionality should be determined and the lactate levels controlled accordingly.
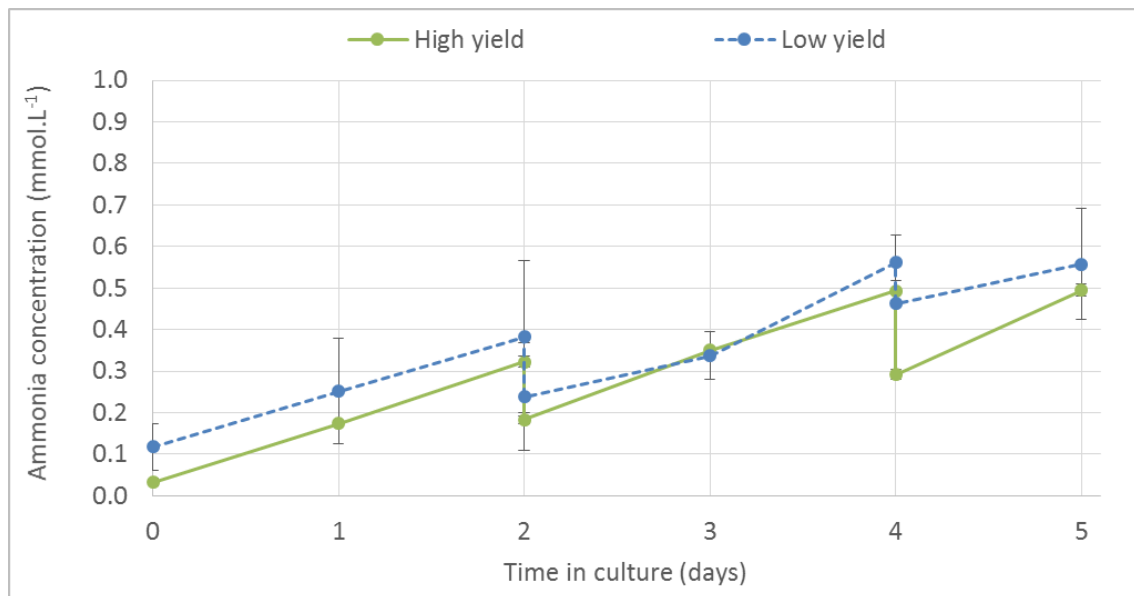
Figure 8.6. Ammonia concentration of BM-hMSCs in a controlled bioreactor process at low and high yield showing a similar production in high and low yield culture. Data shows mean ± SD, n = 3

In contrast to the differences in the consumption of glucose and the production of lactate, the production of ammonia in low and high yield culture was similar over the five days of expansion (Figure 8.6). The maximum ammonia concentration reached during culture was 0.56 ± 0.01 mmol.L^{-1}, which is again far below the previously determined inhibitory level of 2.4 mmol.L^{-1}

(Schop *et al.* 2009b). This again demonstrates that despite increasing the cell density to above $1 \cdot 10^6$ cells.mL^{-1}, the fed-batch strategy employed was sufficient to maintain below-inhibitory levels of process metabolites. In order to control the relative level of desired nutrients and metabolites in the process, however, a perfusion strategy could be employed to constantly monitor and control these concentrations, as has previously demonstrated benefits to BM-hMSC suspension-based expansion processes (Cunha *et al.* 2015).
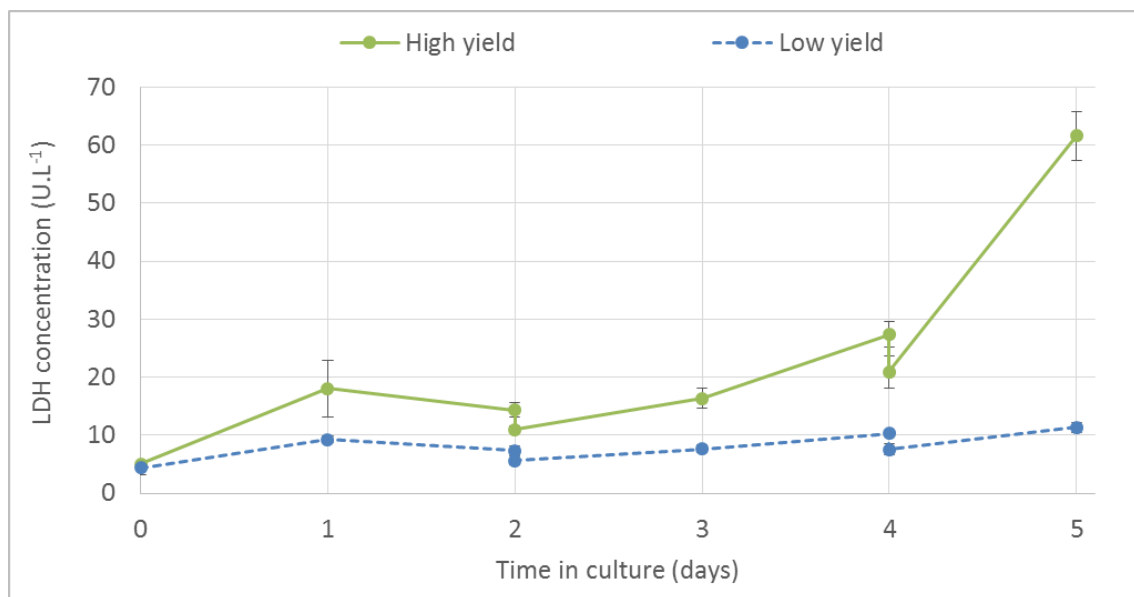
Figure 8.7. Lactate dehydrogenase concentration of BM-hMSCs in a controlled bioreactor process at low and high yield showing the increased production in high yield culture. Data shows mean ± SD, n = 3

In addition to the levels of glucose, lactate and ammonia, the concentration of LDH and total protein have been monitored throughout culture. Figure 8.7 shows the concentration of LDH over the five days of culture which demonstrates a significant increase ($p < 0.05$) in the high yield expansion process. An increase in supernatant concentrations of LDH has previously been linked to rising cell stress (Lavrentieva *et al.* 2010b), which has previously been shown to occur at high BM-hMSC culture density (Song *et al.* 2009) and higher glucose concentrations in culture (Stolzing *et al.* 2012). The implications of this increase in LDH concentrations on BM-hMSC function are currently unclear, however, as the concentration of total protein or the non-viable

cell number during this period did not increase (Figure 8.8) it is unlikely that this increase in LDH is associated with cell death.
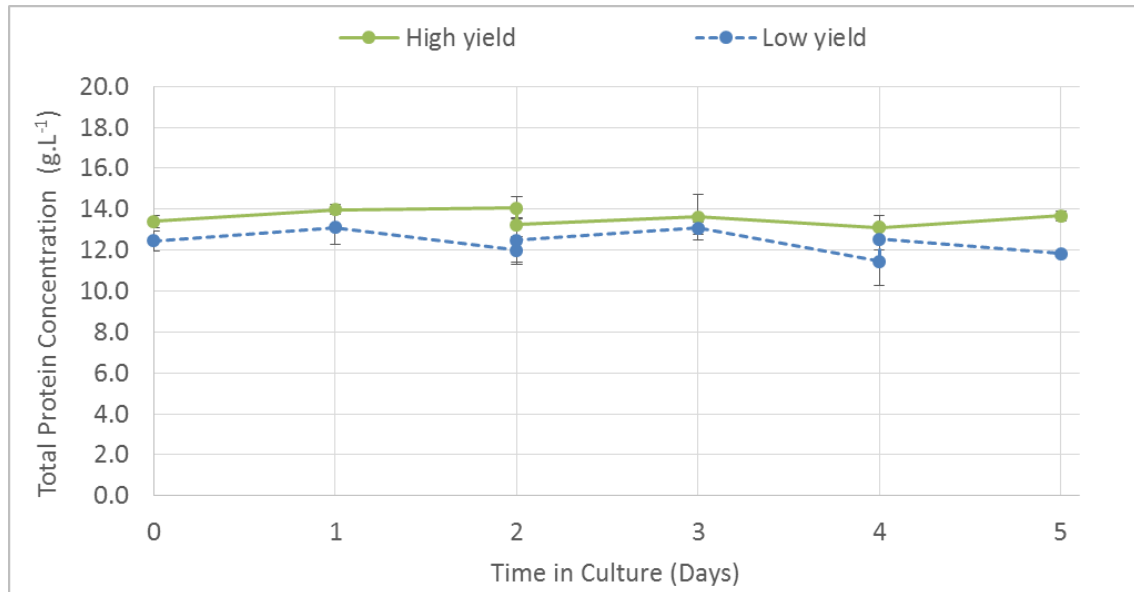
Figure 8.8. Total protein concentration in the supernatant of a controlled BM-hMSC bioreactor process at low and high yield showing no increase in the total protein concentration throughout culture. Data shows mean ± SD, n = 3

The per cell flux of the various metabolites can be seen in Figure 8.9, which shows clear differences in the metabolic pathways utilised under the different conditions. The high yield expansion process demonstrated significant increase in the consumption of glucose and production of lactate ($p < 0.05$) combined with a significant reduction in the production of ammonia ($p < 0.05$). This indicates a shift in the metabolic pathway utilisation between high and low yield cultures, with energy utilisation in the low glucose/low yield process predominantly by oxidative phosphorylation, whereas the high yield/high glucose process has made a relative shift towards energy production *via* anaerobic glycolysis. This effect of increased glucose concentrations on BM-hMSC metabolism has previously been hypothesised (Weil *et al.* 2009) but not demonstrated and the shift towards energy production by anaerobic glycolysis would be largely undesirable as it represents a less efficient mechanism for energy production in BM-

hMSCs. It is important to note also that the consumption rate of glucose and the production rate of lactate in controlled high yield culture is still less than BM-hMSC cultured in a controlled FBS based process, developed in Chapter 7.
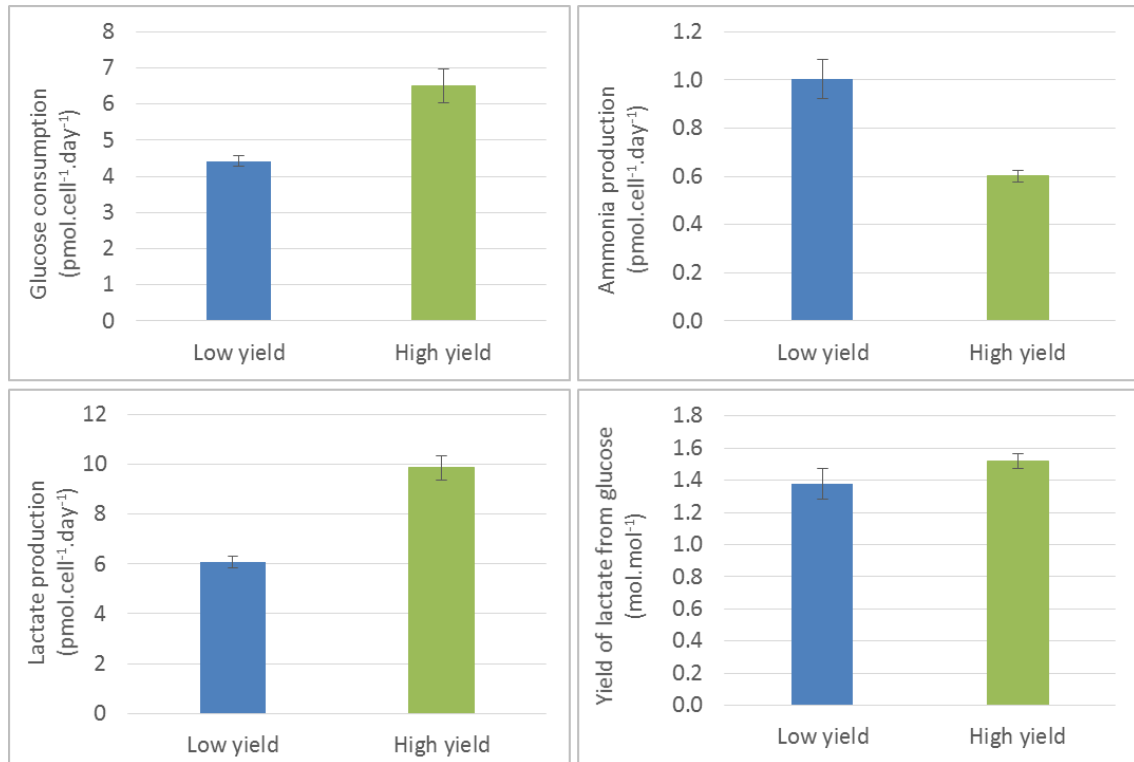
Figure 8.9. Per cell metabolite concentrations of glucose, lactate, ammonia and yield of lactate from glucose for high and low yield culture. Showing the increased consumption of glucose and production of lactate in high yield culture. Data shows mean ± SD, n = 3

8.2.4 Post-harvest characterisation of BM-hMSCs at increased yield

The post-harvest characteristics from the high and low yield expansion processes in SFM have been assessed to ensure that the expansion process is not having a detrimental impact on the BM-hMSC characteristics. The specific outgrowth rate of BM-hMSCs from both the high and low yield controlled bioreactor processes can be seen in Figure 8.10 which shows that the post-harvest outgrowth kinetics of BM-hMSC have been maintained compared to pre-expansion and post-spinner flasks. The post-harvest colony-forming potential of the BM-hMSCs can also be seen in Figure 8.11, which shows that the CFU potential has either increased or been maintained

compared to pre-expansion. This is particularly apparent for the high yield process, which showed a significant increase ($p < 0.05$) in the post-harvest CFU potential.
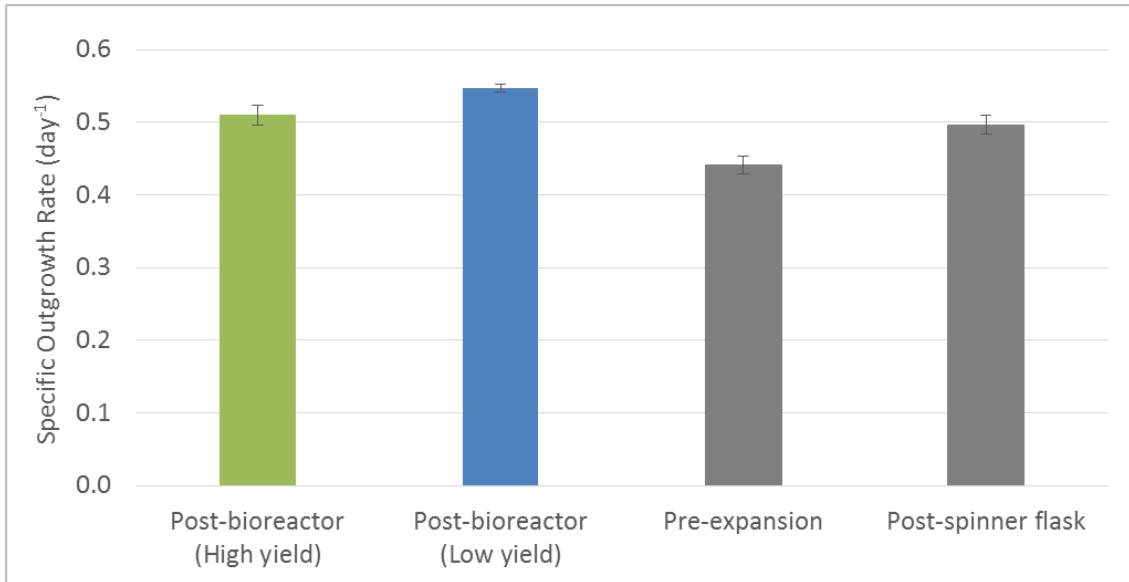
Figure 8.10. Post-harvest BM-hMSC specific outgrowth rate from high and low yield controlled bioreactor processes showing the increased post-harvest growth kinetics compared to pre-expansion ($p < 0.05$). Data shows mean ± SD, n = 3
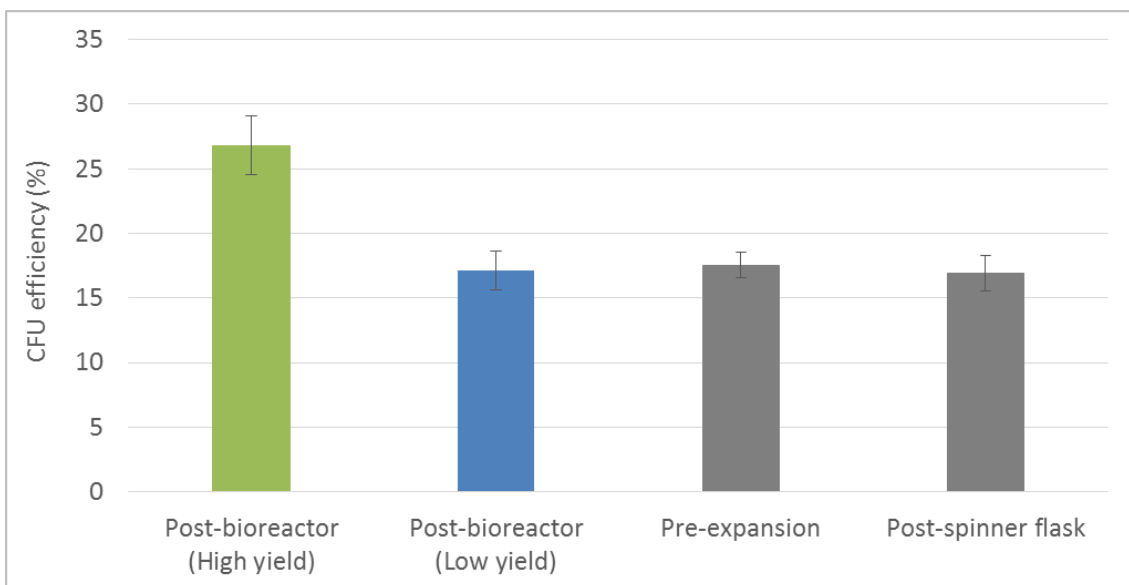
Figure 8.11. Post-harvest BM-hMSC colony forming efficiency from high and low yield controlled bioreactor processes showing the increased post-harvest colony forming efficiency in high yield culture compared to low yield ($p < 0.05$). Data shows mean ± SD, n = 3

The BM-hMSCs harvested from the microcarrier process must also retain their identity in accordance with the ISCT criteria (Dominici *et al.* 2006). Figure 8.12 shows the multiparameter flow cytometry plots of post-harvest BM-hMSCs demonstrating the maintained positive co-expression of CD105, 90, 44 and 73 throughout the microcarrier expansion process (Chan *et al.* 2014a). Further to this, BM-hMSC have retained the negative co-expression of CD45, CD34, CD11b, CD19 and HLA-DR following the high yield controlled microcarrier expansion process in SFM.
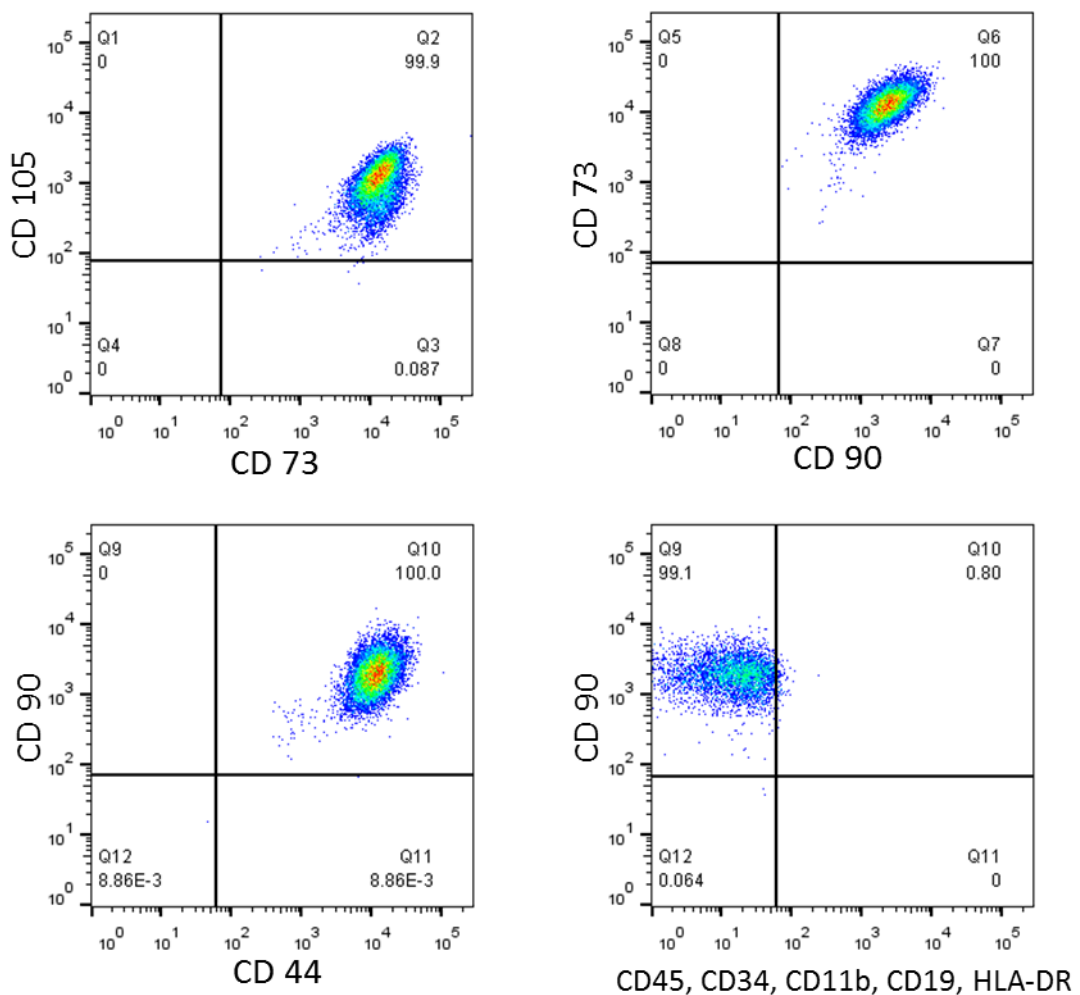
Figure 8.12. Multiparameter flow cytometry plots showing co-expression of CD90+, CD73+, CD105+, CD44+, CD34-, CD45-, CD11b-, CD19- & HLA-DR- for M2 expanded and harvested from a high yield SFM microcarrier process. Representative plots from n = 3

In addition to demonstration of immunophenotype expression, BM-hMSC harvested from the microcarrier process must also retain their tri-lineage differentiation potential. **Figure 8.13** shows the tri-lineage differentiation potential of the BM-hMSC following high yield microcarrier expansion in SFM down the adipogenic, osteogenic and chondrogenic lineages. This demonstrates that the BM-hMSCs have retained their tri-lineage differentiation potential following high yield controlled microcarrier expansion in SFM.
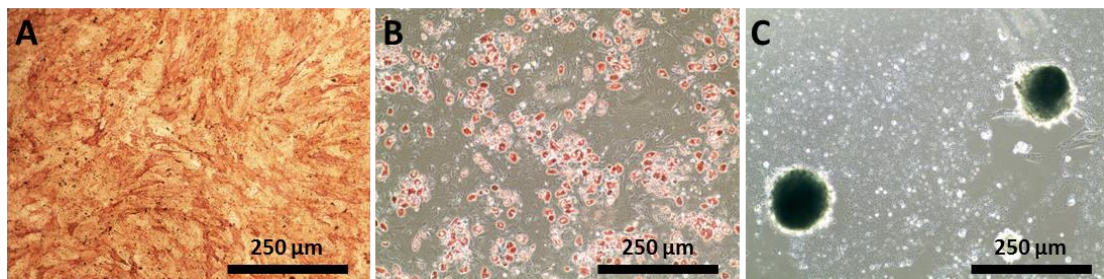
Figure 8.13. Post-harvest tri-lineage differentiation potential of BM-hMSCs from a high yield SFM microcarrier process using phase contrast microscopy. Showing (A) osteogenic differentiation by staining for alkaline phosphatase and calcium deposition, (B) adipogenic differentiation by staining with Oil Red O and (C) chondrogenic differentiation by staining with Alcian Blue. Representative plots from n = 3

8.3 Serum-free downstream process for BM-hMSCs

8.3.1 Experimental overview

Following the successful development of a controlled serum-free microcarrier process for the high yield expansion and harvest of BM-hMSCs, the effect of a serum-free downstream process on two BM-hMSC donors can be evaluated. For this, three DASbox culture vessels of 100 mL working volume per condition were cultured for five days (see Section 3.3.5) using BM-hMSC donor M2 and M3. The pH control set-point was 7.4, the impeller speed was controlled to 115 rpm, the temperature was controlled to 37 °C and the dissolved oxygen concentration was controlled to 10 %. Following the harvest of BM-hMSCs from each DASbox reactor system, the BM-hMSCs were subjected to either a long (7 h) or short (5 h) downstream process in accordance with Figure 8.1. Firstly, the post-harvest BM-hMSCs were held in an agitated suspension of PlasmaLyte-A (PLA) for two or three hours to simulate a potential holding time that is likely to occur as the process is scaled. Following this, the BM-hMSCs were formulated into three formulations (n = 6 for each). The BM-hMSCs were held in their respective cryopreservation solutions for one or two hours before undergoing analysis, these were:

1. PlasmaLyte-A supplemented with 10% (v/v) DMSO
2. PlasmaLyte-A supplemented with 5% (v/v) DMSO
3. PlasmaLyte-A supplemented with 2% (v/v) DMSO
4. Irvine Scientific PRIME-XV® MSC FreezIS DMSO-Free

During this downstream process, the BM-hMSC were analysed immediately post-harvest (2 h total), following the agitated holding step in PLA (4 or 5 h total) and following formulation in each cryopreservation solution (5 or 7 h total). The BM-hMSCs were analysed for membrane integrity, cell aggregation, mean cell diameter (Section 3.4.2), colony forming efficiency (Section 3.4.9) and outgrowth potential were also assessed throughout the downstream process.

8.3.2 Short-term downstream holding process for BM-hMSCs

For the successful development of integrated manufacturing processes for BM-hMSCs, sequential unit operations from expansion to cryopreservation must be evaluated in order to determine the accumulated detrimental effect that this process might be having on the BM-hMSC product. Taking BM-hMSCs from a potentially scalable expansion and harvest process is critical for this, as the upstream process must be representative of the expansion technology

that will be used at the large-scale. In this sense, process development for BM-hMSC manufacture must be carried out using a scaled-down end-to-end process, rather than developing each process step independently and assuming they will successfully integrate together.   Previous experiments have demonstrated maintained BM-hMSC viability after prolonged holding for up to four (Heathman *et al.* 2015a) and eight hours (Pal *et al.* 2008), however breaking down the process to assess the impact of each individual process step provides increased insight into the effect of the downstream process on BM-hMSCs. In addition to breaking down the process, considering the impact of these unit operation on multiple BM-hMSC identity and quality characteristics will provide deeper insight into the potential limitations on the allowable downstream processing times for large-scale off-the-shelf BM-hMSCs manufacturing processes.
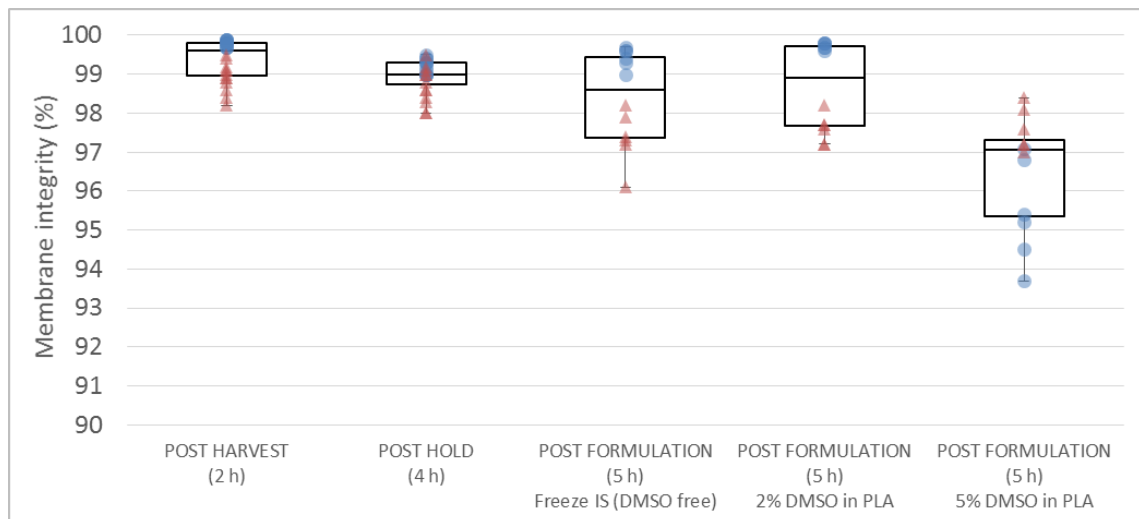
Figure 8.14. Short-term serum-free downstream holding process for BM-hMSCs showing the effect of different holding times on cell membrane integrity (DAPI and acridine orange) with a decrease toward the end of the downstream process. Blue dots represent BM-hMSC line M2, red triangles represent BM-hMSC line M3. Box and whisker plots show n = 12

The downstream process following the controlled serum-free microcarrier expansion and harvest process has been split into a short process (total of five hours) and a long process (total of seven hours). The effect of the short-term downstream process on BM-hMSC viability can be seen in Figure 8.14 across the two BM-hMSC donors, which shows a general decrease in membrane integrity throughout the downstream process. This is from a median post-harvest BM-hMSC membrane integrity of 99.6 % to 97.1 % following a two hour holding and one hour

formulation step in a solution containing 5 % DMSO. Figure 8.14 also demonstrates the variation between the M2 and M3 BM-hMSC donors in terms of membrane integrity throughout the downstream process and also the increase in product divergence, the longer the BM-hMSCs progress through the downstream unit operations. This provides the first indication that the BM-hMSC donor variability experienced in the initial expansion and characterisation processes in Chapter 4 (Heathman *et al.* 2015c) is also having an impact on the downstream process.

8.3.3 Long-term downstream holding process for BM-hMSCs

In addition to the short-term downstream process lasting five hours, a long-term process has also been evaluated lasting a total of seven hours, which has the potential to allow for the handling of commercially relevant BM-hMSC manufacturing batch sizes (Pattasseril *et al.* 2013), with an operating window of five to seven hours. Figure 8.15 shows the result of this extended holding process on BM-hMSC membrane integrity, which is similar to the short-term holding process. This demonstrates that a downstream process window of five to seven hours is satisfactory to maintain a BM-hMSC viability greater than 90 %, which will be critical as the process increases in scale towards commercially relevant batch sizes and also for patient specific therapies, where procedural delays may require extended product holding times.
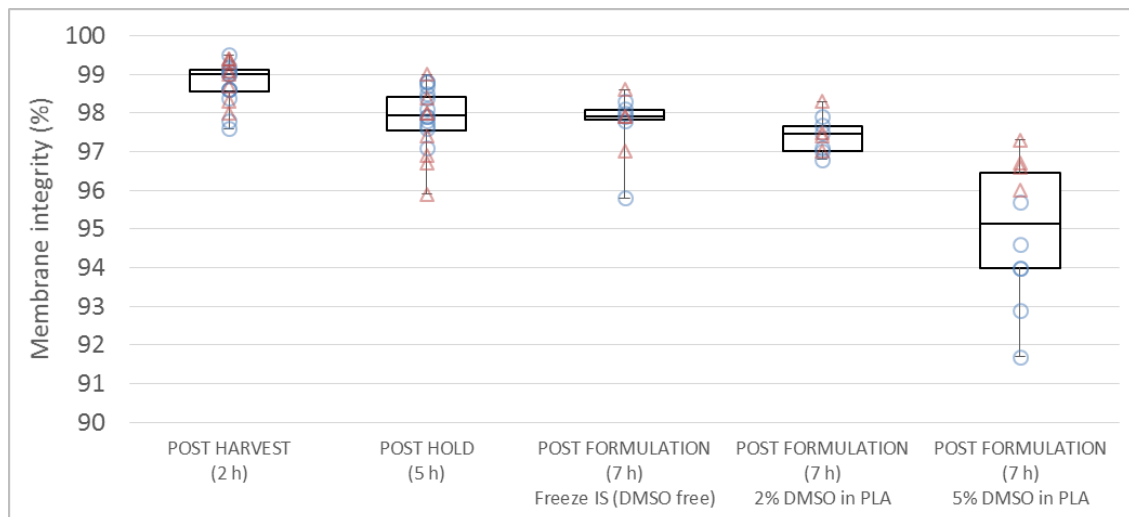
Figure 8.15. Long-term serum-free downstream holding process for BM-hMSCs showing the effect of different holding times on cell membrane integrity with a decrease toward the end of the downstream process. Blue dots represent BM-hMSC line M2, red triangles represent BM-hMSC line M3. Box and whisker plots show n = 12

It is important to note however, that an increase in the concentration of the cryoprotective agent (CPA), in this case DMSO, may contribute to a reduction in BM-hMSC membrane integrity. With many current BM-hMSC cryopreservation processes using up to 10 % DMSO as the CPA in their formulations, it will be important to consider that as these processes are scaled, that prolonged holding times for the product formulation unit operation may not result in the optimum cryopreservation strategy. This is because the cells will experience an irreversible loss in membrane integrity prior to the cryopreservation process, which is not considered when developing a cryopreservation strategy at the bench scale.

8.3.4 Increased concentrations of cryoprotective agents in the downstream process

As mentioned previously, the DMSO concentration in the final product has implications for the downstream process, with holding times for cells in DMSO (and potentially alternative CPAs) dictating allowable process timing and therefore overall scale. Current formulation technology has the ability to fill several thousand vials per hour, however, which should enable lot sizes of least three to five thousand vials per lot (Rowley *et al.* 2012b). This allowable formulation processing time will be dependent on the specific cell-based therapy product, the dose size required and how tolerant the product's quality and functional characteristics are to prolonged exposure to CPAs.

Figure 8.16 shows the effect of holding BM-hMSCs in a formulation containing 10 % DMSO for one and three hours on membrane integrity. This shows a significant drop ($p < 0.05$) in BM-hMSC membrane integrity throughout this holding process to a median of 92.2 % after one hour and 78.4 % after three hours. Considering the time it will take to formulate a large batch of BM-hMSC in the CPA prior to final fill and finish, this will have a dramatic impact on the potential scale to which a cryopreserved product can be manufactured with high concentrations of DMSO. It should be noted also, that the donor variability in post-formulation membrane integrity at a DMSO concentration of 5 % seen previously, has been further compounded with an increase concentration of DMSO.

In the clinic, the therapeutic cells should have a minimum viability of 70% (preferably more than 85%) (Pattasseril *et al.* 2013) prior to delivery into the patient. Therefore in this BM-hMSC downstream process containing high concentrations of DMSO, 33 % of M2 events would fail this criteria after one hour post-formulation and 85 % would fail after three hours post-formulation, before the cryopreservation process has taken place. In contrast, the M3 donor BM-hMSC line

would not experience any failure events based on this criteria after either one or three hours post-formulation. This highlights the potential donor variability that can occur, not only in the expansion process, but also in the downstream process of BM-hMSC manufacture, as the M3 BM-hMSC donor line was initially considered to be far from desirable (Chapter 4).
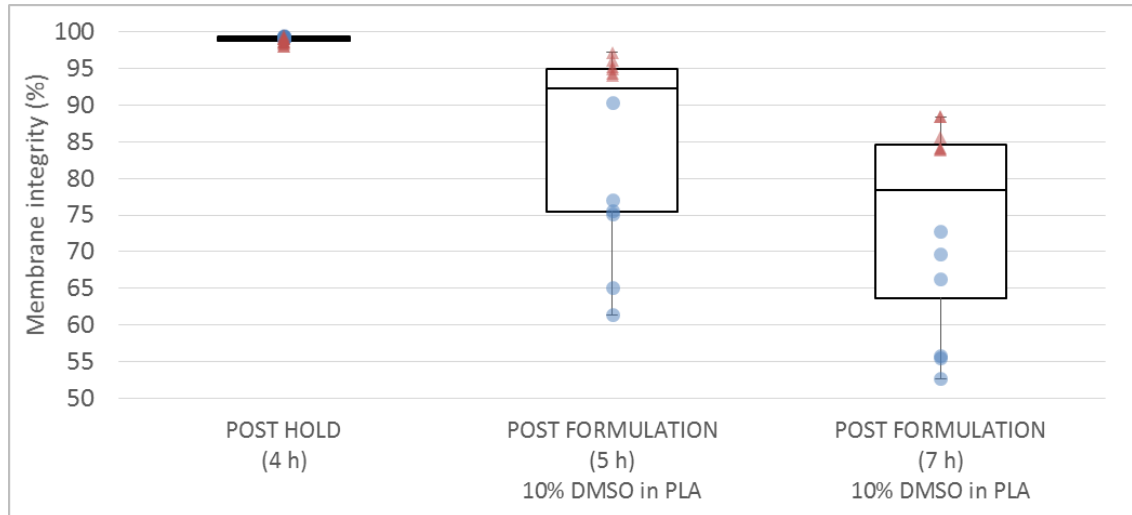
Figure 8.16. The effect of using 10% DMSO in a serum-free downstream process for BM-hMSCs. Showing the dramatic loss in membrane integrity through the downstream process. Blue dots represent BM-hMSC line M2, red triangles represent BM-hMSC line M3. Box and whisker plots for n = 12

Associated with this decrease in membrane integrity of BM-hMSCs post-formulation, is an increase in the cell aggregation, most likely caused by the release of intra-cellular proteins as the BM-hMSC membrane ruptures. This increase in cell aggregation will cause a number of further issues to the process, as aggregation is likely to cause increasing cell death throughout the cryopreservation process, compounding the detriment to the product. This is mainly due to a limitation of nutrients within the aggregates, which will cause increased cell death (Suzuki *et al.* 2012). In addition, an increase in the aggregation level of the product during the downstream process will increase the variation in the vialing process between batches, as the accuracy of current cell counting methods relies upon having an evenly distributed single-cell suspension.
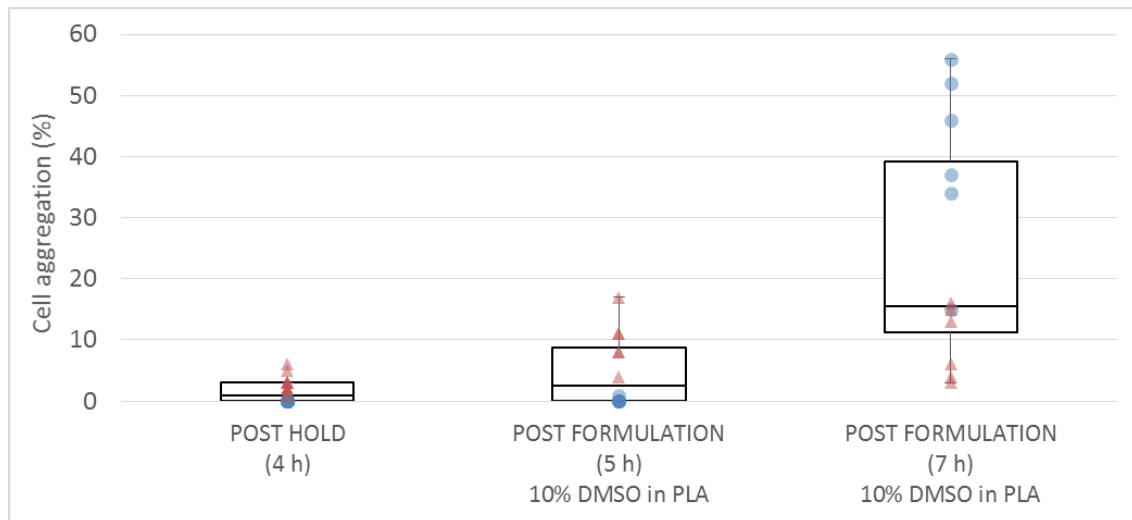
Figure 8.17. The effect of using 10% DMSO in a serum-free downstream process for BM-hMSCs. Showing the dramatic increase in BM-hMSC aggregation that coincides with the decreased membrane integrity through the downstream process. Blue dots represent BM-hMSC line M2, red triangles represent BM-hMSC line M3. Box and whisker plots for n = 12

The use of DMSO for the cryopreservation of BM-hMSCs has been linked to adverse effects in the product such as genetic mutation (Rodrigues *et al.* 2008) as well as potential detriment to the patient (Windrum and Morris 2003) once infused. Therefore, the development of cryopreservation processes should seek to drive down the use of DMSO to not only reduce the toxicity risk to the patient, but also to enable increasing scale to be achieved in the downstream and product formulation processes, which will be required to drive down the cost of manufacture.

8.3.5 Effect of the downstream process on BM-hMSC characteristics

It is clearly important to maintain an acceptable level of BM-hMSC membrane integrity throughout the downstream process as this will have a profound impact on the product efficacy. Despite this however, additional BM-hMSC characteristics should be measured in order to assess subtle changes to the BM-hMSCs throughout the downstream process.
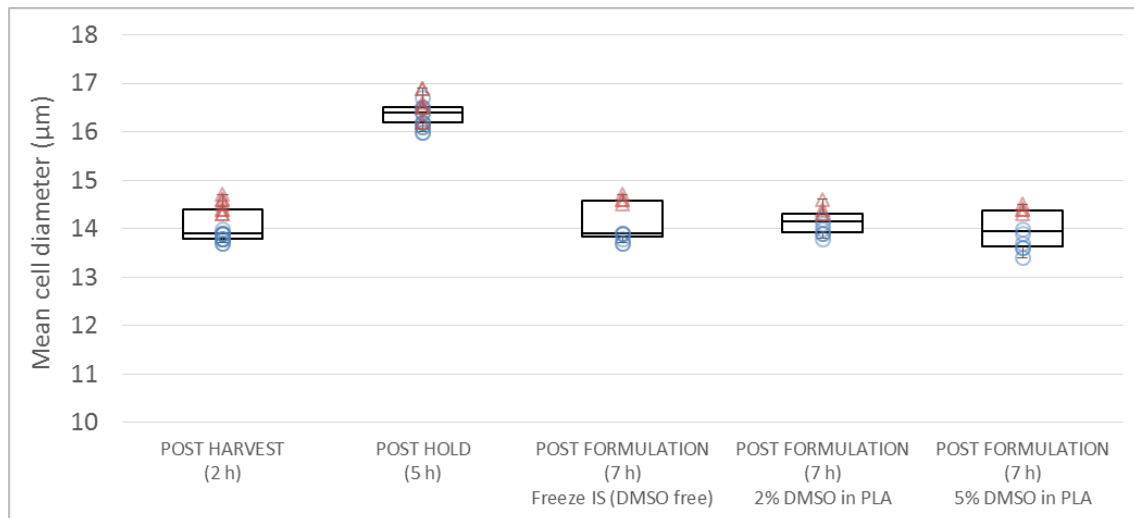
Figure 8.18. The effect of the serum-free downstream process on the mean cell diameter of BM-hMSCs. Showing the increase in mean cell diameter after the holding process. Blue dots represent BM-hMSC line M2, red triangles represent BM-hMSC line M3. Box and whisker plots for n = 12

Figure 8.19 shows the effect of the downstream process on mean BM-hMSC diameter, with a significant increase ($p < 0.05$) following the holding process in PLA, which subsequently reduces post-formulation. This cell swelling through the holding process should be carefully controlled as it will likely increase the likelihood of a loss in membrane integrity and increased cell stress throughout the subsequent process. This can be achieved through the development of BM-hMSC parenteral solutions that support a consistent osmotic balance throughout the entire downstream process.

In addition to an assessment of the BM-hMSC size throughout the downstream process, the BM-hMSC outgrowth kinetics have been assessed for both donors for the formulation in PRIME-XV® SFM FreezIS. The result of this can be seen in Figure 8.19A, which shows that BM-hMSC donor line M3 maintained its outgrowth potential throughout the downstream process above 0.4 day^{-1}. In contrast, BM-hMSC donor M2 not only demonstrated a significant reduction in outgrowth kinetics ($p < 0.05$), but also showed an increasing inter-batch variation throughout the downstream process. This reduction in the stability of the M2 donor line through the downstream process raises serious concerns about the impact of donor variation, not just on the expansion unit operation, but on the entire manufacturing process.
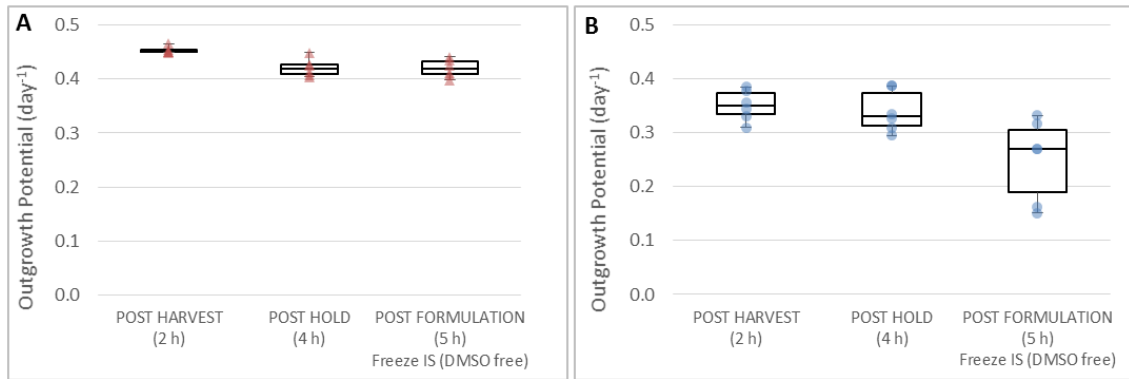
Figure 8.19. Serum-free downstream holding process for BM-hMSCs showing the effect on outgrowth potential for BM-hMSC line M3 (A) and M2 (B). Demonstrating the donor variability in the downstream process. Box and whisker plots, n = 6 for each donor BM-hMSC line.

Colony forming potential has been highlighted as an important assay for the quality of BM-hMSC preparations (Pochampally 2008) and has previously been shown to deteriorate as BM-hMSC age in culture (Stolzing and Scutt 2006). As with the outgrowth potential, the colony-forming potential for BM-hMSC donor M3 saw a slight decrease from a median of 19.2 % post-harvest to 16.2 % post hold, which subsequently stabilised post-formulation in FreezIS (Figure 8.20A). This supports the previous results that suggest that BM-hMSC donor M3 is able to maintain key characteristics throughout the downstream process following serum-free microcarrier expansion. In contrast, Figure 8.20B shows a significant decline ($p < 0.05$) in the CFU potential for BM-hMSC donor M2 from a median of 16.8 % post-harvest to 12.8 % post-hold and finally 6.4 % post-formulation in FreezIS. This represents a dramatic loss in CFU potential throughout the downstream process as was previously seen for the membrane integrity and outgrowth potential of BM-hMSC donor M2.
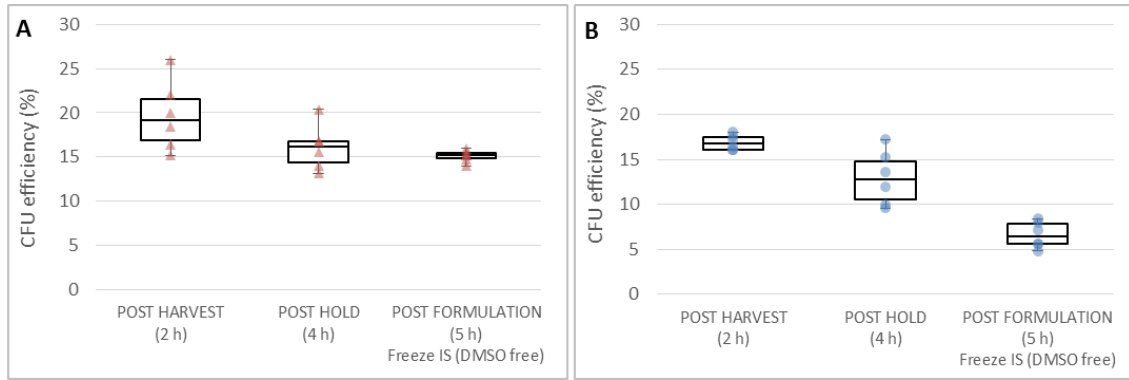
Figure 8.20. Serum-free downstream holding process for BM-hMSCs showing the effect on colony forming efficiency for BM-hMSC line M3 (A) and M2 (B). Demonstrating the donor variability in the downstream process. Box and whisker plots, n = 6 for each donor BM-hMSC line.

Given the impact of the cell survival during prolonged holding times has on the potential scale that can be achieved, careful assessment of the allowable tolerances on the BM-hMSC characteristics should be completed early in process development as this will determine the overall process scalability. For the development of an off-the-shelf BM-hMSC manufacturing process, it will also be important to screen potential donors through the entire process rather than simply having exclusion criteria based on growth and functionality through the upstream process. This is because initial growth and characteristics of BM-hMSC donors in the serum-based process in Chapter 4 highlighted BM-hMSC donor M2 as a favourable donor and M3 as being sub-optimal for the expansion process. This conclusion has been reversed, however, after considering the impact of the downstream on BM-hMSC characteristics in a serum-free process. For future off-the-shelf process development, it would be advised to operate a scaled-down version of the final manufacturing and delivery process, in order to screen desirable BM-hMSC donors through the entire process to take forward into commercial production.

8.4 Serum-free cryopreservation and thaw of BM-hMSCs

8.4.1 Experimental overview

Following the evaluation of a scalable and serum-free downstream process for BM-hMSCs, the effect of a cryopreservation and thaw on two BM-hMSC donors has been evaluated. For this, BM-hMSC from M2 and M3 donors were taken through a cryopreservation and thaw process, following controlled microcarrier expansion, harvest and downstream processing described in Section 8.3. This involved a post-formulation controlled-rate freezing process from 4 °C to -80 °C at -1 °C.min^{-1}, followed by transfer and storage to the vapour phase of monitored liquid nitrogen tank at -196 °C for a least two weeks. A total of six vials were cryopreserved from each bioreactor (n = 18) in each of the three serum-free cryopreservation formulas, these were:

1. PlasmaLyte-A supplemented with 5% (v/v) DMSO
2. PlasmaLyte-A supplemented with 2% (v/v) DMSO
3. Irvine Scientific PRIME-XV® MSC FreezIS DMSO-Free

After at least two weeks at -196 °C, vials of $1 \cdot 10^6$ BM-hMSCs were directly thawed in a water bath at 37 °C, before being washed and re-suspended in SFM. Post-thaw analysis was carried out for n = 3 from the downstream process, for n = 3 vials and n = 2 measurements (n = 18) for both donors in each of the cryopreservation conditions. The BM-hMSCs from both donors were assessed for post-thaw membrane integrity, attachment efficiency, colony forming efficiency (Section 3.4.9) and outgrowth potential.

8.4.2 Post-thaw membrane integrity and attachment efficiency of BM-hMSCs

In order to facilitate the successful development of off-the-shelf BM-hMSC therapies, the impact of cryopreservation, following the controlled serum-free microcarrier expansion, harvest and downstream processes should be evaluated. The post-thaw cell viability prior to clinical infusion into a patient should have a minimum viability of 70% (preferably more than 85%) (Pattasseril *et al.* 2013). The BM-hMSC percentage membrane integrity one hour post-thaw can be seen in Figure 8.21 for both BM-hMSC donors in 5 % and 2 % DMSO as well as FreezeIS, a DMSO-free formulation. The BM-hMSC donor M3 demonstrates a high post-thaw membrane integrity across all conditions with a minimum viability 80.3 % and > 94 % of thawing events above the preferable product viability of > 85 % for clinical delivery. In contrast, the M2 BM-hMSC donor line as with the stability through the downstream process, demonstrated a significant reduction

(p < 0.05) in post-thaw membrane integrity. This is particularly apparent at reduced DMSO concentrations, with 5 % DMSO supporting a similar post-thaw membrane integrity to M3, with only two events below the 85 % threshold.
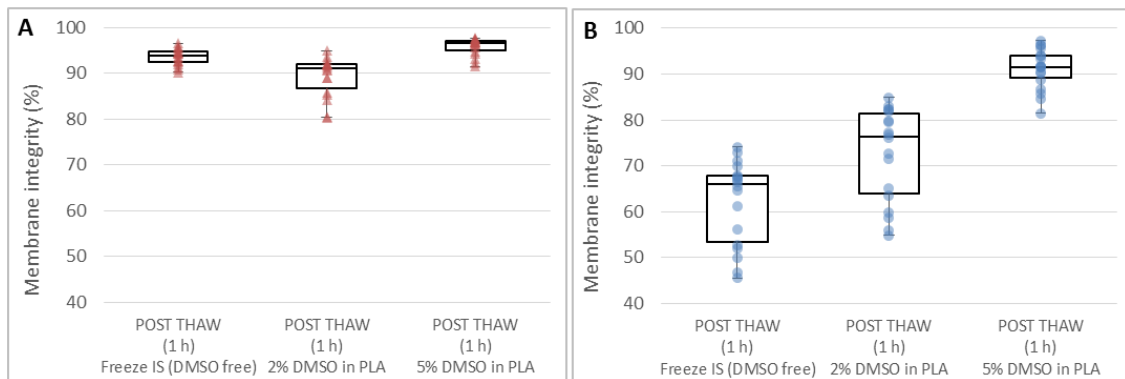
Figure 8.21. Post-thaw membrane integrity of BM-hMSCs following the serum-free downstream holding and cryopreservation process for M3 (A) and M2 (B). Demonstrating the donor variability in the post-thaw BM-hMSC characteristics following cryopreservation. Box and whisker plots show n = 18 for each donor BM-hMSC line in each condition

In addition to the post-thaw membrane integrity, the BM-hMSC attachment efficiency has been evaluated, demonstrating the percentage of BM-hMSCs that have retained the ability to adhere to tissue culture plastic post-thaw. This is important, as the ability of the BM-hMSC to attach to the culture surface demonstrates a higher level of function than simply assessing the cell membrane integrity. The attachment ability of BM-hMSCs has been shown to be a critical part of their putative function to home to the site of injury once delivered (Karp and Leng Teo 2009; Sohni and Verfaillie 2013) and therefore a dramatic reduction post-thaw, prior to clinical delivery, would be highly undesirable. Figure 8.22 shows the post-thaw attachment efficiency of M2 and M3 in each of the cryopreservation solutions, which shows a lower attachment efficiency although a similar trend to the post-thaw membrane integrity. This generally represents a reduction in post-thaw attachment efficiency compared to membrane integrity of 20 - 30 % for M3 and 30 -40 % for M2. This again demonstrates the increased stability of the M3 BM-hMSC donor line through the downstream and cryopreservation process in all three

cryopreservation solutions, whereas the M2 BM-hMSC donor line demonstrated poor recovery and attachment, particularly at lower levels of DMSO.
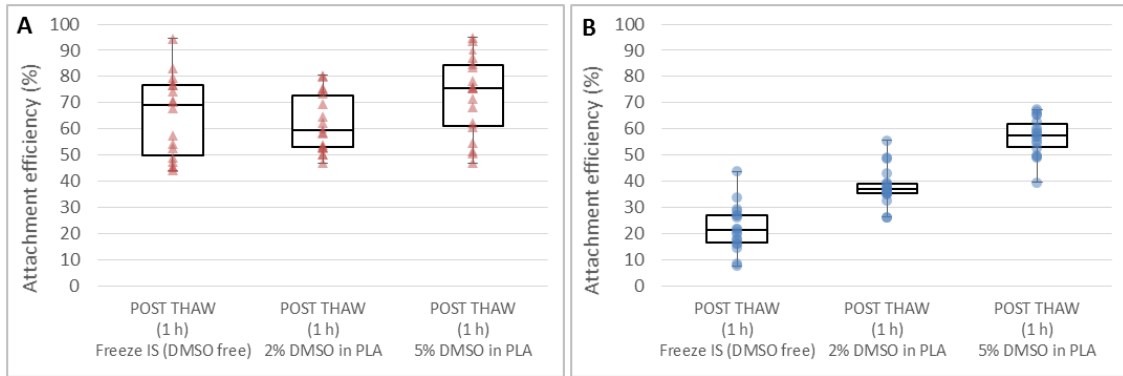
Figure 8.22. Post-thaw attachment efficiency of BM-hMSCs following the serum-free downstream holding and cryopreservation process for M3 (A) and M2 (B). Demonstrating the donor variability in the post-thaw BM-hMSC characteristics following cryopreservation. Box and whisker plots show n = 18 for each donor BM-hMSC line in each condition

In addition to the instability of the M2 BM-hMSC donor throughout the downstream process, it can be seen that the cryopreservation process is also having a detrimental impact on the membrane integrity of the cells. The difference in the median post-formulation and post-thaw membrane integrity of the M3 BM-hMSC donor line was 3.4, 6.7 and 0.7 % for the FreezIS, 2 % DMSO and 5 % DMSO, respectively. In contrast, the difference in the median post-formulation and post-thaw membrane integrity of the M2 BM-hMSC donor line was 33.5, 23.3 and 3.7 % for the FreezIS, 2 % DMSO and 5 % DMSO, respectively. This demonstrates that it is not only the downstream process that is having a detrimental effect on the M2 BM-hMSC line, but also the freeze-thaw process, particularly at reduced DMSO concentrations.
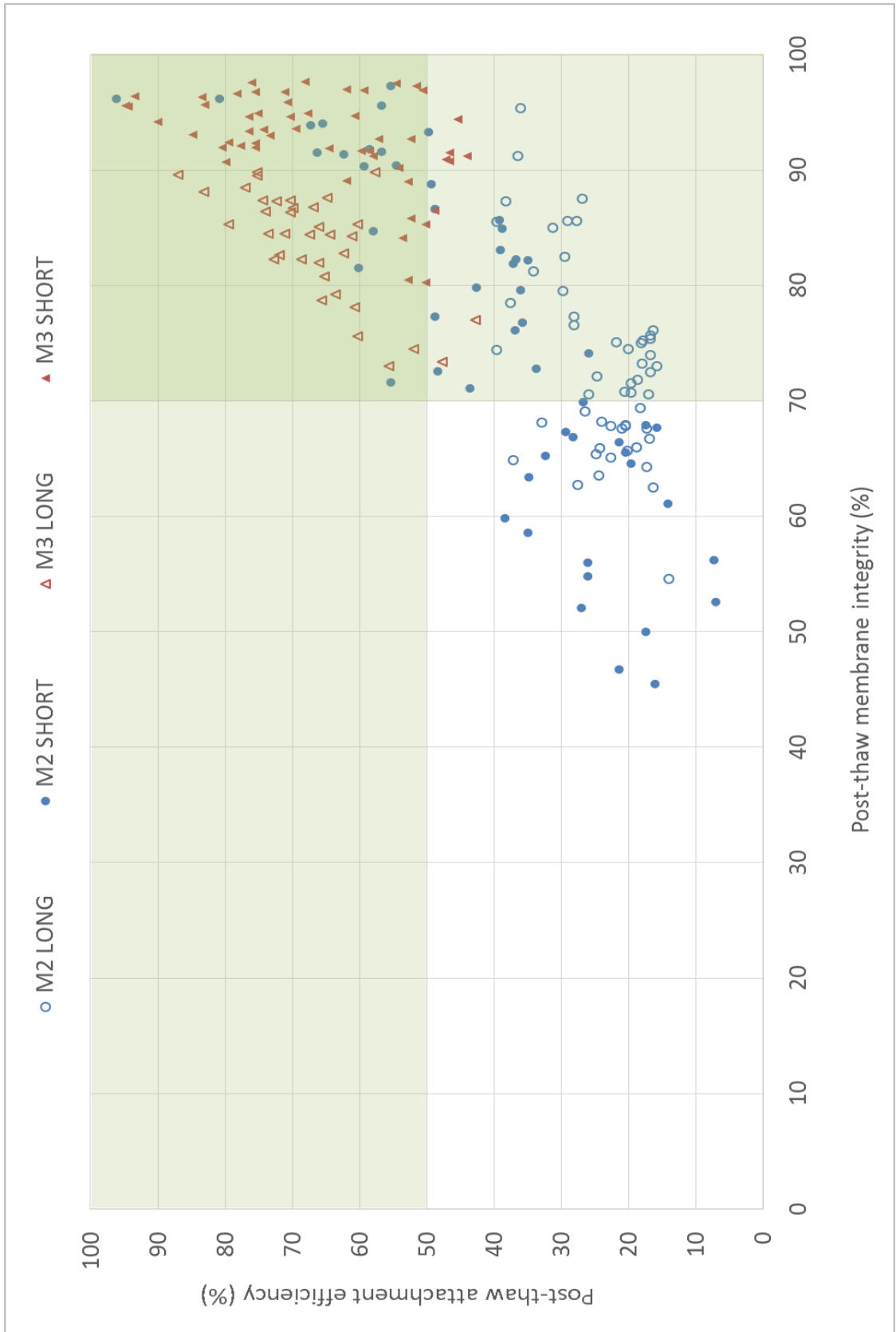
Figure 8.23. Post-thaw membrane integrity versus attachment efficiency of BM-hMSCs following the serum-free downstream holding and cryopreservation process. Showing the improved performance in one of the donor BM-hMSC lines. Data shows n = 198

Figure 8.23 shows the post-thaw membrane integrity against the attachment efficiency for both of the BM-hMSC lines in the short-term and long-term downstream processes. This again demonstrates the difference between the two donors in terms of recoverability through the entire process. Figure 8.23 also shows the effect of the long-term downstream process on the M3 BM-hMSC line, which shows a slight reduction in the post-thaw membrane integrity compared to the short-term downstream process, although not a single event dropped below < 70 % viability after one hour post-thaw. In contrast, almost 40 % of the thaw events for BM-hMSC line M2 were below this 70 % viability benchmark and almost all demonstrated less than 50 % post-thaw attachment efficiency.

8.4.3 Post-thaw BM-hMSC characteristics

The BM-hMSC outgrowth kinetics have also been evaluated post-thaw in each cryopreservation solution for both donors. The result of this can be seen in Figure 8.24 which shows a similar level of outgrowth potential across all conditions in M3 and a slight increase in outgrowth kinetics of M2 as the concentration of DMSO is increased. In terms of the difference between post-formulation and post-thaw outgrowth kinetics, BM-hMSC donor M3 shows a median decrease of 12 % compared to a decrease of 72 % for the M2 BM-hMSC donor for the DMSO-free FreezIS cryopreservation solution. It is clear that the freeze-thaw process is also having a detrimental impact on the BM-hMSC outgrowth kinetics of M2, which also demonstrates increased intra-donor variability compared to M3.
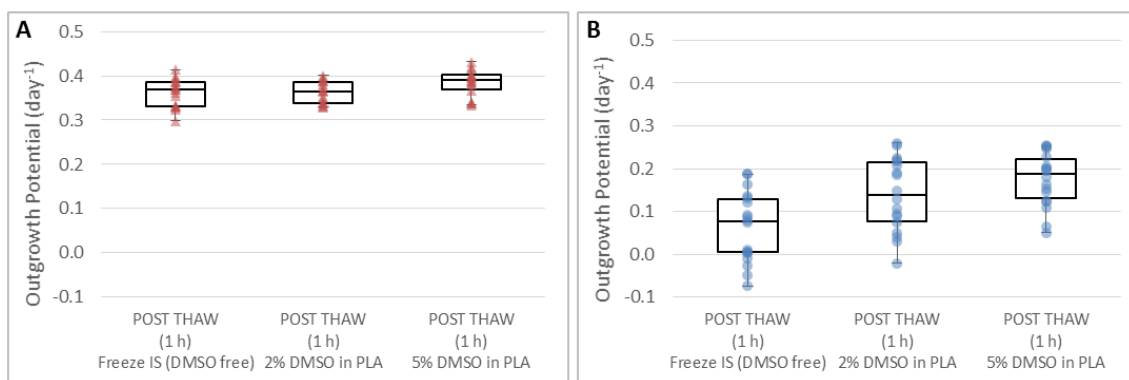
Figure 8.24. Post-thaw outgrowth potential of BM-hMSCs following the serum-free downstream holding and cryopreservation process for BM-hMSC line M3 (A) and M2 (B). Demonstrating the donor variability in the post-thaw BM-hMSC characteristics following cryopreservation. Box and whisker plots show n = 9 for each donor

A reduction in BM-hMSC characteristics as well as an increase in variability, has the potential to increase the likelihood of suffering a batch failure in the product and therefore pre-selecting BM-hMSC donors to mitigate this risk will be critical for the development of successful manufacturing processes.

Maintaining the CFU potential of the BM-hMSCs throughout the cryopreservation process is also important, as key cellular characteristics must remain present right up until the point of product delivery to the patient. Figure 8.25 shows the post-thaw CFU potential of M2 and M3 donor lines in 5 % DMSO, 2 % DMSO and DMSO-free FreezIS. This shows the relative maintenance in the post-thaw CFU potential for the M3 BM-hMSC donor compared with M2 across all three cryopreservation solutions. Despite this, the relative difference between the post-formulation and post-thaw CFU potential for the DMSO-free FreezIS formulation for the M3 and M2 BM-hMSC lines was similar, with a 23 and 19 % reduction, respectively. Considering that the post-harvest CFU potential for M3 and M2 was 19.2 and 16.8% respectively, it is clear that the reduction in CFU potential for the M2 BM-hMSC line has been during the downstream process, before cryopreservation has taken place, whereas M3 CFU potential has been maintained throughout. Placing limits and controls on the downstream, as well as the expansion process will be critical therefore to maintain BM-hMSC quality throughout the entire manufacturing process.
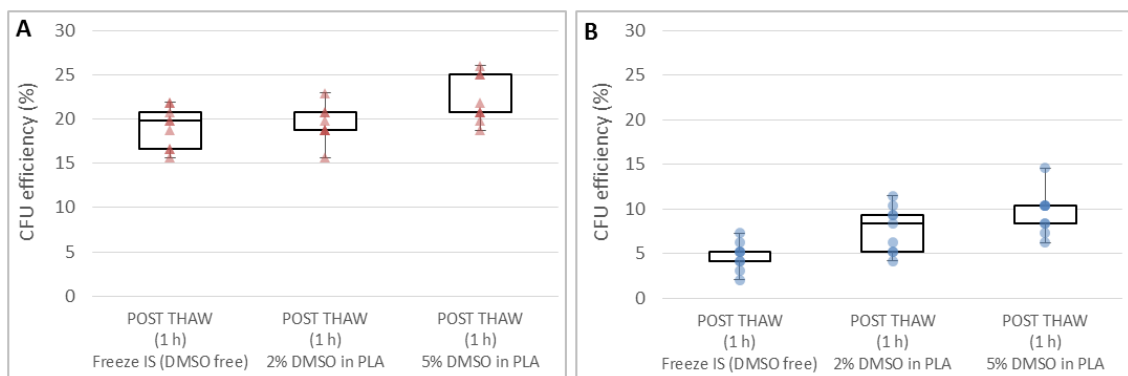
Figure 8.25. Post-thaw colony forming efficiency of BM-hMSCs following the serum-free downstream holding and cryopreservation process for BM-hMSC line M3 (A) and M2 (B). Demonstrating the donor variability in the post-thaw BM-hMSC characteristics following cryopreservation. Box and whisker plots show n = 9 for each donor

8.5 Chapter conclusions

This Chapter has demonstrated that increased BM-hMSC yield can be obtained in a serum-free microcarrier process to above $1 \cdot 10^6$ cells.mL^{-1} without having a detrimental impact on the product characteristics. Increasing the yield of BM-hMSC expansion processes in this way will drive the development of cost-effective manufacturing processes, since reduced bioreactor volumes will be required to manufacture commercially relevant batch sizes within a reduced timescale. It will also be important to control the level of glucose in the culture medium, to avoid requiring increased concentrations to achieve these yields in a fed batch approach. This will likely require the operation of perfused bioreactors, to enable online measurement and control of the nutrient concentration in the culture medium.

Systematic investigation of the downstream and cryopreservation process following microcarrier expansion and harvest of BM-hMSCs has highlighted the need to develop scalable end-to-end processes during development. The allowable time that the BM-hMSCs are exposed to non-adherent conditions during the downstream process will have a significant impact on the potential scale the process can reach, as the product characteristics degrade through these downstream unit operations. It will be critical early in process development, therefore, to determine the allowable tolerances on the quality of the product and the allowable downstream exposure time that does not take the BM-hMSCs outside of this operating window. In conjunction with this, reducing the concentration of cryoprotective agents such as DMSO should be minimised, not only to avoid patient toxicity, but also because increased concentrations are detrimental to the product due to prolonged exposure during the product formulation stage. Reducing the DMSO concentration in the final product will allow for increased product formulation times, which will increase the number of doses that can be manufactured per batch, reducing the overall cost of production per dose.

This Chapter has also highlighted the importance of considering the entire process before selection of master bank material for an off-the-shelf BM-hMSC therapy, as significant levels of donor variability have been experienced in the downstream and cryopreservation processes. Considering that the BM-hMSC donor that was most favourable in terms of growth, identity and quality throughout the entire production process, was evaluated due to its poor growth and characteristics, scaled-down versions of the entire process should be used to evaluate BM-hMSC donors for the product master bank that maintain functional characteristics throughout.

Publications arising from this Chapter:

Heathman TRJ, Picken A, Glyn VAM, Cheeseman E, Rafiq QA, Nienow AW, Kara B, Hewitt CJ, Coopman K. Development of a human mesenchymal stem cell cryopreservation process from a microcarrier process: Implications for large-scale manufacture. Cytotherapy, (2015) (*in preparation*)

9 Conclusions and Future Work

9.1 Conclusions

- This work has first of all demonstrated the high level of variation in BM-hMSCs growth and characteristics from different donors in a monolayer expansion process under FBS-based culture. This has implications for the development of both patient specific and off-the-shelf manufacturing processes and will likely increase the cost of production. These increased costs will be largely driven by this increased variation, which will increase the risk of product batch failure as well as reducing potential BM-hMSC production rates.

- Serum-free medium has demonstrated the ability to reduce this process variability, as well as the potential to reduce the variation in the future supply of process raw materials, associated with the use of serum in the manufacturing process. The increased yield and convergence of BM-hMSC characteristics throughout this monolayer expansion process demonstrates a level of control over the product, which has the potential to increase the cost-effectiveness and reduce the risk in the operation of serum-free BM-hMSC manufacturing processes.

- Transfer of this monolayer BM-hMSC expansion process into a scalable microcarrier-based process has been achieved in serum-based and serum-free medium by the development of a fibronectin coating protocol for microcarriers. This is an important process transfer step as the development of a scalable microcarrier expansion process has the potential to take advantage of increasing economies of scale to cost-effectively manufacture BM-hMSCs at the lot-sizes required for commercial production.

- Furthermore, the increased yield and donor consistency that was experienced for the monolayer process in HPL and serum-free medium, has also directly transferred to the microcarrier process, indicated that this improved efficiency has the potential to be carried through increasing process scales.

- This work has also demonstrated that the BM-hMSCs harvested from this serum-free microcarrier process can be further processed, formulated and cryopreserved downstream, providing the first demonstration of successfully integrated unit operations for BM-hMSC production on microcarriers.

- Unnecessarily increasing the impeller agitation speed during the microcarrier expansion of BM-hMSCs decreased the growth kinetics but did not have a detrimental impact on the BM-hMSC post-harvest characteristics.

- Direct aeration of the culture medium *via* a sparger has also been shown to be detrimental to BM-hMSC growth and post-harvest quality characteristics. Sparging of the medium during bioreactor culture is likely to be required at the large-scale to supply oxygen to the cells and remove carbon dioxide and is currently the preferred method of aeration in large-scale bioreactors. It will be important during process scale-up, therefore, to ensure that bioreactor parameters such as maximum energy dissipation and sparging rates are not increased above levels which might affect the growth and quality characteristics of the BM-hMSC product at the commercial scale. Alternative technology such as membrane based aeration could also be investigated for supplying oxygen to the BM-hMSC expansion process, which might be possible considering that the oxygen demand of these cells is far below that experienced by traditional cell bioprocesses.

- The effect of exposing low oxygen bioreactor culture to atmospheric conditions during the culture period has highlighted the importance of operating closed and controlled processes to avoid large fluctuation of the dissolved oxygen concentration of the medium. Operating the microcarrier expansion process for BM-hMSCs in a functionally closed and controlled manner, has demonstrated improved growth and post-harvest BM-hMSC quality characteristics at 10 and 25 % dissolved oxygen in FBS-based medium.

- The introduction of serum-free medium into this low dissolved oxygen controlled bioreactor process has further increased the yield across two BM-hMSC donors, however, with reduced harvest efficiency compared to the FBS-based process, which has lower cell numbers at harvest. Considering that this was primarily due to cell losses in the cell-microcarrier separation unit operation, it will be imperative to develop specific downstream technology to effectively separate the cells from the microcarriers, particularly as the number of BM-hMSCs per unit volume is increased during future process development.

- The development of a process control strategy has also significantly increased the yield and consistency between BM-hMSC donors with a combined coefficient of variance between and within these donors under serum-free conditions of less than 15 %. This is in conjunction with a significant increase in the BM-hMSCs produced per volume of medium per unit time under serum-free conditions, which will be critical in increasing the economies of scale and reducing the subsequent cost of BM-hMSC therapies.

- The introduction of the process control strategy has significantly reduced the inter- and intra-donor variation in FBS-based culture from 79.1 to 37.5 %, which will again be

critical in further reducing the development costs of both patient specific and off-the-shelf BM-hMSC manufacturing processes.

- This work has demonstrated that increased BM-hMSC yield can be obtained in a serum-free microcarrier process to above $1 \cdot 10^6$ cells.mL^{-1} without having a detrimental impact on the product characteristics post-harvest. Increasing the yield of BM-hMSC expansion processes in this way is likely to drive the development of cost-effective manufacturing processes, as reduced bioreactor volumes will be required to manufacture commercially relevant batch sizes within a reduced timescale.

- It will be important to control the level of glucose in the culture medium, to avoid requiring increased concentrations to achieve these yields in a fed batch approach. This will likely require the operation of perfused bioreactors, to enable online measurement and control of the nutrient concentration, in addition to other critical process parameters such as the pH and dissolved oxygen concentration of the culture medium.

- Systematic investigation of the downstream and cryopreservation process following microcarrier expansion and harvest of BM-hMSCs has highlighted the need to develop scalable end-to-end processes during development. The allowable time that the BM-hMSCs are exposed to non-adherent conditions during the downstream process will have a significant impact on the potential scale that the process can reach, as the product characteristics degrade through these downstream unit operations.

- It will be critical early in process development to determine the allowable tolerances on the quality of the product and the allowable downstream exposure time that does not take the BM-hMSCs outside of this operating window. In conjunction with this, the concentration of cryoprotective agents such as DMSO should be minimised, not only to avoid patient toxicity, but also because increased concentrations are detrimental to the product due to prolonged exposure during the product formulation stage.

- Reducing the DMSO concentration in the final product will allow for increased product formulation times, which will increase the number of doses that can be manufactured per batch, reducing the overall cost of production per dose.

- Finally, this work has highlighted the importance of considering the entire process before selection of master bank material for an off-the-shelf BM-hMSC therapy, as significant levels of donor variability have been experienced in the downstream and cryopreservation processes. The BM-hMSC donor that was most favourable in terms of growth, identity and quality throughout the entire production process, was initially selected due to its poor growth and characteristics in FBS-based medium. It is critical

therefore, that scaled-down versions of the entire process are used to evaluate BM-hMSC donors for the product master bank that maintain functional characteristics throughout the entire manufacturing process.

9.2 Future work

This work has demonstrated the increased yield and consistency that can be achieved by the systematic development of a process control strategy within a scalable and serum-free expansion, harvest, downstream and cryopreservation process for BM-hMSCs. This has provided important findings which can inform future development of BM-hMSC manufacturing processes, however a number of challenges remain:

9.2.1 Development and operation of a functionally closed and end-to-end process

In order to enable the successful development of commercially relevant and scalable BM-hMSC manufacturing processes, future process development should focus on integrating functionally closed unit-operations into an entire end-to-end process. The work presented in this thesis has demonstrated the importance of controlling the culture environment and considering the entire process as a sequential set of unit-operations rather than developing individual process steps in isolation. The key points to consider are as follows:

- Development of scalable downstream technology specifically for microcarrier separation and subsequent BM-hMSCs concentration. Much of the current downstream technology has been adapted for this but there is an opportunity to generate intellectual property around separation technology specific to cells and microcarriers. This should ensure that BM-hMSC harvest and downstream at high cell densities can also be achieved, as this will continue to increase in order to reduce the manufacturing costs per dose, which are currently too high.

- Part of this bioreactor and downstream development should also look to validate and integrate single-use components, as it is widely acknowledged for cell therapies that the risk vs. cost of traditional clean-in-place procedures are too high and single-use processes will be utilised to reduce the risk of contamination. In fact, an EPSRC-funded PhD student will build on the work in this PhD thesis, investigating single-use bioreactors for the expansion of BM-hMSCs on microcarriers in collaboration with PALL Life Sciences.

- Given the importance of reduced oxygen concentrations and serum-free conditions on the growth and characteristics of BM-hMSCs, the initial isolation of the BM-hMSCs should take place under these conditions to provide material for future bioreactor experiments that has not been exposed to serum components. Reducing process input variation will be integral in driving BM-hMSC consistency throughout the entire process

and will act as an initial BM-hMSC selection step for each donor, for cells that adhere and proliferate best on fibronectin under serum-free conditions, which has been shown to be advantageous here.

- Integrating the controlled bioreactor expansion process with the downstream in a closed manner will ensure that the BM-hMSC environment remains stable throughout. Developing functionally closed processes also demonstrates increased scalability, ensuring that unit-operations are amenable to automation, with the potential to replace traditional manual manipulations that are not cost-effective at the commercial scale.

- During the development of these end-to-end processes, it will also be important to consider the regulatory requirements for this BM-hMSC manufacturing technology, to ensure that it has the potential to be GMP compliant. This will drastically increase the commercial relevance of any developed technology, which will be critical in order to successfully exploit any potential intellectual technology arising from this development.

9.2.2 Integration of functional and purity assays within the end-to-end process

Perhaps the biggest challenge facing the successful development of BM-hMSC manufacturing processes is the development and integration of functional BM-hMSC assays into the process. This is critical to the successful development of manufacturing processes, providing metrics to assess the impact of process unit operations on BM-hMSC quality. Setting allowable tolerances on these measurements will be important in order to determine downstream process timings and the subsequent scale that is achievable during manufacture. The development of these functional assays has proved difficult, however, due to the multifaceted and poorly understood mechanism of action of BM-hMSCs. Despite this, assays are beginning to appear that look at a particular aspect of BM-hMSC function such as protein secretion in response to environmental cues, which can be integrated into BM-hMSC characterisation. The key points to consider are as follows:

- These BM-hMSC functional assays are specific to each clinical indication, therefore a couple of lead candidate indications can be selected as exemplars during development, such as immune modulation and angiogenesis that have been previously shown to be important to BM-hMSC function *in vivo*.

- These assays can then be used to assess whether there have been any relative changes to these functions through the process and if so, at which point in the process. This can

then inform the direction of future development, to target particular unit-operations and minimise these product changes during manufacture.

- In addition to measures of BM-hMSC functionality throughout the process, an assessment of the plastic particulate content through the microcarrier expansion, harvest and separation unit-operations should be made as this is becoming an important regulatory consideration for cell-based therapies.

- The maintenance of acceptable levels of product purity remains a key consideration for microcarrier-based expansion processes and downstream technology that can remove plastic particulates from the product prior to formulation may be required for future regulatory approval.

- It is also likely that the evolution of cell-based therapy manufacturing processes will have to consider the product purity in terms of virus and DNA content as has been seen in traditional bioprocesses. Therefore, assessment and integration of this measurement technology into the BM-hMSC manufacturing process will be critical for future process development.

9.2.3 Control of nutrients within a perfused bioreactor process

The control of nutrients in the microcarrier expansion process will be an important consideration in driving further consistency into the process, avoiding bulk fluctuations in the concentrations available to the cells, which has been shown to be detrimental. This will require the development of a perfusion bioreactor processes, where the constant measurement and control of key nutrients such as glucose and glutamine is possible. This will avoid having to adopt a fed-batch approach where large quantities of nutrients are added and depleted by the increasingly high BM-hMSC densities. The key points to consider are as follows:

- The design and operation of the bioreactor perfusion loop must ensure that microcarriers do not pass through as this will not only cause issues in supernatant analysis, but can potentially cause issues as BM-hMSCs attached to microcarriers move through the pumping circuit. This can be achieved using an impeller spin filter, or initially by adopting the same filtered sample port modification demonstrated here.

- In conjunction with this, the validation and integration of a biomass probe into the bioreactor system would allow for the development of a mathematical model to form the basis of an optimisation strategy for this nutrient control system. This is a potential way in which sufficient nutrients can be supplied to the system, based on BM-hMSC

- growth kinetics and the calculated per cell flux, alleviating the need for off-line metabolite analysis as the basis for the control of nutrients and providing a basis for process optimisation.

- This perfused bioreactor system with increased nutrient control can then be assessed in terms of its impact on BM-hMSC yield and consistency across multiple BM-hMSC donors and potentially other BM-hMSC sources (such as umbilical cord and adipose tissue). A comparison can then be made in terms of the number of recovered cells, per volume of medium, per unit time of both the perfused and fed-batch processes.

9.2.4 Further commercial development with HPL and serum-free medium

The work presented here has demonstrated the potential of both HPL and SFM-based processes for the expansion of BM-hMSCs on microcarriers. There remains, however, potential opportunities for further development of these formulations, continuing the current collaborative partnerships that have been hugely beneficial to all parties. The key points to consider are as follows:

- The fibronectin coating of the microcarriers directly prior to BM-hMSC expansion would be undesirable due to the risk of a coating quality assurance failure impacting the subsequent expansion step. In order to decouple the developed fibronectin coating protocol of the microcarriers from the subsequent expansion of BM-hMSCs in serum-free medium, the fibronectin coated microcarriers would have to be stored long-term. The development and validation of a low temperature storage method for the fibronectin coated microcarriers, without compromising the quality of the coating would be a valuable step in this process, decoupling the coating from the expansion.

- As the field moves forward, the development of defined and custom serum-free medium formulations for BM-hMSC production is becoming ever more important. A continuation of commercial partnerships, looking at developing defined medium formulations and culture protocols specifically for the microcarrier culture and harvest of BM-hMSCs would add significant value to the field. This work would specifically look to drive medium costs down during manufacture and identify ways in which these formulations can be developed to minimised donor variation from a variety of BM-hMSC isolation sources.

- There is further scope to investigate the impact of HPL for the controlled expansion, downstream processing and cryopreservation of BM-hMSCs. This would build upon the

contract research projects established with Cook Regentec (USA) to focus on reduced quantities of HPL in the medium (5% rather than 10%) without impacting BM-hMSC growth and characterisation for adipose and bone marrow derived BM-hMSCs on microcarriers. This would from part of a wider economic assessment of the potential scalability of HPL in terms of available supply and batch-to-batch variation, to demonstrate that at reduced concentrations, it is a viable alternation to FBS at the large-scale.

- In terms of demonstrating the physical scalability of the serum-free and HPL-based processes developed here, an increase in scale of the bioreactor system by one order of magnitude to the litre-scale based on sound engineering principles would provide an invaluable demonstration of the true scalability of the system. This would be in conjunction with harvesting the BM-hMSC from the microcarriers in situ and separating the entire batch of BM-hMSCs from the microcarriers using scalable downstream technology, such as tangential flow filtration or fluidised bed centrifugation. Maintaining the relationships with commercial partners will be critical for this moving forward, as the cost of running these experiments is prohibitive without these valuable collaborative partnerships.

- Increasing the hMSC yield during the expansion phase will also be important to drive future process development. A potential mechanism to achieve this would be to add additional microcarriers to the bioreactor during expansion, so that the BM-hMSCs have additional surface area to utilise and higher cell densities can be achieved with an increased cell expansion ratio.

References

Abraham EJ, Slater KA, Sanyal S, Linehan K, Flaherty PM, Qian S. 2011. Scale-up of mammalian cell culture using a new multilayered flask. J Vis Exp(58).

Adams V, Challen GA, Zuba-Surma E, Ulrich H, Vereb G, Tarnok A. 2009. Where New Approaches Can Stem From: Focus on Stem Cell Identification. Cytometry Part A 75A(1):1-3.

Adewumi O, Aflatoonian B, Ahrlund-Richter L, Amit M, Andrews PW, Beighton G, Bello PA, Benvenisty N, Berry LS, Bevan S *and others*. 2007. Characterization of human embryonic stem cell lines by the International Stem Cell Initiative. Nat Biotechnol 25(7):803-16.

Aggarwal S, Pittenger MF. 2005. Human mesenchymal stem cells modulate allogeneic immune cell responses. Blood 105(4):1815-1822.

Anchordoguy TJ, Cecchini CA, Crowe JH, Crowe LM. 1991. Insights into the cryoprotective mechanism of dimethyl sulfoxide for phospholipid bilayers. Cryobiology 28(5):467-73.

Anisimov VN, Ukraintseva SV, Yashin AI. 2005. Cancer in rodents: does it tell us about cancer in humans? Nat Rev Cancer 5(10):807-19.

Antwiler GD, Windmiller DA, Givens M; Terumo Bct, Inc., assignee. 2014. Method of reseeding adherent cells grown in a hollow fiber bioreactor system.

Arakawa T, Carpenter JF, Kita YA, Crowe JH. 1990. The basis for toxicity of certain cryoprotectants: A hypothesis. Cryobiology 27(4):401-415.

Archibald PRT, Chandra A, Thomas D, Morley G, Lekishvili T, Devonshire A, Williams DJ. 2015. Comparability of scalable, automated hMSC culture using manual and automated process steps. Biochemical Engineering Journal (*In press*).

Atala A. 2012. Human embryonic stem cells: early hints on safety and efficacy. Lancet 379(9817):689-90.

Bakker J, Coffernils M, Leon M, Gris P, Vincent JL. 1991. Blood lactate levels are superior to oxygen-derived variables in predicting outcome in human septic shock. Chest 99(4):956-62.

Baraniak PR, Cooke MT, Saeed R, Kinney MA, Fridley KM, McDevitt TC. 2012. Stiffening of human mesenchymal stem cell spheroid microenvironments induced by incorporation of gelatin microparticles. J Mech Behav Biomed Mater 11:63-71.

Basciano L, Nemos C, Foliguet B, de Isla N, de Carvalho M, Tran N, Dalloul A. 2011. Long term culture of mesenchymal stem cells in hypoxia promotes a genetic program maintaining their undifferentiated and multipotent status. BMC Cell Biol 12:12.

References

Becker AJ, Till JE, McCulloch EA. 1963. CYTOLOGICAL DEMONSTRATION OF CLONAL NATURE OF SPLEEN COLONIES DERIVED FROM TRANSPLANTED MOUSE MARROW CELLS. Nature 197(486):452-&.

Beckermann BM, Kallifatidis G, Groth A, Frommhold D, Apel A, Mattern J, Salnikov AV, Moldenhauer G, Wagner W, Diehlmann A *and others*. 2008. VEGF expression by mesenchymal stem cells contributes to angiogenesis in pancreatic carcinoma. Br J Cancer 99(4):622-631.

Beggs KJ, Lyubimov A, Borneman JN, Bartholomew A, Moseley A, Dodds R, Archambault MP, Smith AK, McIntosh KR. 2006. Immunologic consequences of multiple, high-dose administration of allogeneic mesenchymal stem cells to baboons. Cell Transplant 15(8-9):711-21.

Ben-David U, Benvenisty N. 2011. The tumorigenicity of human embryonic and induced pluripotent stem cells. Nat Rev Cancer 11(4):268-77.

Bianco P, Barker R, Brustle O, Cattaneo E, Clevers H, Daley GQ, De Luca M, Goldstein L, Lindvall O, Mummery C *and others*. 2013a. Regulation of stem cell therapies under attack in Europe: for whom the bell tolls. EMBO J 32(11):1489-95.

Bianco P, Cao X, Frenette PS, Mao JJ, Robey PG, Simmons PJ, Wang CY. 2013b. The meaning, the sense and the significance: translating the science of mesenchymal stem cells into medicine. Nat Med 19(1):35-42.

Bianco P, Kuznetsov SA, Riminucci M, Robey PG. 2006. Postnatal skeletal stem cells. In: Klimanskaya I, Lanza R, editors. Adult Stem Cells. San Diego: Elsevier Academic Press Inc. p 117-148.

Bianco P, Robey PG. 2004. Skeletal stem cells. In: Lanza R, editor. Handbook of Adult and Fetal Stem Cells. San Dieog: Academic Press. p 415-424.

Bianco P, Robey PG, Saggio I, Riminucci M. 2010. "Mesenchymal'' Stem Cells in Human Bone Marrow (Skeletal Stem Cells): A Critical Discussion of Their Nature, Identity, and Significance in Incurable Skeletal Disease. Human Gene Therapy 21(9):1057-1066.

Bianco P, Robey PG, Simmons PJ. 2008. Mesenchymal stem cells: Revisiting history, concepts, and assays. Cell Stem Cell 2(4):313-319.

Bieback K. 2013. Platelet Lysate as Replacement for Fetal Bovine Serum in Mesenchymal Stromal Cell Cultures. Transfusion Medicine and Hemotherapy 40(5):326-335.

Blashki D, Short B, Bertoncello I, Simmons P, Brouard N. 2006. Identification of stromal MSC canditates from multiple adult mouse tissues. International Society of Stem Cell Research 4th Annual Meeting 206.

References

Bosch P, Musgrave DS, Lee JY, Cummins J, Shuler T, Ghivizzani TC, Evans T, Robbins TD, Huard. 2000. Osteoprogenitor cells within skeletal muscle. J Orthop Res 18(6):933-44.

Brandenberger R, Burger SR, Campbell AM, Fong T, Lapinskas E, Rowley JA. 2011. Integrating Process and Product Development for the Next Generation of Biotherapeutics BioProcess International 9(1):30-37.

Bravery CA. 2010. Regulating interface science healthcare products: myths and uncertainties. Journal of the Royal Society Interface 7:S789-S795.

Breyer A, Estharabadi N, Oki M, Ulloa F, Nelson-Holte M, Lien L, Jiang Y. 2006. Multipotent adult progenitor cell isolation and culture procedures. Exp Hematol 34(11):1596-601.

Brindley DA, Davie NL, Culme-Seymour EJ, Mason C, Smith DW, Rowley JA. 2012. Peak serum: implications of serum supply for cell therapy manufacturing. Regen Med 7(1):7-13.

Brooke G, Rossetti T, Pelekanos R, Ilic N, Murray P, Hancock S, Antonenas V, Huang G, Gottlieb D, Bradstock K *and others*. 2009. Manufacturing of human placenta-derived mesenchymal stem cells for clinical trials. Br J Haematol 144(4):571-9.

Brown MF, Gratton TP, Stuart JA. 2007. Metabolic rate does not scale with body mass in cultured mammalian cells. Am J Physiol Regul Integr Comp Physiol 292(6):R2115-21.

Bruder SP, Fink DJ, Caplan AI. 1994. MESENCHYMAL STEM-CELLS IN IN BONE-DEVELOPMENT, BONE REPAIR, AND SKELETAL REGENERATION THERAPY. Journal of Cellular Biochemistry 56(3):283-294.

Buchanan SS, Gross SA, Acker JP, Toner M, Carpenter JF, Pyatt DW. 2004. Cryopreservation of stem cells using trehalose: evaluation of the method using a human hematopoietic cell line. Stem Cells Dev 13(3):295-305.

Burger SR, Bravery CA. 2011. ISCT webinar: potency testing. www.celltherapysociety.org. In: Therapy ISfC, editor.

Butler M. 2005. Animal cell cultures: recent achievements and perspectives in the production of biopharmaceuticals. Appl Microbiol Biotechnol 68(3):283-91.

Byrne JA, Pedersen DA, Clepper LL, Nelson M, Sanger WG, Gokhale S, Wolf DP, Mitalipov SM. 2007. Producing primate embryonic stem cells by somatic cell nuclear transfer. Nature 450(7169):497-U3.

Caplan AI. 1991. MESENCHYMAL STEM-CELLS. Journal of Orthopaedic Research 9(5):641-650.

Caplan AI. 2005. Mesenchymal stem cells: Cell-based reconstructive therapy in orthopedics. Tissue Engineering 11(7-8):1198-1211.

Caplan AI. 2007. Adult mesenchymal stem cells for tissue engineering versus regenerative medicine. Journal of Cellular Physiology 213(2):341-347.

Caplan AI. 2008. All MSCs are pericytes? Cell Stem Cell 3(3):229-30.

Caplan AI. 2009. Why are MSCs therapeutic? New data: new insight. J Pathol 217(2):318-24.

Caplan AI. 2010. What's in a name? Tissue Eng Part A 16(8):2415-7.

Caplan AI, Correa D. 2011. The MSC: an injury drugstore. Cell Stem Cell 9(1):11-5.

Caplan AI, Dennis JE. 2006a. Mesenchymal stem cells as trophic mediators. Journal of Cellular Biochemistry 98(5):1076-1084.

Caplan AI, Dennis JE. 2006b. Mesenchymal stem cells as trophic mediators. J Cell Biochem 98(5):1076-84.

Caplan AI, Sorrell JM. The MSC curtain that stops the immune system. Immunology Letters(0).

Carlos Sepúlveda J, Tomé M, Eugenia Fernández M, Delgado M, Campisi J, Bernad A, González MA. 2014. Cell Senescence Abrogates the Therapeutic Potential of Human Mesenchymal Stem Cells in the Lethal Endotoxemia Model. STEM CELLS 32(7):1865-1877.

Carmen J, Burger SR, McCaman M, Rowley JA. 2012a. Developing assays to address identity, potency, purity and safety: cell characterization in cell therapy process development. Regen Med 7(1):85-100.

Carmen J, Burger SR, McCaman M, Rowley JA. 2012b. Developing assays to address identity, potency, purity and safety: cell characterization in cell therapy process development. Regenerative Medicine 7(1):85-100.

Carpenter MK, Frey-Vasconcells J, Rao MS. 2009. Developing safe therapies from human pluripotent stem cells. Nat Biotechnol 27(7):606-13.

Chan AC, Heathman TJ, Coopman K, Hewitt C. 2014a. Multiparameter flow cytometry for the characterisation of extracellular markers on human mesenchymal stem cells. Biotechnology Letters 36(4):731-741.

Chan AK, Heathman TR, Coopman K, Hewitt CJ. 2014b. Multiparameter flow cytometry for the characterisation of extracellular markers on human mesenchymal stem cells. Biotechnol Lett 36(4):731-41.

Chen AK-L, Reuveny S, Oh SKW. 2013. Application of human mesenchymal and pluripotent stem cell microcarrier cultures in cellular therapy: Achievements and future direction. Biotechnology Advances 31(7):1032-1046.

Chen K, Perez-Stable C, D'Ippolito G, Schiller PC, Roos BA, Howard GA. 2011. Human bone marrow-derived stem cell proliferation is inhibited by hepatocyte growth factor via increasing the cell cycle inhibitors p53, p21 and p27. Bone 49(6):1194-204.

References

Cherry RS, Papoutsakis ET. 1986. Hydrodynamic effects on cells in agitated tissue culture reactors. Bioprocess Engineering 1(1):29-41.

Cheuvront SN, Kenefick RW, Heavens KR, Spitz MG. 2014. A Comparison of Whole Blood and Plasma Osmolality and Osmolarity. Journal of Clinical Laboratory Analysis 28(5):368-373.

Christodoulou I, Kolisis FN, Papaevangeliou D, Zoumpourlis V. 2013. Comparative Evaluation of Human Mesenchymal Stem Cells of Fetal (Wharton's Jelly) and Adult (Adipose Tissue) Origin during Prolonged In Vitro Expansion: Considerations for Cytotherapy. Stem Cells Int 2013:246134.

Cierpka K, Elseberg CL, Niss K, Kassem M, Salzig D, Czermak P. 2013. hMSC Production in Disposable Bioreactors with Regards to GMP and PAT. Chemie Ingenieur Technik 85(1-2):67-75.

Crapnell K, Blaesius R, Hastings A, Lennon DP, Caplan AI, Bruder SP. 2013. Growth, differentiation capacity, and function of mesenchymal stem cells expanded in serum-free medium developed via combinatorial screening. Exp Cell Res 319(10):1409-18.

Crigler L, Robey RC, Asawachaicharn A, Gaupp D, Phinney DG. 2006. Human mesenchymal stem cell subpopulations express a variety of neuro-regulatory molecules and promote neuronal cell survival and neuritogenesis. Exp Neurol 198(1):54-64.

Croughan MS, Hamel JF, Wang DI. 1987. Hydrodynamic effects on animal cells grown in microcarrier cultures. Biotechnol Bioeng 29(1):130-41.

Cruz HJ, Moreira JL, Carrondo MJ. 1999. Metabolic shifts by nutrient manipulation in continuous cultures of BHK cells. Biotechnol Bioeng 66(2):104-13.

Cui L-l, Kerkela E, Bakreen A, Nitzsche F, Andrzejewska A, Nowakowski A, Janowski M, Walczak P, Boltze J, Lukomska B *and others*. 2015. The cerebral embolism evoked by intra-arterial delivery of allogeneic bone marrow mesenchymal stem cells in rats is related to cell dose and infusion velocity. Stem Cell Research & Therapy 6(1):11.

Cunha B, Aguiar T, Silva MM, Silva RJ, Sousa MF, Pineda E, Peixoto C, Carrondo MJ, Serra M, Alves PM. 2015. Exploring continuous and integrated strategies for the up- and downstream processing of human mesenchymal stem cells. J Biotechnol.

Das R, Jahr H, van Osch GJ, Farrell E. 2010. The role of hypoxia in bone marrow-derived mesenchymal stem cells: considerations for regenerative medicine approaches. Tissue Eng Part B Rev 16(2):159-68.

Deans RJ, Moseley AB. 2000. Mesenchymal stem cells: biology and potential clinical uses. Exp Hematol 28(8):875-84.

Deskins DL, Bastakoty D, Saraswati S, Shinar A, Holt GE, Young PP. 2013. Human Mesenchymal Stromal Cells: Identifying Assays to Predict Potency for Therapeutic Selection. Stem Cells Translational Medicine 2(2):151-158.

Di Nicola M, Carlo-Stella C, Magni M, Milanesi M, Longoni PD, Matteucci P, Grisanti S, Gianni AM. 2002. Human bone marrow stromal cells suppress T-lymphocyte proliferation induced by cellular or nonspecific mitogenic stimuli. Blood 99(10):3838-43.

Doherty MJ, Canfield AE. 1999. Gene expression during vascular pericyte differentiation. Crit Rev Eukaryot Gene Expr 9(1):1-17.

Dolley-Sonneville PJ, Romeo LE, Melkoumian ZK. 2013. Synthetic surface for expansion of human mesenchymal stem cells in xeno-free, chemically defined culture conditions. PLoS One 8(8):e70263.

Dominici M, Le Blanc K, Mueller I, Slaper-Cortenbach I, Marini F, Krause D, Deans R, Keating A, Prockop D, Horwitz E. 2006. Minimal criteria for defining multipotent mesenchymal stromal cells. The International Society for Cellular Therapy position statement. Cytotherapy 8(4):315-7.

dos Santos F, Andrade PZ, Abecasis MM, Gimble JM, Chase LG, Campbell AM, Boucher S, Vemuri MC, da Silva CL, Cabral JMS. 2011a. Toward a Clinical-Grade Expansion of Mesenchymal Stem Cells from Human Sources: A Microcarrier-Based Culture System Under Xeno-Free Conditions. Tissue Engineering. Part C, Methods 17(12):1201-1210.

Dos Santos F, Andrade PZ, Abecasis MM, Gimble JM, Chase LG, Campbell AM, Boucher S, Vemuri MC, Silva CL, Cabral JM. 2011b. Toward a clinical-grade expansion of mesenchymal stem cells from human sources: a microcarrier-based culture system under xeno-free conditions. Tissue Eng Part C Methods 17(12):1201-10.

Dos Santos F, Andrade PZ, Boura JS, Abecasis MM, da Silva CL, Cabral JM. 2010. Ex vivo expansion of human mesenchymal stem cells: a more effective cell proliferation kinetics and metabolism under hypoxia. J Cell Physiol 223(1):27-35.

dos Santos F, Campbell A, Fernandes-Platzgummer A, Andrade PZ, Gimble JM, Wen Y, Boucher S, Vemuri MC, da Silva CL, Cabral JMS. 2014. A xenogeneic-free bioreactor system for the clinical-scale expansion of human mesenchymal stem/stromal cells. Biotechnology and Bioengineering 111(6):1116-1127.

Doucet C, Ernou I, Zhang Y, Llense JR, Begot L, Holy X, Lataillade JJ. 2005. Platelet lysates promote mesenchymal stem cell expansion: a safety substitute for animal serum in cell-based therapy applications. J Cell Physiol 205(2):228-36.

References

Dreher L, Elvers-Hornung S, Brinkmann I, Huck V, Henschler R, Gloe T, Kluter H, Bieback K. 2013. Cultivation in human serum reduces adipose tissue-derived mesenchymal stromal cell adhesion to laminin and endothelium and reduces capillary entrapment. Stem Cells Dev 22(5):791-803.

Ellington AA, Kullo IJ, Bailey KR, Klee GG. 2010. Antibody-Based Protein Multiplex Platforms: Technical and Operational Challenges. Clinical Chemistry 56(2):186-193.

Erices A, Conget P, Minguell JJ. 2000. Mesenchymal progenitor cells in human umbilical cord blood. British Journal of Haematology 109(1):235-242.

Estrada JC, Torres Y, Benguria A, Dopazo A, Roche E, Carrera-Quintanar L, Perez RA, Enriquez JA, Torres R, Ramirez JC *and others*. 2013. Human mesenchymal stem cell-replicative senescence and oxidative stress are closely linked to aneuploidy. Cell Death Dis 4:e691.

Faris RA, Konkin T, Halpert G. 2001. Liver stem cells: a potential source of hepatocytes for the treatment of human liver disease. Artif Organs 25(7):513-21.

Farrington-Rock C, Crofts NJ, Doherty MJ, Ashton BA, Griffin-Jones C, Canfield AE. 2004. Chondrogenic and adipogenic potential of microvascular pericytes. Circulation 110(15):2226-32.

FDA. 2004. PAT - A framework for Innovative Pharmaceutical Development, Manufacturing and Quality Assurance. In: Center of Drug Evaluation and Research FaDA, editor.

FDA. 2008a. Content and Review of Chemistry, Manufacturing, and Control (CMC) Information for Human Gene Therapy Investigational New Drug Applications (INDs). In: Services USDoHaH, editor.

FDA. 2009. Guidance for Industry Q8(R2) Pharmaceutical Development In: Services USDoHaH, editor. www.fda.gov/downloads/Drugs/Guidances/ucm073507.pdf.

FDA. 2011a. Guidance for Industry. Potency tests for cellular and gene therapy products. In: Administration USFaD, editor. http://www.fda.gov/downloads/BiologicsBloodVaccines/GuidanceComplianceRegulatoryInformation/Guidances/CellularandGeneTherapy/UCM243392.pdf.

FDA U. 1997. FDA summary for basis of approval: BLA Ref No. 96-0372, Carticel. p 1-23.

FDA U. 1998. Guidance for Industry. Guidance for Human Somatic Cell Therapy and Gene Therapy. . In: Services UDoHaH, editor. Rockville, MD, USA.

FDA U. 2002. www.accessdata.fda.gov/scripts/cdrh/cfdocs/cfcfr/CFRSearch.cfm?fr=610.15. Code of Federal Regulations, general biological products standards, constituent materials.

.

FDA U. 2008b. Guidance for FDA Reviewers and Sponsors. Content and Review of Chemistry, Manufacturing, and Control (CMC) Information for Human Somatic Cell Therapy Investigational New Drug Applications (INDs). In: Services UDoHaH, editor. Rockville, MD, USA. p 1-39.

FDA U. 2010. 21 CFR 610.12. Code of Federal Regulations, general biological products standards, sterility www.accessdata.fda.gov/scripts/cdrh/cfdocs/cfcfr/CFRSearch.cfm?fr=610.12.

FDA U. 2011b. Final Guidance for Industry. Potency Tests for Cellular and Gene Therapy Products. In: Services UDoHaH, editor. Rockville, MD, USA. p 1-19.

Festjens N, Vanden Berghe T, Vandenabeele P. 2006. Necrosis, a well-orchestrated form of cell demise: signalling cascades, important mediators and concomitant immune response. Biochim Biophys Acta 1757(9-10):1371-87.

Friedens.Aj, Chailakh.Rk, Lalykina KS. 1970. DEVELOPMENT OF FIBROBLAST COLONIES IN MONOLAYER CULTURES OF GUINEA-PIG BONE MARROW AND SPLEEN CELLS. Cell and Tissue Kinetics 3(4):393-&.

Friedens.Aj, Deriglas.Uf, Kulagina NN, Panasuk AF, Rudakowa SF, Luria EA, Rudakow IA. 1974. PRECURSORS FOR FIBROBLASTS IN DIFFERENT POPULATIONS OF HEMATOPOIETIC CELLS AS DETECTED BY INVITRO COLONY ASSAY METHOD. Experimental Hematology 2(2):83-92.

Friedens.Aj, Piatetzk, II, Petrakov.Kv. 1966. OSTEOGENESIS IN TRANSPLANTS OF BONE MARROW CELLS. Journal of Embryology and Experimental Morphology 16:381-&.

Friedenstein AJ, Chailakhyan RK, Gerasimov UV. 1987. BONE-MARROW OSTEOGENIC STEM-CELLS - INVITRO CULTIVATION AND TRANSPLANTATION IN DIFFUSION-CHAMBERS. Cell and Tissue Kinetics 20(3):263-272.

Friedenstein AJ, Gorskaja UF, Kulagina NN. 1976. FIBROBLAST PRECURSORS IN NORMAL AND IRRADIATED MOUSE HEMATOPOIETIC ORGANS. Experimental Hematology 4(5):267-274.

Galipeau J. 2013. The mesenchymal stromal cells dilemma—does a negative phase III trial of random donor mesenchymal stromal cells in steroid-resistant graft-versus-host disease represent a death knell or a bump in the road? Cytotherapy 15(1):2-8.

Ganguly J, Vogel G. 2006. Process analytical technology (PAT) and scalable automation for bioprocess control and monitoring—A case study. Pharmaceutical Eng 26(1):1-9.

Gao F, He T, Wang H, Yu S, Yi D, Liu W, Cai Z. 2007. A promising strategy for the treatment of ischemic heart disease: Mesenchymal stem cell-mediated vascular endothelial growth factor gene transfer in rats. The Canadian Journal of Cardiology 23(11):891-898.

References

Gao T, Zhang N, Wang Z, Wang Y, Liu Y, Ito Y, Zhang P. 2015. Biodegradable Microcarriers of Poly(Lactide-co-Glycolide) and Nano-Hydroxyapatite Decorated with IGF-1 via Polydopamine Coating for Enhancing Cell Proliferation and Osteogenic Differentiation. Macromol Biosci.

Ge J, Guo L, Wang S, Zhang Y, Cai T, Zhao RC, Wu Y. 2014. The size of mesenchymal stem cells is a significant cause of vascular obstructions and stroke. Stem Cell Rev 10(2):295-303.

Gigout A, Buschmann MD, Jolicoeur M. 2008. The fate of Pluronic F-68 in chondrocytes and CHO cells. Biotechnol Bioeng 100(5):975-87.

Glacken MW. 1988. Catabolic Control of Mammalian Cell Culture. Nat Biotech 6(9):1041-1050.

Goldring CEP, Duffy PA, Benvenisty N, Andrews PW, Ben-David U, Eakins R, French N, Hanley NA, Kelly L, Kitteringham NR *and others*. 2011. Assessing the Safety of Stem Cell Therapeutics. Cell Stem Cell 8(6):618-628.

Goujon E. 1869. Recherches experimentales sur les proprietes physiologiques de la moelle des os. Journal de L'Anat et de La Physiol. 6:399-412.

Grayson WL, Zhao F, Izadpanah R, Bunnell B, Ma T. 2006. Effects of hypoxia on human mesenchymal stem cell expansion and plasticity in 3D constructs. J Cell Physiol 207(2):331-9.

Guilloton F, Caron G, Menard C, Pangault C, Ame-Thomas P, Dulong J, De Vos J, Rossille D, Henry C, Lamy T *and others*. 2012. Mesenchymal stromal cells orchestrate follicular lymphoma cell niche through the CCL2-dependent recruitment and polarization of monocytes. Blood 119(11):2556-67.

Gurdon JB. 1962. DEVELOPMENTAL CAPACITY OF NUCLEI TAKEN FROM INTESTINAL EPITHELIUM CELLS OF FEEDING TADPOLES. Journal of Embryology and Experimental Morphology 10(4):622-&.

Hampson B. 2014. Closed Processing for Cell Therapies: Engineering Risk Reduction and Patient Safety during Manufacturing. Genetic Engineering & Biotechnology News 34(9).

Hampson B, Rowley J, Venturi N. 2008. Manufacturing Patient-Specific Cell Therapy Products. BioProcess International 6(8):60-72.

Hare JM, Traverse JH, Henry TD, Dib N, Strumpf RK, Schulman SP, Gerstenblith G, DeMaria AN, Denktas AE, Gammon RS *and others*. 2009. A randomized, double-blind, placebo-controlled, dose-escalation study of intravenous adult human mesenchymal stem cells (prochymal) after acute myocardial infarction. J Am Coll Cardiol 54(24):2277-86.

Hartmann I, Hollweck T, Haffner S, Krebs M, Meiser B, Reichart B, Eissner G. 2010. Umbilical cord tissue-derived mesenchymal stem cells grow best under GMP-compliant culture

conditions and maintain their phenotypic and functional properties. J Immunol Methods 363(1):80-9.

Hassan S, Simaria AS, Varadaraju H, Gupta S, Warren K, Farid SS. 2015. Allogeneic cell therapy bioprocess economics and optimization: downstream processing decisions. Regenerative Medicine 10(5):591-609.

Hatlapatka T, Moretti P, Lavrentieva A, Hass R, Marquardt N, Jacobs R, Kasper C. 2011. Optimization of culture conditions for the expansion of umbilical cord-derived mesenchymal stem or stromal cell-like cells using xeno-free culture conditions. Tissue Eng Part C Methods 17(4):485-93.

Hayman EG, Pierschbacher MD, Suzuki S, Ruoslahti E. 1985. Vitronectin--a major cell attachment-promoting protein in fetal bovine serum. Exp Cell Res 160(2):245-58.

Heathman T. 2015. Development of a controlled bioreactor process to drive the consistent manufacture of human mesenchymal stem cells from multiple donors. Cytotherapy 17(6):S81-S82.

Heathman TRJ, Glyn VAM, Picken A, Rafiq QA, Coopman K, Nienow AW, Kara B, Hewitt CJ. 2015a. Expansion, harvest and cryopreservation of human mesenchymal stem cells in a serum-free microcarrier process. Biotechnology and Bioengineering 112(8):1696-1707.

Heathman TRJ, Nienow AW, McCall MJ, Coopman K, Kara B, Hewitt CJ. 2015b. The translation of cell-based therapies: clinical landscape and manufacturing challenges. Regen Med 10(1):49-64.

Heathman TRJ, Rafiq QA, Chan AKC, Coopman K, Nienow AW, Kara B, Hewitt CJ. 2015c. Characterisation of human mesenchymal stem cells from multiple donors and the implications for large scale bioprocess development. Biochemical Engineering Journal *(in press)*((presented at ECI Conference on . Scale-up and Manufacture of Cell-based Therapies IV, San Diego, California, January 2015)).

Heathman TRJ, Rafiq QA, Coopman K, Nienow AW, Hewitt CJ. 2015d. Chapter 10: The scale-up of human mesenchymal stem cell expansion and recovery. (in Bioprocessing for Cell-Based Therapies). In: Sons JW, editor.

Heathman TRJ, Stolzing A, Fabian C, Rafiq QA, Coopman K, Nienow AW, Kara B, Hewitt CJ. 2015e. Serum-free process development: improving the yield and consistency of human mesenchymal stromal cell production. Cytotherapy 17(11):1524-1535.

Heid CA, Stevens J, Livak KJ, Williams PM. 1996. Real time quantitative PCR. Genome Research 6(10):986-994.

Heiskanen A, Satomaa T, Tiitinen S, Laitinen A, Mannelin S, Impola U, Mikkola M, Olsson C, Miller-Podraza H, Blomqvist M *and others*. 2007. N-glycolylneuraminic acid xenoantigen contamination of human embryonic and mesenchymal stem cells is substantially reversible. Stem Cells 25(1):197-202.

Herzog EL, Chai L, Krause DS. 2003. Plasticity of marrow-derived stem cells. Blood 102(10):3483-3493.

Hewitt CJ, Lee K, Nienow AW, Thomas RJ, Smith M, Thomas CR. 2011. Expansion of human mesenchymal stem cells on microcarriers. Biotechnol Lett 33(11):2325-35.

Higuera-Sierra G, Schop D, Janssen F, Dijkhuizen-Radersma R, Boxtel vAJB, Blitterswijk vCA. 2009. Quantifying in vitro growth and metabolism kinetics of human mesenchymal stem cells using a mathematical model. Tissue Engineering. Part A 15(9):2653 - 2663.

Higuera GA, Schop D, Spitters TW, van Dijkhuizen-Radersma R, Bracke M, de Bruijn JD, Martens D, Karperien M, van Boxtel A, van Blitterswijk CA. 2012. Patterns of amino acid metabolism by proliferating human mesenchymal stem cells. Tissue Eng Part A 18(5-6):654-64.

Honczarenko M, Le Y, Swierkowski M, Ghiran I, Glodek AM, Silberstein LE. 2006. Human bone marrow stromal cells express a distinct set of biologically functional chemokine receptors. Stem Cells 24(4):1030-41.

Hong SH, Gang EJ, Jeong JA, Ahn C, Hwang SH, Yang IH, Park HK, Han H, Kim H. 2005. In vitro differentiation of human umbilical cord blood-derived mesenchymal stem cells into hepatocyte-like cells. Biochem Biophys Res Commun 330(4):1153-61.

Horwitz EM. 2008. Mesenchymal stromal cells moving forward. Cytotherapy 10(1):5-6.

Horwitz EM, Dominici M. 2008. How do mesenchymal stromal cells exert their therapeutic benefit? Cytotherapy 10(8):771-4.

Horwitz EM, Gordon PL, Koo WK, Marx JC, Neel MD, McNall RY, Muul L, Hofmann T. 2002. Isolated allogeneic bone marrow-derived mesenchymal cells engraft and stimulate growth in children with osteogenesis imperfecta: Implications for cell therapy of bone. Proc Natl Acad Sci U S A 99(13):8932-7.

Horwitz EM, Prockop DJ, Fitzpatrick LA, Koo WW, Gordon PL, Neel M, Sussman M, Orchard P, Marx JC, Pyeritz RE *and others*. 1999. Transplantability and therapeutic effects of bone marrow-derived mesenchymal cells in children with osteogenesis imperfecta. Nat Med 5(3):309-13.

Hourd P, Chandra A, Alvey D, Ginty P, McCall M, Ratcliffe E, Rayment E, Williams DJ. 2014a. Qualification of academic facilities for small-scale automated manufacture of autologous cell-based products. Regen Med 9(6):799-815.

Hourd P, Chandra A, Medcalf N, Williams DJ. 2008. Regulatory challenges for the manufacture and scale-out of autologous cell therapies. StemBook. Cambridge MA: : 2014 Paul Hourd, Amit Chandra, Nick Medcalf and David J. Williams.

Hourd P, Ginty P, Chandra A, Williams DJ. 2014b. Manufacturing models permitting roll out/scale out of clinically led autologous cell therapies: regulatory and scientific challenges for comparability. Cytotherapy 16(8):1033-47.

Huttenlocher A, Horwitz AR. 2011. Integrins in cell migration. Cold Spring Harb Perspect Biol 3(9):a005074.

Hwang SM, See C-j, Choi J, Kim SY, Choi Q, Kim JA, Kwon J, Park SN, Im K, Oh I-H *and others*. 2013. The application of an in situ karyotyping technique for mesenchymal stromal cells: a validation and comparison study with classical G-banding. Exp Mol Med 45:e68.

ICH. 2005. Quality Risk Management Q9. In: Group IEW, editor.

International Conference on Harmonisation of Technical Requirements for Registration of Pharmaceuticals for Human Use I. 2008. Pharmaceutical Quality System Q10.

Isakova IA, Dufour J, Lanclos C, Bruhn J, Phinney DG. 2010. Cell-dose-dependent increases in circulating levels of immune effector cells in rhesus macaques following intracranial injection of allogeneic MSCs. Exp Hematol 38(10):957-967 e1.

Isakova IA, Lanclos C, Bruhn J, Kuroda MJ, Baker KC, Krishnappa V, Phinney DG. 2014. Allo-reactivity of mesenchymal stem cells in rhesus macaques is dose and haplotype dependent and limits durable cell engraftment in vivo. PLoS One 9(1):e87238.

Jaiswal N, Haynesworth SE, Caplan AI, Bruder SP. 1997. Osteogenic differentiation of purified, culture-expanded human mesenchymal stem cells in vitro. Journal of Cellular Biochemistry 64(2):295-312.

James D. 2011. Therapies of Tomorrow Require More Than Factories from the Past. BioProcess International 9:4-11.

Janowski M, Lyczek A, Engels C, Xu J, Lukomska B, Bulte JW, Walczak P. 2013. Cell size and velocity of injection are major determinants of the safety of intracarotid stem cell transplantation. J Cereb Blood Flow Metab 33(6):921-7.

Jiang Y, Vaessen B, Lenvik T, Blackstad M, Reyes M, Verfaillie CM. 2002a. Multipotent progenitor cells can be isolated from postnatal murine bone marrow, muscle, and brain. Exp Hematol 30(8):896-904.

Jiang YH, Jahagirdar BN, Reinhardt RL, Schwartz RE, Keene CD, Ortiz-Gonzalez XR, Reyes M, Lenvik T, Lund T, Blackstad M *and others*. 2002b. Pluripotency of mesenchymal stem cells derived from adult marrow. Nature 418(6893):41-49.

Joeris K, Frerichs JG, Konstantinov K, Scheper T. 2002. In-situ microscopy: Online process monitoring of mammalian cell cultures. Cytotechnology 38(1-3):129-34.

Johnstone B, Hering TM, Caplan AI, Goldberg VM, Yoo JU. 1998. In vitro chondrogenesis of bone marrow-derived mesenchymal progenitor cells. Experimental Cell Research 238(1):265-272.

Jones E, English A, Churchman SM, Kouroupis D, Boxall SA, Kinsey S, Giannoudis PG, Emery P, McGonagle D. 2010. Large-scale extraction and characterization of CD271+ multipotential stromal cells from trabecular bone in health and osteoarthritis: implications for bone regeneration strategies based on uncultured or minimally cultured multipotential stromal cells. Arthritis Rheum 62(7):1944-54.

Jones EA, English A, Kinsey SE, Straszynski L, Emery P, Ponchel F, McGonagle D. 2006. Optimization of a flow cytometry-based protocol for detection and phenotypic characterization of multipotent mesenchymal stromal cells from human bone marrow. Cytometry B Clin Cytom 70(6):391-9.

Jorgensen P, Tyers M. 2004. How cells coordinate growth and division. Curr Biol 14(23):R1014-27.

Jung S, Panchalingam KM, Rosenberg L, Behie LA. 2012. Ex Vivo Expansion of Human Mesenchymal Stem Cells in Defined Serum-Free Media. Stem Cells International 2012:21.

Jung S, Sen A, Rosenberg L, Behie LA. 2010. Identification of growth and attachment factors for the serum-free isolation and expansion of human mesenchymal stromal cells. Cytotherapy 12(5):637-57.

Kang SG, Shinojima N, Hossain A, Gumin J, Yong RL, Colman H, Marini F, Andreeff M, Lang FF. 2010. Isolation and Perivascular Localization of Mesenchymal Stem Cells From Mouse Brain. Neurosurgery 67(3):711-720.

Kantoff PW, Higano CS, Shore ND, Berger ER, Small EJ, Penson DF, Redfern CH, Ferrari AC, Dreicer R, Sims RB *and others*. 2010. Sipuleucel-T immunotherapy for castration-resistant prostate cancer. N Engl J Med 363(5):411-22.

Karp JM, Leng Teo GS. 2009. Mesenchymal Stem Cell Homing: The Devil Is in the Details. Cell Stem Cell 4(3):206-216.

References

Kasten P, Beyen I, Egermann M, Suda AJ, Moghaddam AA, Zimmermann G, Luginbuhl R. 2008. Instant stem cell therapy: characterization and concentration of human mesenchymal stem cells in vitro. Eur Cell Mater 16:47-55.

Kasuto H, Drori-carmi N, Zohar B; Pluristem Ltd. (Haifa, IL) assignee. 2014. METHODS AND SYSTEMS FOR HARVESTING CELLS.

Katagiri T, Yamaguchi A, Komaki M, Abe E, Takahashi N, Ikeda T, Rosen V, Wozney JM, Fujisawasehara A, Suda T. 1994. BONE MORPHOGENETIC PROTEIN-2 CONVERTS THE DIFFERENTIATION PATHWAY OF C2C12 MYOBLASTS INTO THE OSTEOBLAST LINEAGE. Journal of Cell Biology 127(6):1755-1766.

Kedong S, Xiubo F, Tianqing L, Macedo HM, LiLi J, Meiyun F, Fangxin S, Xuehu M, Zhanfeng C. 2010. Simultaneous expansion and harvest of hematopoietic stem cells and mesenchymal stem cells derived from umbilical cord blood. J Mater Sci Mater Med 21(12):3183-93.

Kehoe DE, Jing D, Lock LT, Tzanakakis ES. 2010. Scalable stirred-suspension bioreactor culture of human pluripotent stem cells. Tissue Eng Part A 16(2):405-21.

Kern S, Eichler H, Stoeve J, Kluter H, Bieback K. 2006. Comparative analysis of mesenchymal stem cells from bone marrow, umbilical cord blood, or adipose tissue. Stem Cells 24(5):1294-301.

Kharlamova LA. 1975. INHIBITORY FORMATION OF COLONIES OF HUMAN BONE MARROW STROMAL CELLS UNDER THE EFFECT OF THE FACTOR FORMED IN-VITRO BY PERIPHERAL BLOOD LEUKOCYTES. Byulleten' Eksperimental'noi Biologii i Meditsiny 80(7):89-91.

Kilburn DG, Webb FC. 2000. The cultivation of animal cells at controlled dissolved oxygen partial pressure. Reprinted from Biotechnology and Bioengineering Vol. X, Issue 6, Pages 801-814 (1968). Biotechnol Bioeng 67(6):657-70.

Kim J, Seong J, Lee B, Hashimura Y, Groux D, Oh D. 2013. Evaluation of a novel pneumatic bioreactor system for culture of recombinant Chinese hamster ovary cells. Biotechnology and Bioprocess Engineering 18(4):801-807.

Kinnaird T, Stabile E, Burnett MS, Shou M, Lee CW, Barr S, Fuchs S, Epstein SE. 2004. Local delivery of marrow-derived stromal cells augments collateral perfusion through paracrine mechanisms. Circulation 109(12):1543-1549.

Kirouac DC, Zandstra PW. 2008. The systematic production of cells for cell therapies. Cell Stem Cell 3(4):369-81.

Klyushnenkova E, Mosca JD, Zernetkina V, Majumdar MK, Beggs KJ, Simonetti DW, Deans RJ, McIntosh KR. 2005. T cell responses to allogeneic human mesenchymal stem cells: immunogenicity, tolerance, and suppression. J Biomed Sci 12(1):47-57.

Kocaoemer A, Kern S, Kluter H, Bieback K. 2007. Human AB serum and thrombin-activated platelet-rich plasma are suitable alternatives to fetal calf serum for the expansion of mesenchymal stem cells from adipose tissue. Stem Cells 25(5):1270-8.

Kogler G, Sensken S, Airey JA, Trapp T, Muschen M, Feldhahn N, Liedtke S, Sorg RV, Fischer J, Rosenbaum C *and others*. 2004. A new human somatic stem cell from placental cord blood with intrinsic pluripotent differentiation potential. Journal of Experimental Medicine 200(2):123-135.

Kolf CM, Cho E, Tuan RS. 2007. Mesenchymal stromal cells. Biology of adult mesenchymal stem cells: regulation of niche, self-renewal and differentiation. Arthritis Res Ther 9(1):204.

Kubista M, Andrade JM, Bengtsson M, Forootan A, Jonak J, Lind K, Sindelka R, Sjoback R, Sjogreen B, Strombom L *and others*. 2006. The real-time polymerase chain reaction. Molecular Aspects of Medicine 27(2-3):95-125.

Kuczewski M, Schirmer E, Lain B, Zarbis-Papastoitsis G. 2011. A single-use purification process for the production of a monoclonal antibody produced in a PER.C6 human cell line. Biotechnol J 6(1):56-65.

Kuznetsov SA, Mankani MH, Gronthos S, Satomura K, Bianco P, Robey PG. 2001. Circulating skeletal stem cells. Journal of Cell Biology 153(5):1133-1139.

Langheinrich C, Nienow AW, Eddleston T, Stevenson NC, Emery AN, Clayton TM, Slater NKH. 2002. Oxygen Transfer in Stirred Bioreactors Under Animal Cell Culture Conditions. Food and Bioproducts Processing 80(1):39-44.

Lavery M, Nienow AW. 1987. Oxygen transfer in animal cell culture medium. Biotechnol Bioeng 30(3):368-73.

Lavon N, Yanuka O, Benvenisty N. 2004. Differentiation and isolation of hepatic-like cells from human embryonic stem cells. Differentiation 72(5):230-8.

Lavrentieva A, Majore I, Kasper C, Hass R. 2010a. Effects of hypoxic culture conditions on umbilical cord-derived human mesenchymal stem cells. Cell Communication and Signaling 8(1):1-9.

Lavrentieva A, Majore I, Kasper C, Hass R. 2010b. Effects of hypoxic culture conditions on umbilical cord-derived human mesenchymal stem cells. Cell Commun Signal 8:18.

Lavrentieva A, Majore I, Kasper C, Hass R. 2010c. Effects of hypoxic culture conditions on umbilical cord-derived human mesenchymal stem cells. Cell Communication and Signaling 8(18):1-9.

Le Blanc K. 2006. Mesenchymal stromal cells: Tissue repair and immune modulation. Cytotherapy 8(6):559-61.

Le Blanc K, Frassoni F, Ball L, Locatelli F, Roelofs H, Lewis I, Lanino E, Sundberg B, Bernardo ME, Remberger M *and others*. 2008. Mesenchymal stem cells for treatment of steroid-resistant, severe, acute graft-versus-host disease: a phase II study. Lancet 371(9624):1579-86.

Le Blanc K, Rasmusson I, Sundberg B, Gotherstrom C, Hassan M, Uzunel M, Ringden O. 2004. Treatment of severe acute graft-versus-host disease with third party haploidentical mesenchymal stem cells. Lancet 363(9419):1439-41.

Le Blanc K, Tammik C, Rosendahl K, Zetterberg E, Ringden O. 2003. HLA expression and immunologic properties of differentiated and undifferentiated mesenchymal stem cells. Exp Hematol 31(10):890-6.

Lee B, Fang D, Croughan M, Carrondo M, Paik S-H. 2011. Characterization of novel pneumatic mixing for single-use bioreactor application. BMC Proceedings 5(8):1-2.

Lefort N, Perrier AL, Laabi Y, Varela C, Peschanski M. 2009. Human embryonic stem cells and genomic instability. Regen Med 4(6):899-909.

Li B, Moshfegh C, Lin Z, Albuschies J, Vogel V. 2013. Mesenchymal Stem Cells Exploit Extracellular Matrix as Mechanotransducer. Sci. Rep. 3.

Li MD, Atkins H, Bubela T. 2014. The global landscape of stem cell clinical trials. Regen Med 9(1):27-39.

Li YM, Schilling T, Benisch P, Zeck S, Meissner-Weigl J, Schneider D, Limbert C, Seufert J, Kassem M, Schutze N *and others*. 2007. Effects of high glucose on mesenchymal stem cell proliferation and differentiation. Biochem Biophys Res Commun 363(1):209-15.

Liu JY, Hafner J, Dragieva G, Burg G. 2004. Bioreactor microcarrier cell culture system (Bio-MCCS) for large-scale production of autologous melanocytes. Cell Transplant 13(7-8):809-16.

Liu Y, Xu X, Ma X, Martin-Rendon E, Watt S, Cui Z. 2010. Cryopreservation of human bone marrow-derived mesenchymal stem cells with reduced dimethylsulfoxide and well-defined freezing solutions. Biotechnol Prog 26(6):1635-43.

Livak KJ, Schmittgen TD. 2001. Analysis of relative gene expression data using real-time quantitative PCR and the 2(T)(-Delta Delta C) method. Methods 25(4):402-408.

Lo T, Ho JH, Yang M-H, Lee OK. 2011. Glucose Reduction Prevents Replicative Senescence and Increases Mitochondrial Respiration in Human Mesenchymal Stem Cells. Cell Transplantation 20:813-825.

Lu B, Malcuit C, Wang S, Girman S, Francis P, Lemieux L, Lanza R, Lund R. 2009. Long-term safety and function of RPE from human embryonic stem cells in preclinical models of macular degeneration. Stem Cells 27(9):2126-35.

Lubkowska A, Dolegowska B, Banfi G. 2012. Growth factor content in PRP and their applicability in medicine. J Biol Regul Homeost Agents 26(2 Suppl 1):3S-22S.

Luo W, Xiong W, Zhou J, Fang Z, Chen W, Fan Y, Li F. 2011. Laminar shear stress delivers cell cycle arrest and anti-apoptosis to mesenchymal stem cells. Acta Biochimica et Biophysica Sinica 43(3):210-216.

Lysaght MJ, Hazlehurst AL. 2004. Tissue engineering: the end of the beginning. Tissue Eng 10(1-2):309-20.

Majore I, Moretti P, Hass R, Kasper C. 2009. Identification of subpopulations in mesenchymal stem cell-like cultures from human umbilical cord. Cell Communication and Signaling : CCS 7:6-6.

Majumdar MK, Thiede MA, Mosca JD, Moorman M, Gerson SL. 1998. Phenotypic and functional comparison of cultures of marrow-derived mesenchymal stem cells (MSCs) and stromal cells. J Cell Physiol 176(1):57-66.

Mason C. 2013. House of Lords Regenerative Medicine Report. In: Committee SaT, editor. London.

Mason C, Brindley DA, Culme-Seymour EJ, Davie NL. 2011. Cell therapy industry: billion dollar global business with unlimited potential. Regen Med 6(3):265-72.

Mason C, Dunnill P. 2007. Translational regenerative medicine research: essential to discovery and outcome. Regenerative Medicine 2(3):227-229.

Mason C, Dunnill P. 2008. A brief definition of regenerative medicine. Regen Med 3(1):1-5.

Mason C, Hoare M. 2006. Regenerative medicine bioprocessing: the need to learn from the experience of other fields. Regenerative Medicine 1(5):615-623.

Mason C, Manzotti E. 2009. Regen: the industry responsible for cell-based therapies. Regen Med 4(6):783-5.

Mason C, Manzotti E. 2010. The Translation Cycle: round and round in cycles is the only way forward for regenerative medicine. Regen Med 5(2):153-5.

Mather ML, Crowe JA, Morgan SP, White LJ, Shakesheff KM, Howdle SM, Thomas RJ, Byrne HM, Waters SL, Williams DJ. 2009. Remedi: A Research Consortium Applying Engineering

Strategies to Establish Regenerative Medicine as a New Industry. In: VanderSloten J, Verdonck P, Nyssen M, Haueisen J, editors. 4th European Conference of the International Federation for Medical and Biological Engineering. New York: Springer. p 2209-2212.

Maziarz RT, Devos T, Bachier CR, Goldstein SC, Leis JF, Devine SM, Meyers G, Gajewski JL, Maertens J, Deans RJ *and others*. 2015. Single and multiple dose MultiStem (multipotent adult progenitor cell) therapy prophylaxis of acute graft-versus-host disease in myeloablative allogeneic hematopoietic cell transplantation: a phase 1 trial. Biol Blood Marrow Transplant 21(4):720-8.

Meier SJ, Hatton TA, Wang DI. 1999. Cell death from bursting bubbles: role of cell attachment to rising bubbles in sparged reactors. Biotechnol Bioeng 62(4):468-78.

Meirelles LDS, Chagastelles PC, Nardi NB. 2006. Mesenchymal stem cells reside in virtually all post-natal organs and tissues. Journal of Cell Science 119(11):2204-2213.

Mendicino M, Bailey AM, Wonnacott K, Puri RK, Bauer SR. 2014. MSC-based product characterization for clinical trials: an FDA perspective. Cell Stem Cell 14(2):141-5.

Merten OW, Dante J, Noguiez-Hellin P, Laune S, Klatzmann D, Salzmann JL. 1997. New Process for Cell Detachment: Use of Heparin. In: Carrondo MT, Griffiths B, Moreira JP, editors. Animal Cell Technology: Springer Netherlands. p 343-348.

Mikola M, Seto J, Amanullah A. 2007. Evaluation of a novel Wave Bioreactor® cellbag for aerobic yeast cultivation. Bioprocess and Biosystems Engineering 30(4):231-241.

Mimeault M, Batra SK. 2006. Concise review: Recent advances on the significance of stem cells in tissue regeneration and cancer therapies. Stem Cells 24(11):2319-2345.

Mimeault M, Hauke R, Batra SK. 2007. Stem cells: A revolution in therapeutics - Recent advances in stem cell biology and their therapeutic applications in regenerative medicine and cancer therapies. Clinical Pharmacology & Therapeutics 82(3):252-264.

Mitchell PD, Ratcliffe E, Hourd P, Williams DJ, Thomas RJ. 2014. A quality-by-design approach to risk reduction and optimization for human embryonic stem cell cryopreservation processes. Tissue Eng Part C Methods 20(12):941-50.

Moelker AD, Baks T, Wever KM, Spitskovsky D, Wielopolski PA, van Beusekom HM, van Geuns RJ, Wnendt S, Duncker DJ, van der Giessen WJ. 2007. Intracoronary delivery of umbilical cord blood derived unrestricted somatic stem cells is not suitable to improve LV function after myocardial infarction in swine. J Mol Cell Cardiol 42(4):735-45.

Mohyeldin A, Garzón-Muvdi T, Quiñones-Hinojosa A. 2010. Oxygen in Stem Cell Biology: A Critical Component of the Stem Cell Niche. Cell Stem Cell 7(2):150-161.

References

Moll G, Alm JJ, Davies LC, von Bahr L, Heldring N, Stenbeck-Funke L, Hamad OA, Hinsch R, Ignatowicz L, Locke M *and others*. 2014a. Do cryopreserved mesenchymal stromal cells display impaired immunomodulatory and therapeutic properties? Stem Cells 32(9):2430-42.

Moll G, Alm JJ, Davies LC, von Bahr L, Heldring N, Stenbeck-Funke L, Hamad OA, Hinsch R, Ignatowicz L, Locke M *and others*. 2014b. Do Cryopreserved Mesenchymal Stromal Cells Display Impaired Immunomodulatory and Therapeutic Properties? STEM CELLS 32(9):2430-2442.

Moon YJ, Lee MW, Yang MS, Kim SK, Park JS, Kim HC, Kim HS, Lee KH, Kim YJ, Choi J. 2005. Expression profile of genes representing varied spectra of cell lineages in human umbilical cord blood-derived mesenchymal stem cells. Acta Haematol 114(2):117-20.

Mostafa SS, Gu X. 2003. Strategies for improved dCO2 removal in large-scale fed-batch cultures. Biotechnol Prog 19(1):45-51.

Mullis K, Faloona F, Scharf S, Saiki R, Horn G, Erlich H. 1992. Specific enzymatic amplification of DNA in vitro: the polymerase chain reaction. 1986. Biotechnology (Reading, Mass.) 24:17-27.

Muntion S, Sanchez-Guijo FM, Carrancio S, Villaron E, Lopez O, Diez-Campelo M, San Miguel JF, del Canizo MC. 2012. Optimisation of mesenchymal stromal cells karyotyping analysis: implications for clinical use. Transfus Med 22(2):122-7.

Naing MW, Gibson DA, Hourd P, Gomez SG, Horton RB, Segal J, Williams DJ. 2015a. Improving umbilical cord blood processing to increase total nucleated cell count yield and reduce cord input wastage by managing the consequences of input variation. Cytotherapy 17(1):58-67.

Naing MW, Gibson DA, Hourd P, Gomez SG, Horton RBV, Segal J, Williams DJ. 2015b. Improving umbilical cord blood processing to increase total nucleated cell count yield and reduce cord input wastage by managing the consequences of input variation. Cytotherapy 17(1):58-67.

Nienow AW. 1997. The suspension of solid particles. In: Harnby N, Edwards MF, Nienow AW (eds) Mixing in the process industries, 2nd edn.: Butterworth Heinemann, London. p 364-393.

Nienow AW. 2003. Aeration-biotechnology. In: Kirk Othmer encyclopaedia of chemical technology, 5th edn.: Wiley, New York.

Nienow AW. 2006. Reactor engineering in large scale animal cell culture. Cytotechnology 50(1-3):9-33.

References

Nienow AW, Hewitt CJ, Heathman TRJ, Coopman K, Rafiq QA. 2015a. Bioreactor Engineering Fundamentals for Stem Cell Manufacturing (In Stem Cell Manufacturing). In: Elsevier, editor.

Nienow AW, Hewitt CJ, Heathman TRJ, Glyn VAM, Fonte GN, Hanga MP, Coopman K, Rafiq QA. 2015b. Agitation Conditions for the Culture and Detachment of hMSCs from Microcarriers in Multiple Bioreactor Platforms. Biochemical Engineering Journal (in press).

Nienow AW, Langheinrich C, Stevenson NC, Emery AN, Clayton TM, Slater NK. 1996. Homogenisation and oxygen transfer rates in large agitated and sparged animal cell bioreactors: Some implications for growth and production. Cytotechnology 22(1-3):87-94.

Nienow AW, Rafiq QA, Coopman K, Hewitt CJ. 2014. A potentially scalable method for the harvesting of hMSCs from microcarriers. Biochemical Engineering Journal 85(0):79-88.

Nienow AW, Rielly CD, Brosnan K, Bargh N, Lee K, Coopman K, Hewitt CJ. 2013. The physical characterisation of a microscale parallel bioreactor platform with an industrial CHO cell line expressing an IgG4. Biochemical Engineering Journal 76(0):25-36.

Noaksson K, Zoric N, Zeng X, Rao MS, Hyllner J, Semb H, Kubista M, Sartipy P. 2005. Monitoring differentiation of human embryonic stem cells using real-time PCR. Stem Cells 23(10):1460-7.

O'Cearbhaill ED, Ng KS, Karp JM. 2014. Emerging medical devices for minimally invasive cell therapy. Mayo Clin Proc 89(2):259-73.

Oh SH, Hatch HM, Petersen BE. 2002. Hepatic oval 'stem' cell in liver regeneration. Semin Cell Dev Biol 13(6):405-9.

Oh SKW, Chen AK, Mok Y, Chen X, Lim UM, Chin A, Choo ABH, Reuveny S. 2009. Long-term microcarrier suspension cultures of human embryonic stem cells. Stem Cell Research 2(3):219-230.

Oh SKW, Nienow AW, Al-Rubeai M, Emery AN. 1989. The effects of agitation intensity with and without continuous sparging on the growth and antibody production of hybridoma cells. Journal of Biotechnology 12(1):45-61.

Owen M, Friedenstein AJ. 1988. STROMAL STEM-CELLS - MARROW-DERIVED OSTEOGENIC PRECURSORS. Ciba Foundation Symposia 136:42-60.

Ozturk SS, Palsson BO. 1991. Growth, metabolic, and antibody production kinetics of hybridoma cell culture: 2. Effects of serum concentration, dissolved oxygen concentration, and medium pH in a batch reactor. Biotechnol Prog 7(6):481-94.

Pal R, Hanwate M, Totey SM. 2008. Effect of holding time, temperature and different parenteral solutions on viability and functionality of adult bone marrow-derived mesenchymal stem cells before transplantation. J Tissue Eng Regen Med 2(7):436-44.

Pattappa G, Heywood HK, de Bruijn JD, Lee DA. 2011. The metabolism of human mesenchymal stem cells during proliferation and differentiation. J Cell Physiol 226(10):2562-70.

Pattasseril J, Varadaraju H, Lock L, Rowley JA. 2013. Downstream Technology Landscape for Large-Scale Therapeutic Cell Processing. BioProcess International 11(3):38-47.

Peault B, Rudnicki M, Torrente Y, Cossu G, Tremblay JP, Partridge T, Gussoni E, Kunkel LM, Huard J. 2007. Stem and progenitor cells in skeletal muscle development, maintenance, and therapy. Mol Ther 15(5):867-77.

Peled A, Petit I, Kollet O, Magid M, Ponomaryov T, Byk T, Nagler A, Ben-Hur H, Many A, Shultz L *and others*. 1999. Dependence of human stem cell engraftment and repopulation of NOD/SCID mice on CXCR4. Science 283(5403):845-8.

Pensler JM, Bauer BS, Christensen M, Jones JCR. 1988. DIFFERENTIATION AND FORMATION OF BONE TISSUE IN CELL CULTURE FROM CHICK EMBRYO MESENCHYMAL PROGENITOR CELLS. Surgical Forum (Chicago) 39:616-618.

Pereira RF, Halford KW, O'Hara MD, Leeper DB, Sokolov BP, Pollard MD, Bagasra O, Prockop DJ. 1995. Cultured adherent cells from marrow can serve as long-lasting precursor cells for bone, cartilage, and lung in irradiated mice. Proc Natl Acad Sci U S A 92(11):4857-61.

Pereira RF, O'Hara MD, Laptev AV, Halford KW, Pollard MD, Class R, Simon D, Livezey K, Prockop DJ. 1998. Marrow stromal cells as a source of progenitor cells for nonhematopoietic tissues in transgenic mice with a phenotype of osteogenesis imperfecta. Proc Natl Acad Sci U S A 95(3):1142-7.

Peters JM, Ansari MQ. 2011. Multiparameter Flow Cytometry in the Diagnosis and Management of Acute Leukemia. Archives of Pathology & Laboratory Medicine 135(1):44-54.

Petersen BE, Bowen WC, Patrene KD, Mars WM, Sullivan AK, Murase N, Boggs SS, Greenberger JS, Goff JP. 1999. Bone marrow as a potential source of hepatic oval cells. Science 284(5417):1168-70.

Pittenger MF, Le Blanc K, Phinney DG, Chan JKY. 2015. MSCs: Scientific Support for Multiple Therapies. Stem Cells International 2015:2.

Pittenger MF, Mackay AM, Beck SC, Jaiswal RK, Douglas R, Mosca JD, Moorman MA, Simonetti DW, Craig S, Marshak DR. 1999. Multilineage potential of adult human mesenchymal stem cells. Science 284(5411):143-7.

Pittenger MF, Martin BJ. 2004. Mesenchymal stem cells and their potential as cardiac therapeutics. Circulation Research 95(1):9-20.

Pochampally R. 2008. Colony forming unit assays for MSCs. Methods Mol Biol 449:83-91.

Pochampally RR, Smith JR, Ylostalo J, Prockop DJ. 2004. Serum deprivation of human marrow stromal cells (hMSCs) selects for a subpopulation of early progenitor cells with enhanced expression of OCT-4 and other embryonic genes. Blood 103(5):1647-52.

Ponomaryov T, Peled A, Petit I, Taichman RS, Habler L, Sandbank J, Arenzana-Seisdedos F, Magerus A, Caruz A, Fujii N *and others*. 2000. Induction of the chemokine stromal-derived factor-1 following DNA damage improves human stem cell function. J Clin Invest 106(11):1331-9.

Prado-Lopez S, Conesa A, Armiñán A, Martínez-Losa M, Escobedo-Lucea C, Gandia C, Tarazona S, Melguizo D, Blesa D, Montaner D *and others*. 2010. Hypoxia Promotes Efficient Differentiation of Human Embryonic Stem Cells to Functional Endothelium. STEM CELLS 28(3):407-418.

Prasad VK, Lucas KG, Kleiner GI, Talano JA, Jacobsohn D, Broadwater G, Monroy R, Kurtzberg J. 2011. Efficacy and safety of ex vivo cultured adult human mesenchymal stem cells (Prochymal) in pediatric patients with severe refractory acute graft-versus-host disease in a compassionate use study. Biol Blood Marrow Transplant 17(4):534-41.

Preffer F, Dombkowski D. 2009. Advances in Complex Multiparameter Flow Cytometry Technology: Applications in Stem Cell Research. Cytometry Part B-Clinical Cytometry 76B(5):295-314.

Prockop DJ. 1997. Marrow stromal cells as steam cells for nonhematopoietic tissues. Science 276(5309):71-74.

Qu-Petersen Z, Deasy B, Jankowski R, Ikezawa M, Cummins J, Pruchnic R, Mytinger J, Cao B, Gates C, Wernig A *and others*. 2002. Identification of a novel population of muscle stem cells in mice: potential for muscle regeneration. J Cell Biol 157(5):851-64.

Rafiq QA, Brosnan KM, Coopman K, Nienow AW, Hewitt CJ. 2013a. Culture of human mesenchymal stem cells on microcarriers in a 5 l stirred-tank bioreactor. Biotechnol Lett 35(8):1233-45.

Rafiq QA, Coopman K, Hewitt CJ. 2013b. Scale-up of human mesenchymal stem cell culture: current technologies and future challenges. Current Opinion in Chemical Engineering 2(1):8-16.

Rafiq QA, Coopman K, Nienow AW, Hewitt CJ. 2013c. A quantitative approach for understanding small-scale human mesenchymal stem cell culture – implications for large-scale bioprocess development. Biotechnology Journal 8(4):459-471.

Rafiq QA, Heathman TRJ, Coopman K, Nienow AW, Hewitt CJ. 2015a. Chapter 10. Scale-up of stem cell manufacture for cell therapy needs in "Bioreactors: Design, Operation and Novel Applications". Wiley VCH.

Rafiq QA, Heathman TRJ, Coopman K, Nienow AW, Hewitt CJ. 2015b. Culture of human mesenchymal stem cells on microcarriers in multiple stirred-tank bioreactor platforms. (In Bioreactors for Stem Cells Biology: Methods and Protocols). In: Biology SsMiM, editor.

Rasini V, Dominici M, Kluba T, Siegel G, Lusenti G, Northoff H, Horwitz EM, Schafer R. 2013. Mesenchymal stromal/stem cells markers in the human bone marrow. Cytotherapy 15(3):292-306.

Rayment EA, Williams DJ. 2010. Concise review: mind the gap: challenges in characterizing and quantifying cell- and tissue-based therapies for clinical translation. Stem Cells 28(5):996-1004.

Reya T, Morrison SJ, Clarke MF, Weissman IL. 2001. Stem cells, cancer, and cancer stem cells. Nature 414(6859):105-111.

Reyes M, Verfaillie CM. 2001. Characterization of multipotent adult progenitor cells, a subpopulation of mesenchymal stem cells. In: Orlic D, Brummendorf TH, Sharkis SJ, Kanz L, editors. Hematopoietic Stem Cells 2000 Basic and Clinical Sciences. New York: New York Acad Sciences. p 231-235.

Rich IN, Hall KM. 2005. Validation and development of a predictive paradigm for hemotoxicology using a multifunctional bioluminescence colony-forming proliferation assay. Toxicol Sci 87(2):427-41.

Riekstina U, Cakstina I, Parfejevs V, Hoogduijn M, Jankovskis G, Muiznieks I, Muceniece R, Ancans J. 2009. Embryonic stem cell marker expression pattern in human mesenchymal stem cells derived from bone marrow, adipose tissue, heart and dermis. Stem Cell Rev 5(4):378-86.

Rodrigues JP, Paraguassu-Braga FH, Carvalho L, Abdelhay E, Bouzas LF, Porto LC. 2008. Evaluation of trehalose and sucrose as cryoprotectants for hematopoietic stem cells of umbilical cord blood. Cryobiology 56(2):144-51.

Rowley J, Abraham E, Campbell A, Brandwein H, Oh S. 2012a. Meeting lot-size challenges of manufacturing adherent cells for therapy. BioProcess International 10(1):16-22.

Rowley J, Abraham E, Campbell A, Brandwein H, Oh S. 2012b. Meeting Lot-Size Challenges of Manufacturing Adherent Cells for Therapy. BioProcess International 10(3):16-22.

Ruan ZB, Zhu L, Yin YG, Chen GC. 2014. Karyotype stability of human umbilical cord-derived mesenchymal stem cells during culture. Exp Ther Med 8(5):1508-1512.

S. Rathore A, Kapoor G, Flickinger MC. 2009. Process Analytical Technology: Strategies for Biopharmaceuticals. Encyclopedia of Industrial Biotechnology: John Wiley & Sons, Inc.

Saiki RK, Gelfand DH, Stoffel S, Scharf SJ, Higuchi R, Horn GT, Mullis KB, Erlich HA. 1988. PRIMER-DIRECTED ENZYMATIC AMPLIFICATION OF DNA WITH A THERMOSTABLE DNA-POLYMERASE. Science 239(4839):487-491.

Saiki RK, Scharf S, Faloona F, Mullis KB, Horn GT, Erlich HA, Arnheim N. 1985. ENZYMATIC AMPLIFICATION OF BETA-GLOBIN GENOMIC SEQUENCES AND RESTRICTION SITE ANALYSIS FOR DIAGNOSIS OF SICKLE-CELL ANEMIA. Science 230(4732):1350-1354.

Sakaguchi Y, Sekiya I, Yagishita K, Muneta T. 2005. Comparison of human stem cells derived from various mesenchymal tissues: superiority of synovium as a cell source. Arthritis Rheum 52(8):2521-9.

Saki N, Jalalifar MA, Soleimani M, Hajizamani S, Rahim F. 2013. Adverse Effect of High Glucose Concentration on Stem Cell Therapy. International Journal of Hematology-Oncology and Stem Cell Research 7(3):34-40.

Samsonraj RM, Rai B, Sathiyanathan P, Puan KJ, Rotzschke O, Hui JH, Raghunath M, Stanton LW, Nurcombe V, Cool SM. 2015. Establishing criteria for human mesenchymal stem cell potency. Stem Cells 33(6):1878-91.

Santos F, Andrade PZ, Abecasis MM, Gimble JM, Chase LG, Campbell AM, Boucher S, Vemuri MC, Silva CL, Cabral JM. 2011. Toward a clinical-grade expansion of mesenchymal stem cells from human sources: a microcarrier-based culture system under xeno-free conditions. Tissue Eng Part C Methods 17(12):1201-10.

Sarugaser R, Lickorish D, Baksh D, Hosseini MM, Davies JE. 2005. Human umbilical cord perivascular (HUCPV) cells: a source of mesenchymal progenitors. Stem Cells 23(2):220-9.

Schallmoser K, Bartmann C, Rohde E, Bork S, Guelly C, Obenauf AC, Reinisch A, Horn P, Ho AD, Strunk D *and others*. 2010. Replicative senescence-associated gene expression changes in mesenchymal stromal cells are similar under different culture conditions. Haematologica 95(6):867-74.

References

Schellenberg A, Stiehl T, Horn P, Joussen S, Pallua N, Ho AD, Wagner W. 2012. Population dynamics of mesenchymal stromal cells during culture expansion. Cytotherapy 14(4):401-11.

Schop D, Janssen FW, Borgart E, de Bruijn JD, van Dijkhuizen-Radersma R. 2008. Expansion of mesenchymal stem cells using a microcarrier-based cultivation system: growth and metabolism. J Tissue Eng Regen Med 2(2-3):126-35.

Schop D, Janssen FW, van Rijn LD, Fernandes H, Bloem RM, de Bruijn JD, van Dijkhuizen-Radersma R. 2009a. Growth, metabolism, and growth inhibitors of mesenchymal stem cells. Tissue Eng Part A 15(8):1877-86.

Schop D, Janssen FW, van Rijn LDS, Fernandes H, Bloem RM, de Bruijn JD, van Dijkhuizen-Radersma R. 2009b. Growth, Metabolism, and Growth Inhibitors of Mesenchymal Stem Cells. Tissue Engineering Part A 15(8):1877-1886.

Schwartz RE, Reyes M, Koodie L, Jiang YH, Blackstad M, Lund T, Lenvik T, Johnson S, Hu WS, Verfaillie CM. 2002. Multipotent adult progenitor cells from bone marrow differentiate into functional hepatocyte-like cells. Journal of Clinical Investigation 109(10):1291-1302.

Schwartz SD, Hubschman J-P, Heilwell G, Franco-Cardenas V, Pan CK, Ostrick RM, Mickunas E, Gay R, Klimanskaya I, Lanza R. 2012. Embryonic stem cell trials for macular degeneration: a preliminary report. The Lancet 379(9817):713-720.

Seaberg RM, Smukler SR, Kieffer TJ, Enikolopov G, Asghar Z, Wheeler MB, Korbutt G, van der Kooy D. 2004. Clonal identification of multipotent precursors from adult mouse pancreas that generate neural and pancreatic lineages. Nat Biotechnol 22(9):1115-24.

Services USDoHaH. 2004. Guidance for industry: PAT—a framework for innovative pharmaceutical development, manufacturing and quality assurance. http://www.fda.gov/downloads/Drugs/GuidanceComplianceRegulatoryInformation/Guidances/ucm070305.pdf Food and Drug Administration.

Sethe S, Scutt A, Stolzing A. 2006. Aging of mesenchymal stem cells. Ageing Res Rev 5(1):91-116.

Shaffer AL, Shapiro-Shelef M, Iwakoshi NN, Lee AH, Qian SB, Zhao H, Yu X, Yang L, Tan BK, Rosenwald A *and others*. 2004. XBP1, downstream of Blimp-1, expands the secretory apparatus and other organelles, and increases protein synthesis in plasma cell differentiation. Immunity 21(1):81-93.

Shi S, Gronthos S. 2003. Perivascular niche of postnatal mesenchymal stem cells in human bone marrow and dental pulp. J Bone Miner Res 18(4):696-704.

References

Shih DT, Lee DC, Chen SC, Tsai RY, Huang CT, Tsai CC, Shen EY, Chiu WT. 2005. Isolation and characterization of neurogenic mesenchymal stem cells in human scalp tissue. Stem Cells 23(7):1012-20.

Siddappa R, Licht R, van Blitterswijk C, de Boer J. 2007. Donor variation and loss of multipotency during in vitro expansion of human mesenchymal stem cells for bone tissue engineering. Journal of Orthopaedic Research 25(8):1029-1041.

Sieblist C, Hägeholz O, Aehle M, Jenzsch M, Pohlscheidt M, Lübbert A. 2011. Insights into large-scale cell-culture reactors: II. Gas-phase mixing and CO2 stripping. Biotechnology Journal 6(12):1547-1556.

Siegel G, Kluba T, Hermanutz-Klein U, Bieback K, Northoff H, Schäfer R. 2013. Phenotype, donor age and gender affect function of human bone marrow-derived mesenchymal stromal cells. BMC Medicine 11(1):1-20.

Simaria AS, Hassan S, Varadaraju H, Rowley J, Warren K, Vanek P, Farid SS. 2014. Allogeneic cell therapy bioprocess economics and optimization: Single-use cell expansion technologies. Biotechnology and Bioengineering 111(1):69-83.

Siminovitch L, McCulloch EA, Till JE. 1963. DISTRIBUTION OF COLONY-FORMING CELLS AMONG SPLEEN COLONIES. Journal of Cellular and Comparative Physiology 62(3):327-&.

Singh V. 1999. Disposable bioreactor for cell culture using wave-induced agitation. Cytotechnology 30(1-3):149-158.

Small EJ, Schellhammer PF, Higano CS, Redfern CH, Nemunaitis JJ, Valone FH, Verjee SS, Jones LA, Hershberg RM. 2006. Placebo-controlled phase III trial of immunologic therapy with sipuleucel-T (APC8015) in patients with metastatic, asymptomatic hormone refractory prostate cancer. J Clin Oncol 24(19):3089-94.

Sohni A, Verfaillie CM. 2013. Mesenchymal Stem Cells Migration Homing and Tracking. Stem Cells International 2013:8.

Soncini M, Vertua E, Gibelli L, Zorzi F, Denegri M, Albertini A, Wengler GS, Parolini O. 2007. Isolation and characterization of mesenchymal cells from human fetal membranes. J Tissue Eng Regen Med 1(4):296-305.

Song I-H, Caplan AI, Dennis JE. 2009. Dexamethasone inhibition of confluence-induced apoptosis in human mesenchymal stem cells. Journal of Orthopaedic Research 27(2):216-221.

Spees JL, Gregory CA, Singh H, Tucker HA, Peister A, Lynch PJ, Hsu SC, Smith J, Prockop DJ. 2004. Internalized antigens must be removed to prepare hypoimmunogenic mesenchymal stem cells for cell and gene therapy. Mol Ther 9(5):747-56.

Stolzing A, Bauer E, Scutt A. 2012. Suspension cultures of bone-marrow-derived mesenchymal stem cells: effects of donor age and glucose level. Stem Cells Dev 21(14):2718-23.

Stolzing A, Coleman N, Scutt A. 2006. Glucose-induced replicative senescence in mesenchymal stem cells. Rejuvenation Res 9(1):31-5.

Stolzing A, Scutt A. 2006. Age-related impairment of mesenchymal progenitor cell function. Aging Cell 5(3):213-24.

Streitz M, Miloud T, Kapinsky M, Reed MR, Magari R, Geissler EK, Hutchinson JA, Vogt K, Schlickeiser S, Kverneland AH *and others*. 2013. Standardization of whole blood immune phenotype monitoring for clinical trials: panels and methods from the ONE study. Transplantation Research 2:17-17.

Stroncek DF, Jin P, Wang E, Ren J, Sabatino M, Marincola FM. 2009. Global Transcriptional Analysis for Biomarker Discovery and Validation in Cellular Therapies. Molecular Diagnosis & Therapy 13(3):181-193.

Sun X, Long X, Yin Y, Jiang Y, Chen X, Liu W, Zhang W, Du H, Li S, Zheng Y *and others*. 2008. Similar biological characteristics of human embryonic stem cell lines with normal and abnormal karyotypes. Hum Reprod 23(10):2185-93.

Sunil N, Punreddy S, Niss K, Jing D. 2014. Expansion of Human Mesenchymal Stem Cells: Using Microcarriers and Human Platelet Lysate. BioProcess International 12(8):74-78.

Suzuki S, Muneta T, Tsuji K, Ichinose S, Makino H, Umezawa A, Sekiya I. 2012. Properties and usefulness of aggregates of synovial mesenchymal stem cells as a source for cartilage regeneration. Arthritis Res Ther 14(3):R136.

Takahashi K, Tanabe K, Ohnuki M, Narita M, Ichisaka T, Tomoda K, Yamanaka S. 2007. Induction of pluripotent stem cells from adult human fibroblasts by defined factors. Cell 131(5):861-872.

Takahashi K, Yamanaka S. 2006. Induction of pluripotent stem cells from mouse embryonic and adult fibroblast cultures by defined factors. Cell 126(4):663-676.

Tamama K, Kawasaki H, Kerpedjieva SS, Guan J, Ganju RK, Sen CK. 2011. Differential roles of hypoxia inducible factor subunits in multipotential stromal cells under hypoxic condition. Journal of cellular biochemistry 112(3):804-817.

Tan KY, Teo KL, Lim JF, Chen AK, Reuveny S, Oh SK. 2015. Serum-free media formulations are cell line-specific and require optimization for microcarrier culture. Cytotherapy 17(8):1152-65.

Tarnok A, Ulrich H, Bocsi J. 2010. Phenotypes of Stem Cells from Diverse Origin. Cytometry Part A 77A(1):6-10.

Tavassol.M, Crosby WH. 1968. TRANSPLANTATION OF MARROW TO EXTRAMEDULLARY SITES. Science 161(3836):54-&.

Tchkonia T, Zhu Y, Deursen Jv, Campisi J, Kirkland JL. 2013. Cellular senescence and the senescent secretory phenotype: therapeutic opportunities. The American Society for Clinical Investigation 123(3):966-972.

The Emerging Risk Factors C. 2010. Diabetes mellitus, fasting blood glucose concentration, and risk of vascular disease: a collaborative meta-analysis of 102 prospective studies. Lancet 375(9733):2215-2222.

Thomas RJ, Chandra A, Liu Y, Hourd PC, Conway PP, Williams DJ. 2007. Manufacture of a human mesenchymal stem cell population using an automated cell culture platform. Cytotechnology 55(1):31-9.

Thomson JA, Itskovitz-Eldor J, Shapiro SS, Waknitz MA, Swiergiel JJ, Marshall VS, Jones JM. 1998. Embryonic stem cell lines derived from human blastocysts. Science 282(5391):1145-1147.

Till JE. 1961. RADIATION EFFECTS ON DIVISION CYCLE OF MAMMALIAN CELLS IN VITRO. Annals of the New York Academy of Sciences 95(2):911-&.

Till JE, McCulloch EA. 1961. DIRECT MEASUREMENT OF RADIATION SENSITIVITY OF NORMAL MOUSE BONE MARROW CELLS. Radiation Research 14(2):213-&.

Timmins NE, Kiel M, Gunther M, Heazlewood C, Doran MR, Brooke G, Atkinson K. 2012. Closed system isolation and scalable expansion of human placental mesenchymal stem cells. Biotechnol Bioeng 109(7):1817-26.

Toma JG, Akhavan M, Fernandes KJ, Barnabe-Heider F, Sadikot A, Kaplan DR, Miller FD. 2001. Isolation of multipotent adult stem cells from the dermis of mammalian skin. Nat Cell Biol 3(9):778-84.

Tondreau T, Lagneaux L, Dejeneffe M, Massy M, Mortier C, Delforge A, Bron D. 2004. Bone marrow-derived mesenchymal stem cells already express specific neural proteins before any differentiation. Differentiation 72(7):319-326.

Trainor N, Pietak A, Smith T. 2014. Rethinking clinical delivery of adult stem cell therapies. Nat Biotech 32(8):729-735.

Tremain N, Korkko J, Ibberson D, Kopen GC, DiGirolamo C, Phinney DG. 2001. MicroSAGE analysis of 2,353 expressed genes in a single cell-derived colony of undifferentiated human mesenchymal stem cells reveals mRNAs of multiple cell lineages. Stem Cells 19(5):408-18.

Trummer E, Fauland K, Seidinger S, Schriebl K, Lattenmayer C, Kunert R, Vorauer-Uhl K, Weik R, Borth N, Katinger H *and others*. 2006. Process parameter shifting: Part I. Effect of DOT, pH, and temperature on the performance of Epo-Fc expressing CHO cells cultivated in controlled batch bioreactors. Biotechnol Bioeng 94(6):1033-44.

Tse WT, Pendleton JD, Beyer WM, Egalka MC, Guinan EC. 2003. Suppression of allogeneic T-cell proliferation by human marrow stromal cells: implications in transplantation. Transplantation 75(3):389-97.

Tuschong L, Soenen SL, Blaese RM, Candotti F, Muul LM. 2002. Immune response to fetal calf serum by two adenosine deaminase-deficient patients after T cell gene therapy. Hum Gene Ther 13(13):1605-10.

Uccelli A, Moretta L, Pistoia V. 2006. Immunoregulatory function of mesenchymal stem cells. Eur J Immunol 36(10):2566-73.

Uccelli A, Moretta L, Pistoia V. 2008. Mesenchymal stem cells in health and disease. Nature Reviews Immunology 8(9):726-736.

Unger C, Skottman H, Blomberg P, Dilber MS, Hovatta O. 2008. Good manufacturing practice and clinical-grade human embryonic stem cell lines. Hum Mol Genet 17(R1):R48-53.

Veevers-Lowe J, Ball SG, Shuttleworth A, Kielty CM. 2011. Mesenchymal stem cell migration is regulated by fibronectin through alpha5beta1-integrin-mediated activation of PDGFR-beta and potentiation of growth factor signals. J Cell Sci 124(Pt 8):1288-300.

Viswanathan S, Keating A, Deans R, Hematti P, Prockop D, Stroncek DF, Stacey G, Weiss DJ, Mason C, Rao MS. 2014. Soliciting strategies for developing cell-based reference materials to advance mesenchymal stromal cell research and clinical translation. Stem Cells Dev 23(11):1157-67.

von Bahr L, Batsis I, Moll G, Hagg M, Szakos A, Sundberg B, Uzunel M, Ringden O, Le Blanc K. 2012. Analysis of tissues following mesenchymal stromal cell therapy in humans indicates limited long-term engraftment and no ectopic tissue formation. Stem Cells 30(7):1575-8.

Vrábel P, van der Lans RGJM, Luyben KCAM, Boon L, Nienow AW. 2000. Mixing in large-scale vessels stirred with multiple radial or radial and axial up-pumping impellers: modelling and measurements. Chemical Engineering Science 55(23):5881-5896.

Wada MR, Inagawa-Ogashiwa M, Shimizu S, Yasumoto S, Hashimoto N. 2002. Generation of different fates from multipotent muscle stem cells. Development 129(12):2987-95.

Wagner W, Feldmann RE, Jr., Seckinger A, Maurer MH, Wein F, Blake J, Krause U, Kalenka A, Burgers HF, Saffrich R *and others*. 2006. The heterogeneity of human mesenchymal

stem cell preparations--evidence from simultaneous analysis of proteomes and transcriptomes. Exp Hematol 34(4):536-48.

Wagner W, Ho AD, Zenke M. 2010. Different facets of aging in human mesenchymal stem cells. Tissue Eng Part B Rev 16(4):445-53.

Wagner W, Wein F, Seckinger A, Frankhauser M, Wirkner U, Krause U, Blake J, Schwager C, Eckstein V, Ansorge W *and others*. 2005. Comparative characteristics of mesenchymal stem cells from human bone marrow, adipose tissue, and umbilical cord blood. Exp Hematol 33(11):1402-16.

Wakitani S, Saito T, Caplan AI. 1995. MYOGENIC CELLS DERIVED FROM RAT BONE-MARROW MESENCHYMAL STEM-CELLS EXPOSED TO 5-AZACYTIDINE. Muscle & Nerve 18(12):1417-1426.

Wang HS, Hung SC, Peng ST, Huang CC, Wei HM, Guo YJ, Fu YS, Lai MC, Chen CC. 2004. Mesenchymal stem cells in the Wharton's jelly of the human umbilical cord. Stem Cells 22(7):1330-1337.

Wang M, Crisostomo PR, Herring C, Meldrum KK, Meldrum DR. 2006. Human progenitor cells from bone marrow or adipose tissue produce VEGF, HGF, and IGF-I in response to TNF by a p38 MAPK-dependent mechanism. Am J Physiol Regul Integr Comp Physiol 291(4):R880-4.

Wappler J, Rath B, Laufer T, Heidenreich A, Montzka K. 2013. Eliminating the need of serum testing using low serum culture conditions for human bone marrow-derived mesenchymal stromal cell expansion. Biomed Eng Online 12:15.

Weil BR, Abarbanell AM, Herrmann JL, Wang Y, Meldrum DR. 2009. High glucose concentration in cell culture medium does not acutely affect human mesenchymal stem cell growth factor production or proliferation. Am J Physiol Regul Integr Comp Physiol 296(6):R1735-43.

Williams DJ, Thomas RJ, Hourd PC, Chandra A, Ratcliffe E, Liu Y, Rayment EA, Archer JR. 2012. Precision manufacturing for clinical-quality regenerative medicines. Philos Trans A Math Phys Eng Sci 370(1973):3924-49.

Windrum P, Morris TC. 2003. Severe neurotoxicity because of dimethyl sulphoxide following peripheral blood stem cell transplantation. Bone Marrow Transplant 31(4):315.

Woodbury D, Schwarz EJ, Prockop DJ, Black IB. 2000. Adult rat and human bone marrow stromal cells differentiate into neurons. Journal of Neuroscience Research 61(4):364-370.

Wu J, Rostami MR, Cadavid Olaya DP, Tzanakakis ES. 2014. Oxygen Transport and Stem Cell Aggregation in Stirred-Suspension Bioreactor Cultures. PLoS ONE 9(7):e102486.

Wuchter P, Bieback K, Schrezenmeier H, Bornhauser M, Muller LP, Bonig H, Wagner W, Meisel R, Pavel P, Tonn T *and others*. 2014. Standardization of Good Manufacturing Practice-compliant production of bone marrow-derived human mesenchymal stromal cells for immunotherapeutic applications. Cytotherapy.

Wuertz K, Godburn K, Iatridis JC. 2009. MSC response to pH levels found in degenerating intervertebral discs. Biochemical and biophysical research communications 379(4):824-829.

Yamachika E, Iida S. 2013. Bone regeneration from mesenchymal stem cells (MSCs) and compact bone-derived MSCs as an animal model. Japanese Dental Science Review 49(1):35-44.

Yamaguchi A, Katagiri T, Ikeda T, Wozney JM, Rosen V, Wang EA, Kahn AJ, Suda T, Yoshiki S. 1991. RECOMBINANT HUMAN BONE MORPHOGENETIC PROTEIN-2 STIMULATES OSTEOBLASTIC MATURATION AND INHIBITS MYOGENIC DIFFERENTIATION INVITRO. Journal of Cell Biology 113(3):681-687.

Yang H, Acker JP, Cabuhat M, Letcher B, Larratt L, McGann LE. 2005. Association of post-thaw viable CD34+ cells and CFU-GM with time to hematopoietic engraftment. Bone Marrow Transplant 35(9):881-7.

Yu Y, Li K, Bao C, Liu T, Jin Y, Ren H, Yun W. 2009. Ex vitro expansion of human placenta-derived mesenchymal stem cells in stirred bioreactor. Appl Biochem Biotechnol 159(1):110-8.

Zeikus G; PRS Biotech, Inc., assignee. 2009. Pneumatic bioreactor.

Zisa D, Shabbir A, Suzuki G, Lee T. 2009. Vascular endothelial growth factor (VEGF) as a key therapeutic trophic factor in bone marrow mesenchymal stem cell-mediated cardiac repair. Biochemical and Biophysical Research Communications 390(3):834-838.

Zuk PA, Zhu M, Ashjian P, De Ugarte DA, Huang JI, Mizuno H, Alfonso ZC, Fraser JK, Benhaim P, Hedrick MH. 2002. Human adipose tissue is a source of multipotent stem cells. Molecular Biology of the Cell 13(12):4279-4295.

Zuk PA, Zhu M, Mizuno H, Huang J, Futrell JW, Katz AJ, Benhaim P, Lorenz HP, Hedrick MH. 2001. Multilineage cells from human adipose tissue: Implications for cell-based therapies. Tissue Engineering 7(2):211-228.

Appendices

Appendix A. Development of a quantitative osteogenesis assay

For the development of the quantitative osteogenesis assay, a method to measure the amount of deposited collagen by BM-hMSCs under osteogenic differentiation must be validated. This is important as traditional qualitative methods of demonstrating BM-hMSC differentiation potential are not useful for comparing changing conditions during process development. In order to compare the effect of different process conditions on the osteogenic potential of BM-hMSCs, an assay must be developed to facilitate this.

Experimental Protocol

The details of the osteogenic assay protocol can be found in Section 3.4.8. The aim of this investigation was to quantify the amount of collagen deposited under osteogenic conditions by producing a collagen standard and to determine whether this was more than is typically produced in normal culture.

For the collagen standards, acid-soluble collagen Type I at 0, 0.1, 0.2 and 0.4 $g.L^{-1}$ were formulated in sterile filtered deionised water at an n = 5. Each of these was treated with Sircol-red dye reagent and washed three times with deionised water to dilute unbound dye reagent. This solution was then washed with ice-cold acid salt wash reagent to remove traces of dye reagent, so that only dye reagent bound to collagen remained. An alkali reagent was then added to each of the standards to released bound dye reagent from the collagen and five samples of 100 µL for each concentration were transferred to a 96 well plate for analysis. This plate was then analysed on a plate reader at an absorbance of 555 nm and values normalised to the reagent blanks (0 $µ.L^{-1}$ collagen).

To compare the levels of collagen production under osteogenic differentiation and normal culture, two 12-well plates were set up with 38,000 BM-hMSCs per well, both containing six wells of DMEM and 10% FBS and six wells containing PRIME-XV® Serum-free Osteogenic Medium. The first of these 12-well plates was cultured for three days before being sacrificed and analysed as per the protocol in Section 3.4.8, with the other being cultured for six days with a complete medium exchange taking place on day three.

Results

The results of the collagen standard can be seen in Figure 11.1 which shows a strong correlation of R^2 = 0.975 and an equation of y = 0.3869x. Using this correlation, the actual amount of collagen deposition can be calculated for future experimental conditions.
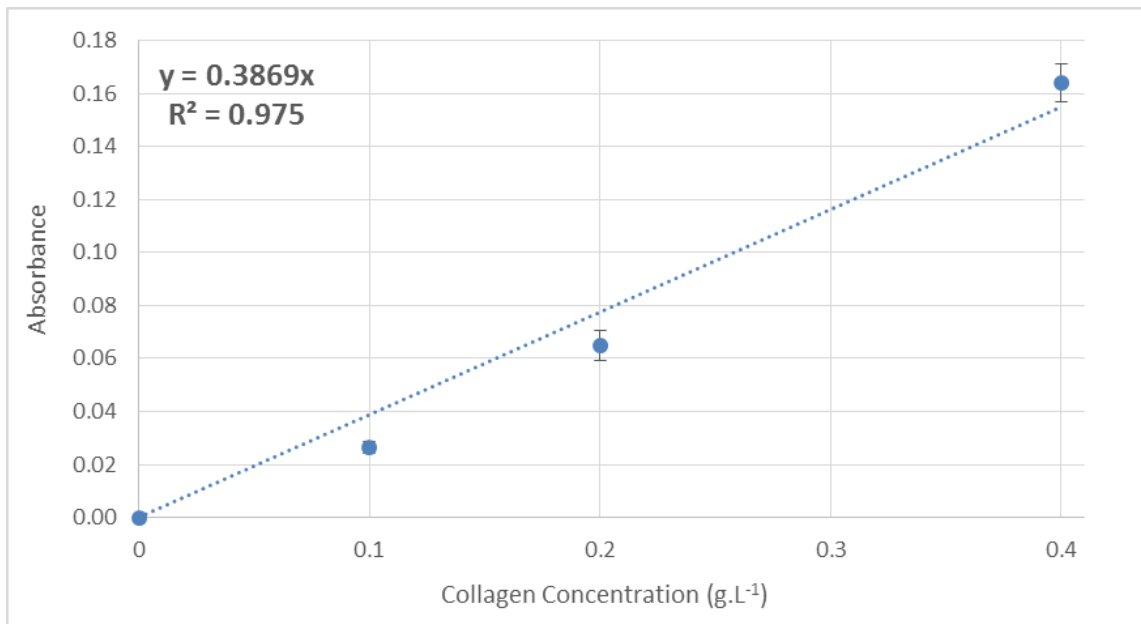

Figure 11.1. Collagen standard to quantify the amount of collagen produced during osteogenic culture of BM-hMSCs based on the plate reader absorbance

In order to assess whether the BM-hMSCs produce more collagen under osteogenic conditions a comparison was made between BM-hMSCs under osteogenic conditions and under normal culture conditions. Figure 11.2 shows the level of expression between these conditions with the day three level of collagen produced under osteogenic conditions being significantly higher (p < 0.05) than under normal culture conditions. The level of collagen under osteogenic conditions at day six was still higher, although not significantly so in this instance (p > 0.05). This is likely caused by the BM-hMSC population under normal culture conditions continuing proliferation and increasing the number of BM-hMSCs per well, whereas under osteogenic conditions the BM-hMSC proliferation is limited and there are less cells per well at day six. For a direct

comparison of the osteogenic potential of BM-hMSCs for different process conditions, however, this assay can be used as an aid to process development.
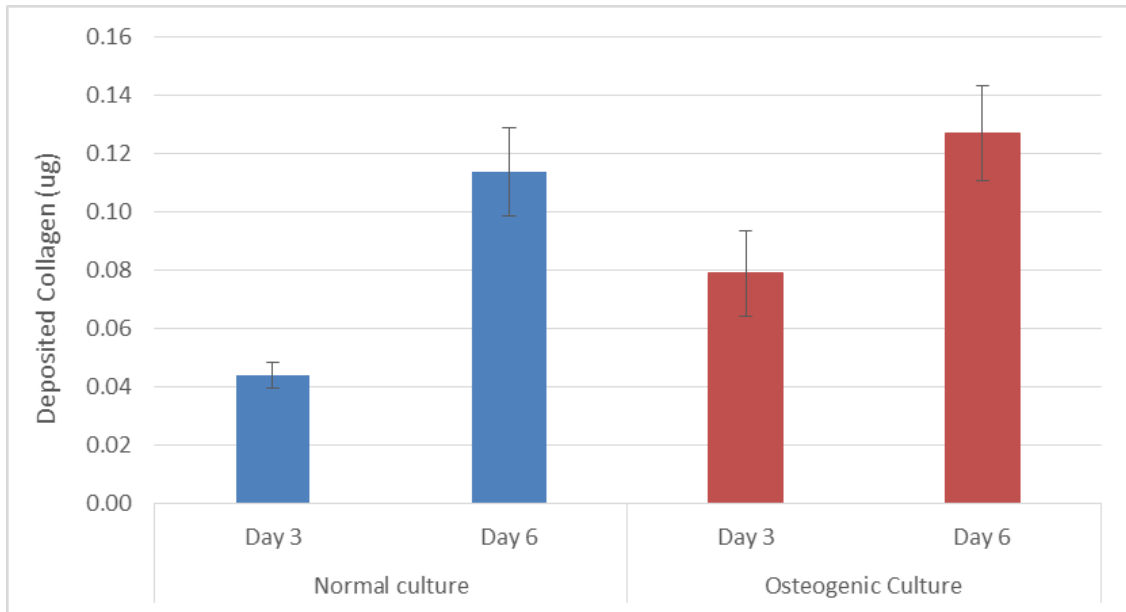

Figure 11.2. The level of collagen deposition in normal culture and osteogenic culture showing the higher level of collagen production under osteogenic conditions

Appendix B. Screening of HPL concentration in DMEM

Human platelet lysate (HPL) has been previously demonstrated as a viable alternative to FBS to supplement the culture medium for the expansion of BM-hMSCs. Prior to carrying out experiments using HPL, a screening study must be undertaken to find the concentration of HPL that best reflects the BM-hMSC performance in 10% FBS. This is important as the amount of serum used in culture should be minimised, without having a detrimental impact of the growth and characteristics of the BM-hMSCs.

Experimental Protocol

In order to make a direct comparison to 10% FBS, BM-hMSC line M2 was selected due to its stable growth characteristics in FBS culture. This was compared to 2, 5 and 10% (v/v) HPL in DMEM, formulated according to the protocol described in Section 3.2.1. To make this comparison, four T-75 flasks were seeded with M2 BM-hMSCs per experimental condition giving a total of 16 flasks, which were cultured for three passages according to the protocol described in Section 3.2.5. At the end of each passage, the cell number was determined using the protocol in Section 3.4.2 and the growth kinetics calculated. In conjunction with this, daily medium samples were taken and analysed on the Nova BioProfile FLEX for glucose, lactate and ammonium concentrations as described in Section 3.4.6. From the growth kinetics data and the relative metabolite concentrations over each passage, the net flux per cell of each metabolite was calculated.

Results

The growth kinetics of M2 BM-hMSCs can be seen in Figure 11.3 which shows the increased BM-hMSC growth kinetics as the concentration of HPL is increased up to 10% (v/v). It is clear also that the BM-hMSCs undergo an adaption passage in HPL as the first passage in all concentration of HPL is significantly higher ($p < 0.05$) than the subsequent passages. This is likely due to the presence of residual FBS in the culture which supplies additional proteins to support BM-hMSC growth that is diluted out through the first passage (Dolley-Sonneville *et al.* 2013). Following this first passage, the number of population doublings stabilises for passages four and five. This is also an important finding as it demonstrates that one adaption passage is required prior to subsequent experiments involving HPL to allow the growth kinetics of the BM-hMSCs to stabilise.
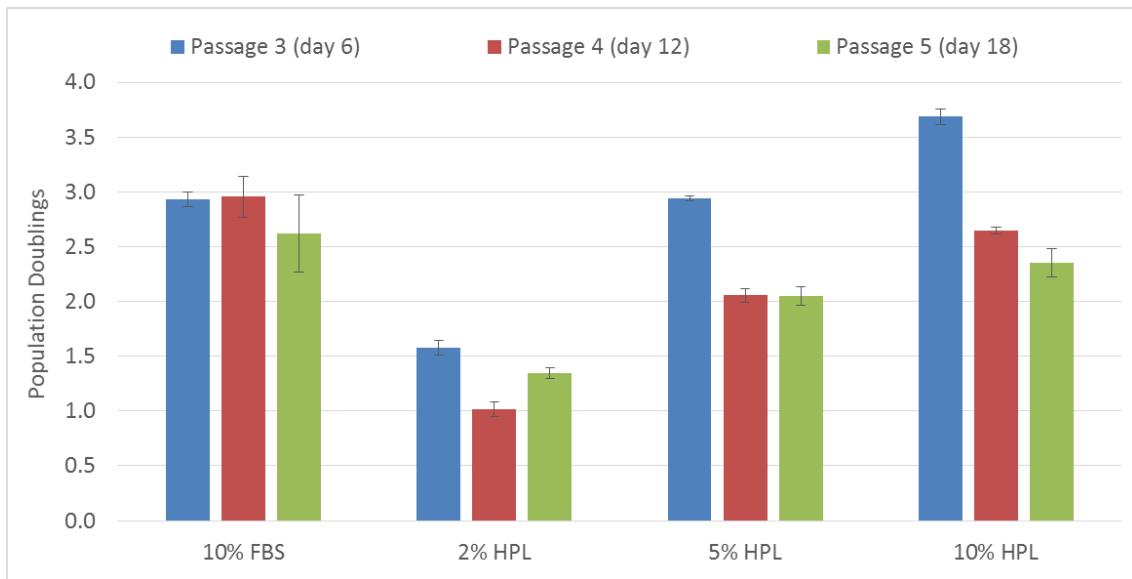
Figure 11.3. Population doublings of BM-hMSCs in various concentrations of HPL compared with 10% FBS, showing the increased proliferation in the first passage under HPL and the increased proliferation at the concentration of HPL in increased. Data shows mean ± SD, n = 4

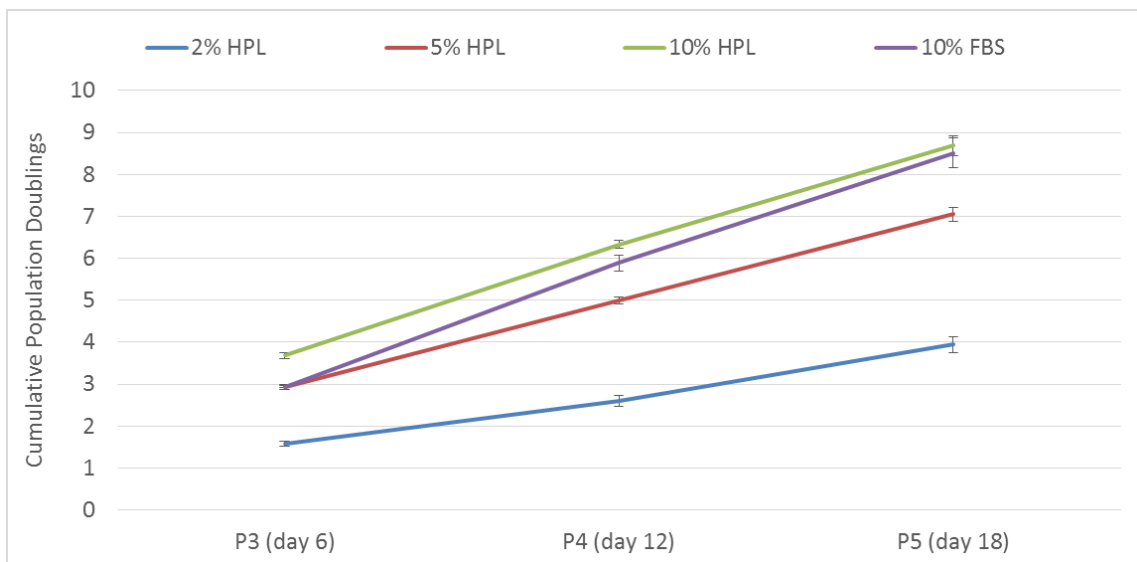**Figure 11.4. Cumulative population doublings of BM-hMSCs in various concentration of HPL compared with 10% FBS over three passages. Showing a similar number of cumulative population doublings in 10% HPL and 10% FBS. Data shows mean ± SD, n = 4**

The number of cumulative population doublings for each condition can be seen in Figure 11.4, which shows that the BM-hMSCs cultured in 2% HPL had significantly reduced cumulative population doublings ($p < 0.01$) compared to the other conditions over the three experimental passages. Despite the similar number of population doublings at passage three, BM-hMSCs cultured in 5% HPL showed a decline in growth kinetics over the subsequent two passages and finished with a lower number of cumulative population doublings. In contrast, BM-hMSCs cultured in 10% HPL demonstrated a similar number of cumulative population doublings after three passages ($p > 0.05$) compared to BM-hMSCs cultured in 10% FBS. From these data, it can be concluded that in terms of BM-hMSC growth kinetics over three passages, 10% HPL is the most comparable to 10% FBS.
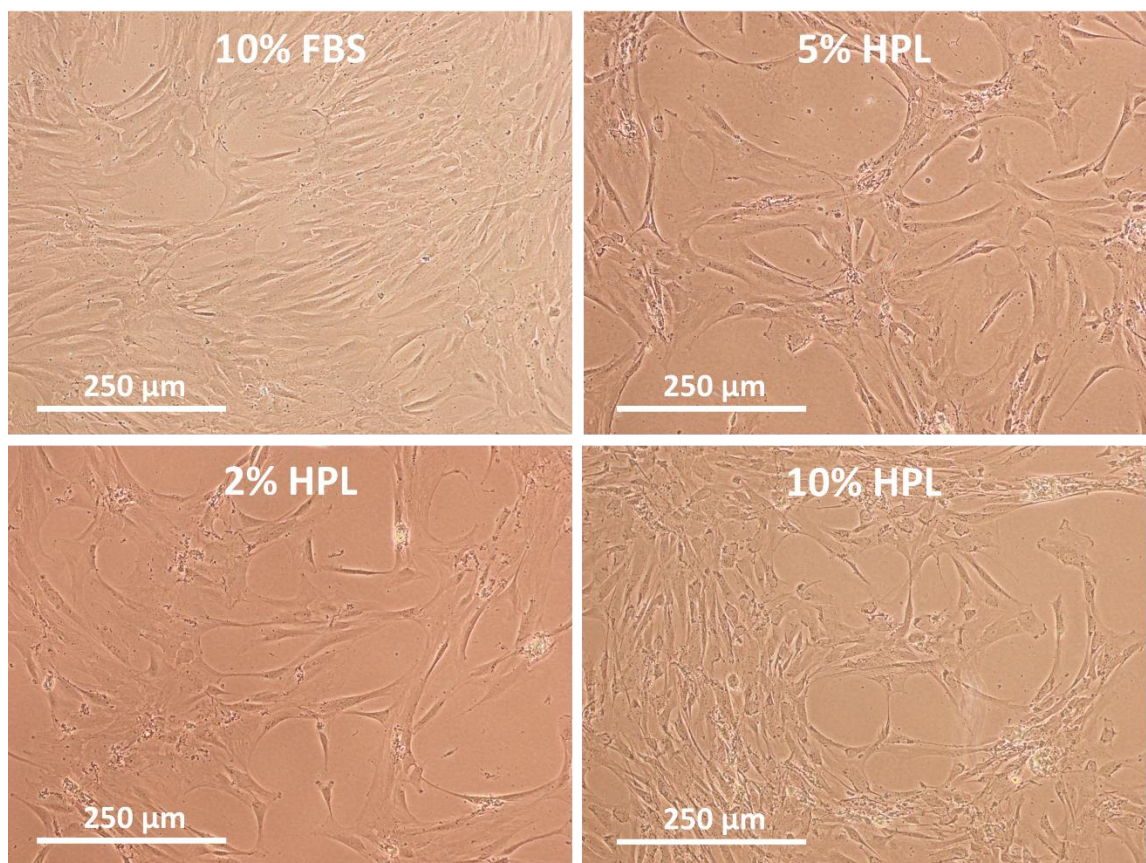

Figure 11.5. Phase contrast images showing the morphological changes to M2 BM-hMSCs in HPL compared with FBS.

The morphology of M2 BM-hMSCs in 2, 5, and 10% HPL compared with 10% FBS can be seen in Figure 11.5. The morphology of the BM-hMSCs cultured in HPL shows a marked difference compared with FBS, with BM-hMSCs in FBS demonstrating a more spindle-shaped and elongated morphology. It is apparent, however, that the concentration of HPL the BM-hMSCs are cultured in does not affect their morphology, which is similar for 2, 5 and 10% HPL. Despite the differences in morphology compared to FBS, this demonstrates that the concentration of HPL used in culture will not affect their morphology, an important characteristics for adherent cell expansion.

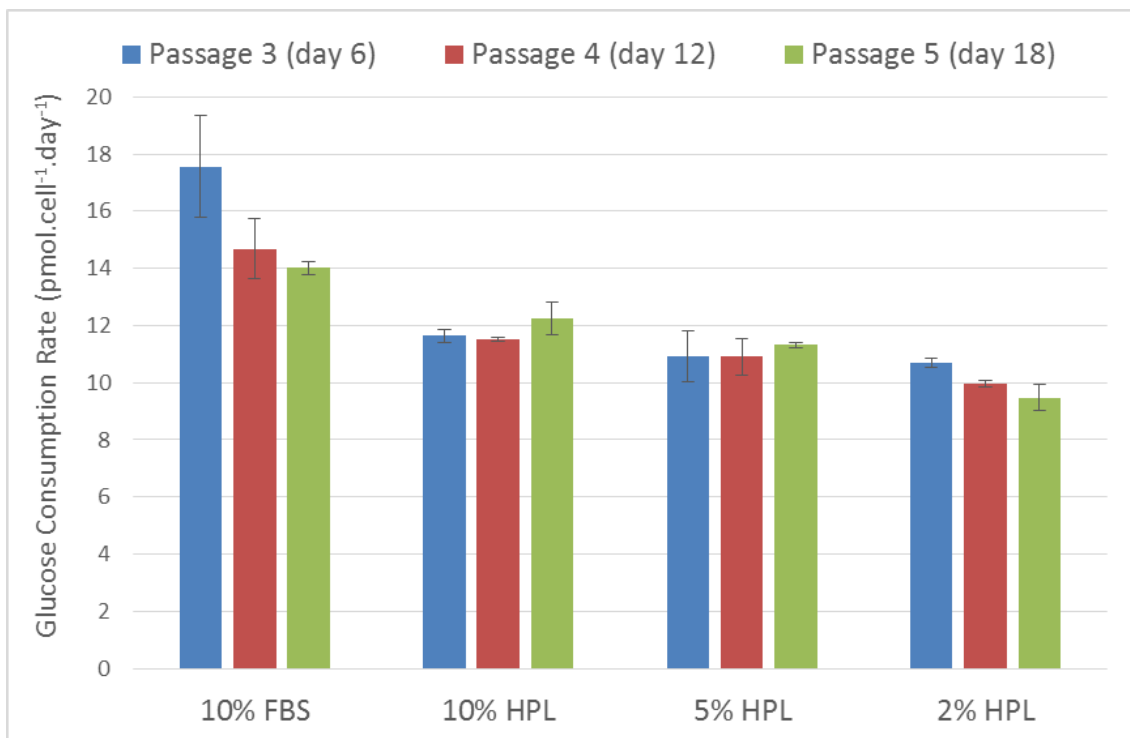**Figure 11.6. Glucose consumption rate of BM-hMSCs over three passages in various concentrations of HPL and 10% FBS. Data shows mean ± SD, n = 4**

The net metabolite flux of BM-hMSCs between experimental conditions is an important parameter to assess, as it provides a quantitative indication of the effect that varying the concentration of HPL in culture has on the metabolic profile of BM-hMSCs. Considering that

metabolite concentrations are key process parameters that can be measured online, it will be important to ensure they remain stable under different culture conditions.

Figure 11.6 shows the glucose consumption rate of M2 BM-hMSCs over the three experimental passages in each condition. The net glucose consumption rate in 2, 5 and 10% HPL remained between 10 – 12 pmol.cell^{-1}.day^{-1} across the three passages, which was reduced compared with 10% FBS. In contrast, Figure 11.7 shows that the relative lactate production rate of the BM-hMSCs decreases as the concentration of HPL in culture is reduced. Furthermore, the net production rate of lactate in 10% FBS culture of BM-hMSCs is similar to 10% HPL, a further indication that 10% HPL supports the expansion of BM-hMSCs in a similar way to 10% FBS.

Figure 11.7. Lactate production rate of BM-hMSCs over three passages in various concentrations of HPL and 10% FBS. Showing the reduction in lactate production rate as the level of HPL decreases. Data shows mean ± SD, n = 4

The relative production rate of ammonium for BM-hMSCs in all conditions can be seen in Figure 11.8, which in contrast to the net lactate production rate, increases as the concentration of HPL is decreased. This is an indication that reducing the concentration of HPL in the culture medium

encourages BM-hMSCs to reduce the flux through the aerobic glycolysis pathway and increase the utilisation of the glutamine to glutamate pathway, as demonstrated by the increase in ammonium production. It can be seen from Figure 11.8, however, that the net production of ammonium in 10% HPL is the most similar to 10% FBS, in accordance with the similarity in the BM-hMSC growth kinetics over the three passages.
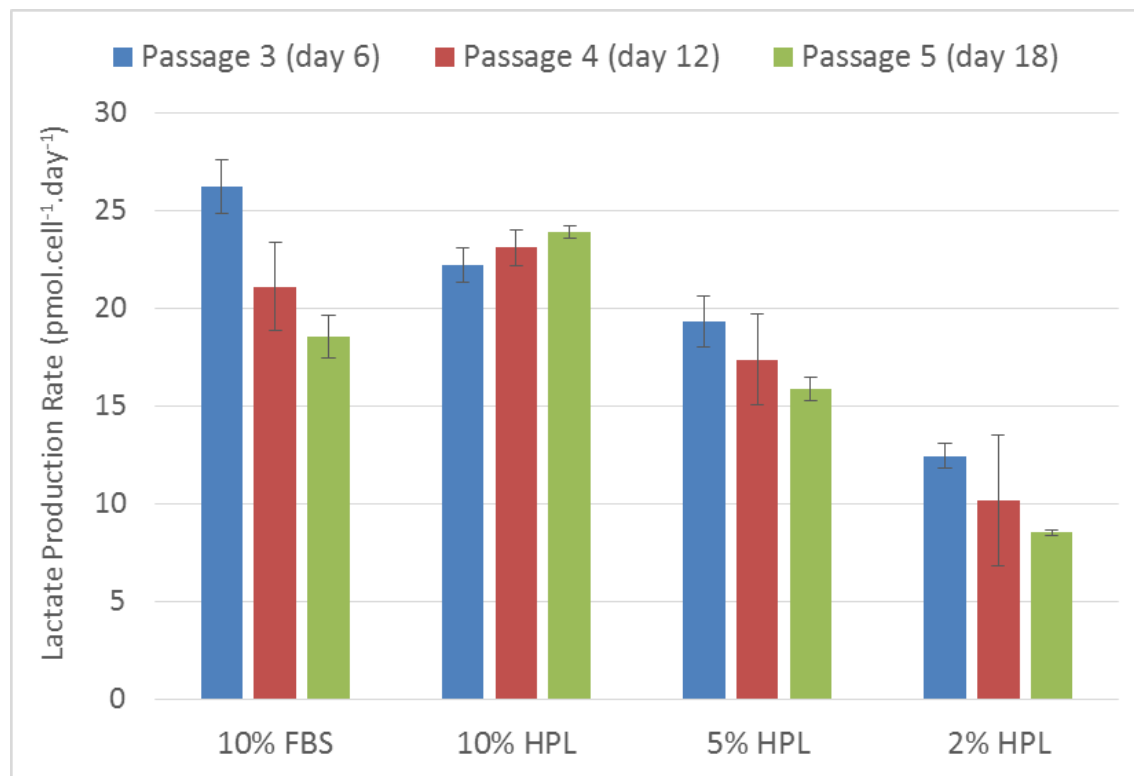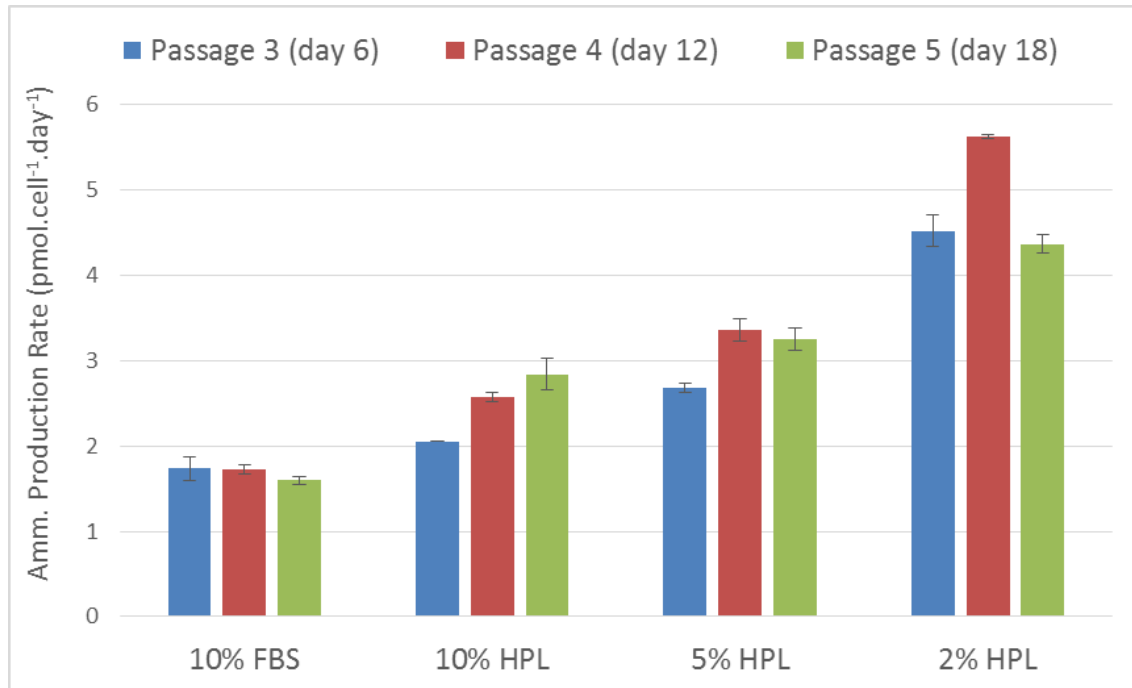

Figure 11.8. Ammonium production rate of BM-hMSCs over three passages in various concentrations of HPL and 10% FBS. Showing the increase in ammonium production rate as the level of HPL decreases. Data shows mean ± SD, n = 4

The yield of lactate from glucose can be seen in Figure 11.9, with around 2 $mol.mol^{-1}$ in 10% HPL, demonstrating that glutamine was also metabolised as a carbon source into lactate. Figure 11.9 also shows that the net flux through the oxidative phosphorylation pathway is increased as the concentration of HPL is reduced, although the general trend in the data demonstrates that BM-hMSCs predominantly utilise aerobic glycolysis as the main metabolic pathway for energy production (Dos Santos *et al.* 2010).
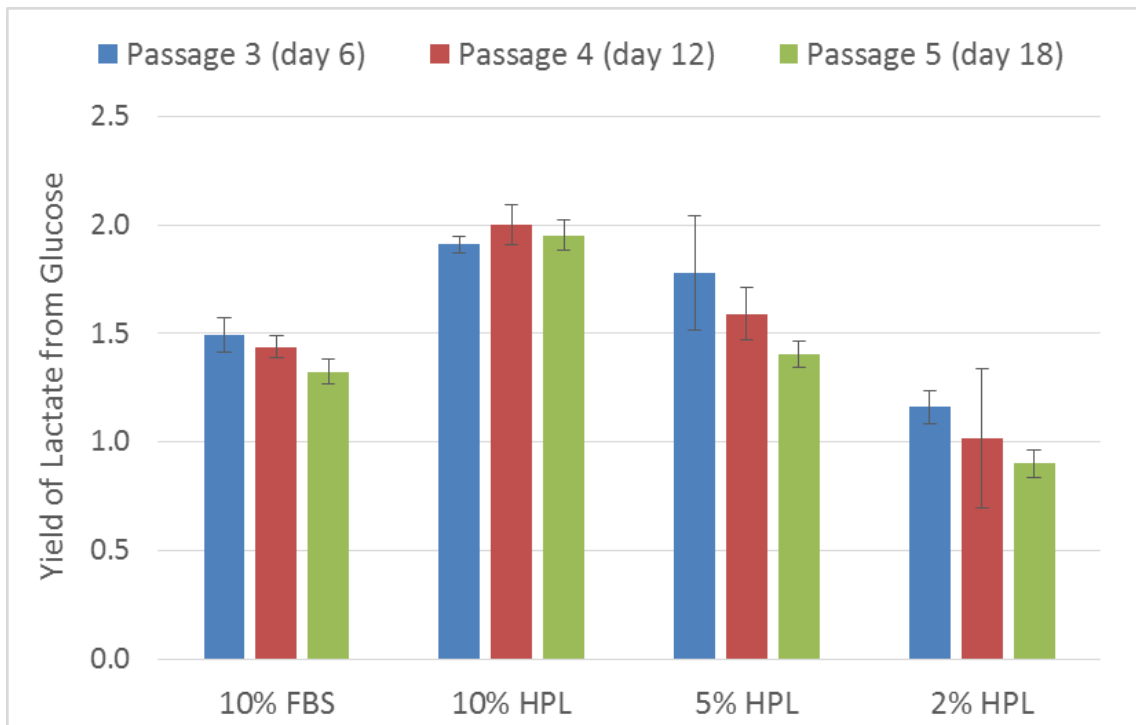
Figure 11.9. Yield of lactate from glucose of BM-hMSCs over three passages in various concentrations of HPL and 10% FBS. Showing the decrease in yield of lactate from glucose as the level of HPL decreases. Data shows mean ± SD, n = 4

This study has assessed the effect of various concentrations of HPL to support the proliferation of BM-hMSCs. From these data it is clear that 10% HPL is the most comparable to 10% FBS for the support of BM-hMSC proliferation in monolayer culture. Therefore, an HPL concentration of 10% will be used for further experiments involving BM-hMSCs with at least one adaption passage prior to any experiments taking place.

Appendix C. Assessment of PRIME-XV® SFM for BM-hMSC expansion

The development of serum-free BM-hMSC manufacturing processes will be critical for future process development as reducing and eventually eliminating the use of FBS from the cell culture medium has many key benefits. In addition to lot-to-lot variability, there are further process constraints on the use of FBS such as limited supply, spiralling cost, potential for pathogen transmission, increased risk of recipient immune reaction and reduced scope for process optimization. All of these considerations mean that moving towards a serum-free process would be beneficial in achieving scalable and consistent BM-hMSC manufacturing processes. In addition, serum-free culture has been shown to be amenable to scalable expansion technology such as microcarriers and stirred bioreactors (dos Santos *et al.* 2011a), producing higher BM-hMSC yields per unit time than serum-based processes, which will be important for driving down the production cost of BM-hMSC therapies.

It is important that prior to using a serum-free medium for BM-hMSC process development, that it is assessed for its impact on BM-hMSC expansion to ensure that it provides a favourable growth and identity profile. With this in mind an experiment was designed to compare the use of PRIME-XV® MSC Expansion SFM to the process baseline of 10% FBS culture for two BM-hMSC donors to ensure that any measured effect is not donor specific.

Experimental Protocol

In order to make a direct comparison to 10% FBS, BM-hMSC lines M0 and M2 were selected due to their stable growth characteristics in FBS culture. This was compared to PRIME-XV® MSC Expansion SFM over three passages. To make this comparison, four T-75 flasks were seeded with M0 and M2 BM-hMSCs per experimental condition giving a total of 16 flasks, which were cultured for three passages according to the protocol described in Section 3.2.5. At the end of each passage, the cell number was determined using the protocol in Section 3.4.2 and the growth kinetics calculated. In conjunction with this, daily medium samples were taken and analysed on the Nova BioProfile FLEX for glucose, lactate and ammonium concentrations as described in Section 3.4.6. From the growth kinetics data and the relative metabolite concentrations over each passage, the per cell flux of each metabolite was calculated. At the end of the third passage, the cells were assessed for immunophenotype using the flow cytometry protocol described in Section 3.4.5.

Results

The number of cumulative population doublings for each condition can be seen in Figure 11.10, which shows that both M0 and M2 BM-hMSCs cultured in SFM had between 12 -14 cumulative population doublings compared with 8 – 10 cumulative population doublings in FBS over the same time period. This represents a significantly higher number of cumulative population doublings in SFM ($p > 0.01$) compared to FBS culture. From these data, it can be concluded that PRIME-XV® SFM significantly increases the proliferation potential of BM-hMSCs compared to 10% FBS. This has the potential to offer advantages during process development as more BM-hMSCs can be produced per unit time.
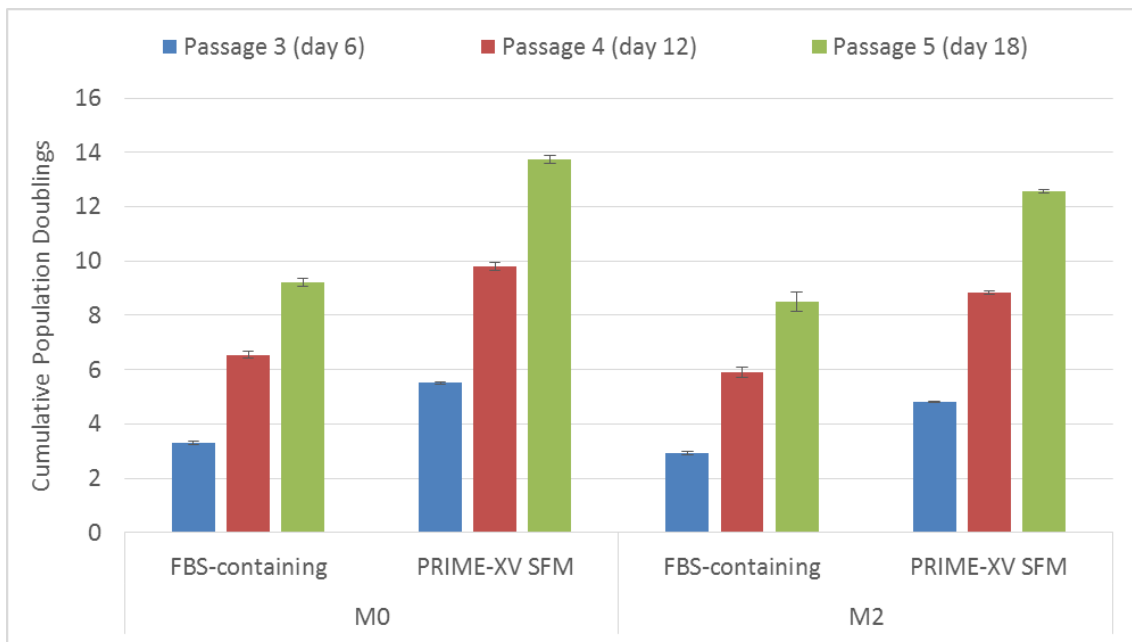
Figure 11.10. Cumulative population doublings of BM-hMSC lines M0 and M2 in 10% FBS and PRIME-XV® SFM over three passages. Showing the increased growth kinetics under serum-free conditions. Data shows mean ± SD, n = 4

As mentioned previously, the net metabolite flux of BM-hMSCs between experimental conditions is an important parameter to assess, as it provides a quantitative indication of the effect that different culture media has on the metabolic profile of BM-hMSCs.

Figure 11.11 shows the glucose consumption rate of M0 and M2 BM-hMSCs over the three experimental passages in SFM and FBS. The net glucose consumption rate in SFM remained between 5 - 7 pmol.cell^{-1}.day^{-1} across the three passages, which was significantly reduced (p < 0.01) compared with the 15 - 20 pmol.cell^{-1}.day^{-1} measured in 10% FBS. Further to this, Figure 11.12 shows that the relative lactate production rate of the BM-hMSCs in SFM is significantly lower (p < 0.01) than BM-hMSCs in FBS culture.

Figure 11.11. Glucose consumption rate of BM-hMSC lines M0 and M2 over three passages in 10% FBS and PRIME-XV® SFM. Showing the reduced glucose consumption rate in SFM. Data shows mean ± SD, n = 4

This reduction in the per cell flux of both glucose and lactate demonstrates an increase in the metabolic efficiency of BM-hMSC culture in SFM, which has potential advantages with increasing process yield, as a reduced concentration of glucose will be required and the potential inhibitory effects of lactate build up will be reduced.
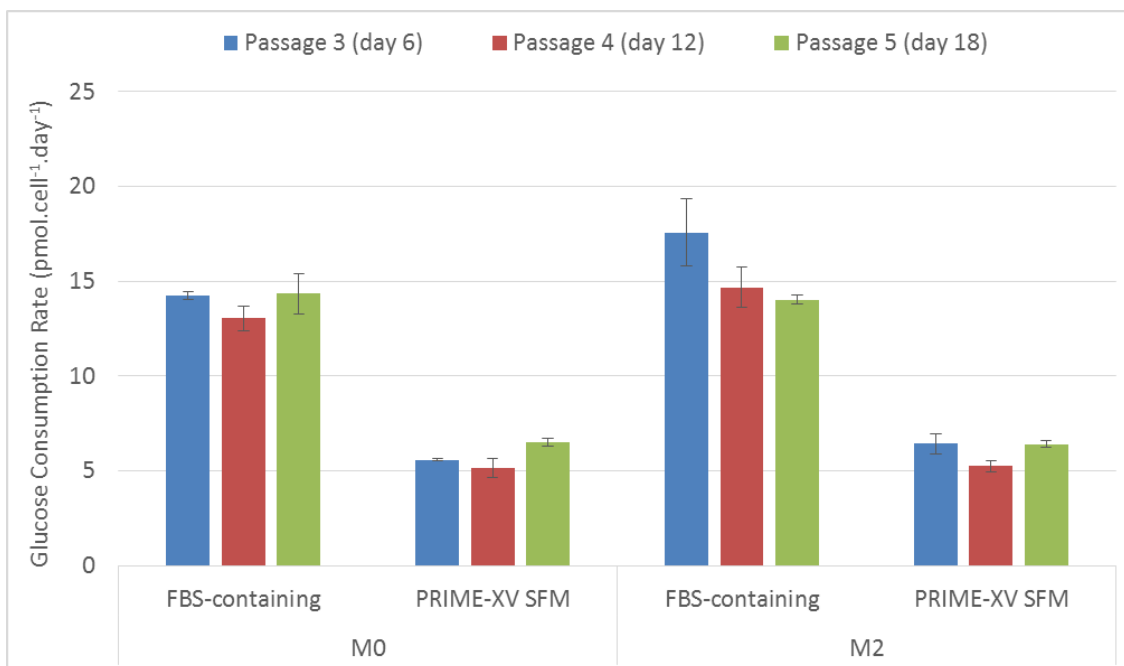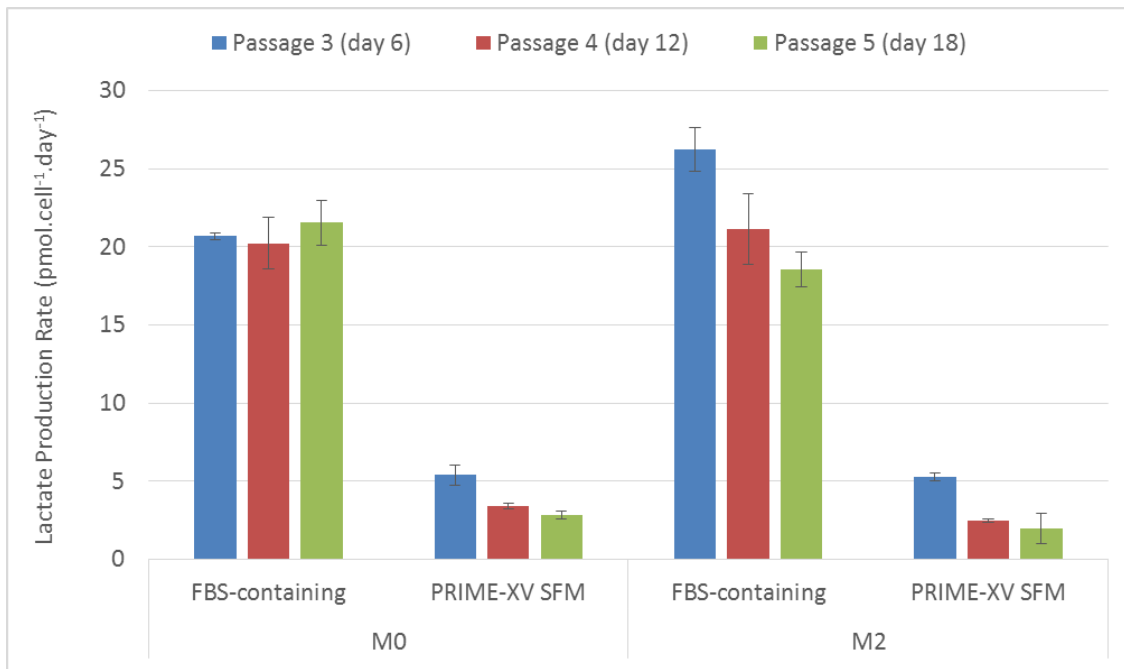
Figure 11.12. Lactate production rate of BM-hMSC lines M0 and M2 over three passages in 10% FBS and PRIME-XV® SFM. Showing the reduced lactate production rate in SFM. Data shows mean ± SD, n = 4

Despite the reduced consumption of glucose and production of lactate over the three passages in SFM, Figure 11.13 shows that the per cell flux of ammonium for both BM-hMSC lines in FBS and SFM are between $1 - 2$ pmol.cell^{-1}.day^{-1}. As before, this is an indication that reducing the concentration of serum in the culture medium encourages BM-hMSCs to reduce the flux through the aerobic glycolysis pathway and increase the utilisation of the glutamine to glutamate pathway, as demonstrated by the measured increase in ammonium production of BM-hMSCs in SFM.

The yield of lactate from glucose can be seen in Figure 11.14, with below 1 mol.mol^{-1} in SFM, supporting the previous statement that BM-hMSCs cultures in SFM favour the production of energy *via* oxidative phosphorylation, whereas BM-hMSCs cultured in FBS tend to increase the flux through the aerobic glycolysis pathway. This again demonstrates that BM-hMSCs cultured in SFM have a more efficient metabolic profile compared to the same BM-hMSCs cultured in FBS.

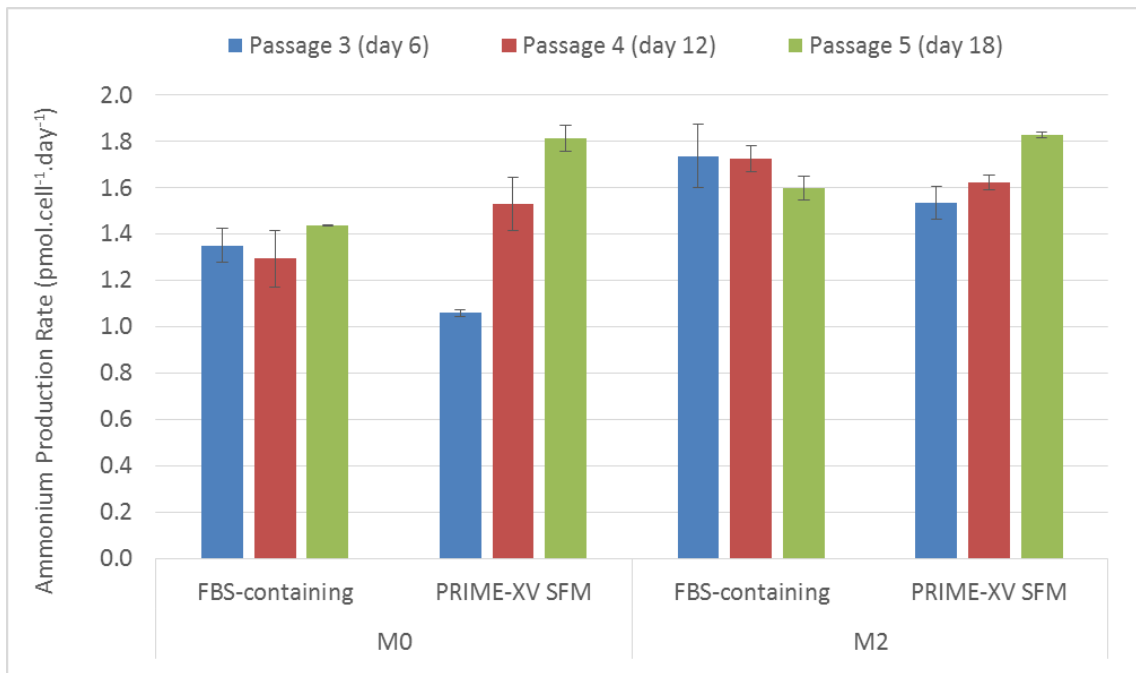**Figure 11.13. Ammonium production rate of BM-hMSC lines M0 and M2 over three passages in 10% FBS and PRIME-XV® SFM. Showing similar ammonium production rate in both 10% FBS and SFM. Data shows mean ± SD, n = 4**
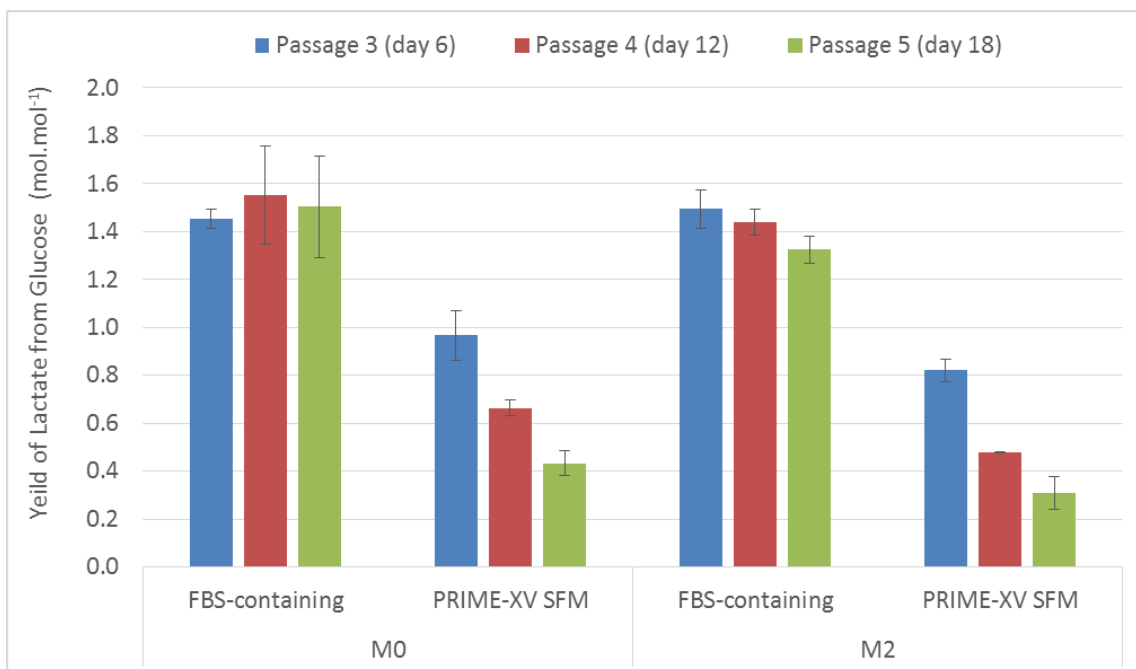

Figure 11.14. Yield of lactate from glucose of BM-hMSC lines M0 and M2 over three passages in 10% FBS and PRIME-XV® SFM. Showing the decrease in yield of lactate from glucose in SFM. Data shows mean ± SD, n = 4

The morphology of M2 BM-hMSCs in SFM compared with 10% FBS can be seen in Figure 11.15. The morphology of the BM-hMSCs cultured in SFM demonstrate differences in morphology with smaller, more spindle-shaped BM-hMSCs which are also packed more tightly together in monolayer culture. This is likely to greatly increase the available number of BM-hMSCs per area in culture, which will offer advantages for the manufacture of adherent cells as the yield per area will also increase.
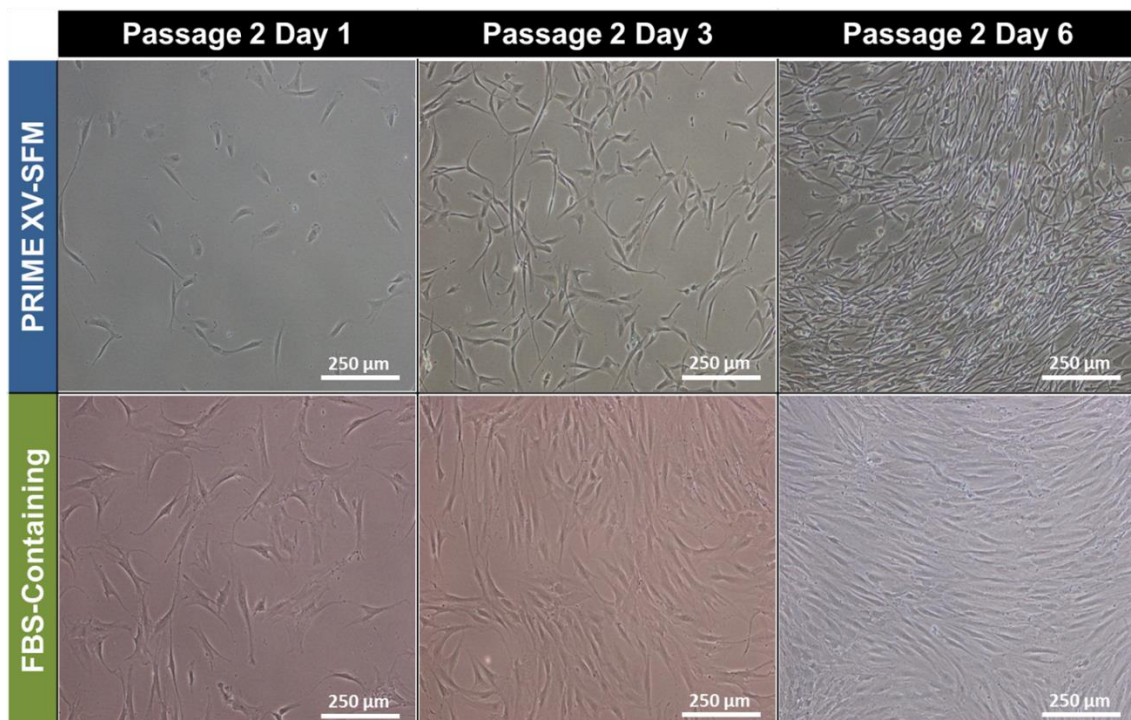
Figure 11.15. Phase contrast images showing morphology of BM-hMSC line M2 in 10% FBS and PRIME-XV® SFM over six days of culture.

Immunophenotype analysis of M0 and M2 after the three experimental passages can be seen in Figure 11.16, which demonstrates the maintenance of $CD73^+$, $CD90^+$, $CD105^+$, $CD34^-$ and HLA-DR^- BM-hMSCs in SFM compared with FBS culture. There was an increase in the positive expression of CD34 above the 2% positive threshold, which can be attributed to an increase in non-specific antibody binding caused by the culture of BM-hMSCs on a fibronectin substrate, as the upregulation of CD34 is not biologically possible for BM-hMSCs after selection by plastic adherence (Wagner *et al.* 2005).

Figure 11.16. Flow cytometry plots showing expression of CD90+, CD73+, CD105+, CD34- and HLA-DR- at the end of passage three in 10% FBS and SFM. In all cases 10,000 events were measured.

Appendix D. Fibronectin coating in glass bioreactor vessels
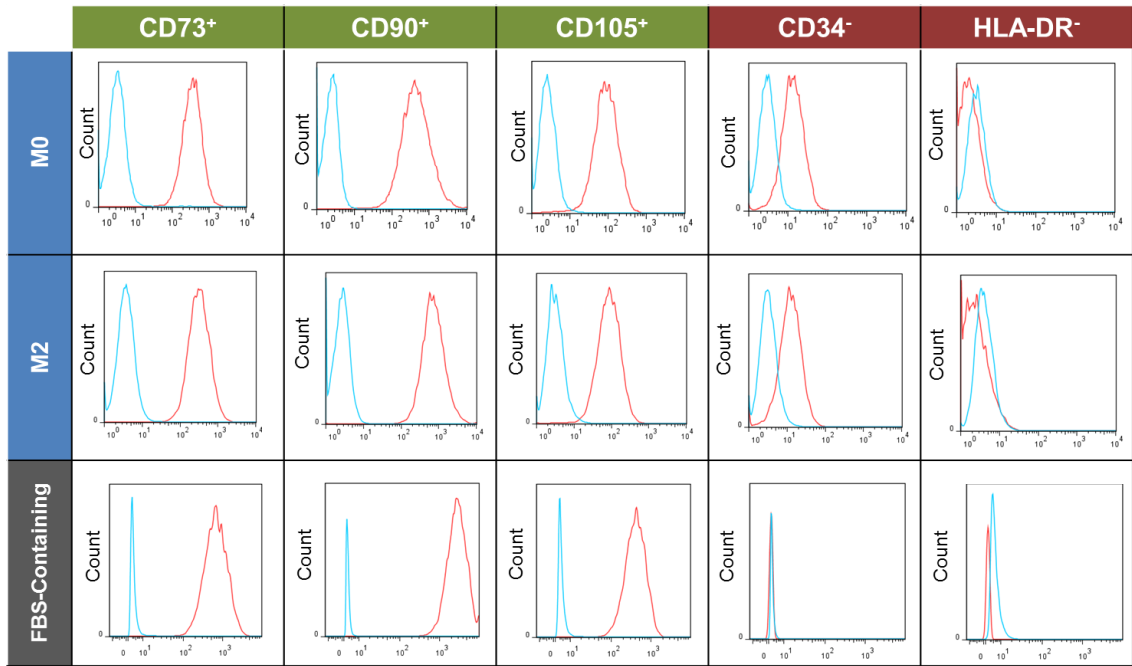
In order to transfer the microcarrier culture of BM-hMSC from a serum based process to a serum-free process, the coating of the plastic microcarrier surface with an attachment protein is required to achieve BM-hMSC attachment to the surface. This is because the serum used for BM-hMSC culture contains a high level of these attachment proteins that coat the microcarrier surface during the microcarrier conditioning phase and promote BM-hMSC attachment to the surface and subsequent growth. For the expansion of BM-hMSCs in PRIME-XV® SFM in monolayer, fibronectin has successfully been used to coat the surface of the tissue culture flask prior to culture and therefore will be used to coat the microcarrier surface in suspension prior to BM-hMSC suspension culture. This fibronectin coating of the microcarriers will take place immediately before the start of the BM-hMSC culture process to ensure that the coating substrate remains active on the surface of the microcarrier prior to BM-hMSC addition. This does present a challenge however, as both the coating step and the culture step will take place within the same spinner flask vessel to avoid the transfer of material between spinner vessels, reducing the potential for loss of material and culture contamination. With the coating of the microcarriers with fibronectin taking place in the same spinner flask, it must be confirmed that the fibronectin is not able to coat the internal glass surface of the spinner flask, therefore allowing BM-hMSCs to attach and grow on a surface other than the microcarriers in suspension. With this in mind, an experiment was designed to test whether the BM-hMSCs were able to attach to the glass surface of the spinner flask following the fibronectin coating protocol developed in Section 6.3.

Experimental Protocol

In order to test whether the fibronectin was able to coat the internal glass surface of the spinner flask, four experimental conditions were assessed. The first condition aimed to test the normal attachment of BM-hMSCs to tissue culture plastic as a positive control, with the second condition testing the relative BM-hMSC attachment in an ultra-low attachment well plate to provide a negative experimental control. To assess whether the BM-hMSC were able to attach to the spinner flask surface after the fibronectin coating step, the attachment assay was performed on a glass vessel treated with Sigmacoat before and after the fibronectin coating procedure. For the attachment assay, 10,000 BM-hMSCs per cm^2 were seeded into each condition at n = 3 with an appropriate volume of culture medium and placed into an incubator (see Section 3.2.5) for three hours to allow for BM-hMSC attachment. After this three hour period, the culture vessels were removed, washed with PBS and trypsin added to remove BM-

hMSCs attached to the surface (see Section 3.2.5). The BM-hMSCs in this solution were then counted (see Section 3.4.2) and the percentage of BM-hMSC that had attached was calculated from the amount initially seeded.

Results

The three hour attachment efficiency of each condition can be seen in Figure 11.17. This demonstrates that under normal culture conditions, a high percentage (80 – 90 %) of BM-hMSCs are able to attach to the culture surface within this three hour period. In contrast, the attachment efficiency of the BM-hMSCs in the ultra-low attachment plate was measured to be < 10%, the presence of this low amount of BM-hMSC is likely due to the presence of residual cells following the PBS washing step. It is clear from Figure 11.17 that the BM-hMSCs were not able to attach to either the spinner flask surface before or after the fibronectin coating step with < 30% attachment measured in both conditions. This is significantly lower (p < 0.01) than the positive control and the presence of BM-hMSCs in the final solution was likely the result of performing the PBS washing step in a spinner flask, which is even more inefficient than the ultra-low attachment well plate. This is clear evidence that the fibronectin is not able to coat the spinner flask and therefore it is possible to perform the fibronectin coating of the microcarriers in the same spinner flask that the culture takes place within.
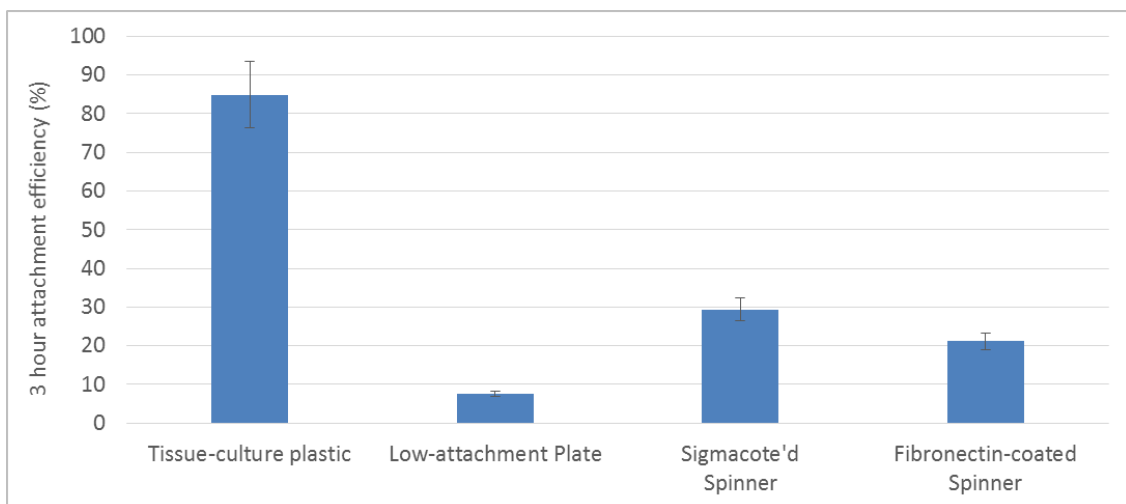

Figure 11.17. Comparison of BM-hMSC attachment to tissue culture plastic, low-attachment plate, sigma-coated spinner flask and fibronectin coated spinner flask. Demonstrating that BM-hMSCs do not attach to the spinner flask surface after fibronectin coating. Data shows mean ± SD, n = 3.

Appendix E. Controller tuning of the DASGIP DASbox bioreactor platform

The development of a process control strategy will be important to drive increased yield and consistency into the production of BM-hMSC in suspension. The goal of this process control strategy is to maintain tight control on key process parameters effecting BM-hMSC expansion such as dissolved oxygen concentration and the pH of the culture medium.

The DASGIP DASbox bioreactor system has been selected to perform these studies as it can maintain the same culture volume as the spinner flasks and has physical characteristics similar to bioreactor systems at the litre scale, with the possibility of online monitoring and control of these key parameters. The DASbox bioreactor system has been primarily developed for the culture of mammalian cells for the production of protein and therefore must be validated for the expansion of BM-hMSCs. The key part of this validation is to ensure that the DASbox bioreactor system can maintain a tight control of key process parameters for BM-hMSC culture, where the consumption of oxygen and production of pH-altering substrates is far lower than traditional cell culture processes. With this in mind, an experiment was carried out to tune the settings of the pH control loop, which was initially found to be unstable. In contrast, the regulation of oxygen in the DASbox system was stable using the default settings and therefore these settings were used for all controlled BM-hMSC experiments.

Experimental Protocol

In order to stabilise the pH control system on the DASbox an experiment was set up with the system set to control at pH = 7.4 and the culture vessels sterilised, filled with 100 mL of DMEM supplemented with 10% FBS and connected to the DASbox bioreactor platform. Following calibration of the pH probes, the system was set to control at 100% dissolved oxygen and 37°C in order to simulate normal operating conditions. Once stabilised, the control loop parameters were adjusted with the software recording and allowed to stabilise to assess the pH range obtained under those parameters. This process was repeated until an acceptable control range was obtained for the pH in the bioreactor system.

Results

The result of this iterative process can be seen in Figure 11.18. The default settings of the DASbox pH controller (point A) created a pH range of 7.42 − 7.67 which is clearly very large,

particularly considering the sensitivity of BM-hMSCs to the pH of culture medium (Wuertz *et al.* 2009), although these fluctuations are typical within an uncontrolled monolayer process. In the first instance, the proportional gain was doubled to 50 in order to increase the magnitude of the response of the controller to changes in process disturbances and the reset time was halved to increase the response time following a process disturbance. Additionally, the pre-set overlay of 6% CO_2 was applied to prevent the control system from dropping below this value during controller fluctuation. This intervention reduced the pH range by 0.11 (see Table 11.4), however this range was still too large for BM-hMSC culture.
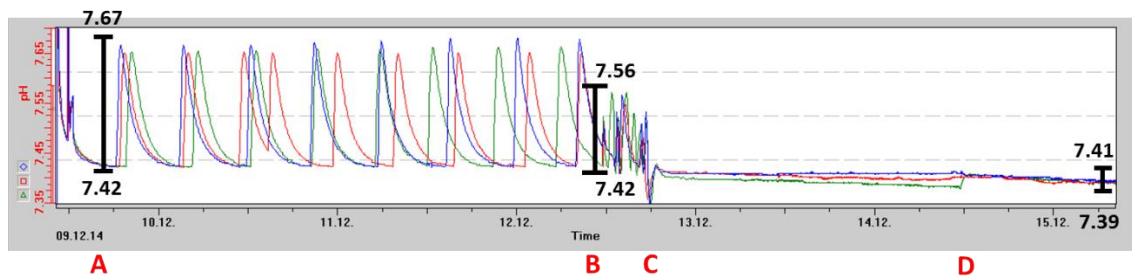

Figure 11.18. Loop tuning of the DASGIP DASbox pH controller for BM-hMSCs showing the evolution of the control strategy to obtain a stable process control system.

The second intervention was to further reduce the reset time of the controller to 300 seconds and therefore reduce the lag time of response to process disturbance. In addition to this, the auto-reset function was disabled, which is in place to protect the culture process from going below the control set-point (pH = 7.4). It was determined that a reduction of the pH to below this set-point would not be detrimental to the BM-hMSC culture (Schop *et al.* 2009b) and therefore this layer of protection could be removed as it was the main cause of the fluctuations in the culture pH. At this point, it was also decided that the pre-set overlay should be removed as this had the potential to cause issues if the pH was reduced enough during expansion that the CO_2 concentration in the inlet gas was required to be lower than the pre-set value of 6%.

Table 11.4. Proportional-integral (PI) controller settings for the pH controller on the DASGIP DASbox bioreactor relating to Figure 11.18. Demonstrating the reduced pH range achieved after tuning the control settings for BM-hMSC culture on microcarriers.

	pH set-point	Proportional gain, K_p	Reset time, K_i (s)	Deadband	Auto reset	Pre-set overlay	pH range
A	7.4	25	3600	0.02	On	Off	0.25
B	7.4	50	1800	0.02	On	6% CO_2	0.14
C	7.4	50	300	0.02	Off	Off	0.04
D	7.4	50	300	0.01	Off	Off	0.02

These changes to the control parameters on the DASbox system greatly reduced the control range of the pH to 0.04. It can be seen from Figure 11.18, however, that there was still drift in the pH control setting which could be mitigated. To achieve this, the deadband (or neutral zone) in the controller was adjusted from 0.02 to 0.01 which acts to decrease the region in which no control action occurs. It can be seen from Figure 11.18 that this eliminated the drift in the pH and halved the pH control range to 0.02. This was determined to be a satisfactory range for the pH controller and represented a reduction in the pH fluctuation of 0.23.